TECHNISCHE UNIVERSITÄT MÜNCHEN

Fakultät für Chemie

Lehrstuhl für Organische Chemie

# Tissue kallikrein-related peptidases as novel biomarkers in cancer: Cellular analysis of expression, epigenetic regulation and relation to course of the disease.

Apostolos Gkazepis

TECHNISCHE UNIVERSITÄT MÜNCHEN

Lehrstuhl für Organische Chemie

# Tissue kallikrein-related peptidases as novel biomarkers in cancer: Cellular analysis of expression, epigenetic regulation and relation to course of the disease

Apostolos Gkazepis

Vollständiger Abdruck der von der Fakultät für Chemie

der Technischen Universität München zur Erlangung des akademischen Grades eines

Doktors der Naturwissenschaften (Dr. rer. nat.)

genehmigten Dissertation.

Vorsitzender: Univ.- Prof. Dr. H.-J. P. Wester

Prüfer der Dissertation:

1. Univ.- Prof. Dr. Dr. h. c. H. Kessler
2. Univ.-Prof. Dr. M. Schmitt

Die Dissertation wurde am 28.07.2011 bei der Technischen Universität München eingereicht und durch die Fakultät für Chemie am 14.09.2011 angenommen.

# Table of Contents

# 1. Introduction

## 1.1 Biomarkers

Any specific molecular alteration of a cell on DNA, RNA or protein level can be referred as biomarker (Jain 2010). These markers can be found in a wide range of specimens, including body fluids (plasma, serum, urine, saliva, etc.), tissues, and cell lines. A biomarker is a characteristic that can be objectively measured and evaluated as an indicator of a physiological as well as a pathological process or pharmacological response to a therapeutic intervention.

In a multifactor and individually complex disease as cancer, biomarkers are essential for (a) detection and identification of a given type of cancer (diagnostic biomarkers), (b) prediction the course of the disease and (or) its recurrence (prognostic biomarkers), (c) prediction of a drug response (predictive biomarkers) and (d) observation of the disease status (monitoring biomarkers) (Hamdan 2007).

Targeted treatment strategies are not yet available for all cancers. The present approach to systemic treatment of cancer is often referred to, as "trial and error" or "one size fits all"; but this practice is inefficient and frequently results in inappropriate therapy and treatment-related toxicity. Conversely, personalized cancer treatment has the potential to increase efficacy and decrease toxicity. To achieve personalized treatment for cancer, we need meaningful biomarkers (signatures) for characterization of cancer subgroups, determining prognosis, predicting response to therapy, and predicting severe toxicity related to treatment (Dowsett and Dunbier 2008; Duffy and Crown 2008; Koomen 2008).

## 1.2 Cancer

Cancer is the uncontrolled growth of abnormal cells in the body. There are many different kinds of cancers. Cancer can develop in almost any organ or tissue, such as the lung, colon, breast, skin, bones, or nerve tissue. There are many causes of cancers, including benzene and other chemicals, drinking excess alcohol, environmental toxins, such as certain poisonous mushrooms and a type of poison that can grow on peanut plants (aflatoxins), excessive sunlight exposure, genetic predisposition, obesity, radiation and viruses (NIH 2010).

In 2008, approximately 12.7 million cancers were diagnosed (excluding non-melanoma skin cancers and other non-invasive cancers) and 7.6 million people died of cancer worldwide (Jemal 2008). Cancers as a group account for approximately 13 % of all deaths each year with the most common being: lung cancer (1.3 million deaths), stomach cancer (803,000 deaths), colorectal cancer (639,000 deaths), liver cancer (610,000 deaths), and breast cancer (519,000 deaths) (WHO 2008). This makes invasive cancer the leading cause of death in the developed world and the second leading cause of death in the developing world.

Some cancers are more common in certain parts of the world. For example, in Japan, there are many cases of stomach cancer, but in the United States, this type of cancer is rare. Differences in diet may play a role.

Like symptoms, the signs of cancer vary based on the type and location of the tumor. Common tests include the following: biopsy of the tumor, blood tests, bone marrow biopsy (for lymphoma or leukemia), chest x-ray, complete blood count (CBC), CT scan and MRI scan.

Treatment varies based on the type of cancer and its stage. The stage of a cancer refers to how much it has grown and whether the tumor has spread from its original location.

- If the cancer is confined to one location and has not spread, the most common treatment approach is surgery to cure the cancer. This is often the case with skin cancers, as well as cancers of the lung, breast, and colon.
- If the tumor has spread to local lymph nodes only, sometimes these can be removed.
- If surgery cannot remove all of the cancer, the options for treatment include radiation, chemotherapy, or both. Some cancers require a combination of surgery, radiation, and chemotherapy.
- Lymphoma, or cancer of the lymph glands, is rarely treated with surgery. Chemotherapy and radiation therapy are most often used to treat lymphoma (NIH 2010).

### 1.2.1 Gynecological cancers

**Ovarian cancer**

Approximately 125,000 deaths and 204,000 new ovarian cancer cases worldwide were reported in 2002 (Parkin 2005) whereas the incidence rates display the highest level in the Western world (Jemal 2008).The high mortality rate is usually due to late diagnosis, since epithelial ovarian tumors commonly lack early warning symptoms (Cannistra 2004); almost 75 % of patients are diagnosed with metastasis beyond the ovaries (FIGO stages III and IV) and require combined surgery and chemotherapy (Dinh 2008).

Heterogeneity of ovarian cancer and unidentified molecular pathways prohibit efficient individualized treatment strategies. Shortage of clinical, histomorphological and tumor biological markers suitable for diagnosis, prognosis and therapy response intensifies the critical state (Rosen 2005).

Staging (FIGO I–IV) of the disease at the time of diagnosis according to the guidelines of the International Federation of Gynecology and Obstetrics, nuclear grade, patient age, presence or absence of ascitic fluid, and residual tumor mass after primary surgery are the most common prognostic factors. On the other hand, there are no diagnostic factors apart from CA125.

Therefore, tumor biomarkers risk predictors of ovarian cancer patients with disease recurrence, early death, or response to preoperative, adjuvant or palliative therapy are in demand. Numerous studies have focused on improved understanding of the underlying tumor biology in ovarian cancer and biomarkers associated with this fatal disease (Kim 2009; Meani 2009; Na 2009; Safra 2009; Yoshida 2009; Kulasingam 2010). Still, despite of that, staging of the disease at the time of diagnosis according to the guidelines of the International Federation of Gynecology and Obstetrics (FIGO I-IV) represents the major prognostic factor in ovarian cancer.

**Breast cancer**

In women, breast cancer is the most common class of cancer worldwide with more than one million cases diagnosed annually, followed by cancer of the lung and colon, making it the leading cause of cancer deaths in women with >400,000 deaths per year (Parkin 2005).

Histological, immunohistochemical, mRNA expression, and genomic analyses have indicated that breast cancer is a heterogeneous disease that varies in morphology, biology, behavior, and response to therapy (Perou 2000; Sorlie 2001; Voduc and Nielsen 2008; Geyer 2009).

TNM staging, tumor grading, receptor status (ER and PR) as well as Her-2 status are established prognostic factors in breast cancer. uPA and PAI-1 have recently reached LOE (Level Of Evidence) 1, while BRCA-1 genetic tests are often used for screening.

Consequently, in breast cancer, specific biomarkers indicating the course of the disease and/or response to therapy are very much needed to help systemic treatment move from the current trial-and-error approach to more personalized cancer care.

### 1.3 Kallikrein-related peptidases (KLKs)

All human KLK genes consist of five coding exons and four intervening introns. Sizes of the genes range from 4-10 kb with most of the differences relating to variable intron sizes (Luo 1998). The five coding exons are very similar both in size and in organization. Coding exon 1 harbors the start codon, coding exons 2, 3, and 5 contain the histidine (H), aspartic acid (D), and serine (S) codons of the catalytic triad. In contrast to the "classical" *KLK* genes, most of the new members of the human tissue kallikrein family have one or two non-coding exons in the 5′ untranslated region (UTR). The 3′ UTR typically varies in length (Borgono 2004).

KLK proteins are single-chain secreted serine endopeptidases of 25-30 kDa. They are synthesized as pre-pro-enzymes containing an amino-terminal single peptide (Pre), that directs them to the endoplasmic reticulum for secretion, followed by a pro-peptide (Pro) of four to nine amino acids, that maintains them as inactive precursors (zymogen) and a catalytic domain, which comprises the mature, enzymatically active protein. KLK proteins have fully conserved amino acids around the catalytic residues, as well as overall amino acid sequence identity of 40-80 % (Obiezu and Diamandis 2005). Most of the tissue kallikrein enzymes denote a trypsin-like activity, while enzymatic activity of KLK3, KLK7, and KLK9 are chymotrypsin-like (Clements 2004).

Alternatively processed mRNA transcripts are common among members of the tissue kallikrein family. In fact, all *KLK* genes possess at least two transcripts. A total of 70 alternative *KLK* mRNA isoforms have been identified to date, exclusive the classical form. Most of alternative

splicing characterizes coding regions plus limited splicing within the 5′ UTR, involving exon skipping, exon extension/truncation and intron retention (Obiezu and Diamandis 2005).

All KLKs are synthesized as inactive precursors or zymogens with an inhibitory pro-peptide that sterically blocks the active site and thereby prevents substrate binding. Zymogen conversion to the active enzyme generally occurs by limited proteolysis of the pro-peptide via diverse mechanisms.

## Normal physiology

KLKs are expressed in several tissues, at both mRNA and protein level. Employing Northern blot, RT-PCR, and/or ELISA, KLKs are found to express at highest levels within a few major tissues such as the salivary gland, the CNS, the prostate and the breast (**Table 1**). The parallel expression of many KLKs in the same tissue under physiologic and/or pathologic conditions implies potential participation in enzyme cascade reactions similar to those established for the processes of digestion, fibrinolysis, coagulation, complement activation, wound healing, angiogenesis, and apoptosis (Yousef and Diamandis 2002). The aberrant expression in human tissues reflects tissue-specific substrate specificity.

Kallikrein 1 promotes the release of kallidin from low-molecular-weight kininogen specifically into different cell types and towards the processing of growth factors and peptide hormones (Schachter 1979; Bhoola 1992). KLK2, on the other hand, demonstrates very low kininogenase activity compared to kallikrein 1 (Charlesworth 1999). Seminal plasma KLK2 cleaves seminogelin I and seminogelin II, but at different cleavage sites and at a lower efficiency than PSA (Deperthes 1996). KLK2 has also been implicated in regulating growth factors, through insulin-like growth factor binding protein-3 (IGFBP-3) proteolysis. KLK3 (prostate-specific antigen/PSA) is present at very high concentrations in seminal plasma, rapidly hydrolyzing both seminogelin I and seminogelin II, as well as fibronectin, provoking liquefaction of the seminal plasma clot after ejaculation (Lilja 1985). Potential substrates for KLK3 have been identified such as IGFBP-3, tumor growth factor-β, basement membrane, parathyroid hormone-related peptide, and plasminogen (Diamandis and Yousef 2002). KLK3 is found in nipple aspirate fluid, breast cancer cyst fluid, milk of lactating women, amniotic fluid, and breast cancer tumor tissue (Diamandis 1995).

Among the additional twelve KLKs, only a few have been attributed to physiologic processes and/or pathologic conditions (**Table 1**). Putative functions have been suggested for several of the KLKs, based on the sites of expression and/or the activity of orthologue proteins. Isolation or cloning of KLKs from specific tissues such as skin (*KLK5, KLK7, KLK11*) and brain (*KLK6, KLK8, KLK11*) proposes a role at these sites (Gan 2000; Clements and Atkins 2001). Cascade models simulate efficiently skin desquamation and semen liquefaction, and may be applied in tumor invasion and metastasis. Specifically, KLK6 is hypothesized to be involved in the deposition of amyloid plaques in Alzheimer´s disease (Little 1997). KLK7 is directly linked to the physiological skin desquamation process as a key serine protease, which deconstructs the cohesive bonds that maintain the integrity of corneodesmosomes. It has been reported that KLK7 is present in different layers of the epidermis like the dendritic cells (Sondell 1997), the keratinizing squamous epithelia (Sondell 1994) and that it is stored in lamellar bodies in the stratum granulosum and transported via these structures to the stratum corneum extracellular space (Sondell 1995). KLK7 is moreover located in the sebaceous follicles, in luminal parts of the pilary canal, common sebaceous ducts and proximal sebaceous ducts and in cells apparently situated within the distal parts of the glandular lobules (Ekholm 1998). It has been shown that proKLK7 in skin is activated by KLK5 at a slightly acidic/neutral environment (Brattsand 2005; Hachem 2005) and that KLK7 acts in a water-depleted environment of the stratum corneum (Watkinson 2001) cleaving key corneodesmosomal proteins like CDSN and DSC1, leading to cohesive bond disruption and furthermore desquamation of the corneocytes (Caubet 2004). Theories adapting skin cascade theories are developed for many tissues (e.g. pancreas) (Johnson 2007).

Pro-KLK proteins can serve as substrates for activated KLKs, thereby setting the stage, potentially, for a proteolytic cascade, whereby differentially expressed kallikreins within the tissue microenvironment proteolytically activate other KLK proenzymes, with the entire array of activated species subsequently acting on extracellular substrates to either mediate physiological functions or contribute to disease progression (Mikolajczyk 1997; Magklara 2003; Bayes 2004; Caubet 2004).

**Table 1:** Differential expression of kallikrein-related peptidases in normal physiological conditions

| KLK | Normal physiology | | |
|---|---|---|---|
| | **Highest (RT-PCR)** | **Other tissues (RT-PCR)** | **Reference** |
| **KLK1** | Pancreas, kidney, salivary glands | Sweat glands, intestine, CNS, b neutrophils, uterus, prostate, testis, breast, placenta | (Bhoola 1992; Clements 1997) |
| **KLK2** | Prostate | Breast, thyroid, salivary glands | (Catalona 1991; Lovgren 1999; Black 2000) |
| **KLK3** | Prostate | Breast, thyroid, salivary glands, lung, trachea | (Wang 1979; Papsidero 1980; Wang 1981; Oesterling 1991; Diamandis and Yu 1995; 1997; Diamandis 1998b; a; Rittenhouse 1998; Black and Diamandis 2000) |
| **KLK4** | Prostate | Breast, thyroid, testis, uterus, adrenal, colon, spinal cord | (Nelson 1999; Stephenson 1999; Yousef 1999b) |
| **KLK5** | Breast, brain, testis, skin | Salivary glands, thymus, CNS, prostate, thyroid, trachea, pancreas | (Brattsand and Egelrud 1999; Yousef and Diamandis 1999; Dong 2008) |
| **KLK6** | CNS, breast, kidney, uterus | Salivary gland, spleen, testis | (Anisowicz 1996; Little 1997; Yamashiro 1997; Yousef 1999a) |
| **KLK7** | Skin, CNS, kidney, breast | Salivary glands, thymus, uterus, thyroid, placenta, trachea, testis, ovary, pancreas | (Hansson 1994; Tanimoto 1999; Yousef 2000d; Dong 2008) |
| **KLK8** | CNS, skin, ovary | | (Yoshida 1998a; Underwood 1999) |
| **KLK9** | Thymus, testis, CNS, trachea | Breast, prostate, salivary glands, ovary, skin | (Yousef and Diamandis 2000) |
| **KLK10** | Breast, ovary, testis, prostate | Small intestine, lung, colon, pancreas, uterus, CNS, salivary glands, trachea | (Liu 1996) |
| **KLK11** | Brain, skin, salivary gland, stomach, uterus, lung, thymus, prostate, spleen, liver, small intestine, trachea | Heart, fetal liver, breast, thyroid, skeletal muscle | (Yoshida 1998b; Yousef 2000c) |
| **KLK12** | Salivary glands, stomach, uterus, trachea, prostate, thymus, lung, colon, brain, breast, thyroid | Testis, pancreas, small intestine, spinal cord | (Yousef 2000d) |
| **KLK13** | Breast, prostate, salivary glands, testis | Lung, heart, thymus, adrenal, colon, thyroid, trachea | (Yousef 2000a; Planque 2008a) |
| **KLK14** | CNS, skin, breast, prostate, ovary | thyroid, uterus, thymus, colon, spleen, placenta, small intestine, kidney, bone marrow, lung (localized in the cytoplasm of epithelial cells of normal bronchus and NSCLC, as determined by immunohistochemistry), salivary glands | (Hashem ; Yousef 2001b; Borgono 2007; Planque 2008a) |
| **KLK15** | Thyroid, salivary glands, prostate | Adrenal, colon, testis, kidney | |

## Kallikrein-related peptidases in cancer

**Growth and survival:** KLKs promote or inhibit cancer cell proliferation by modulating the availability and activity of latent growth factors. Kallikrein 1, KLK2, KLK3 and KLK11 degrade insulin-like growth factor binding proteins (IGFBP2, 3, 4, 5) *in vitro* and liberate insulin-like growth factor 1 (IGF1), which, by binding to its receptor (IGF1R), has a proliferative and anti-apoptotic activity (Cohen 1992; Rajah 1997; Sutkowski 1999; Rehault 2001; Sano 2007). KLK2 and KLK4 interact with the urokinase plasminogen activator system by activating single-chain pro-uPA (Frenette 1997; Takayama 2001), and inactivating (only KLK4) plasminogen inhibitor type-1 (PAI-1) (Mikolajczyk 1999), leading to release and/or activation of growth factors from the extracellular matrix (ECM). KLKs may also act as growth factors themselves by activating protease-activated receptor (PAR) signaling (Ohta 2003; Oikonomopoulou 2010). Interestingly, KLK3 can also release transforming growth factor-β (TGF-β) from its latent complex, which, bound to its receptor, might suppress tumor growth (Derynck 2001).

**Angiogenesis:** KLKs might promote angiogenesis by modulating its activation, facilitating endothelial-cell proliferation, migration and capillary-tube formation through direct or indirect ECM degradation. KLKs *in vitro* cleave structural components of the subendothelial basement membrane (BM) and extracellular matrix (ECM) (Watt 1986; Bernett 2002; Cloutier 2002; Magklara 2003). KLKs also interact with the plasminogen activation system (Frenette 1997; Mikolajczyk 1999; Takayama 2001) and matrix metalloproteinases (MMPs) (Tschesche 1989; Desrivieres 1993; Menashi 1994). These systems promote ECM degradation through plasmin, activation of proangiogenic growth factors such as vascular endothelial growth factor (VEGF) and pro-MMPs and therefore tumor invasion and metastasis. Activation of TGF-β (by KLK3) (Derynck 2001) and release of bradykinin from kininogen (by kallikrein 1) (Emanueli 2001) leads to stimulation of angiogenesis. PAR signaling induces endothelial cell proliferation (Jin 2003). Angiogenesis may be inhibited by KLK3, KLK6, and KLK13 by generating angiostatin-like fragments from plasminogen (Heidtmann 1999; Sotiropoulou 2003; Bayes 2004). Angiostatin is a potent inhibitor of endothelial cell proliferation and angiogenesis *in vivo* (Borgono and Diamandis 2004).

**Invasion and metastasis:** KLKs may directly or indirectly regulate invasion by dissolution of ECM barriers. KLKs could activate PAR signaling with a consequent stimulatory or inhibitory effect on tumor cell invasion (Henrikson 1999; Kamath 2001). KLK3 liberates TGF-β (Derynck 2001) from its latent complex and therefore promotes epithelial-to-mesenchymal transition (EMT), which is necessary for tumor cells to detach, invade, and metastasize.

In breast cancer tissues and/or cell lines, *KLK3, KLK10, KLK12, KLK13,* and *KLK14* genes are downregulated at the mRNA level (Yu 1995; Liu 1996; Yu 1996; Goyal 1998; Yu 1998; Yousef 2000a; Yousef 2000b; Dhar 2001; Yousef 2001b). Contradictory to that fact a study on (mRNA)*KLK14,* where its expression seems to be upregulated in the malignant samples compared to their benign counterparts (Papachristopoulou 2011). *KLK6* gene is down-regulated in metastatic breast cancer and upregulated in primary breast cancer (Anisowicz 1996). *In silico* analysis of KLK mRNA expression levels in normal and cancerous breast tissues and cell lines proposes that *KLK5, KLK6, KLK8,* and *KLK10* genes are down-regulated in breast cancer (Yousef 2004e). In a recent study, disease-free interval (DFI) and overall survival (OS) were significantly associated with KLK10 methylation suggesting it as an independent prognostic factor for DFI and OS. KLK3 expression is not only associated with prostate but also with breast diseases (Yu 1996) and has been suggested to be a useful prognostic marker for breast cancer (Black and Diamandis 2000). Although (mRNA)*KLK5* and (mRNA)*KLK14* levels are reduced in breast cancer, elevated serum levels of the KLK5 and KLK14 proteins were observed in a subgroup of breast cancer patients (Yousef 2003c). For some KLKs, a prognostic impact in breast cancer can be observed: higher mRNA expression of *KLK5, KLK7* and *KLK14* is associated with poor prognosis (Yousef 2002a; Yousef 2002d; Talieri 2004), while expression levels of *KLK9, KLK13,* and *KLK15* as well as KLK3 protein content are indicative for a favorable disease outcome (Yu 1995; Yu 1998; Foekens 1999; Chang 2002; Yousef 2002e; Yousef 2003f). High levels of KLK3 and KLK10 proteins in breast carcinomas predict a poor response to tamoxifen therapy (Foekens 1999; Luo 2002).

Six of the fifteen KLKs (KLK4, 5, 6, 7, 10, 15) are markers of poor prognosis, whereas higher levels of five other tissue kallikreins (KLK8, 9, 11, 13, 14) in ovarian cancer patients are associated with favorable prognosis (Yousef 2001a; Yousef 2003a; Yousef 2003c; Yousef 2003e; Borgono 2004; Obiezu and Diamandis 2005; Borgono 2006; White 2009). Numerous studies employing Northern-Blot, RT-PCR, or immunoassay have demonstrated that KLK4,

KLK5, KLK6, KLK7, KLK8, KLK10, KLK11, KLK13, KLK14, and KLK15 are overexpressed in ovarian carcinoma tissues, serum and/or cell lines at the mRNA and/or protein levels. The up-regulation of *KLK5, KLK6, KLK7, KLK8, KLK10, KLK11,* and *KLK14* genes was further verified by *in silico* analysis of KLK gene expression in normal and cancerous ovarian tissues and cell lines (Yousef 2003d). *KLK4, KLK5/KLK5, KLK6/KLK6, KLK7, KLK10,* and *KLK15* seem to be markers of poor prognosis, while *KLK8, KLK9,* KLK11, KLK13, and *KLK14* markers of favorable prognosis. By means of ELISA, elevated serum or tissue levels of KLK5, KLK6, KLK8, KLK10, KLK11, KLK13, and KLK14 protein were discovered in a proportion of ovarian cancer patients and correspond to clinical significance either as biomarkers for detection or diagnosis or as prognostic indicators (Diamandis 2000a; Luo 2001a; Diamandis 2002; Borgono 2003b; Diamandis 2003b; Kishi 2003; Luo 2003a; Yousef 2003c; Scorilas 2004; Kountourakis 2009; White 2009; Batra 2011). Differential KLK expression is summarized in **Table 2**.

**Table 2:** Differential expression of kallikrein-related peptidases in various types of cancer. ND= Not defined

| KLK | Cancer | | | |
|---|---|---|---|---|
| | **Type** | **Expression** | **Clinical relevance** | **Reference** |
| **KLK1** | Breast cancer | ND | ND | (Hermann 1995; Rehbock 1995) |
| | Colon cancer | ↓ Expression in malignant tumors compared to normal tissues | ND | (Yousef 2004a) |
| | Pancreatic cancer<br>Cancer cells<br>Fibroblasts<br>Neutrophils<br>Lymphocytes | ND | ND | (Wolf 2001) |
| | Renal cell carcinoma | ND | ND | (Moodley 2005) |
| **KLK2** | Ovarian cancer | ↑ Expression in malignant tumors compared to normal tissues | ND | (Adib 2004) |
| | Prostate cancer | ↓ Expression in malignant tumors compared to normal tissues | Diagnosis | (Darson 1997; Rittenhouse 1998; Magklara 2000) |
| **KLK3** | Breast cancer Cancer cells | ↓ Expression in malignant tumors compared to benign tissues | Favorable prognosis (↑ survival) | (Yu and Diamandis 1995; Yu 1995; Yu 1996; Howarth 1997; Yu 1998; Foekens 1999) |
| | Serum | | Predictive value (predicts response to tamoxifen therapy) | |
| | Ovarian cancer | ↑ Expression in malignant tumors compared to normal tissues | ND | (Adib 2004; Gilks 2005) |
| | | ↑ Expression in low malignant potential serous tumors compared to serous carcinomas | | |
| | Prostate cancer | ↓ Expression in malignant tumors compared to normal tissues | Population screening, Diagnosis, Prognosis, Monitoring | (Hakalahti 1993; Rittenhouse 1998; Magklara 2000) |

| KLK | Cancer | | | |
|---|---|---|---|---|
| | **Type** | **Expression** | **Clinical relevance** | **Reference** |
| **KLK4** | Ovarian cancer Cancer cells Stromal Cells | ↑ Expression in malignant tumors and cell lines compared to benign and normal tissues | Unfavorable prognosis (↑ stage, ↑ tumor grade, ↓ survival) | (Dong 2001; Obiezu 2001; Xi 2004a; Davidson 2005) |
| | | ↑ Expression in tumor cells in effusions compared with primary tumors and solid metastases. | Expression not correlated with survival | |
| | | ↑ Expression in stromal cells of primary tumors than from solid metastases | Predictive value (predicts resistance to paclitaxel resistance) | |
| | Prostate cancer Cancer cells | ↑ Expression in malignant tumors compared to benign and normal tissues | ND | (Nelson 1999; Day 2002; Obiezu 2002; Xi 2004b; Dong 2005; Obiezu 2005; Veveris-Lowe 2005; Avgeris 2011) |
| | Oral squamous cell carcinoma | ↑ Expression in tumors | Unfavorable prognosis (↓ survival) | (Zhao 2010) |
| | Endometrial cancer | ↑ Expression in endometroid endometrial cancer than in hyperplasia or normal endometrium | The expression of KLK4 was significantly associated with tumor grade | (Zhang 2009) |
| | Breast cancer Stromal cells | ↑ Expression | Monitoring (↑ tumor grade) | (Mange 2008; Papachristopoulou 2009) |
| | | ↑ Expression in malignant compared to benign tumor | ND | |
| **KLK5** | Breast cancer Serum | ↓ Expression in malignant tumors compared to normal tissues | Diagnosis | (Yousef 2002d; Yousef 2003c; Yousef 2004d) |
| | | ↑ Levels in serum of cancer patients compared to normal | Unfavorable prognosis (↓ survival) | |
| | Lung cancer | ↑ Expression in squamous cell tumors compared to normal tissues | ND | (Planque 2005; Planque 2008b) |
| | | ↓ Expression in NSCLC compared to normal tissues | ND | |
| | Ovarian cancer Serum, Ascites | ↑ Expression in malignant tumors and cell lines compared to benign and normal tissues | Diagnosis | (Kim 2001; Diamandis 2003a; Dong 2003; Yousef 2003c; Yousef 2003d; Hibbs 2004; Dorn 2011) |
| | | ↑ Levels in serum and ascites fluid of cancer patients compared to normal | Unfavorable prognosis (↑ stage, ↑ tumor grade,↓ survival) | |
| | Prostate cancer | ↓ Expression in malignant tumors compared to normal tissues | Favorable prognosis (↓ tumor grade, ↓ Gleason score) | (Yousef 2002c) |
| | Renal cell carcinoma | ↓ Expression in malignant tumors compared to normal tissues | ND | (Petraki 2006a) |
| | Testicular cancer | ↓ Expression in malignant tumors compared to normal tissues | Favorable prognosis (↓ stage) | (Yousef 2002b) |
| | Urinary bladder carcinoma | ↑ Expression in tumors | ND | (Shinoda 2007) |
| | Oral squamous cell carcinoma | ↑ Expression | ND | (Jiang 2011) |

| KLK | Cancer | | | |
|---|---|---|---|---|
| | **Type** | **Expression** | **Clinical relevance** | **Reference** |
| **KLK6** | Brain cancer | ↓ Expression in malignant tumors compared to normal tissues | ND | (Yousef 2004b) |
| | Breast cancer | ↓ Expression in metastatic tumors, ↑ expression in primary tumors | ND | (Anisowicz 1996; Yousef 2004b; Yousef 2004e) |
| | | ↓ Expression in malignant tumors compared to normal tissues | | |
| | Colon cancer | ↑ Expression in malignant tumors compared to normal tissues | ND | (Yousef 2004a; Yousef 2004b; Kim 2011) |
| | | | ↓ survival ↑Dukes disease stage | |
| | Colorectal cancer | ↑ Expression in malignant tumors compared to normal tissues | Unfavorable prognosis (↑ stage, ↑ survival) | (Ogawa 2005) |
| | Esophageal cancer | ↑ Expression in malignant tumors compared to normal tissues | ND | (Yousef 2004b) |
| | Gastric cancer | ↑ Expression in malignant tumors and cell lines compared to normal tissues | Unfavorable prognosis (↓ survival) | (Yousef 2004a; Nagahara 2005) |
| | Ovarian cancer Cancer cells Serum | ↑ Expression in malignant tumors and tumors of low malignant potential compared to benign and normal tissues | Diagnosis | (Anisowicz 1996; Diamandis 2000a; Tanimoto 2001; Hoffman 2002; Diamandis 2003b; Welsh 2003; Yousef 2003d; Adib 2004; Hibbs 2004; Lu 2004; Ni 2004; Santin 2004b; Yousef 2004b; Gilks 2005; Rosen 2005; Shan 2007; White 2009) |
| | | ↑ Expression in low malignant potential serous tumors compared to serous carcinomas | Unfavorable prognosis (↑ stage, ↑ tumor grade, ↓ survival) | |
| | | ↑ Levels in serum of cancer patients compared to normal women and those with benign disease | Monitoring | |
| | | ↑Expression KLK13 mRNA in invasive cancers relative to normal ovaries | Unfavorable prognosis (↓recurrence-free survival ↓overall survival | |
| | Pancreatic cancer | ↑ Expression in malignant tumors compared to normal tissues | ND | (Yousef 2004a; Yousef 2004b; Ruckert 2008) |
| | | ↑ Expression in PDAC | Unfavorable prognosis (↓ survival) | |
| | Prostate cancer | ↓ Expression in malignant tumors compared to normal and benign tissues | ND | (Petraki 2003a) |
| | Renal cell cancer | ↓ Expression in malignant tumors compared to normal tissues | Unfavorable prognosis (↑ stage, ↓ survival) | (Petraki 2006a) |
| | | ↑ Expression in high malignant compared to low malignant tumors | | |
| | Salivary gland tumor | ↓ Expression in malignant tumors compared to normal tissues | ND | (Darling 2006) |

| KLK | Cancer | | | |
|---|---|---|---|---|
| | **Type** | **Expression** | **Clinical relevance** | **Reference** |
| **KLK6** | Uterine (Serous papillary) Serum | ↑ Expression in malignant tumors compared to normal tissues | ND | (Santin 2004b; Yousef 2004b; Santin 2005a) |
| | | ↑ Expression in uterine serous papillary tumors compared to endometriod carcinoma | | |
| | | ↑ Levels in serum of patients with uterine serous papillary tumors compared to those with endometroid carcinoma and normal women | | |
| | Lung cancer | ↑ Expression in tumor tissue | Prediction (↓survival) | (Heuzé-Vourc'h 2009) |
| **KLK7** | Breast cancer | ND | Unfavorable prognosis (↑ stage, ↓ survival) | (Talieri 2004; Holzscheiter 2006) |
| | | ↑ Expression | Favorable prognosis | |
| | Cervical cancer | ↑ Expression in tumors compared to normal tissues | Expression not correlated with survival | (Santin 2004a; Tian 2004) |
| | Lung cancer | ↓ Expression in adenocarcinomas compared to normal tissues | ND | (Planque 2005; Planque 2008b) |
| | | ↓ Expression in NSCLC compared to normal tissues | ND | |
| | Ovarian cancer | ↑ Expression in malignant tumors and cell lines compared to benign and normal tissues | Unfavorable prognosis (↑ tumor grade, ↓ survival) | (Tanimoto 1999; Dong 2003; Kyriakopoulou 2003; Yousef 2003d; Adib 2004; Hibbs 2004; Spentzos 2004; Gilks 2005; Shan 2006; Psyrri 2008) |
| | | ↑ Expression in low malignant potential serous tumors compared to serous carcinomas | Favorable prognosis | |
| | Brain cancer | ↑ Expression is associated with a more aggressive phenotype in brain cancer cells. | ND | (Prezas 2006b) |
| | Oral squamous cell carcinoma | ↑ Expression in tumors | Unfavorable prognosis (↓survival) | (Zhao 2010) |
| | Pancreatic cancer | ↑ Expression in tumors compared to normal | ND | (Johnson 2007) |
| | Colorectal cancer | ↑ Expression in cancerous than in normal tissues. | Unfavorable prognosis (↓survival) | (Talieri 2009b) |
| **KLK8** | Breast cancer | ↓ Expression in malignant tumor compared to normal tissues | | (Yousef 2004d) |
| | Cervical cancer | ↑ Expression in cancer cell lines and primary tumor cultures compared to normal tissues | ND | (Cane 2004) |
| | Colon cancer | ↑ Expression in malignant tumors compared to normal tissues | ND | (Yousef 2004a) |
| | Ovarian cancer Cancer cells, Serum Ascites | ↑ Expression in malignant tumors compared to benign and normal tissues | Diagnosis | (Underwood 1999; Magklara 2001; Kishi 2003; Yousef 2003d; Adib 2004; Hibbs 2004; Shigemasa 2004b; Borgono 2006; Kountourakis 2009) |
| | | ↑ Expression in low malignant potential serous tumors compared to serous carcinomas | Favorable prognosis (↓ stage, ↓ tumor grade,↑ survival) | |
| | | ↑ Levels in serum of cancer patients compared to normal | Monitoring | |
| | | ↑ Expression compared to normal | Favorable prognosis (↑survival) | |
| | | ND | ↓ Expression ↑survival | |

| KLK | Cancer | | | |
|---|---|---|---|---|
| | **Type** | **Expression** | **Clinical relevance** | **Reference** |
| **KLK8** | Lung cancer | ↓ Expression in NSCLC compared to normal tissues | ND | (Sher 2006; Planque 2008b; Planque 2010) |
| | | ↑ Expression of the *KLK8* gene and the amounts of the KLK8-T3 and KLK8-T4 mRNAs were significantly increased in lung tumor tissue | Unfavorable prognosis (↓ survival) Cox multivariate analysis indicated that the amount of KLK8-T4 mRNA was an independent prognostic factor for OS | |
| | | ↑ Expression | Favorable prognosis | |
| | Salivary gland tumors | ↑ Expression | ND | (Darling 2008) |
| **KLK9** | Breast cancer | ND | Favorable prognosis (↓ stage, ↑ survival) | (Yousef 2003f) |
| | Ovarian cancer | | Favorable prognosis (↓ stage, ↑ survival) | (Yousef 2001a) |
| **KLK10** | Acute lymphoblastic leukemia (ALL) | ↓ Expression (↑ methylation) in ALL cell lines compared to normal fresh bone marrow mononuclear cells | Unfavorable prognosis ↓ survival) | (Roman-Gomez 2004) |
| | Breast cancer | ↓ Expression in malignant tumors and cell lines compared to normal and benign tissues | Predictive value (predicts response to tamoxifen therapy) | (Liu 1996; Dhar 2001; Luo 2002; Sidiropoulos 2005; Yousef 2005; Kioulafa 2009) |
| | | ↑ Expression in subset of malignant cell lines | | |
| | | ↑ Expression ↑methylation in cancer compared to normal | Unfavorable prognosis Disease-free interval (DFI) and overall survival (OS) were significantly associated with methylation | |
| | Colon cancer | ↑ Expression in malignant tumors compared to normal tissues | ND | (Yousef 2004a; Yousef 2005) |
| | Colorectal cancer | ↑ Expression in malignant tumors compared to normal tissues | Unfavorable prognosis (↑ TNM, ↓ disease-free survival and ↓ overall survival) | (Feng 2006; Talieri 2011) |
| | | ↑ Expression in tumor than normal mucosa | Unfavorable prognosis (↑ stage) | |
| | Gastric cancer | ↑ Expression in malignant tumors and cell lines compared to normal tissues | ND | (Yousef 2005; Feng 2006; Li 2011) |
| | | ↑ Upregulation | ND | |
| | | ↑ Expression in tumor than normal mucosa | Unfavorable prognosis (↑ stage) | |
| | Lung cancer | ↑ Presence of splice variants in non-small-cell lung cancer | ND | (Planque 2006; Planque 2008b; Zhang 2010) |
| | | ↓ Expression in NSCLC compared to normal tissues | ND | |
| | | ↓ Expression in NSCLC as compared to non-cancer samples | ↑ Methylation was associated with advanced stage and lymph metastasis | |

| KLK | Cancer | | | |
|---|---|---|---|---|
| | **Type** | **Expression** | **Clinical relevance** | **Reference** |
| **KLK10** | Ovarian cancer | ↑ Expression in malignant tumors and cell lines compared to benign and normal tissues | Diagnosis | (Luo 2001a; Luo 2001b; Luo 2003a; Shvartsman 2003; Welsh 2003; Yousef 2003d; Adib 2004; Lu 2004; Santin 2004b; Gilks 2005; Rosen 2005; Sidiropoulos 2005; Yousef 2005; Batra 2010) |
| | | ↑ Expression in low malignant potential serous tumors compared to serous carcinomas | Unfavorable prognosis (↑ tumor grade, ↑ stage, ↓ survival) | |
| | | ↑ Levels in serum of cancer patients compared to normal women and those with benign disease | Monitoring | |
| | | ↑ Expression after steroid hormone treatment of ovarian cell lines showed | No effect | |
| | Pancreatic cancer | ↑ Expression in malignant tumors compared to benign and normal tissues | ND | (Iacobuzio-Donahue 2003; Yousef 2004a; Yousef 2005; Ruckert 2008) |
| | | ↑ Expression in PDAC | Unfavorable prognosis (↓survival | |
| | Prostate cancer | ↓ Expression in malignant tumors compared to normal and benign tissues | ND | (Goyal 1998; Petraki 2003a; Sidiropoulos 2005) |
| | | ↓ Expression in subset of malignant cell lines | | |
| | Renal cell carcinoma | ↓ Expression in malignant tumors compared to normal tissues | ND | (Petraki 2006a) |
| | | ↑ Expression in high malignant compared to low malignant tumors | | |
| | Squamous cell carcinoma: head and neck | ↑ Expression in ‘‘Group 1’’ tumor subtype | Unfavorable prognosis (↓ survival): worst outcome for ‘‘Group 1’’ tumor subtype compared to others | (Chung 2004) |
| | Testicular cancer | ↓ Expression in malignant tumors compared to normal tissues | ND | (Luo 2001c) |
| | Uterine (serous papillary) | ↑ Expression in malignant tumors compared to normal tissues | ND | (Santin 2005b) |
| | Hepatocellular carcinoma | ↓ Expression↑methylation in HCC ↑ Methylation associated with cirrhosis and HCV infection | ND | (Lu 2009) |
| **KLK11** | Lung cancer | ↑ Expression in a subgroup (cluster ‘‘C2) of neuroendocrine tumors | Unfavorable prognosis (↓ survival): worst outcome | (Bhattacharjee 2001; Planque 2006; Planque 2008b) |
| | | ↑ Presence of splice variants non-small-cell lung cancer | For ‘‘C2’’ tumor subtype compared to others | |
| | | ↑ Expression in NSCLC compared to normal tissues | Higher risk | |
| | Ovarian cancer | ↑ Expression in malignant tumors compared to benign and normal tissues | Diagnosis | (Diamandis 2002; Borgono 2003a; Yousef 2003d; Adib 2004; Diamandis 2004a; Shigemasa 2004a; Gilks 2005) |
| | | ↑ Expression in low malignant potential serous tumors compared to serous carcinomas | Favorable prognosis (↓ stage, " survival) | |
| | | ↑ Levels in serum of cancer patients compared to normal | Unfavorable prognosis (↑ stage,↓ survival) | |

| KLK | Cancer | | | |
|---|---|---|---|---|
| | **Type** | **Expression** | **Clinical relevance** | **Reference** |
| **KLK11** | Prostate cancer | ↑ Expression in malignant tumors compared to normal | Diagnosis | (Diamandis 2002; Nakamura 2003a; Nakamura 2003b; Stavropoulou 2005; Jamaspishvili 2011) |
| | | ↑ Levels in serum of cancer patients compared to normal | Favorable prognosis (↓ stage, ↓ tumor grade, ↓ Gleason score) | |
| | | ↓ Expression in prostate cancer cells compared to normal/benign prostate cells. ↓ Expression in CaP compared to BPH ↑ Expression in advanced tumors compared to localized ones | Diagnosis | |
| | Renal cell cancer | ↓ Expression in malignant tumors compared to normal tissues | Unfavorable prognosis (↑ stage) | (Petraki 2006a) |
| | Gastric cancer | ↓ Expression in gastric cancer compared with that in normal gastric mucosa Furthermore, ↓ Expression in poorly differentiated cancer samples than that in well-differentiated group | Unfavorable prognosis | (Wen 2011) |
| | Breast cancer | ↑Expression in histological grade I/II than in grade III breast cancers. | ND | (Sano 2007) |
| **KLK12** | Breast cancer | ↓ Expression in malignant tumors compared to normal tissues | ND | (Yousef 2000d) |
| | Lung cancer | ↓ Expression in NSCLC compared to normal tissues | Higher risk | (Planque 2008b) |
| **KLK13** | Breast cancer | ↓ Expression in malignant tumors and cell lines compared to normal tissues | Favorable prognosis (↑ survival) | (Yousef 2000a; Chang 2002) |
| | Ovarian cancer Ascites | ↑ Expression in malignant tumors compared to benign and normal tissues | Favorable prognosis (↓ stage, ↑ survival) | (Kapadia 2003; Adib 2004; Scorilas 2004; White 2009) |
| | | ↑ Expression KLK13 mRNA in invasive cancers relative to normal ovaries | Unfavorable prognosis (↓ recurrence-free survival ↓ overall survival | |
| | Prostate cancer | ↓ Expression in malignant tumors compared to normal and benign tissues | ND | (Kapadia 2003; Petraki 2003b) |
| | Lung cancer | Significant difference in malignant tissues compared to adjacent non-malignant tissues | mRNA overexpression in tumors (1/3 of the patients) was associated with a (+) nodal status and adenocarcinoma histotype (↓survival) | (Planque 2008a; Planque 2008b; Chou 2011) |
| | | ↑ Expression in NSCLC compared to normal tissues | Higher risk | |
| | | ↑ Expression in metastatic lung adenocarcinoma | ND | |
| | Gastric cancer | ↓ Expression in cancerous compared with their matching nonmalignant pairs (p=0.002) and in poorly differentiated gastric tumors (p=0.029) | Favorable prognosis (↑ survival, ↓ recurrence) | (Konstantoudakis 2010) |

| KLK | Cancer | | | |
|---|---|---|---|---|
| | **Type** | **Expression** | **Clinical relevance** | **Reference** |
| **KLK14** | Breast cancer | ↓ Expression in malignant tumors and cell lines compared to normal tissues | Diagnosis | (Yousef 2001b; Yousef 2002a; Borgono 2003b; Papachristopoulou 2011) |
| | Breast cancer | ↑ Levels in serum of cancer patients compared to normal | Unfavorable prognosis (↑ stage, ↓ survival) | |
| | | ↑ Expression in the malignant, compared to the benign tumor samples | Diagnosis (↑ tumor grade, ↑ tumor size) | |
| | Ovarian cancer | ↓ Expression in malignant tumors compared to normal tissues | Diagnosis | (Yousef 2001b; Borgono 2003b; Yousef 2003a; Yousef 2003d) |
| | | ↑ Expression in malignant tumors compared to benign and normal tissues | Favorable prognosis (↓ stage, ↑ survival) | |
| | | ↑ Levels in serum of cancer patients compared to normal | | |
| | Prostate cancer | ↑ Expression in malignant tumors compared to normal tissues | Unfavorable prognosis (↑ stage, ↑ tumor grade, ↑ Gleason score) | (Hooper 2001; Yousef 2003g; Borgono 2007; Rabien 2008) |
| | | ↑ Expression in malignant tumors compared to normal tissues | Unfavorable prognosis (↑tumor grade) | |
| | | ↑ Expression (Serum) in prostate cancer patients compared with healthy males. | ND | |
| | Testicular cancer | ↓ Expression in malignant tumors compared to normal tissues | ND | (Yousef 2001b) |
| | Colorectal cancer | No significant difference in expression between malignant and normal | Unfavorable prognosis (↓ survival) | (Talieri 2009a) |
| | Lung cancer | Significant difference in malignant tissues compared to adjacent non-malignant tissues | mRNA overexpression in tumors (1/3 of the patients) was associated with a (+) nodal status and tumor size | (Planque 2008a; Planque 2008b) |
| | | ↑ Expression in NSCLC compared to normal tissues | Higher risk | |
| | Salivary gland tumors | ↑ Expression in pleomorphic adenoma and adenoid cystic carcinoma than normal glands and mucoepidermoid carcinoma tissues. | ND | (Hashem 2010) |
| **KLK15** | Breast cancer | ND | Favorable prognosis (↑ survival) | (Yousef 2002e) |
| | Ovarian cancer | ↑ Expression in malignant tumors compared to benign tissues | Unfavorable prognosis (↓ survival) | (Yousef 2003e; Batra 2011) |
| | | aggressive phenotype due to SNP rs266851 | ↓ survival | |
| | Prostate cancer | | Unfavorable prognosis (↑ stage, ↑ tumor grade, ↑ Gleason score) | (Yousef 2001c; Stephan 2003; Mavridis 2010; Rabien 2011) |

### 1.3.1 KLKs under investigation in this study (KLK4-5-6-7)

KLK4, 5, 6, 7 were under closer investigation based on their tumorigenic potential in ovarian cancer, which was discovered and analyzed by Prezas et al. (Prezas 2006a). Gynecological cancers are a field of interest due to their high mortality and the lack of powerful prognostic tools.

All of the fifteen kallikrein-related peptidases show differential gene and/or protein expression patterns in a variety of normal tissues (Petraki 2006b; Shaw and Diamandis 2007) yet these peptidases are also expressed in various types of cancer tissues, with breast, ovarian, and prostate cancer being the most prominent ones studied (Borgono 2004). KLK4, 5, 6, 7 are not expressed in the normal ovary but are overexpressed in ovarian carcinoma tissues at the mRNA and/or protein level or both (Obiezu and Diamandis 2005; Paliouras and Diamandis 2006; Shan 2007; White 2009). KLK4 and KLK5 are indicators of poor prognostic outcome (Kim 2001; Obiezu 2001; Dorn 2011). Ovarian cancer patients show also express KLK6 protein in their tumor tissues which is associated with disease-free and overall survival (Diamandis 2000a; Tanimoto 2001; Hoffman 2002; Diamandis 2003b). Like KLK4, 5, and 6, KLK7 is expressed in ovarian tumor tissues. Elevated KLK7 expression in ovarian cancer tissue is associated with poorer prognosis of ovarian cancer patients, especially those with lower grade disease and those who have been optimally debulked (Kyriakopoulou 2003).

Less than for ovarian cancer regarding the expression and clinical impact of kallikrein-related peptidases is known for incidence and clinical value in breast cancer. KLK4 protein is expressed in normal breast ductal epithelium and in cancer tumor tissue (Davidson 2007), with the latter to demonstrate higher levels compared to the normal status (Mange 2008; Papachristopoulou 2009). KLK5 is expressed in normal breast ductal epithelium but is decreased in breast cancer tissue. KLK5 is a prognostic factor in patients with large tumors and tumor-bearing lymph nodes, indicating unfavorable prognosis (Yousef 2003c; Yousef 2004c; Yousef 2004e). KLK6 is also expressed in the normal breast ductal epithelium and decreased in breast cancer tissue. (Yousef 2004e; Obiezu and Diamandis 2005). Like KLK5 and KLK6, KLK7 is expressed in normal ductal epithelium of the breast but downregulated in breast cancer tissues. Within breast cancer, high KLK7 expression is associated with good prognosis (Yousef 2000d; Talieri 2004; Holzscheiter 2006). In addition to PSA (KLK3) (Rittenhouse

1998; de Koning 2002), a prostate tumor-screening marker, other kallikrein-related peptidases are expressed in the normal and cancer-afflicted prostate, including KLK4-7.

KLK4 protein is significantly overexpressed in malignant prostate compared with the normal prostate. Interestingly, two major isoforms of KLK4 were detected of which $KLK4_{254}$ is cytoplasmically localized, while $KLK4_{205}$ is in the nucleus of prostate cancer cells (Xi 2004a; Xi 2004b; Dong 2005; Klokk 2007; Avgeris 2011). Other than KLK4, expression of KLK5, and a KLK5 variant (KLK5-SV1), is significantly lower in prostate cancer tissue compared to their normal counterparts (Yousef 2002c; Kurlender 2004). KLK6 is also expressed by normal prostatic epithelium, benign prostate; and prostatic intraepithelial neoplasia, but expression of KLK6 is decreased in neoplasia. Expression of KLK6 does not correlate with aggressiveness or prostate cancer prognosis. KLK7 is expressed moderately at the mRNA level in the normal prostate but was not detected at the protein level (Shaw and Diamandis 2007). Reports regarding clinical impact of KLK7 in prostate cancer are not available, yet.

Expression of KLK4 has also been reported for mesothelioma, oral squamous cell carcinoma and endometrial cancer (Zhang 2009; Zhao 2011); for KLK5 reports have been issued for endometrium cancer, testicular cancer, kidney cancer, lung cancer, salivary gland cancer, and brain tumor (**Table 2**). Expression of KLK6 and clinical implications has been described for endometrium cancer, urothelial and kidney cancer, colon, gastric, and pancreatic cancer, salivary gland cancer, and brain tumor (**Table 2**). KLK7 is also expressed in cancer tissues of the cervix uteri, pancreas, and lung, in brain tumor tissues, and in melanoma (**Table 2**).

KLK5 is elevated in 69 % of ovarian cancer patient serum samples compared to almost undetectable serum levels of normal individuals or patients suffering from other malignancies (Yousef 2003c). KLK5 can also be detected in ascitic fluid of ovarian cancer patients (Yousef 2003c) and in the specimens: analysis of ovarian tumor tissue extracts has indicated that KLK5 is elevated in cancerous compared to normal or benign ovarian tissue cytosols (Yousef 2003c), also compared to tumors with low malignant potential (LMP) (Diamandis 2003a). KLK5 overexpression in ovarian cancer patients, defined by exceeding the optimized cut-off value, predicts poor outcome and is associated with more aggressive forms of ovarian cancer (Diamandis 2003a).

KLK6, like KLK5, is significantly elevated in malignant tumor serum samples compared to normal or benign ovarian tumor serum samples (higher levels associated with unfavorable prognosis)(Shan 2007). Pre-surgical serum KLK6 levels increase the diagnostic sensitivity of CA125 in patients with early stage (I/II) ovarian cancer and predict overall and progression-free survival (Diamandis 2003b). Analysis of KLK6 in tumor cytosols using ELISA indicates that KLK6-positive tumors are more likely attached to advanced disease, serous histology, and suboptimal debulking. KLK6 has a prognostic impact on overall survival and progression-free survival, especially in subgroups with a favorable prognosis at first sight, e.g. optimally debulked and low-grade tumors.

### 1.3.2 KLK7

Purification and preliminary characterization of kallikrein-related peptidase 7 (KLK7) had been initially performed by Egelrud et al.(Egelrud 1993a), followed by cloning and expression of the recombinant protein (Hansson 1994). Precise mapping of KLK7 has indicated that it is located at chromosomal locus 19q13. 3- q13.4 between KLK6 and KLK8 (Yousef 2000d). Later on, antibodies to KLK7 epitopes were generated to formulate an immunofluorometric assay (ELISA) for the quantification of KLK7 in tissue extracts and biological fluids (Kishi 2004). KLK7 displayed an elevated expression at healthy state in esophagus, heart, liver and skin (Shaw and Diamandis 2007). KLK7 belongs to the family of serine endoproteinases specific for amino acid residues with aromatic side chains in the P1 position (Skytt 1995). The resolved KLK7 structure revealed unique features (short 70-80 loop and the unique S1 pocket, which prefers P1 Tyr residues) as well as large positively charged surface patches, representing putative exosites for prime side substrate recognition (Debela 2007), which match a diverse set of sequences (substrates) that they could recognize (Fernandez 2007).

KLK7 is known to be inhibited by a serpin as all kallikrein-related peptidases are. Kallistatin, a member of the serpin family, exhibited fast inhibition when incubated with KLK7 (Luo and Jiang 2006). Antileukoprotease, a secretory leukocyte protease inhibitor produced by human keratinocytes, inhibits sufficiently KLK7 (Franzke 1996). But the well-studied KLK7 inhibitor is LEKTI, a skin development protein encoded by the gene SPINK5 (Schechter 2005). LEKTI fragments show specific inhibition of KLK7 (Egelrud 2005; Deraison 2007) and it is hypothesized that in normal skin the lamellar granule system transports and secretes LEKTI

earlier than KLK7 preventing premature loss of stratum corneum integrity (Ishida-Yamamoto 2005). Absence or lack of LEKTI is responsible for a severe skin disease, the Netherton syndrome, as protease activity such as KLK5 or KLK7 cannot be anymore regulated (Komatsu 2002). In Netherton syndrome patients, desmoglein 1 (DSG1) and desmocollin 1 (DSC1) were dramatically reduced in the upper most living layers of the epidermis and these defects were associated with premature degradation of corneodesmosomes (Descargues 2006). In parallel, KLK5 and KLK7 activities were increased at a magnitude that correlated with the barrier effect and clinical severity (Hachem 2006). In another skin disease, atopic dermatitis, excessive proteolytic activity is also observed, mainly of KLK7 (Komatsu 2007a). An extra gene sequence in the KLK7 gene might also be responsible for the protease hyperactivity in some cases (Vasilopoulos 2004). In psoriasis (Ekholm and Egelrud 1999; Komatsu 2007b) as well as in other skin diseases like peeling skin syndrome (Komatsu 2006) and chronic dermatitis (Hansson 2002), elevated chymotryptic activity is observed.

KLK7, initially described as human stratum corneum chymotryptic enzyme, was first identified in human skin extracts (Lundstrom and Egelrud 1991) and is supposed to be involved in the process of skin desquamation (Sondell 1995; Caubet 2004). KLK7 is predominantly produced in the esophagus and kidney (Shaw and Diamandis 2007) but is upregulated in tumor tissues of patients afflicted with cancer of the kidney (Gabril 2010), cervix (Termini 2010), colon (Talieri 2009b), or ovary (Dorn 2006; Shan 2006; Dorn 2007; Psyrri 2008) while downregulated in breast cancer (Holzscheiter 2006), prostate cancer (Xuan 2008), and melanoma (Winnepenninckx 2006).

KLK7 is suggested to play a role in pancreatic cancer, through its high expression translated into reduction of cell adhesion components DSG1 and DSG2 (Ramani 2008), diminishment of cell adhesion to vitronectin and enhancement of uPAR shedding (Ramani and Haun 2008a). It is also known that fibronectin, main component of the pancreatic extracellular matrix, can be cleaved in physiological conditions by KLK7. This also implies a potential tumorigenic role for KLK7 (Ramani and Haun 2008b). In lung cancer, KLK7 is aberrantly expressed in certain subtypes, highly in the squamous cell and small cell carcinoma, whereas low in the adenocarcinoma (Planque 2005; Singh 2008). In oral squamous cell carcinoma, KLK7 is highly expressed together with KLK4, 5, 8 and 10 (Pettus 2009; Zhao 2011). In prostate cancer, KLK7 and its potential inhibitor display decreased expression both at the mRNA and protein level, in

comparison with the healthy state (Xuan 2008). In colorectal as well as brain cancer, overexpression observed at the malignant state is associated with shorter disease-free (Talieri 2009b) and overall survival (Prezas 2006b). In breast cancer, there is a controversy. Some researchers state that elevated KLK7 expression in the malignant state is correlated with better patient outcome (Holzscheiter 2006), others support that it is correlated with shorter disease-free and overall survival (Talieri 2004). Li at al., however, suggest that low KLK7 expression is correlated with postmenauposal status and positive estrogen receptor status (Li 2009). In cervical cancer, KLK7 is highly expressed in the malignant state in comparison with the healthy one (Santin 2004a; Tian 2004).

There is a plethora of reports on KLK7 overexpression in ovarian cancer. KLK7 expression in normal and cancerous tissues has been determined by assessing mRNA expression levels by microarray analysis (Winnepenninckx 2006) or RT-PCR (Kyriakopoulou 2003; Holzscheiter 2006), and by quantifying KLK7 protein expression levels by immunoenzymometric assays (ELISA) (Dorn 2006; Shan 2006) or immunohistochemical techniques (Psyrri 2008; Gabril 2010). Both at the protein and at the mRNA level (Tanimoto 1999), there are reports that KLK7 is upregulated in the malignant state, sometimes in co-expression with other kallikrein-related peptidase, like KLK5, KLK6, KLK8, KLK10, and KLK14 (Yousef 2003d). KLK7 undergoes differential splicing in ovarian cancer (Prezas 2006a; Dong 2008) and it displays tumor-associated overexpression according to animal experiments performed by Prezas et al (Prezas 2006a). KLK7, additionally, is associated to unfavorable patient outcome (Shan 2006; Psyrri 2008), especially related to lower grade and optimal debulking surgery (Kyriakopoulou 2003).

### 1.4 uPA/PAI-1

The plasminogen activation system comprises three major constituents: serine proteases, inhibitors to these serine proteases and a cell-surface receptor specific for one of the serine proteases, urokinase-type plasminogen activator (uPA). Pro-uPA is produced and secreted by endothelial cells, muscle cells, specific types of leukocytes, fibroblasts, granulosa cells in the follicles, several epithelial-like cell types including proximal and distal kidney tubule cells and bladder urothelium cells, trophoblast cells, migrating keratinocytes and cancer cells (Mengele 2010). uPA content, released into the bloodstream is low but in case of malignant processes, uPA expression and secretion are often increased (Schmitt 1997). uPA, may activate the protein

plasminogen into its proteolytically active form, the serine protease plasmin (Dano 1985; Schmitt 1992; Rijken 1995; Schmitt 1997), but other substrates are also known, such as $a_6$-integrin, fibronectin, fibrinogen, uPAR and uPA itself. Plasmin cleaves fibrin and other constituents of the ECM (fibrinolysis). uPA influences cell signaling cascades, such as matrix metalloproteinase (MMP) activation, directly or by plasmin (Zhao 2008) and can therefore affect cell adherence, cell migration, cell growth and cell survival.

The proteolytic activity of the protease activation system is regulated by inhibitors, such as plasminogen activator inhibitor type-1 (PAI-1) (van Mourik 1984), targeting uPA. Several other proteases may target PAI-1 by cleavage at different positions, e.g. MMP-3 (amino acids 337 and 341)(Lijnen 2002). PAI-1 is secreted by platelets, endothelial cells, stromal cells, monocytes, smooth muscle cells, trophoblasts, adipocytes, hepatocytes, myofibroblasts and cancer cells. Moderate levels of PAI-1 were reported in the liver, pancreas, thyroid gland, lung, skin, nerve cells and connective tissue, with higher levels in the placenta and bone marrow (Mengele 2010). PAI-1 expression can rise locally in tumor tissue. PAI-1 is involved in blood coagulation, angiogenesis, wound healing, tissue remodeling, cell attachment, cell detachment, cell migration and tumor-cell invasion (Czekay 2003; Lijnen 2005; Takahashi 2005; Milliat 2008; Vial and McKeown-Longo 2008; Angenete 2009).

The interaction among plasminogen activator system (uPA, PAI-1) and kallikrein-related peptidases has been a well-known hypothesis over the past decade, mainly due to the proteolytic cascade theory (Yousef and Diamandis 2002). Since uPA and kallikrein-related peptidases belong to the serine-protease family and in some cases co-reside in normal or malignant tissues, many scientists examined this theory. PSA (KLK3) as well as KLK2 were found to activate the single chain preform of uPA (scuPA) (Yoshida 1995; Mikolajczyk 1999), while KLK4 is suggested to cleave uPAR (uPA receptor) and activate pro-uPA (Takayama 2001; Beaufort 2006).

uPA is present in normal and malignant tissues, e.g. ovarian cancer tissues (Astedt and Holmberg 1976) and in plasma (Tissot 1982; Wun 1982). Additionally, elevated uPA concentrations in tumor tissues compared with normal ones have been reported (Wu 1977; Svanberg and Astedt 1979; Corasanti 1980; Markus 1980). Clinical findings have demonstrated that elevated tumor antigen levels of uPA and/or PAI-1 are conductive to tumor cell spread and

metastasis and are associated with poor disease outcome in a variety of solid tumors, like in cancer of the breast, ovary, lung, prostate, stomach, pancreas, cervix, and colon (Andreasen 1986; Oka 1991; Kobayashi 1994; Nekarda 1994; Pedersen 1994a; Pedersen 1994b; Wang 1994; Schmitt 1997; Skelly 1997; Herszenyi 1999; Duffy 2002; Horn 2002; Kaneko 2003). The uPA and PAI-1 assessment in cancer tumors is a routine practice and it is performed by means of ELISA on fresh or fresh-frozen tissue. This requirement is always a drawback in terms of practicability. Immunohistochemistry is candidate alternative, since it performed on formalin-fixed paraffin-embedded (FFPE) tissue specimens, easy to archive and assess. Immunohistochemical analysis, however, is difficult in this case, due to the co-localization of uPA and PAI-1 in tumor cells and surrounding stroma cells and their internalization by cells or their release into the tissue or ECM (Schmitt 2008; Schmitt 2010).

In the literature, a comparative study of uPA values for breast cancer, obtained by ELISA and by immunohistochemical score, noted a statistically significant increase in the uPA values by ELISA with increasing uPA staining intensity by immunohistochemistry (Jänicke 1990). Similar work on PAI-1 was published later (Reilly 1992) and in the following years numerous publications employing various antibodies to uPA and PAI-1 by immunohistochemistry were distributed, with the only target to establish an alternative to ELISA method for worldwide quantification of these cancer biomarkers in breast cancer specimens (Schmitt 2008).

Due to the large number of assessment efforts of uPA and PAI-1 in the literature, it was essential to begin with appropriate tools. In our hands, within the frame of collaboration with American Diagnostica Inc., a number of antibodies directed to uPA and to PAI-1 were employed for immunohistochemical assessment of the respective molecules. Ultimate goal was to achieve a Standard Operating Procedure (S.O.P.) as a basis for immunohistochemical assessment.

## 1.5 Epigenetics

Epigenetic mechanisms are essential for normal development and maintenance of tissue-specific gene expression patterns in mammals. Disruption of epigenetic processes can lead to altered gene function and malignant cellular transformation. Methylation of cytosine bases in DNA provides a layer of epigenetic control in many eukaryotes that has important implications for normal state and disease (Watanabe and Maekawa 2010). Cancer research possesses a

major share of this attention to DNA methylation. Epigenetic research and discovery of methylation markers has been boosted by new and improved high throughput technology that has improved the efficacy and enabled the rapid progress of biomarker evaluation and validation. (Ballestar 2011; Khandige 2011)**.** Furthermore, several epigenetic drugs that have proved to prolong survival and to be less toxic than conventional chemotherapy were recently approved by the FDA for cancer treatment, e.g. Decitabine (5-aza-dC) (Boumber and Issa 2011).

To study epigenetic regulation in cancer, it is essential to obtain information about Alu elements and LINE-1 sequences. Total methylation content of Alu elements and LINE-1 sequences is highly correlated with global DNA methylation content (Ehrlich 2002). Estimation of total methylation content of Alu elements is useful for evaluation of the global genomic methylation status and level of homologous and non-homologous chromatin recombination in gene-rich regions.

Methylation of CpG islands of genes causes epigenetic changes in chromatin structure without altering DNA sequence to regulate transcription of these genes. This epigenetic regulation of gene expression plays an important role in the process of tumor invasion, growth and metastasis in malignancies (Pakneshan 2005). Urokinase type plasminogen activator (uPA), plus its inhibitor PAI-1, are associated with invasive and metastatic potential of malignancies. Added to this, novel serine proteases potentially playing a physiological role in these processes, such as KLK7, might be implicated in interactions with uPA. DNA methylation might be the regulatory mechanism of the uPA/PAI-1 system expression.

It is already known in the literature, that demethylating drugs, such as Decitabine (Christman 2002), affect the expression of uPA in breast cancer cell lines by altering the methylation status of CpG island (Xing and Rabbani 1996; Rabbani and Xing 1998; Xing and Rabbani 1999; Guo 2002). Employing an established commercial uPA/PAI-1 methylation system (Hs_PLAU_1_SG QuantiTect Primer Assay (200), #QT00013426, Qiagen, Hilden, Germany), we set several tumor cell lines under investigation, including KLK7 overexpressing cells to check whether there is any correlation between uPA and KLK7 expression.

## 1.6 Triple negative breast cancer patients (TNBC) and *BRCA1*

In search of new target biomarkers, it was recently discovered that triple negative breast cancer (TNBC), a subgroup of breast cancer (15 %), is characterized by loss of estrogen and progesterone receptor (ER, PR) and diminished expression of human epidermal growth factor receptor-2 (HER2) (Kang 2008; Reis-Filho and Tutt 2008). TNBC is associated with reduced disease-free and overall survival rates compared to other subtypes and constitutes the leading cause of 25 % of all death cases related to breast cancer (Kang 2008; Chacon and Costanzo 2010). Finally, more than 60 % of breast cancer patients with an inherited *BRCA1* germ line mutation are diagnosed for basal-like TNBC. The DNA repair gene *BRCA1* might be alternatively downregulated in TNBC by epigenetic mechanisms (Esteller 2000; Turner 2007; Toyama 2008) and/or loss of heterozygosity (Wei 2005; Rhiem 2010).

BRCA status identification could be essential for personalized treatment decision, as failure of BRCA1-mediated DNA-double-strand-break repair sensitizes the respective tumors to DNA-damaging agents (Kennedy 2004; Byrski 2009) to the newly developed Poly(ADP-ribose)Polymerase (PARP) inhibitors (Fong 2009; Tuma 2009; O'Shaughnessy 2011)

## 2. Aim of the study

The strong prognostic value of tumor tissue expression of proteases such as the kallikrein-related peptidases (KLKs) and the urokinase-type plasminogen activator (uPA) and its inhibitor PAI-1 in predicting poor outcome in patients afflicted with cancer of the ovary or breast is well established and is gaining attention as a diagnostic tool to refine clinical management in terms of choice of the right drug for the right patient. Previous work demonstrated the strong clinical value of determination of certain KLKs or uPA/PAI-1 in tumor tissue extracts by enzymoimmunometric assays (ELISA); evaluation of the clinical utility of these markers by immunohistochemistry was lacking. Likewise, epigenetic tests for these biomarkers have not been established yet for clinical utility, regarding breast or ovarian cancer.

Since there have been no definitive protocols available for identification of KLKs by use of antibodies, no standard-operating-procedures for the quantitative assessment of these markers by immunohistochemistry and no data on the clinical utility of epigenetic testing of these biomarkers, aims and objectives of the thesis were: 1) Production, testing, and set-up of standard operating procedures for immunohistochemical localization and quantification of KLK-proteases and the protease uPA (urokinase) and its inhibitor PAI-1. 2) Validation of the clinical relevance of KLK7 protein expression to predict outcome in advanced ovarian cancer patients. 3) Exploration of the DNA-methylation status of KLKs, uPA/PAI-1 and the caretaker gene BRCA1.

Tissue specimens and clinical data were provided by the Dept. Obstetrics and Gynecology and the biobank of the Klinikum rechts der Isar, Technical University of Munich, Germany; histological evaluation was performed in collaboration with the Institute of Pathology of the Technical University of Munich.

# 3. Materials and methods

## 3.1. Reagents and materials

| **Immunohistochemistry, immunocytochemistry** | |
|---|---|
| Acetone | In-house acetone provided by Department of Pathology, Technical University of Munich |
| AEC | #K3464, Dako, Glostrup, Denmark |
| Antibody diluent | #S2022, Dako, Glostrup, Denmark |
| AP Enzyme (ENHANCER) | #K5355 kit, Dako, Glostrup, Denmark |
| APAAP complex | #D0652, Dako, Glostrup, Denmark |
| Bovine Serum Albumin (BSA) | #A-3912, Sigma, St. Louis, USA |
| Citrate buffer | 1 L $H_2O_{dist}$; 2.1 g citric acid monohydrate (C1909 Sigma, St. Louis, USA), adjusted by sodium hydroxide (1.09136 Merck, Darmstadt, Germany) at pH 6 |
| DAB chromogen | #K5001 kit, Dako, Glostrup, Denmark |
| Dako wash buffer | #S3006 (containing 0.05 % Tween 20), 10 x concentrated, Dako, Glostrup, Denmark solution for use: 900 mL $H_2O_{dist}$ to 100 mL concentrate |
| Dual Endogenous Enzyme Block | #S2003, Dako, Glostrup, Denmark |
| EnVision system kit | #K4065, Dako, Glostrup, Denmark |
| Eosin | #45380, Roth, Karlsruhe, Germany |
| Ethanol | In-house ethanol provided by Department of Pathology, Technical University of Munich |
| Fast red | #K5000 kit, Dako, Glostrup, Denmark |
| Fast red substrate (tablets) | #F-0775 (Fast Red TR/Naphthol/AS-MX |
| Phosphate Tablets | #T-9043 (Tris Buffer Tablets), Sigma FastTM Fast Red, Sigma-Aldrich, St. Louis, USA |
| Formalin (aqueous solution of formaldehyde) | in-house formalin provided by Department of Pathology, Technical University of Munich |
| Fuchsin chromogen | #K0625, Dako, Glostrup, Denmark |
| Glycerol gelatin | #1.09242, Kaiser´s glycerol gelatin, Merck, Darmstadt, Germany |
| Hematoxylin | Mayer´s acid hematoxylin |
| Human serum | In-house human serum provided by Department of Pathology, Technical University of Munich |
| Hydrogen peroxide 3 % | 45 mL $H_2O_{dist}$, 5 mL 30 % $H_2O_2$ (1.07210, Merck, Darmstadt, Germany) |
| Isopropanol | In-house isopropanol provided by Department of Pathology, Technical University of Munich |
| Levamisole | #L9756, levamisole 1mM (12 mg/50 mL), Sigma Aldrich, St. Louis, USA |
| LSAB AEC kit | #K5001, Dako, Glostrup, Denmark |
| LSAB DAB kit | #K5003, Dako, Glostrup, Denmark |
| Paraffin | In-house paraffin provided by Department of Pathology, Technical University of Munich |
| Paraformaldehyde (PFA) | 1 % (PFA 1%) 200 mL PBS 0.1 M, 2.0 g PFA (1.04005, Merck, Darmstadt, Germany) 2 N sodium hydroxide adjusted by phosphoric acid (No. 9079, Roth, Karlsruhe, Germany) at pH 7.4 |
| PBS/1 % BSA | 20 ml PBS 0.1M, 0.2 g BSA |
| Permanent red | #K5355 kit, Dako, Glostrup, Denmark |
| Pertex (mounting medium) | Medite, Burgdorf, Germany |
| Phosphate buffered saline (PBS) | 80 g sodium chloride, 2.0 g dipotassium phosphate, 11.4 g disodium phosphate, 2.0 g potassium chloride |
| Rabbit/Mouse (LINK) | #K5355 kit, Dako, Glostrup, Denmark |

| | |
|---|---|
| Saponin | 200 mL PBS 0.1 M, 2.0 g BSA, 0.05 g saponin (S-2149, Sigma, St. Louis, USA) |
| Tris buffered saline (TBS) | 60.5 g Trizma Base (T-1503, Sigma, St. Louis, USA), 1 L $H_2O_{dist,}$ 2 N hydrogen chloride, 90 g sodium chloride (1.06404, Merck, Darmstadt, Germany). Adjust at pH 7.6 solution for use: 900 mL $H_2O_{dist}$ to100 mL stock solution |
| Streptavidin/Biotin Blocking Kit | #SP-2002, Vector Labs, BIOZOL DIAGNOSTICA VERTRIEB GMBH, Eching, Germany |
| Xylene | In-house xylene provided by Department of Pathology, Technical University of Munich |
| Centrifuge | Sigma 4K15 refrigerated table top centrifuge, Sigma, Munich, Germany |
| Coverslips | R. Langenbrinck, Teningen, Germany |
| Cytospin centrifuge | Shandon 2 centrifuge, Thermo Fisher Scientific Inc., Waltham, USA |
| Cytospin chamber filter cards | #5991022, Shandon filter cards, Thermo Fisher Scientific Inc., Waltham, USA |
| Cytospin plastic sample chamber | Thermo Fisher Scientific Inc., Waltham, USA |
| Cytospin stainless steel clip | Thermo Fisher Scientific Inc., Waltham, USA |
| Digital camera | Canon PowerShot A640, 10 Mega Pixel, Canon Inc., Tokyo, Japan |
| Light microscope | Axioskop, Carl Zeiss, Jena, Germany |
| Manual tissue microarray instrument | Alpha Metrix Biotech GmbH, Rödermark, Germany |
| Microscope slides | SuperFrost Plus, # 03-0060, R. Langenbrinck, Teningen, Germany |
| Microscope software | AxioVision Rel.4.6.3 (04-2007), Carl Zeiss, Jena, Germany |
| Microtome (electronic, rotary) | Microm HM 335E, Microm GmbH, Walldorf, Germany |
| Pressure cooker | Ankoch-Automatik, WMF, Geislingen/ Steige, Germany |
| Scanning software | NanoZoomer Virtual Microscopy, Hamamatsu Photonics, Hamamatsu, Japan |
| **Cell culture** | |
| DMEM Dulbecco´s modified Eagles medium | Gibco, Darmstadt, Germany |
| Accutase | #L11-007, PAA Laboratories, Pasching, Austria |
| FCS (Fetal Calf Serum) | |
| HEPES (4-(2-hydroxyethyl)-1-piperazineethanesulfonic acid) | #15630-080, Gibco, Invitrogen, Darmstadt, Germany |
| Geneticin (G418) | #10131-019, Gibco, Invitrogen, Darmstadt, Germany |
| Gentamycin | #15750-037, Gibco, Invitrogen, Darmstadt, Germany |
| PBS (*phosphate buffered solution*) | #10010-015**,** Gibco, Invitrogen, Carlsbad, CA, USA |
| Arginine, Asparagine | #A8094, #A7094, Sigma, Munich, Germany |
| Triton X-100 | #9002-93-1, Sigma, Munich, Germany |
| EDTA (Ethylenediaminetetraacetic acid) | #L2113, Biochrom AG, Berlin, Germany |
| Decitabine | #A3656, Sigma, Munich, Germany |
| Trypan Blue | #T-8154, Sigma, Munich, Germany |
| Erythrocyte lysis buffer | 8.29 g $NH_4Cl$/ 1.0 g $Na_2CO_3$/ 0.038 g EDTA (Triplex III) Dissolve EDTA in 500 mL $H_2O_{dist}$. Adjust pH by means of 2 N NaOH to pH 8 at 50 °C. $NH_4Cl$ and $Na_2CO_3$ are added and the solution is left to cool down (RT). The pH value is adjusted to pH 7.2 by means of 2 N NaOH. The solution is adjusted with $H_2O_{dist}$ up to 1 L and then autoclaved immediately. |
| Laminar flow cabinet | Hera Safe, Heraeus, Hanau, Germany |
| Incubator | Heraeus Function Line Serie 7000 |
| $CO_2$-Incubator | HERA Cell, Kendro, Langenselbold, Germany |
| **Protein determination, SDS-Gel electrophoresis, Western Blot-Analysis** | |
| Acrylamide/Bisacrylamide (29:1) | Roth, Karlsruhe, Germany |
| Ammoniumpersulfate (APS) | Amresco, Solon, USA |
| Tween-20 | #P2287, Fluka, Sigma, Munich, Germany |

| | |
|---|---|
| BSA | #A-3912, Sigma, Munich, Germany |
| Ponceau S Staining Solution | Sigma-Aldrich, St. Louis, MO, USA |
| ECL Western Blotting Detection Reagent | #RPN2106, Amersham Biosciences; Little Chalfont, UK |
| CL-XPosure Film | #28-9068-35, Hyperfilm 5 x 7 inches (Amersham Biosciences, Uppsala, Sweden) |
| BCA Protein Assay Kit | #23221, Pierce, Rockford, IL, USA |
| peqGOLD Agarose | #35-1010, PEQLAB Biotechlology GmbH, Erlangen, Germany |
| peqGOLD 100 bp-DNA-Marker | #25-2010, PEQLAB Biotechlology GmbH, Erlangen, Germany |
| PVDF membrane | #66547, PALL; Dreieich, Germany |
| SDS | #2326.1, Carl Roth, Karlsruhe, Germany |
| Bromophenol blue | #1117460005, Merck Chemicals, Darmstadt, Germany |
| β-mercaptoethanol | #444203, Merck Chemicals, Darmstadt, Germany |
| Glycerin | #G5516-100ML, Sigma, Munich, Germany |
| Acetic acid | #695092, Sigma, Munich, Germany |
| Ethanol | In-house |
| DMSO | #317275, Merck Chemicals, Darmstadt, Germany |
| TEMED | #A1148,0100, Applichem, Omnilab, Munich, Germany |
| Ethidium bromide | #E1510, Sigma, Munich, Germany |
| Protease inhibitors (complete, mini EDTA-free) | #11836170001, Roche, Penzberg, Germany |
| Coomassie blue | #27813, Sigma, Munich, Germany |
| Skimmed milk | #70166, Fluka, Sigma, Munich, Germany |
| Whatman blotting paper | #3030672; Biometra, Goettingen, Germany |
| 10 x PBS (phosphate buffered saline) buffer (pH 7.4) | 81.8 g NaCl, 1.99 g KCl , 2.39 g $KH_2PO_4$, 14.4 g $Na_2HPO_4$ (in 1 L $H_2O_{dist}$) |
| 10 x Electrophoresis buffer | 30 g Tris Base (0.25 M), 10 g SDS (1 %), 144 g Glycine (192 mM) (in 1 L $H_2O_{dist}$) |
| Anode blotting buffer (20 %) | 100 mL boric acid buffer 5 x, 100 mL EtOH (in 500 mL $H_2O_{dist}$) |
| Cathode blotting buffer (5 %) | 100 mL boric acid buffer 5 x, 25 mL EtOH (in 500 mL $H_2O_{dist}$) |
| 5 x Boric acid buffer | 7.73 g boric acid in 500 mL $H_2O_{dist}$ (pH 8.5) |
| 50 x TAE buffer | 2 M Tris-HCl (pH 7.9), 0.5 M Sodium acetate, 2 mM EDTA |
| 10 x TBS (Tris buffered saline) buffer (pH 7.6) | 60.5 g Trizma base, 90 g NaCl (in 1 L $H_2O_{dist}$) |
| DNA loading buffer 6 x | 0.1 M EDTA; 50 % w/v Saccharose; 0.1 % w/v Bromophenol blue and 0.1 % v/v Xylenecyanol FF in $H_2O_{dist}$, pH 8.0 |
| Protein sample buffer 3 x | 2 % (w/v) SDS and 5 % (v/v) β-mercaptoethanol |
| Film Developer | Cawomat 2000IR, Cawo, Schrobenhausen, Germany |
| Thermomixer 5436, centrifuge 5417C | Eppendorf, Hamburg, Germany |
| Electrophoresis device | Blue Power 500, 3000, SERVA Electrophoresis GmbH, Heidelberg, Germany |
| **MACS** | |
| FcR blocking reagent | #130-059-901; Miltenyi Biotec, Bergisch Gladbach, Germany |
| VarioMACS Separation Unit | #130-090-282, Miltenyi Biotec, Bergisch Gladbach, Germany |
| Pre-separation filter | #130-041-047, Miltenyi Biotec, Bergisch Gladbach, Germany |
| LS Columns | #130-042-401, Miltenyi Biotec, Bergisch Gladbach, Germany |
| CD326 (EpCAM)-FITC, human | #130-080-301, Miltenyi Biotec, Bergisch Gladbach, Germany |
| CD326 (EpCAM) MicroBeads, human | #130-061-101, Miltenyi Biotec, Bergisch Gladbach, Germany |
| **Cytofluorometry** | |
| FACS Flow Sheath Fluid | BD Biosciences, Franklin Lakes, NJ, USA |
| Polystyrol-tubes (round bottom, 5 mL) | BD Biosciences, Franklin Lakes, NJ, USA |
| Polystyrol-tubes (conical bottom, 4.5 mL) | Greiner Bio-One, Frickenhausen, Germany |
| FACSCalibur Sort Cytofluorometer with CellQuest software | BD Biosciences, Franklin Lakes, NJ, USA |
| **CLSM** | |
| Zeiss Axiovert 35 Confocal Laser Scanning Microscope (CLSM) with laserscan-detection | Zeiss, Jena, Germany |

| | |
|---|---|
| unit from Leica | |
| **ELISA** | |
| Nunc-Immuno-F96 Maxisorp | Thermo-Fisher, Nunc GmbH & Co. KG, Wiesbaden, Germany |
| Wallac 1420 VICTOR 3 | Multilabel counter (Perkin Elmer, Boston, MA, USA) |
| SLT Spectra Elisa Reader, Software easy WIN fitting E 5.0 a | SLT, Crailsheim, Germany |
| **DNA/RNA technology** | |
| QiaAmp DNA Mini kit | #51304, Qiagen, Hilden, Germany |
| Epitect Bisulfite Kit | #59104, Qiagen, Hilden, Germany |
| TaqMan Universal PCR Mastermix (2x) | #4304437, Applied Biosystems Deutschland GmbH, Darmstadt, Germany |
| RNeasy Mini Kit | #74104, Qiagen, Hilden, Germany |
| RNeasy FFPE Kit | #73504, Qiagen, Hilden, Germany |
| Human HPRT ready-to-use mastermix (20x) | #4310890E, Applied Biosystems, Darmstadt, Germany |
| Taq DNA Polymerase, recombinant | #10342-053; Invitrogen GmbH, Darmstadt, Germany |
| Thermal cycler | Biorrad, Munich, Germany |
| Qiacube | Qiagen, Hilden, Germany |
| TaqMan Cycler | ABI Prism 7000 Sequence Detector, ABI, Darmstadt, Germany |
| Nanodrop | Thermo Scientific, Peqlab, Erlangen, Germany |
| **Xcelligence** | |
| RTCA DP Analyzer | #05469759001, Roche, Penzberg, Germany |
| RTCA Software Package 1.2 | #05454433001, Roche, Penzberg, Germany |
| CIM-Plate 16 | #05665817001, Roche, Penzberg, Germany |
| E-Plate 16 | #05469830001, Roche, Penzberg, Germany |
| **Antibodies (secondary)** | |
| Goat IgG HRP (*horseradish peroxidase)*-conjugated | Sigma-Aldrich, St. Louis, MO, USA |
| pab Goat-anti-rabbit IgG Alexa488-conjugated | Molecular Probes, Invitrogen, Carlsbad, CA, USA |
| pab rabbit-anti-goat IgG Alexa488-conjugated | Molecular Probes, Invitrogen, Carlsbad, CA, USA |
| HRP-conjugated goat anti-rabbit IgG | #111-035-003 (WB), Jackson ImmunoResearch |
| HRP-conjugated rabbit anti-mouse IgG | #315-035-045, Dianova, Hamburg, Germany |
| mouse anti-GAPDH | #MAB374; Chemicon, Billerica, MA, USA |
| Alexa Fluor 488 goat anti-mouse IgG, IgM (H+L) | #A-10680, Invitrogen GmbH, Darmstadt, Germany |
| Alexa Fluor 488 goat anti-rabbit IgG, IgM (H+L) | #A-11008, Invitrogen GmbH, Darmstadt, Germany |
| mouse Anti-Tag-100 | #34680, Qiagen, Hilden, Germany |
| mouse Anti-$His_5$ | #34660, Qiagen, Hilden, Germany |
| Wide spectrum CK antibody | #ab9377, Abcam, Cambridge, UK (3 mg/mL stock) |

## 3.2. Patient characteristics

**Ovarian cancer**: A total of 98 patients afflicted with ovarian cancer stage FIGO I–IV (Fédération Internationale de Gynécologie et d'Obstétrique) were enrolled between 1990 - 1999 in a prospective collection conducted at the Department of Obstetrics and Gynecology, Klinikum rechts der Isar, Technical University of Munich, Germany. Standard surgical procedures were performed, including partial resection of the small and large intestine, diaphragmatic peritoneum, peritonectomies and upper abdominal surgery, as well as pelvic and para-aortic lymphadenectomy if indicated (Kuhn 1994; Schmalfeldt 1995; Kuhn 1999). In

younger patients (<35 years) with tumor stage FIGO I, less radical surgery was performed to preserve patient fertility (Schmalfeldt 1995). All of the patients gave written informed consent for the use of tissue material for scientific purposes.

The study to collect tissue from ovarian cancer patients to assess KLK7 expression was approved by the Ethics Committee of the University Hospital Klinikum rechts der Isar of the Technical University of Munich. Following surgery, all patients received adjuvant treatment according to consensus recommendations at that time, mainly including taxanes and platinum-based chemotherapeutics. None of the patients received any neoadjuvant therapy before surgery. The median age of the patients at surgery was 57 years (range 20-85 years). The median follow-up time of the patients was 57 and 32.5 months for overall survival (OS) and progression-free survival (PFS), respectively, (range 1 to 244 months after primary tumor resection, for both). Tumors were staged according to FIGO. Ascitic volume was estimated preoperatively. Clinical and histomorphological information documented at the time of surgery included FIGO stage, ascitic fluid volume, nuclear grade, lymph node status, and presence of residual tumor mass histotype. Tumors were staged according to FIGO criteria (Pettersson 1994) and graded according to the protocol of Day et al. (Day 1975). The classification of histotypes was based on the WHO and FIGO recommendations (Serov 1973). Patients with ovarian carcinoma at all clinical stages (I–IV) and grades (1–3/4) are represented in our cohort of patients study. Of the 98 ovarian tumors, 74 were of serous papillary histotype, followed by 4 endometrioid, 10 undifferentiated, 8 mucinous, and 2 clear cell types. Residual tumor mass (RT) was defined as the size of residual tumor in mm (RT mass 0= no residual tumor, RT mass > 0= residual tumor mass greater/ equal 1 mm. Relevant data on clinical and histomorphologic parameters of the ovarian cancer patients are shown in **Table 3** (Gkazepis 2011).

**Table 3:** Clinical and histomorphologic characteristics of ovarian cancer patients

| Clinicopathological parameters | No. patients (%) |
|---|---|
| Total | 98 |
| Age | |
| ≤ 60 years | 60 (61.2) |
| > 60 years | 38 (38.8) |
| FIGO stage | |
| I | 18 (18.4) |
| II | 3 (3.0) |
| III | 58 (59.2) |
| IV | 19 (19.4) |
| Nuclear grade | |
| G1 | 8 (8.2) |
| G2 | 29 (29.6) |
| G3 (+4) | 61 (62.2) |
| Relapsed[#] | |
| No | 46 (46.9) |
| Yes | 52 (53.1) |
| Deceased[+] | |
| No | 32 (32.7) |
| Yes | 66 (67.3) |
| RT mass | |
| 0 | 52 (53.1) |
| > 0 | 41 (41.8) |
| Unknown | 5 (5.1) |
| Ascitic fluid volume | |
| No ascites | 30 (30.6) |
| < 500ml | 34 (34.7) |
| > 500ml | 32 (32.7) |
| Unknown | 2 (2.0) |
| Nodal status | |
| Negative | 34 (34.7) |
| Positive | 45 (45.9) |
| Unknown | 19 (19.4) |

**Colon cancer:** Tissue specimens of 266 primary colon carcinomas were collected by the Surgery Department, Technical University of Munich (TUM; Munich, Germany), between 1991-2002 (German collective) plus 95 colon carcinoma tissue specimens collected by the Pathology Department of Saint Savvas Hospital in Athens (Greek collective)-. For the German collective, a follow-up for 252 patients was available with a median time of follow-up of 52 months.

**Table 4:** Clinical characteristics of the colon cancer collective

| Clinical parameters | Number of patients (%) |
|---|---|
| Total | 261 (100) |
| **pT** | |
| T1 | 21 (8.05) |
| T2 | 47 (18.01) |
| T3 | 142 (54.4) |
| T4 | 51 (19.54) |
| **pN** | |
| N0 | 157 (60.15) |
| N1 | 65 (24.9) |
| N2 | 31 (11.88) |
| N3 | 8 (3.07) |
| **pM** | |
| M0 | 243 (93.1) |
| M1 | 18 (6.9) |
| **Stage** | |
| I | 57 (21.84) |
| II | 98 (37.55) |
| III | 88 (33.72) |
| IV | 18 (6.9) |
| **Dukes** | |
| A | 57 (21.84) |
| B1 | 0 (0) |
| B2 | 98 (37.55) |
| C1 | 8 (3.07) |
| C2 | 80 (30.65) |
| D | 18 (6.9) |
| **Deceased*** | |
| No | 182 (71.65) |
| Yes | 72 (28.35) |

*Total number of patients enrolled in the follow-up is 254.

**Melanoma:** Tissue microarray constructed out of patient material (n > 100) derived from Institut Gustave-Roussy (IGR, Paris, France). Due to unavailability of clinicopathological data, no statistical analysis was performed.

**Breast cancer (TNBC) (Gross 2011):** 179 primary breast cancer tissues of the TNBC type (triple-negative breast cancer) have been collected between 1989 and 2009 and stored in liquid nitrogen at the Department of Gynecology, Klinikum rechts der Isar, Technische Universität München. Tumors had been classified and assessed for the HER2 and steroid hormone receptor expression at the Department of Pathology before storage as previously described (Aubele et al., 2007). Estrogen receptor (ER) and progesterone receptor (PR) status were defined as negative at less than 10% nuclear staining as assessed by immunohistochemistry (IHC). Tumors assigned as 0 or 1+ in IHC staining for HER2 and/or lack of overexpression of HER2 in FISH staining were classified as HER2-negative. Samples diagnosed for breast cancer before 1999 were retrospectively assessed for HER2 expression. The majority of the patients were treated with an anthracycline/cyclophosphamide-containing chemotherapy protocol in an adjuvant setting. Complete follow up data were available for up to 157 patients. Characteristics are described in **Table 5**.

**Table 5:** Clinical characteristics of the breast cancer collective (TNBC).

| **Clinical parameter** | **all patients (n=179)**<br>**n (%)** |
|---|---|
| **Age** | |
| <50 | 58 (32) |
| ≥50 | 118 (68) |
| Median (range) | 57.5 (25-96) |
| **Tumor size** | |
| pT1 | 76 (42) |
| pT2 | 77 (43) |
| pT3 | 9 (5) |
| pT4 | 12 (7) |
| unknown | 5 (3) |
| **Nodal status** | |
| N0 | 91 (51) |
| N1 | 58 (32) |
| N2 | 16 (9) |
| N3 | 6 (3) |
| unknown | 8 (4) |

| | |
|---|---|
| **Grade** | |
| 1/2 | 44 (25) |
| 3 | 127 (71) |
| unknown | 8 (4) |
| | |
| **Histopathological subtype** | |
| Invasive ductal | 133 (74) |
| medullary | 11 (6) |
| lobular | 11 (6) |
| other | 21 (12) |
| unknown | 3 (2) |
| | |
| **Therapy** | |
| none | 38 (21) |
| Anthracycline-based | 103 (58) |
| CMF | 24 (13) |
| Taxol | 1 (0.6) |
| Other | 12 (4) |
| unknown | 6 (3) |

### 3.3. Tissue collection and preparation of formalin-fixed paraffin-embedded specimens

**Ovarian cancer tissues:** Routinely prepared formalin-fixed (buffered), paraffin-embedded ovarian cancer tissue specimens (Dorn 2006; Dorn 2007) were retrieved from the archives of the Institute of Pathology of the Technical University of Munich, Germany. Ovarian cancer tissue specimens were collected during surgery, examined by a pathologist and then formalin-fixed and paraffin-embedded. Samples were fixed for 8 h in 3.7 % buffered formalin and dehydrated by passing them through 70 % ethanol for one hour once, 96 % ethanol once for one hour and once for 45 min, isopropanol twice for one hour and once for 45 min and xylene twice for one hour. After four baths in liquid paraffin at 60 °C twice for 15 minutes, once for 30 min and once for one hour, the samples were embedded in paraffin. Sectioning of paraffin blocks at 2 µm thickness was performed by means of an electronic rotary microtome. Sections were then floated on a 38 °C distilled water bath, transferred onto Superfrost Plus slides, and dried overnight at room temperature.

The same procedure, as for ovarian cancer tissues, was followed for every in-house processed tissue, such as colon cancer, pancreatic cancer, prostate cancer, etc., as well as for normal tissue specimens.

**Other tissues:** Tissues which were included in Dr. Krajewski's normal organ or malignant tissue microarrays might be processed under different conditions; in case fixatives other than formalin e.g. Bouin's solution or Z-Fix (Anatech, MI, USA) were used.

**List of tissue samples used**

- Ovarian cancer TMA (>140 patient blocks, 98 patients finally used) and single tissue blocks, in-house
- Colon cancer TMA (261 tissue samples), made out of two different collectives, in-house and external (Greece)
- Melanoma TMA (>100 blocks), collection sent by Dr. A. Spatz (Institut Gustave-Roussy, Paris, France)
- Breast cancer (TNBC), 176 human breast cancer tissues of the TNBC type have been collected between 1999 and 2009 and stored in liquid nitrogen at the Department of Gynaecology, Klinikum rechts der Isar, Technische Universität München (Gross 2011).
- Multi-organ TMAs (>30 different tissues), one by Dr. S. Krajewski (Sanford-Burnham Institute, La Jolla, California, US) (various fixatives) and one in-house
- Cancer tissue TMA (>30 different tissues), provided by Dr. S. Krajewski (various fixatives)
- Test blocks (skin and kidney), in-house
- Prostate cancer specimens (app.10), in-house
- Pancreatic cancer specimens (app. 10), in-house

**Tissue microarray (TMA) construction**

The technique of tissue microarray production has been described in detail elsewhere (Skacel 2002). In brief, for the construction of TMAs, tumor areas within the donor paraffin blocks were identified by a pathologist using hematoxylin-eosin stained FFPE tumor tissue sections. Three different tissue cores (∅ 1 mm) were removed from each donor block and inserted into a recipient paraffin block using a MicroArrayer instrument (Alpha Metrix GmbH, Rödermark, Germany). Tissue cores were inserted into the paraffin block according to our own virtual custom-made compartmentalization pattern, using normal kidney and placenta tissue as the reference tissue cores. (Simon 2003). Hematoxylin-and-eosin-stained 2 µm sections were

reviewed by a pathologist to select representative areas of tumor from which to acquire cores for TMA construction. TMAs were constructed by taking core samples from these predefined areas of paraffin-embedded cancer tissue and assembling them in a recipient paraffin block. By using a manual tissue microarray instrument a technician took core needle biopsies with a diameter of 1 mm from donor blocks and arrayed these tissue cores into the 1 mm core-diameter holes of the recipient blocks. All samples were spaced around 1 mm apart. Of every ovarian cancer block 3 different punches were transferred to the recipient block. Two-micrometer thick sections were cut from the TMA and stained with hematoxylin and eosin to confirm the presence of tumor by a pathologist. Core samples of normal tissue blocks including kidney and lung were also placed between tumor core samples due to better orientation during histological evaluation. Sample tracking was based on coordinate positions for each tissue spot and was read according to the tissue microarray map. For construction of human multi-organ normal tissue microarrays a morphologically representative area of interest within the donor block was identified under the microscope by a pathologist using a section stained with hematoxylin and eosin as a guide. The tissues included are kidney, skin, myocardium, skeletal muscle, bone marrow, prostate, sebaceous gland, salivary gland, colon, thyroid, spleen, thymus, brain, lymph node, liver, placenta, and tendon. Colon cancer tissue microarrays, as well as multi-organ TMAs, were constructed in a similar way.

**Table 6:** TMA constructed by the Clinical Research Unit of the Dept. Obstetrics & Gynecology in collaboration with the Sanford-Burnham Institute, La Jolla, USA. The TMA consists of various normal and cancerous tissue specimens with the aim to test the effect of fixation on antibody reactivity and to assess loci of protein expression for the target antigen in question. White for available, green for non-available, yellow for no information.

| | fixative | | | state | |
|---|---|---|---|---|---|
| **Tissue** | **Z-fix** | **BF** | **Bouin** | **normal** | **malignant** |
| **breast** | ● | ● | ● | ● | ● |
| **ovary** | ● | ● | ● | ● | ● |
| **colon** | ● | ● | ● | ● | ● |
| **thyroid** | | ● | | ● | |
| **testis** | ● | | ● | ● | |
| **leiomyoma (uterus)** | ● | | ● | | |
| **bladder** | ● | | ● | | |
| **T cell NHL PB** | | | | | |
| **endometrium** | | ● | | ● | |
| **squamous ca** | ● | | | | ● |
| **NHL small cleaved cells LN** | ● | | | | |
| **thymus** | ● | | ● | ● | |
| | | | | | |
| **cerebral cortex** | | | | ● | |
| **aorta** | | | | ● | |

| Tissue | fixative | | | state | |
|---|---|---|---|---|---|
| | Z-fix | BF | Bouin | normal | malignant |
| heart | | | | ● | |
| adrenal | | | | ● | |
| appendix | ● | | ● | ● | |
| jejunum | ● | ● | ● | ● | ● |
| small intestine | ● | ● | ● | ● | |
| pancreas | ● | ● | ● | ● | ● |
| peritoneum | | | | ● | |
| LN | ● | ● | | ● | |
| stomach | ● | ● | ● | ● | ● |
| placenta | ● | | ● | ● | |
| tonsil | ● | ● | ● | ● | |
| cervix | ● | | ● | ● | ● |
| myometrium | | | | ● | |
| esophagus | ● | ● | ● | ● | ● |
| prostate | ● | ● | ● | ● | ● |
| uterus | | | | ● | |
| fallopian tube | | | | ● | |
| BM | | | | ● | |
| skin | ● | ● | ● | ● | ● |
| liver | ● | | ● | ● | ● |
| kidney | ● | | ● | ● | ● |
| smooth muscle (stomach) | | | | ● | |
| adrenal (cortex) | | | | ● | |
| lung | ● | | ● | ● | |
| spleen | | | | ● | |
| epidermis/dermis | ● | ● | ● | | |
| salivary gland | | | ● | | |
| skeletal muscle | ● | ● | ● | | |
| tongue | ● | | ● | | |
| gallbladder | ● | ● | ● | | |
| adrenal gland | | | ● | | |
| penis | | ● | ● | | |
| umbilical cord | ● | | ● | | |
| mammary gland | ● | ● | ● | ● | ● |
| motor cortex | ● | | ● | | |
| temporal lobe | ● | | ● | | |
| sensory cortex | ● | | ● | | |
| hypothalamus/thalamus | ● | | ● | | |
| striatum | ● | | ● | | |
| brain stem/pons | ● | | ● | | |
| spinal cord | ● | | | | |
| pituitary gland | ● | | | | |
| pineal gland | | | ● | | |
| choroid plexus | | | ● | | |
| mesencephalon | ● | | | | |
| medulla | ● | | ● | | |
| substantia nigra | ● | | ● | | |
| dorsal root ganglia | | | ● | | |
| CA-1, CA-2 | | | ● | | |
| CA-3 | | | ● | | |
| CA-4 | | | ● | | |
| foreskin | ● | | ● | | ● |
| larynx | ● | | ● | ● | ● |

**Z-Fix (buffered zinc formalin fixative)**

Ready-to-use buffered aqueous zinc formalin which prevents formalin pigments. Fixation time 8h.

*Morphology*

- Prevents nuclear and cytoplasmic bubbling artifact
- Creates B-5 (mercuric chloride containing) like fixation, without the toxicity and disposal problems of mercury

*Immunohistochemistry*

- Highly sensitive staining, often without antigen retrieval
- Retains immunoreactivity-even after long term storage of the paraffin blocks
- Preserves formalin-sensitive antigens in paraffin sections

**Neutral buffered formalin - fixation time 12-24 h**

Formalin (~ 40 % aqueous solution of formaldehyde) – 100 mL

- Sodium dihydrogen orthophosphate (monohydrate) – 4 g
- Disodium hydrogen orthophosphate (anhydrous) - 6.5 g
- Distilled water – 900 mL
- This fixative is suitable for most histological purposes. It is to be preferred to formol-saline (a single 10 % solution of formalin in 0.9 % aqueous NaCl) as formalin pigment is avoided. Specimens may be stored in this fluid. The solution is isotonic.

**Bouin's fluid - fixation time 6 h**

- Saturated aqueous solution of picric acid – 75 mL
- Formalin (~ 40 % aqueous solution of formaldehyde) – 25 mL
- Glacial acetic acid – 5 mL
- Fixed tissue should be transferred to 70 % alcohol for storage.

## Cell microarrays (CMA)

For the construction of CMAs, adherently growing tumor cells were cultured in T-125 flasks (3 x $10^7$), detached by the use of PBS/5 % EDTA, washed twice in 3 mL cold PBS (4 °C) and then centrifuged (800 x g, 5 min, 4 °C). For fixation of the cells, the cell pellet was suspended in 5 ml of 10 % formalin in TBS (30 min, 20 °C), centrifuged (800 x g, 5 min, 4° C), washed with TBS (4 °C) and centrifuged. Subsequently, the cell pellet was resuspended in a cocktail consisting of 150 µL thrombin (10 U/mL; Sigma, Munich, Germany), 750 µL casein (Sigma-Aldrich; 10 mg/mL) and 600 µL fibrinogen (25 mg/mL; Sigma, Munich, Germany), all in 0.04 M Tris-HCl, pH 8.0, and the cell suspension left overnight at 4 °C to solidify before paraffin-embedding. Since cells are formalin-fixed and paraffin-embedded, the procedure followed for construction of the CMAs is identical to the way TMAs are prepared (Luther 1996).

## 3.4. Tissue extraction and quantification of protein concentration

Tissue samples from primary ovarian cancer patients were collected during surgery, classified by a pathologist and stored in liquid nitrogen until use. Deep-frozen specimens of 200–500 mg

wet weight were pulverized using the Micro-Dismembrator II bead mill apparatus (Sartorius, Goettingen, Germany) and immediately suspended in 2 ml of Tris-buffered saline (TBS; 0.02 M Tris-HCl, pH 8.5, 125 mM sodium chloride), 1 % (w/v) Triton X-100 (Sigma, Munich, Germany). Extraction was conducted at 4 °C for 12 h followed by ultracentrifugation at 100,000 x g for 45 min to separate cell debris. The supernatant was collected, aliquoted, and stored in liquid nitrogen until further use.

Protein content in cell and tissue extracts was determined using by the BCA protein assay reagent (BiCinchoninic Acid) kit manufactured by Pierce (Rockford, IL, USA) according to the manufacturer's instructions. This method combines the well-known reduction of $Cu^{+2}$ to $Cu^{+1}$ by protein in an alkaline medium (the biuret reaction) with the highly sensitive and selective colorimetric detection of the cuprous cation ($Cu^{+1}$) using a unique reagent containing bicinchoninic acid (chelation of two molecules of BCA with one cuprous ion forms a purple-colored reaction product). After incubation for either 1 h at 37 °C or overnight at RT, absorbance of the colored complexes was determined at 562 nm using an ELISA reader (SLT Spectra, SLT Instruments, Germany). Protein concentrations were determined based on the standard curve of known concentrations (20-400 µg/mL) of the reference protein, bovine serum albumin (BSA). Triton X- 100 up to 1 % did not interfere with the protein determination assay (Janicke 1994).

### 3.5. Culture of tumor cell lines

**Cell lines**

The following human cell lines were cultivated in DMEM- 10 %, FCS- 0.2 %, arginine/asparagine, 1 % HEPES: spontaneously transformed (immortalized) keratinocyte cell line HaCaT (M. Kotzsch, Dresden, Germany), breast adenocarcinoma cell line MDA MB 231 (A. Krueger, Munich, Germany), MCF-7 (M. Kotzsch, Dresden, Germany) and ovarian cancer epithelial cell line OV-MZ-6 (V. Moebus, Frankfurt, Germany) which was used as the wild-type cell line and the one transfected with a vector only (OV-MZ-6 RSV) or transfected with a vector overexpressing *KLK7* (OV-MZ-6 RSV/ ne KLK7). Adherently growing cells were detached by PBS (GIBCO, Karlsruhe, Germany) /EDTA (Versen) (Biochrom AG, Berlin, Germany) 5 %, except for HaCaT, which was detached enzymatically by use of Accumax (L11-008; PAA Labs, Pasching, Austria).

**Table 7:** List of cell lines used in the studies presented.

| Cell line | Origin | Source/information |
|---|---|---|
| **CAL27** | Squamous cell carcinoma of the tongue | German Collection of Microorganisms and Cell Cultures, DSMZ, Braunschweig, Germany |
| **FaDu** | Esophageal squamous cell carcinoma of the hypopharynx | M. Baumann, Dresden, Germany |
| **OV-MZ-6** | Epithelial ovarian cancer (Moebus 1992) | V. Moebus, Frankfurt, Germany |
| **HeLa** | Epithelial cervical cancer | ATCC-CCL-2, American Type Culture Collection (ATCC), Manassas,VA, USA |
| **Caco-2** | Epithelial colon adenocarcinoma | ATCC- HTB-37; K.P. Janssen, Munich |
| **HT-1080** | Fibrosarcoma | ATCC-CCL-121, ATCC |
| **HaCaT** | Spontaneously transformed keratinocyte cell line | M. Kotzsch, Dresden, Germany |
| **MCF7** | Breast adenocarcinoma (pleural effusion) | ATCC-HTB-22, ATCC |
| **MDA-MB-231** | Breast adenocarcinoma (pleural effusion) | ATCC-HTB-26, ATCC |
| **U-937** | Myelomonocytic histiocytic lymphoma cell line | ATCC-CRL-1593.2, ATCC |
| **SKBR-3** | Epithelial breast adenocarcinoma of metastatic origin (pleural effusion) | ATCC-HTB-30, ATCC |
| **MDA-MB-435** | breast ductal carcinoma of metastatic site (pleural effusion) | ATCC-HTB-129, ATCC |
| **BT-20** | Epithelial breast carcinoma | ATCC-HTB-19, ATCC |
| **ZR-75-1** | Epithelial breast ductal carcinoma of metastatic site: ascites | ATCC-CRL-1500, ATCC |
| **OVCAR-3** | Epithelial ovarian adenocarcinoma | ATCC-HTB-161, ATCC |
| **OV-MZ10** | Epithelial ovarian cancer (Moebus 1992) | V. Moebus, Frankfurt, Germany |
| **OV-MZ-15** | Epithelial ovarian cancer (Moebus 1992) | V. Moebus, Frankfurt, Germany |
| **OV-MZ-19** | Epithelial ovarian cancer (Moebus 1992) | V. Moebus, Frankfurt, Germany |
| **EJ 28** | Epithelial bladder carcinoma | A. Lehmer, Munich, Germany |
| **RT-112** | Epithelial bladder carcinoma | DSMZ, Germany |
| **Caki-1** | Epithelial kidney clear cell carcinoma of metastatic site: skin | CLS, Eppelheim, Germany |
| **DU 145** | Epithelial prostate carcinoma of metastatic site: brain | ATCC-HTB-81, ATCC |
| **LNCaP** | Prostate adenocarcinoma | ATCC-CRL-740, ATCC |
| **PC-3** | Prostate adenocarcinoma | ATCC-CRL-1435, ATCC |
| **SW480** | Colorectal adenocarcinoma | ATCC-CCL-228, ATCC |
| **MIA PaCa-2** | Pancreatic cancer | ATCC-CRL-1420, ATCC |
| **PaTu-II** | Pancreatic cancer | D. Saur, Munich, Germany |
| **BHY** | Squamous carcinoma, oral | DSMZ, Germany |
| **U-2 OS** | Osteosarcoma | ATCC-HTB-96, ATCC |
| **Saos-2** | Osteosarcoma | ATCC-HTB-85, ATCC |
| **HT-1080** | Fibrosarcoma | ATCC-CCL-121, ATCC |
| **SNB19** | Glioma | ATCC-CRL-2219, ATCC |
| **Raji** | Burkitt's lymphoma | ATCC-CCL-86, ATCC |
| **HL-60** | Acute promyelocytic leukemia | ATCC-CCL-240, ATCC |
| **Granulocytes** | Normal blood | Dept. Ob & Gyn, TUM, Germany |
| **Lymphocytes** | Normal blood | Dept. Ob & Gyn, TUM, Germany |
| **Trophoblast cells** | Normal placenta | Dept. Ob & Gyn, TUM, Germany |

**Methylation studies**

For DNA methylation studies, cell lines were grown in twin T-125 flasks until 60 % confluency. Then, for one of the twin flasks, 10 mL of the old medium was removed and 200 µL of Decitabine aqueous solution (0.25 mg in 1,095 µL water) together with 9.8 mL of fresh medium. Cells were then incubated for 48 h at 37° C.

**Table 8:** Cell lines employed for methylation studies

| | | |
|---|---|---|
| HaCaT | OVCAR-3 | MCF-7 |
| MDA-MB-435 WT | MDA-MB-435 pRc RSV | MDA-MB-435 pRc RSV/KLK7 |
| OV-MZ-6 WT | OV-MZ-6 pRc RSV | OV-MZ-6 pRc RSV/KLK7 |

**Cell extracts**

Cell extracts were prepared by lysing the cells with the non-ionic detergent Triton X-100 (1 % w/v in TBS; 2 h, 4 °C) and the supernatant containing the KLK7 protein harvested by high-speed centrifugation (25,000 x g, 10 min, 4 °C).

### 3.6. Peritoneal ascitic fluid cell collection

Already in early FIGO stages, such as Ic, accumulation of ascitic fluid in the peritoneal cavity may happen. Metastasis from an ovarian adenocarcinoma is the most common etiology for the presence of malignant cells in effusions in female patients. Tumor cells have disseminated to the peritoneal cavity already at diagnosis in two-thirds of ovarian carcinoma patients. Isolated malignant cells often go undetected among large mesothelial cell and macrophage populations in effusions (Davidson 2004). These floating malignant cells are uniquely capable of proliferation, advancing and developing alternative means for acquisition of survival signals. The ascites of ovarian cancer patients provokes migratory activity on other cancer cell types and can stimulate MMP activation and tumor cell invasion (Kassis 2005).

Original material derived from patients diagnosed with ovarian cancer (age ranged from 64-73 years) and operated at the Department of Gynecology and Obstetrics was collected (4 samples). Ascitic fluid accumulated in the peritoneal cavity of ovarian cancer patients is collected in bags but its volume varies from patient to patient. An experimental protocol was developed to enrich white cells.

After centrifugation at 400 x g, 4 °C, 10 min in 225 mL Falcon tubes. The residual pellet was subjected to Erythrocyte Lysis Buffer (ELB) to eliminate contaminating red blood cells, followed by 2 x volume of TBS plus centrifugation at 400 x g, 5 min, 4 °C. Ascitic fluid supernatant was transferred to separate tubes and stored at -80 °C. The pellet of cells was subsequently fixed with 4 % PFA/PBS for 30 min at RT, followed by three washes 3 with TBS and finally resuspension in 5 ml PBS.

Erythrocyte Lysis buffer preparation

8.29 g $NH_4Cl$/ 1.0 g $Na_2CO_3$/ 0.038 g EDTA (Triplex III)

Dissolve EDTA in 500 mL $H_2O_{dist}$. Adjust pH by means of 2 N NaOH to pH 8 at 50 °C. $NH_4Cl$ and $Na_2CO_3$ are added and the solution is left to cool down (RT).

Finally, the pH value is adjusted to pH 7.2 by means of 2 N NaOH. The solution is adjusted with $H_2O_{dist}$ up to 1 L and then autoclaved immediately.

### 3.7. Antibodies

**KLK7:** The following antibodies, generated against different epitopes of KLK7, were employed both in western blot analyses and immuno(cyto)histochemistry: rabbit polyclonal antibody PA1-8435 against a synthetic peptide derived from the kallikrein loop area of KLK7 (Affinity Bioreagents (Dianova), Hamburg, Germany); rabbit polyclonal antibody H-50 raised against the aa 154-203 epitope near the C-terminus of KLK7 (Santa Cruz, Heidelberg, Germany); goat polyclonal antibodies C-15 and E-16 raised against peptides located within the internal region of KLK7 (Santa Cruz, Heidelberg, Germany); goat polyclonal antibody raised against rhKLK7 encompassing the aa 23-252 epitope of pro-KLK7 (R&D, Wiesbaden-Nordenstadt, Germany); rabbit polyclonal antibody raised against recombinant human pro-KLK7, kindly provided by Prof. T. Egelrud, Umea, Sweden, Arexis-Symbicon); rabbit polyclonal antibody to KLK7 (Tanimoto 1999), kindly provided by Prof. E.P. Diamandis, Toronto, Canada; mouse monoclonal antibody to KLK7 (Kishi 2004), kindly provided by Prof. E.P. Diamandis, Toronto, Canada.

**Table 9:** List of antibodies directed to KLK7, KLK14, KLK4, KLK5 and KLK6. In case of antibodies directed to KLK4, KLK6 and KLK7 and produced in Nijmegen, the 3-digit number after the "#" represents the code number of the each antibody. Code numbers of the host animals are also noted under the "species" column. Purification always takes place in three steps (A, B and C) for the antibodies starting with 6, whereas the rest have been purified in two steps. KLK14 as well as two KLK5 antibodies were developed in collaboration with Agrisera (Agrisera AB, Vännäs, Sweden). The R&D antibodies (the majority of them non-commercial) were gifted in the context of collaboration with the company. All but one, are mouse monoclonal.

| Antibody | Species | Immunogen | Purification |
|---|---|---|---|
| **Affinity Bioreagents PA1-8435** | Rabbit | Synthetic peptide derived from kallikrein loop area of KLK7 | Affinity purified |
| **Arexis Tagena + Domino** | Rabbit | Recombinant pro-KLK7 | 1. Affinity chromatography on a column presenting recombinant proKLK7 coupled to CNBr-sepharose<br>2. Size-exclusion chromatography (95 % purity) |
| **Santa Cruz H-50** | Rabbit | 154-203 aa near the C-terminus of KLK7 | Non-disclosed |
| **Santa Cruz C-15** | Goat | Peptide within an internal region of KLK7 | Affinity chromatography purification |
| **Santa Cruz E-16** | Goat | Peptide within an internal region of KLK7 | Affinity chromatography purification |
| **RnD systems AF2624** | Goat | rhKLK7, aa 23-252 (pro-enzyme) | Affinity chromatography purification on recombinant human KLK7 |
| **Diamandis** | Rabbit | Immunization with a combination of 2 poly-lysine linked multiple Ag peptide derived from the KLK7 protein sequences. | Non-disclosed (Tanimoto 1999) |
| **Diamandis (clone 83-1)** | Mouse | Full-length KLK7 human cDNA | Affinity-chromatography purification (Kishi 2004) |

## KLK14

| Antibody | Species | Immunogen | Purification |
|---|---|---|---|
| **Agrisera anti-KLK14** | Rabbit | A mixture of synthetic peptides conjugated to KLH. Peptides are coming from the N-terminus and the C-terminus of KLK4 | Affinity chromatography purified |

## KLK4/KLK6

| Antibody | Source | Species | Immunogen | Purification |
|---|---|---|---|---|
| ***# 617 A,B,C*** *anti-KLK4* | RUNMC (Nijmegen) | Chicken Ch #51 | rec-KLK4 | A: KLK 4-peptide<br>B: His & EK peptides *<br>C: rec KLK 4 |
| ***# 618 A,B,C*** *anti-KLK4* | | Rabbit Rb #96 | rec-KLK4 | A: KLK 4-peptide<br>B: *<br>C: rec KLK 4 |
| ***# 619 A,B,C*** *anti-KLK4* | | Rabbit Rb #97 | rec-KLK4 | A: KLK 4-peptide<br>B: *<br>C: rec KLK 4 |
| ***# 622 A,B,C*** *anti-KLK6* | | Chicken Ch #43 | rec-KLK6 | A: KLK 6-peptide<br>B: *<br>C: rec KLK 6 |
| ***# 623 A,B,C*** *anti-KLK6* | | Rabbit Rb #77 | rec-KLK6 | A: KLK 6-peptide<br>B: *<br>C: rec KLK 6 |
| ***# 620 A,B,C*** *anti-KLK7* | | Chicken Ch #45 | rec-KLK7 | A: KLK 7-peptide<br>B: *<br>C: rec KLK 7 |
| **# 621 A,B,C** anti-KLK7 | | Rabbit Rb #78 | rec-KLK7 | A: KLK 7-peptide<br>B: *<br>C: rec KLK 7 |
| ***# 578*** *anti-KLK4* | | Chicken | rec-KLK4 | KLK4-peptide |
| ***# 581*** *anti-KLK4* | | Rabbit | rec-KLK4 | KLK4-peptide |
| ***# 430*** *anti-KLK4* | | Chicken | rec-KLK4 | rec-KLK4-13 |
| ***# 431*** *anti-KLK4* | | Rabbit | rec-KLK4 | rec-KLK4-13 |
| ***# 579*** *anti-KLK6* | | Chicken | rec-KLK6 | KLK6-peptide |
| ***# 582*** *anti-KLK6* | | Rabbit | rec-KLK6 | KLK6-peptide |
| ***# 426*** *anti-KLK6* | | Chicken | rec-KLK6 | rec-KLK6 |
| ***# 427*** *anti-KLK6* | | Rabbit | rec-KLK6 | rec-KLK6 |
| ***# 580*** *anti-KLK7* | | Chicken | rec-KLK7 | KLK7-peptide |
| **# 583** anti-KLK7 | | Rabbit | rec-KLK7 | KLK7-peptide |

## KLK5

| Antibody | Source | Species | Immunogen | Purification |
|---|---|---|---|---|
| anti-KLK5<br>IV+2 “Pepsy“<br>AgriSera | AgriSera (Sweden) | Rabbit | Denatured rec-proKLK5 | rec-proKLK5 |
| anti-KLK5<br>IV+4 “Brage“<br>AgriSera | | Rabbit | Denatured rec-proKLK5 | rec-proKLK5 |

## KLK5 and KLK7 antibodies from R&D Systems

| Antibody | Host | Immunogen | Clonality |
|---|---|---|---|
| **MAB2624** | mouse | KLK7 | monoclonal |
| **333901** | mouse | KLK7 | monoclonal |
| **333902** | mouse | KLK7 | monoclonal |
| **333908** | mouse | KLK7 | monoclonal |
| **333909** | mouse | KLK7 | monoclonal |
| **333916** | mouse | KLK7 | monoclonal |
| **333918** | mouse | KLK7 | monoclonal |
| **333924** | mouse | KLK7 | monoclonal |
| **333925** | mouse | KLK7 | monoclonal |
| **333930** | mouse | KLK7 | monoclonal |
| **333945** | mouse | KLK7 | monoclonal |
| **AF1108** | goat | KLK5 | polyclonal |
| **MAB1108** | mouse | KLK5 | monoclonal |
| **MAB11081** | mouse | KLK5 | monoclonal |
| **MAB11082** | mouse | KLK5 | monoclonal |
| **193302** | mouse | KLK5 | monoclonal |
| **193303** | mouse | KLK5 | monoclonal |
| **193304** | mouse | KLK5 | monoclonal |
| **193305** | mouse | KLK5 | monoclonal |
| **193306** | mouse | KLK5 | monoclonal |
| **193308** | mouse | KLK5 | monoclonal |
| **193315** | mouse | KLK5 | monoclonal |

**Antibodies to uPA and PAI-1 employed in the immunohistochemical assessments**

| Antibody | Immunogen/Epitope | Reference |
|---|---|---|
| **uPA #3689** 1 mg/mL | A murine IgG1 monoclonal antibody directed against the B-chain of human urokinase (uPA). The antibody has been grown in cell culture and immunoaffinity purified using a uPA-agarose gel column. Reactivity directed against a B-chain epitope of human urokinase, near the catalytic site. It reacts with free and receptor bound, single and two chain (HMW) urokinase and the B-chain (33 kDa) fragment. The antibody incubated at 1 µg/mL, room temperature for 1 hour, identifies pro-uPA, HMW-uPA and LMW-uPA after electrophoresis under non-reduced conditions and B-chain fragments after electrophoresis under reducing conditions | (Kobayashi 1991; Sier 1991; Jankun 1993; Costantini 1996) |
| **PAI-1 #3785** 1mg/mL | IgG1 (κ). Unknown epitope. Raised against purified active PAI-1 secreted by the human melanoma cell line MJZJ. Interferes with PAI-1 activity. | (Andreasen 1986; Nielsen 1986; Torr-Brown and Sobel 1993; Costantini 1996) |
| **PAI-1 #3786** 0.42 mg/mL | anti-human melanoma PAI-1 (HD PAI-1 14.1) Protein-G purification from cell culture supernatant. Epitope specificity unknown. | No reference |
| **PAI-1 #ADG25** 1.7 mg/mL | Monoclonal mouse IgG2a. Protein-G purification from cell culture supernatant. Epitope specificity unknown. Reacts with: PAI-1 | No reference |

### 3.8. Recombinant KLK protein: generation and purification

Recombinant KLK 3-4 and 6-15 were designed and produced in-house as described previously by Debela et al. (Debela 2006b; Debela 2008). Briefly, KLK DNAs were isolated from breast and ovarian cancer tissue, respectively, or from cancer cell lines, and fusion genes generated encoding pro-forms of the various KLKs with an N-terminally located histidine-tag followed by an enterokinase cleavage site to produce the recombinant KLK proteins in transformed E. coli cells, induced with IPTG. Recombinant KLK proteins were purified under denaturing / slightly reducing conditions and refolded subsequently in decreasing concentrations of urea, ranging from 8 until 2 M. Recombinant KLK1 and KLK2 protein were provided by Prof. E.P. Diamandis, Toronto, Canada. Recombinant KLK5 was kindly provided by Prof. N. Schechter, San Francisco, USA (Schechter 2005)

## 3.9. Various reagents

### Generation of polyclonal antibodies directed to KLK4 and KLK6 in chickens

The procedure has been previously described in detail elsewhere (Seiz 2010). Briefly, purified and refolded recombinant (non-glycosylated) human KLK4 (rec-KLK4) or KLK6 (rec-KLK6), carrying an N-terminal extension of 17 amino acids encompassing a histidine $(His)_6$-tag and an enterokinase (EK) cleavage site (DDDDK↓) was used for immunization of chickens. Chickens were immunized intramuscularly (pectoral muscle) with 20 µg of rec-KLK per injection following the protocol by (McKiernan 2008). Antibodies (IgY, avian analog of IgG) were isolated from egg yolk using a standard step precipitation procedure utilizing increasing concentrations of polyethyleneglycol (PEG precipitation) as described previously (Grebenschikov 1997). Antibodies from the animals were subsequently purified by affinity chromatography by three consecutive procedures: (a) against a unique peptide of KLK4/KLK6 in order to select for monospecific polyclonal antibodies; (b) by a "negative" purification step using columns with immobilized peptides covering the tag of the recombinant protein and (c) against the immunogen.

For affinity purification of the KLK5-directed antibodies recombinant pro-KLK5 was used. The two different sera investigated display different reaction patterns: IV+2 serum is specific for the pro-form of KLK5, while the IV+4 serum recognizes the active part of the protein, which is present both in the active and the pro-form of the KLK5 protein.

### Characterization of polyclonal antibodies directed to KLK in chickens

The reaction pattern of pAb fraction A was analyzed by "one-side ELISA" assays, in which the antigen, the KLK-derived peptide, or control proteins/peptides were used for coating, demonstrating a specific, strong reaction with both the immunogen (rec-KLK) as well as the peptide (a). The flow through was applied to the column linked to the $(His)_6$-tag plus EK site peptides, for negative selection of antibodies generated against the N-terminal, non-KLK related sequences of rec-KLK (b). The flow through of the second column, which now was depleted from antibodies directed to the non-KLK related sequences of rec-KLK, was applied to the third column, coupled with the immunogen (c). As seen in the "one-side ELISA" assay, antibodies eluted from the third column, fraction C, react distinctly with the immunogen (rec-

KLK), but not with peptide, demonstrating that pAb C is the antibody fraction completely depleted from pAb A. Thus, pAb A and pAb C are directed against different epitopes of KLK.

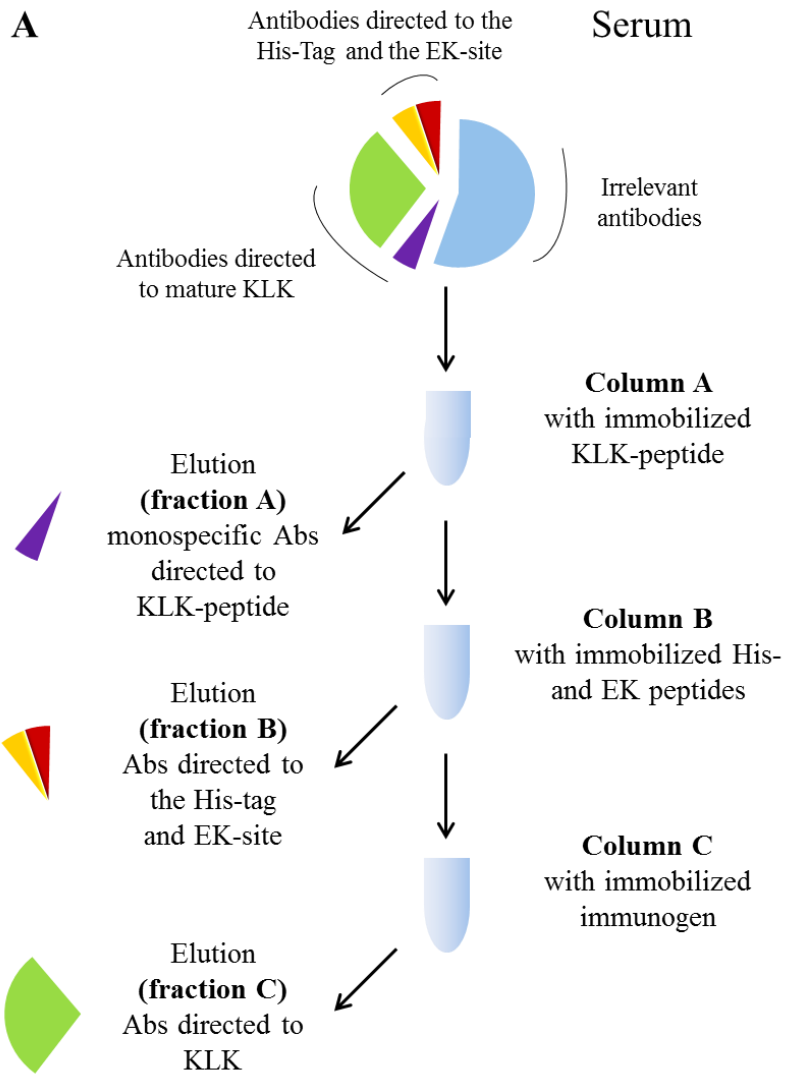


**Figure 1A**: Affinity purification of polyclonal antibodies. Serum of animal, immunized with rec-KLK, is passed over column A with immobilized KLK-peptide. The elution (fraction A) contains monospecific, polyclonal antibodies directed against the linear epitope of the KLK-peptide. The flow through of column A is applied to column B with immobilized His-peptide plus EK-peptide. The elution (fraction B) contains antibodies directed to the N-terminal extension of rec-KLK, i.e. the $(His)_6$-tag and the EK-site. The flow through of column B is passed over column C with immobilized rec-KLK. The elution (fraction C) contains polyclonal antibodies directed against rec-KLK.

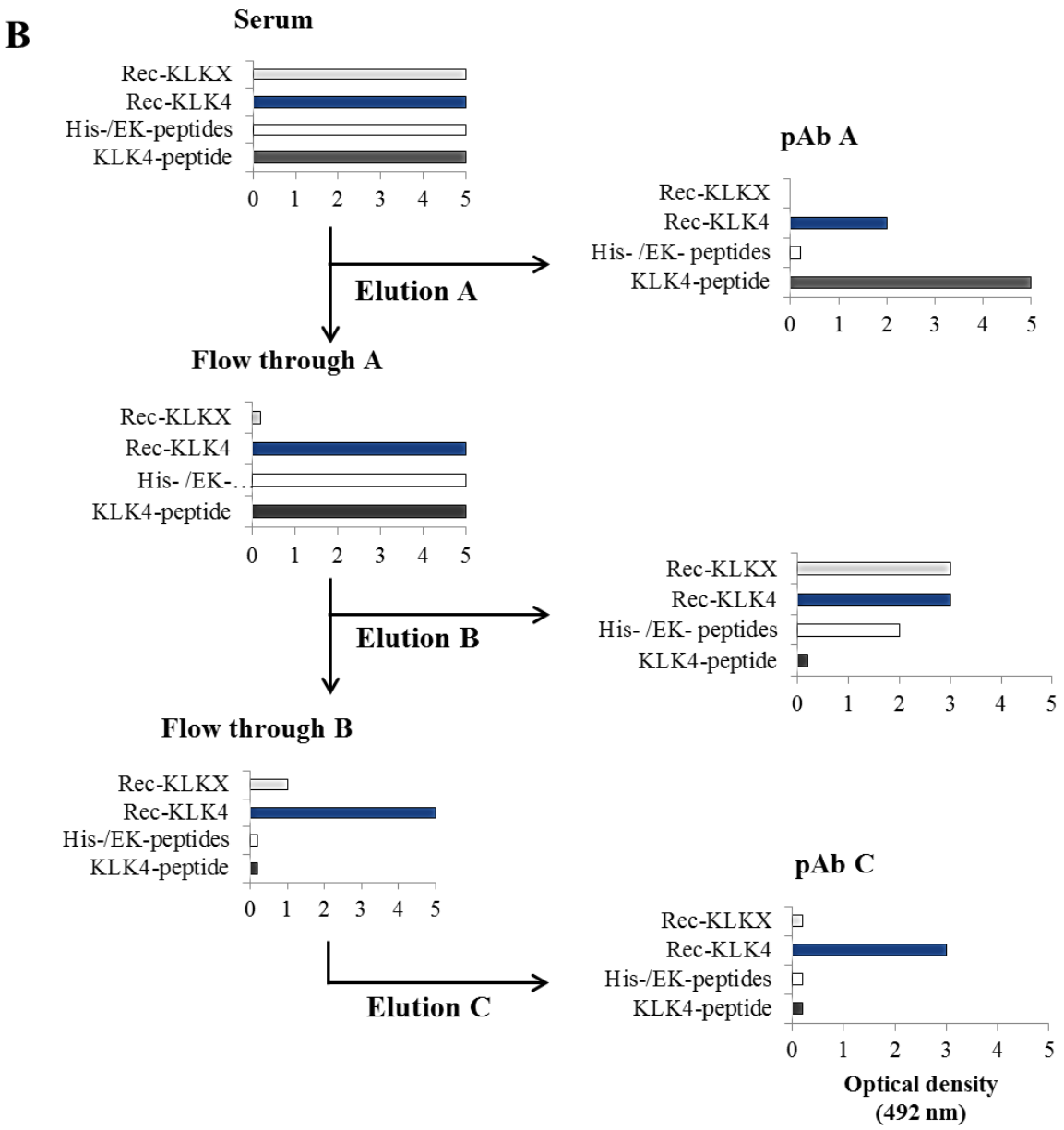


**Figure 1B:** One-side ELISA. Elution A (pAb A) reacts with the KLK-peptide and with the rec-KLK; elution B reacts with the rec-KLK, rec-KLKX and with His- plus EK-peptides. Elution C (pAb C) reacts with the rec-KLK but not with the KLK-peptide, demonstrating that this fraction is completely depleted from antibodies directed against this specific epitope of KLK.

### 3.10. Statistical methods

Distributions of KLK7 expression were characterized in terms of minimum, maximum, median, mean, SD, and number of values detected. Of interest is the distribution of KLK7 in the population as a whole, and particularly in subgroups defined by nuclear grade (G1-3/4) and FIGO classification (I-IV). All correlations are Spearman correlations with respect to the original analytes, missing values were excluded pairwise. We describe correlations R>0.5 as strong. The levels of significance between continuous variables of tumor biological markers were calculated using Spearman rank correlation ($r_s$). The relationship of biological marker expression levels (grouped as tertials) with clinical and histomorphologic parameters was evaluated using the $Chi^2$ –test. Outcome variables were PFS, OS, and residual tumor mass presence, defined as "1" if macroscopic RT mass was visible and "0" if completely absent. Age, nuclear grade, ascitic fluid volume, and nodal status were coded as binary variables (age: >60 years versus younger; nuclear grade: G3/4 versus G1/G2; ascitic fluid volume: >500 mL versus less; nodal status "0" for N0, otherwise "1".FIGO status was coded III/IV versus I/II. For survival analyses, OS and PFS of ovarian cancer patients were used as follow-up end points, respectively. The association of KLK7 parameters as well as of clinical and histomorphological factors with OS and PFS was analyzed by employing Cox univariate and multivariate proportional hazards regression models and data expressed as hazard ratio (HR) and its 95 % confidence interval (95 % CI). The multivariate Cox's regression model was adjusted for known clinical prognostic factors of the ovarian cancer patients: age, FIGO stage, nuclear grade, residual tumor mass, and ascitis volume. In subgroup analysis of FIGO III/IV patients, age, nuclear grade, tumor resection status and ascites volume were considered. Survival curves were generated by Kaplan-Meier analysis using log-rank tests to test for differences. The effects of the different factors on PFS and OS were expressed as hazard ratios (HR) with respect to the above coding and were estimated by Cox proportional hazards regression using forward selection. Univariate and multivariate Cox models were estimated including clinical factors and KLK7 scores (by ELISA and immunohistochemistry). All calculations were performed using the StatView 5.0 statistical package (SAS Institute, Cary, NC). The level of statistical significance was set to $p \leq 0.05$.

In case of TNBC, statistical analysis was performed with the IBM SPSS Statistics version 19.0 (SPSS Inc.) Association of (epi)genetic and categorical clinical data was assessed by the Chi-

square test. Overall survival (OS) and time to progression (TTP) were considered as long-term endpoints. TTP was defined as the time from surgery to the first incidence of disease recurrence (local or distant). OS was defined as the time from surgery until death from any cause. The Cox proportional hazard model was used to investigate the predictive value of the clinical or molecular-genetic parameters. Survival curves were generated according to the Kaplan-Meier method and the log-rank test was used for statistical comparison of event-time distributions between independent subgroups. All statistical tests were conducted two-sided and a p-value $<0.05$ was considered to indicate statistical significance. No correction of p-values was applied to adjust for multiple test issue (Saville 1990). Ninety-five percent confidence intervals were provided for relevant effect estimates such as hazard ratios (HRs) (Gross 2011).

# 4. Techniques

## 4.1. Cytospins

**Cytospin preparation**

Cell suspensions (Noack 1999; Noack 2000) were adjusted to 300,000 per mL of PBS/1 % BSA. Aliquots of 200 µL were loaded into a cytospin sample chamber assembly and centrifuged onto microscope slides for 5 min at 450 rpm by use of a Shandon cytocentrifuge II. Immediately, cells were either fixed in acetone (5 min, 4 °C) or in 1 % buffered paraformaldehyde (30 min, RT). Optionally, slides are subsequently treated with 0.025 % saponin in PBS (30 min, RT) to improve cell permeabilization.Cells from cell culture in PBS were centrifuged at 1214 rpm for 5 min at 10 °C in a refrigerated centrifuge. After removal of supernatant by aspiration with Pasteur pipettes, the cells were resuspended with 2 ml PBS/1 % BSA. Subsequently, centrifugation was performed in the same way as described before and discarding supernatant, resuspension with 1 ml PBS/1 % BSA followed. Having made a dilution of 1 to 10 cells the cells were counted by use of a Neubauer hemocytometer. The cell suspension was adjusted to 300,000 cells/mL in PBS/1 % BSA. Aliquots of 200 µL were loaded into a cytospin sample chamber assembly and cytocentrifuged onto microscope slides for 5 min at 450 rpm. By using centrifugal forces, cells were deposited onto a clearly defined area of a microscope slide. Residual fluid was absorbed into the sample chamber filter card. In order to avoid drying of cells, cell fixation was performed instantaneously after centrifugation. Cells were fixed either in acetone for 5 minutes at 4 °C, in paraformaldehyde 1 % for 30 min at RT or unbuffered formalin 4 % buffered in 0.1 M PBS for 30 min at 4 °C. After fixation with acetone, slides were dried for 10 min and subsequently washed in TBS. In case of fixation with paraformaldehyde or formalin slides were first washed in $H_2O_{dist}$ and then in TBS before permeabilization with saponin 0.025 % (w/v) in PBS/1 % BSA for 30 min at RT was performed. These slides were later compared to slides that were not exposed to the permeabilization procedure. All slides were transferred into TBS to continue with immunohistochemistry. Before proceeding with staining the PAP pen for immunostaining was used to draw a hydrophobic circle around the cell area to prevent loss of reagents.

**Table 10:** Basic protocol for cytospin construction. Multiple fixation variables were tested to achieve fine structure preservation. All variants are cited in literature.

**Cytospin – test conditions for antibody reactivity**

- Cells in medium or PBS
- Centrifuge cells at 300 x g (1,214 rpm) for 5 min at 10 °C
- Discard the supernatant by aspiration with Pasteur pipettes and resuspend the pellet in 2 ml PBS/BSA (1 %)
- Centrifuge cells at 300 x g (1,214 rpm) for 5 min at 10 °C
- Discard the supernatant by aspiration with Pasteur pipettes and resuspend the pellet with 1 ml PBS/BSA (1 %)
- Dilute 1:10 of the cells
- Count the cells by use of Neubauer haemocytometer
- Adjust to $10^6$ cells/mL in PBS/1 % BSA
- Put 200 µL of cells in PBS/1 % BSA into the cytospin cell suspension stage device
- Cytospin at 450 rpm for 5 min
- Don´t let cells dry after centrifugation, but proceed immediately with any of the cell fixative procedure:
  1. **with acetone:**
  a) 5 min in 4 °C
  b) 10 min in -20 °C cold acetone
  2. **with 96 % ethanol:**
  a) 5 min at 4 °C
  b) 10 min at -20 °C
  3. **with 70 % ethanol:**
  a) 5 min at 4 °C
  b) 10 min at -20 °C
  4. **with 100 % methanol in $H_2O_{dist}$:**
  a) 10 min at 4 °C
  b) 30 min at -20 °C
  5. **with 70 % methanol in in $H_2O_{dist}$:**
  a) 10 min at 4 °C
  b) 30 min at -20 °C
  6. **with unbuffered paraformaldehyde 1 %; in $H_2O_{dist}$ or tap water, 30 min RT**
  7. **with buffered paraformaldehyde 1 %; in 0.1 M PBS; pH 7.4; 30 min, RT**
  8. **with unbuffered formalin 4 %; in $H_2O_{dist}$ or tap water; 30 min, 4 °C**
  9. **with buffered formalin 4 %; in 0.1 M PBS; 30 min, 4 °C**

,

After fixation with (1) to (5) let cytospin air-dry for around 10 min, for (6) to (9) wash slides in $H_2O_{dist}$, then in TBS (contains amino groups) to neutralize residual reactive aldehyde groups. For (1) to (5) wash in TBS once. For (6) to (9) permeabilization before immunocytochemistry is needed. Permeabilization should be performed before freezing of the cytospin slides.

**Table 11:** Permeabilization variants. Permeabilization allows for access of antibodies to all cells and subcellular compartments. Saponin is a relatively mild detergent that solvates cholesterol which is present in the plasma membrane. At low concentrations, internal membranes remain intact within the cytoplasm. Digitonin is a detergent which replaces cholesterol in membranes, and creates pores making them water-soluble. Digitonin and saponin form bigger holes and therefore also allow the introduction of large molecules, such as enzymes and immunoglobulins. Triton X-100 efficiently solves cellular membranes without disturbing protein-protein interactions.

**Evaluation of various permeabilization variants:**

1. **Saponin** (0.025 % in PBS/1 % BSA)
2. **Digitonin** (concentration steps: (a) 10 µM, (b) 100 µM, (c) 1 mM and (d) 10 mM in PBS/1 % BSA; duration and temperature optimization: 1st group: (a) 5, (b) 10, (c)15 min on ice; 2nd group: (d) 5, (e) 10, (f) 15 min at RT)
3. Non-ionic detergents (e.g. **Triton X-100**: Validate dilution row: (a) 0.1 % [w/v], (b) 0.01 %, (c) 0.001 %, (d) 0.0001 % and (e) 0.00001 %).

Wash slides in TBS. In order to dry slides and then freeze them (at -80 °C) wash (1) to (9) one more time in $H_2O_{dist}$. For directly passing over from permeabilization to immunochemistry, transfer slides into TBS and proceed with immunostaining protocols.

NOTES
If preparing BSA-containing solutions for blocking of unspecific binding: just let BSA-crystals sink in TBS or PBS-buffer (10 mM; pH 7.4) and subsequently mix solution gently without bringing oxygen into solution (will otherwise cause multimers of BSA).

**Table 12:** Preparation protocol of two fixatives used for cell preservation, paraformaldehyde (PFA) 1 % and formalin 4 %. Fixation variants such as PFA 1 % and formalin 4 % proved to maintain cell structure better than other fixatives.

**Paraformaldehyde 1 %**
-2 g PFA in 200 mL PBS or $H_2O_{dist}$ (50 °C)
-add 2 N NaOH (max 1 mL) until it becomes clear (add slowly dropwise)
-adjust to pH 7.4 by addition of phosphoric acid (slowly)
-use pH paper for control of pH
**Formalin 4 %**
-add 8 mL formaldehyde solution (37 %) to 192 mL PBS or $H_2O_{dist}$
-check pH with pH-paper
-add 2 N NaOH or phosphoric acid to adjust pH to 7.4

## 4.2. Magnetic cell sorting (MACS)

In order to enrich epithelial-origin cells of the white cell pellet mostly containing lymphocytes and neutrophils, a sophisticated technique, called Magnetic Cell Sorting (MACS), was used. This system uses paramagnetic beads, to which cell surface-specific antibodies are bound, to specifically label an epithelial cell specific molecule.

### Background

Epithelial cell adhesion molecule (EpCAM)- 40 kDa transmembrane glycoprotein, which is also known as CD326 and human epithelial antigen (HEA), is broadly expressed on cells of epithelial origin and on epithelial-derived tumor cells (Moldenhauer 1987). CD326 MicroBeads are used for the positive selection of epithelial tumor cells from serous effusions of patients

with carcinomas. In order to prevent FcR-mediated non-specific labeling of non-epithelial cells, FcR blocking reagent (#130-059-901; Miltenyi Biotec, Bergisch Gladbach, Germany) is used before magnetic labeling.

**VarioMACS separation system**

LS columns are assembled via a specific adaptor on the VarioMACS to achieve maximum capacity of 2 x $10^9$ filtered cells. As MACS MicroBeads (diameter of 50 nm) are extremely small, a high-gradient magnetic field is required to retain labeled cells. LS columns contain an optimized matrix to generate this strong magnetic field when placed in a permanent magnet such as the VarioMACS Separator. LS columns contain a hydrophilic coating, which allows rapid filling.

**Protocol**

First, the cell number is determined, then the cell suspension is centrifuged at 300 x g for 10 min and the supernatant is subsequently aspirated completely. Up to $10^8$ cells are resuspended in 500 µL of *buffer* (PBS/ 0.5 % BSA/ 2 mM EDTA) and then cells are passed through a pre-separation filter (#130-041-047; Miltenyi Biotec, Bergisch Gladbach, Germany) [30 µm nylon mesh] to remove clumps. Around 100 µL of FcR Blocking Reagent per 5 x $10^7$ total cells is added. 100 µL of CD326 MicroBeads per 5 x $10^7$ total cells is added. The suspension is mixed well and refrigerated for 20 min at 4 °C. Cells are washed by adding 5-10 mL of *buffer* [buffer: PBS, pH 7.2 0.5 % BSA and 2 mM EDTA, keep cold (2-8 °C)] per 5 x $10^7$ cells and centrifuged at 300 x g for 10 min. Then, the supernatant is removed and the cell pellet is resuspended in 500 µL of buffer. The cell suspension is placed onto the top of the LS column, already assembled in the magnetic field (prepared by rinsing with 3 mL of buffer) and unlabeled cells are collected while they pass through the magnetic field. The magnetically labeled $CD326^+$ cells are retained within the column. However, the unlabeled cells run through this; this cell fraction is depleted of $CD326^+$ cells. Column is then washed with three times of 3 mL buffer and the total effluent collected as the unlabeled cell fraction. Five ml buffer washed the magnetically labeled cells from the column by applying pressure with a plunger and these cells are harvested in a separate collection tube. After removing the column from the magnetic field, the magnetically retained $CD326^+$ cells can be eluted as the positively selected cell fraction (**Figure 2**).

**Table 13:** Properties of the antibody HEA-125 (Miltenyi Biotec, Bergisch Gladbach, Germany) used in the MACS experiments. It specifically recognizes epithelial-like cells.

| Antibody | Immunogen | Immunogen type | Localization | Species | Specificity |
|---|---|---|---|---|---|
| HEA-125 | CD326 (or EpCAM or HEA) | Transmembrane glycoprotein 40 kDa | Basolateral surface of carcinoma and epithelial cells | Mouse IgG1 | Epithelial-like cells |

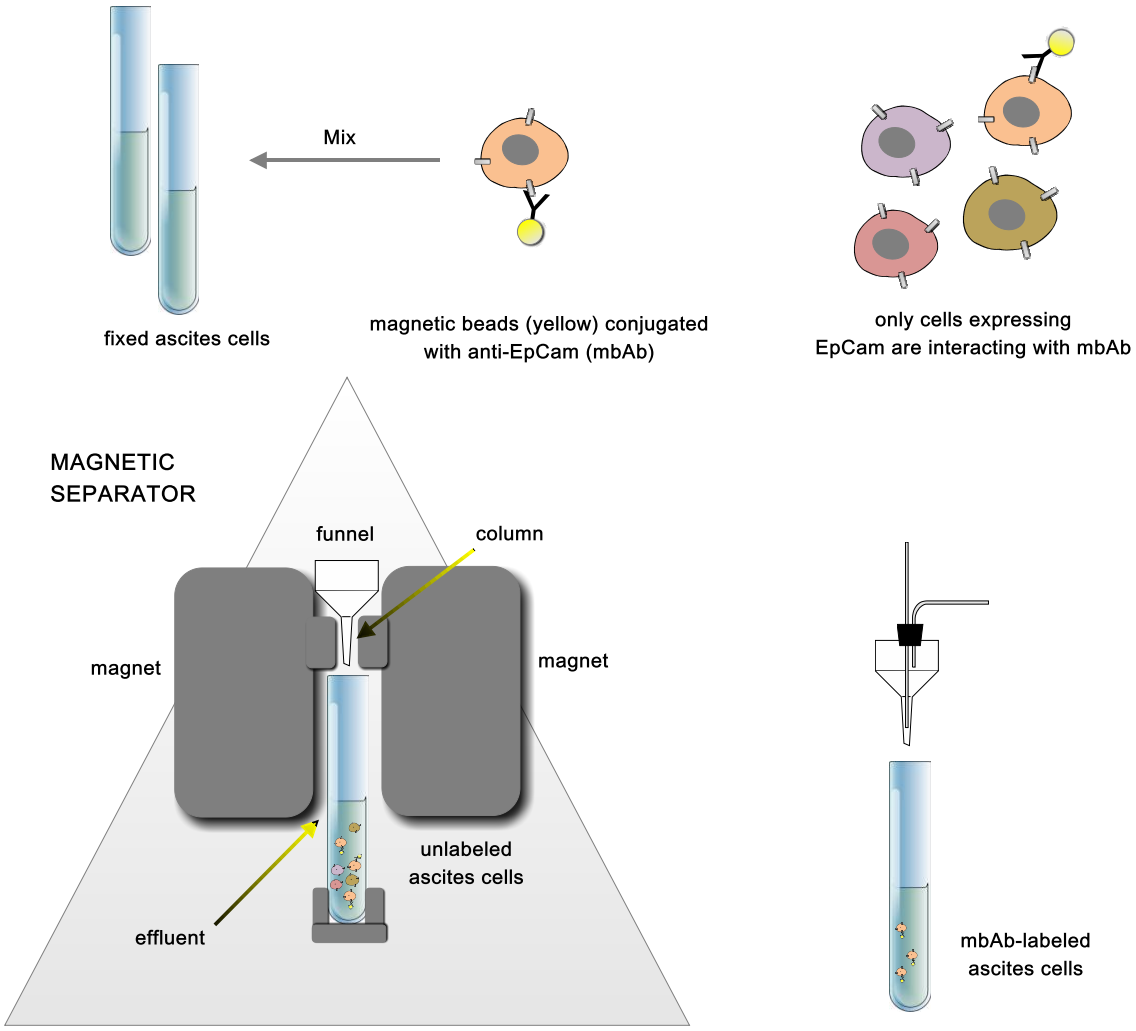


**Figure 2:** Positive selection strategy for epithelial-origin cells using the MACS technology. Positive selection means that the targeted epithelial tumor cells interacting with specific antibodies are enriched as the magnetically retained cell fraction. As a first step, fixed ascitic fluid cells are mixed with a MicroBeads suspension bearing antibodies to EpCam, are conjugated with a magnetically labeled anti-EpCam. The mixture is placed onto a column in the Magnetic Separator, where magnets cell-mbAb constructs, whereas unlabeled cells end up in the effluent. As the last step, the column is removed from the Magnetic Separator and the retained cells are eluted by the addition of *buffer* as the positively selected EpCam-positive cell fraction.

### 4.3. Fluorescence-activated cell sorting (FACS)

MDA-MB-231, HaCaT, OV-MZ-6 and MCF-7 cells were grown to 80 % confluency, washed once with PBS and detached from the culture flask with 0.05 % EDTA in PBS. Detached cell pellets were resuspended in PBS and were counted in a haemocytometer in the presence of Trypan blue to discriminate living from dead cells. Cells ($1 \times 10^6$) were then fixed with 2 % PFA in PBS for 20 min at RT and washed 3 times with TBS. In order to allow penetration of the antibodies into the cells, cells were permeabilized for 10 min with 0.025 % saponin/ PBS and then washed twice with PBS. Unspecific binding sites were blocked using PBS/ 1 % BSA for 30 min at RT. Primary antibodies were diluted in PBS/1 % BSA and incubated together with the cells for 1h at RT. Following extensive washing (4 times) with PBS, secondary antibodies conjugated with Alexa-488 (#A-10680 *goat anti-mouse* or #A-11008 *goat anti-rabbit*, Invitrogen GmbH, Darmstadt, Germany) (dilution 1:1,000 of the stock solution) were added to the cells and then left in the dark for 30 min at 4 °C.

Finally, cells were washed twice with PBS, resuspended with 200 µL PBS/ 1 % BSA and examined using a FACSCalibur flow cytometer (Becton Dickinson, San José, CA, USA). Data analyses were performed using the CellQuest software.

Cytofluorometry was also performed for ascitic fluid cells before and after enrichment (see previous section). Cells were stained for KLK7 with the Arexis and R&D antibodies.

### 4.4. Immunohistochemistry (IHC)

**Antigen retrieval**

Antigen retrieval technique according to the HIER protocol (Heat-Induced Epitope Retrieval) was performed as part of the antibody evaluation process. Briefly, the slides, after deparaffinization, were placed in a plastic rack and put in a household pressure cooker, filled to one-third with 10 mM citrate buffer, pH 6.0. The pressure cooker was brought to the boil point on a hot plate (4 min), placed to cool down (5 min) under running tap water, and then the slides washed twice in TBS (Huang 1996).

**Staining**

IHC was performed on formalin-fixed paraffin-embedded (FFPE) tissue sections. First, deparaffinization and rehydration of the slides was performed by passing the FFPE tissue sections through xylene twice for 10 min at RT and then the slides were exposed to a graded series of ethanol 100 % twice for 5 min to 96 % ethanol once for 5 min and finally to 70 % ethanol for 5 min. Finally, all slides were transferred into TBS.

**Soluble enzyme immune complex technique – APAAP method**

The sections were incubated at 4 °C overnight with the primary antibody diluted in antibody diluent (#S2022, Dako REAL™ Diluent, Dako Hamburg, Germany), followed by a 5-min washing step in TBS. In case a rabbit polyclonal antibody was used as the primary antibody instead of a mouse monoclonal antibody, an intermediate mouse antibody against rabbit IgG (goat anti-rabbit #111-005-003, JIR, Dianova Hamburg, Germany) diluted 1:200 (stock: 1.5 mg) in antibody diluent was applied to all slides and incubated for 30 min at RT. After washes in TBS, a secondary antibody (rabbit anti-mouse IgG, Dako #Z0259) is applied, diluted in TBS/human serum (1:5) at a 1:30 dilution at RT. Subsequent washes for 5 min are followed by incubation with mouse APAAP complex (Dako #D0651, calf intestinal alkaline phosphatase and specific antibody directed to this) for 30 min at a 1:50 dilution (stock: 120 mL, *ready-to-use*) in TBS at RT. After a further washing step in TBS, color was developed choosing one of two different chromogens:

1) Fast Red substrate tablets (Sigma, Munich, Germany) plus 1 mM levamisole for 10 min or
2) Permanent Red plus 1 mM levamisole for 20 min was applied to the slides. Levamisole was used to quench endogenous human alkaline phosphatase activity.

Subsequent to a washing step in TBS, nuclei were counterstained in hematoxylin for 10 seconds and blue-dyed for another 5 min under running tap water. The Fast Red chromogen required the use of aqueous mounting medium without passing through an ascending row of alcohols. Slides treated with Permanent Red chromogen were dehydrated in graded alcohols and mounted with pertex mounting medium (Taylor 2009).

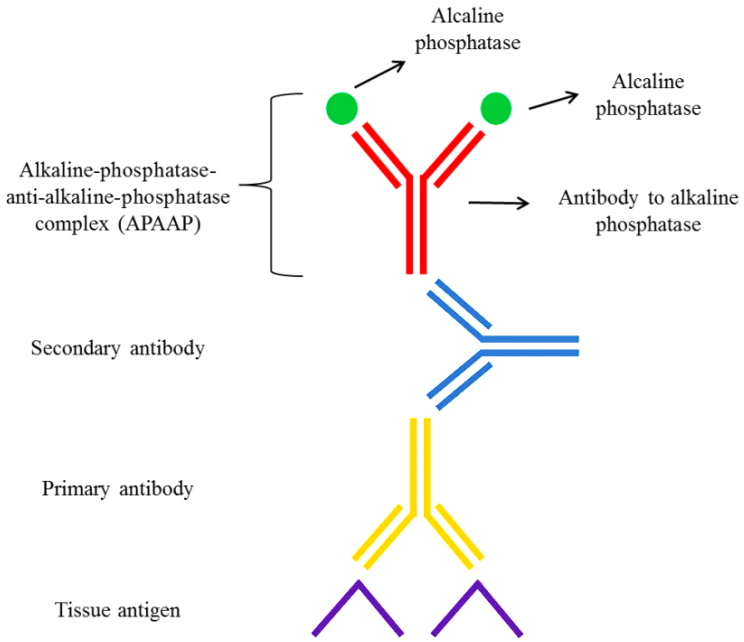


**Figure 3:** Graphic representation of the APAAP (alkaline-phosphatase-anti-alkaline-phosphatase) method. The antigen detection signal is amplified via an enzymatic immunocomplex (2 enzyme units (AP): 1 antibody).

## Streptavidin-biotin technology -LSAB method

First, endogenous biotin activity was quenched by incubating the slides with $H_2O_2$ for 20 min at RT to inhibit endogenous peptidases. Subsequent to a 5-min washing step with tap water and a 5-min washing step with TBS, the streptavidin/ biotin blocking step was installed. The incubation time of streptavidin solution and biotin solution was 15 min, each with a 5-min washing step in between. After another washing step, primary mouse or rabbit antibodies, raised against the target proteins and diluted in antibody diluent, were applied to slides and incubated at 4 °C overnight. Negative control is to test for the specificity of an antibody involved, thus no staining must be shown when omitting primary antibody. The next day a biotin-streptavidin-peroxidase-based detection kit was used subsequent to a 5-min washing step with TBS. The incubation time for the biotinylated link antibody solution (containing goat anti-mouse and anti-rabbit immunoglobulins) and the peroxidase-labeled streptavidin were 30 min each; both were followed by a 5-min washing step. The chromogen used to reveal the labeling was the 3,3´- diaminobenzidine (DAB) for 10 min. After a final washing step, nuclei were counterstained with Mayer's hematoxylin for 10 seconds. Then the slides were rinsed under running tap water, transferred to $H_2O_{dist}$ and mounted.

Dehydration step was performed by passing the slides through an ascending row of graded alcohols (70 % ethanol, 96 % ethanol, 100 % ethanol twice and xylene twice for 5 min each) and mounting the of slides with organic-solvent-based Pertex mounting medium (Taylor 2009).

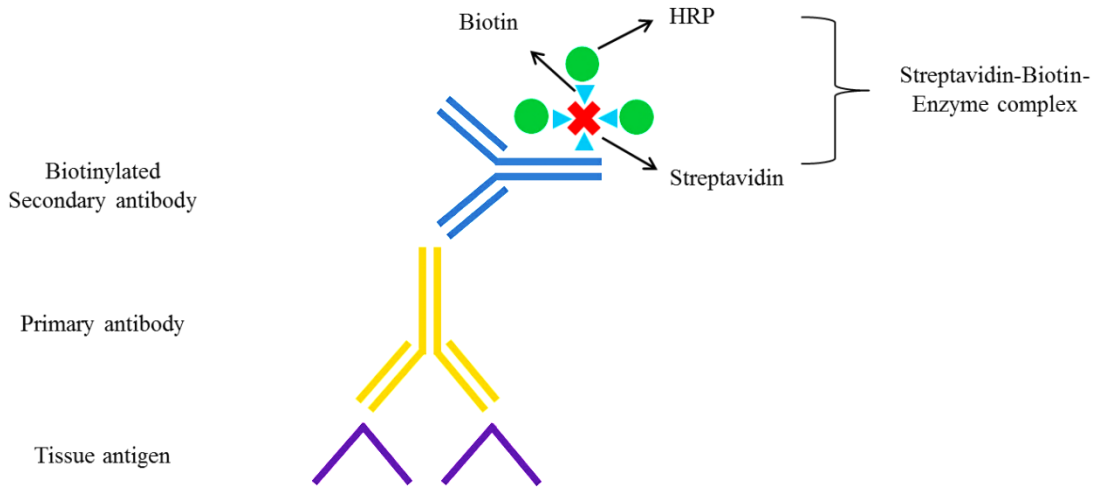


**Figure 4:** Graphic representation of the LSAB method. Signal amplification is achieved via the streptavidin-biotin enzyme complex. Streptavidin shows high affinity to biotin; this property results in an artificial HRP-binding multiplier and eventually in signal amplification.

**Chain polymer-conjugated technology – Dako EnVision system**

FFPE tissue sections (2 µm) were deparaffinized and hydrated by passing them through xylene twice (10 min) and a descending graded series of ethanol (5 min each step) ( see previous §). At this point, sections were treated for antigen retrieval or no antigen retrieval was applied. After a 5-min washing step in TBS at RT including buffer change, endogenous peroxidase activity was quenched by incubating the tissue sections at RT for 5 min with endogenous enzyme block solution (#K5361, DAKO, Hamburg, Germany) , containing 0.5 % hydrogen peroxide, detergents, enzyme inhibitors, and preservative. Subsequent to a 5 min washing step in TBS at RT including buffer change, sections were incubated at 4 °C overnight with the primary antibody, diluted in antibody diluent (#S2022, Dako- contains Tris buffer, 15 mmol/L $NaN_3$ and protein). The procedure resumed the next day with a 5 min washing step in TBS at RT including buffer change. Subsequently, a dextran polymer conjugated with horseradish peroxidase (HRP) and secondary antibodies to mouse plus rabbit primary antibodies was applied. In case of the use of primary goat-anti-KLK7, mouse-anti-goat-IgG (Jackson Immunoresearch, Baltimore, USA) was added as an intermediary step to assign compatibility with the Envision protocol. After an additional washing step, the chromogenic reaction was carried out (RT, 10 min) using the peroxidase substrate 3,3'-diaminobenzidine

tetrahydrochloride chromogen (DAB$^{+}$, K5361, Dako Hamburg, Germany), which forms a brown product at the site of enzyme reaction. After a final washing step, nuclei were counterstained with Mayer's haematoxylin for 10 seconds, rinsed under running tap water, transferred to $H2O_{dist}$ and mounted with mounting medium Histokitt (#1025-250, Assistent, Sondheim, Germany). Stained sections were photographed using a SONY 3CCD COLOR video camera attached to a Zeiss Axioplan 2 microscope and employing the Zeiss AxioVision software 4.5 SP1. Alternatively, slides were scanned by the Aperio Scanscope XT (Aperio, Vista, California, USA) or the Hamamatsu Nanozoomer HT (Hamamatsu Photonics, Herrsching, Germany) slide scanner.

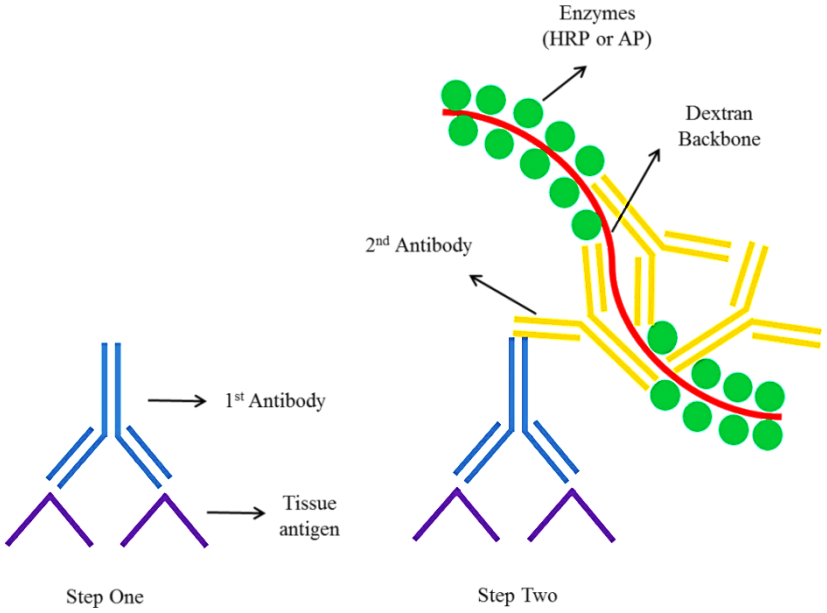


**Figure 5:** Graphic representation of the EnVision system. In this case, a dextran polymer chain with multiple HRP (or AP) molecules attached is employed to achieve greater signal. Despite its great advantage, EnVision could also result in false results due to its high molecular weight (inflexibility). At step one, the primary antibody is employed to detect the tissue antigen. At step two, the polymer chain conjugate reacts with the primary antibody for signal production through an enzymatic chromogenic reaction.

Staining pattern and intensity was evaluated by a pathologist, according to the immunoreactive score method (IRS) according to Remmele, (Beck 1994). Each, tumor cells, normal cells and the extracellular matrix receive a separate score for staining intensity (0-3 scale) and positivity (0-4 scale). IRS (immunoreactive score) occurs when multiplying staining intensity by cell positivity. The lowest score is 0 defining no staining in any of the cells or extracellular matrix,

12 defines a score with strong staining of more than 80 % of the respective cellular or extracellular matrix compartment.

### 4.5. Confocal laser scan microscopy (CLSM)

In order to localize the cellular compartment of KLK7 expression, diverse cell lines (MDA-MB-231, HaCaT, OV-MZ-6 WT, OV-MZ-6 pRc RSV, OV-MZ-6 pRc RSV/KLK7, MCF-7) were harvested and a number of 20,000 cells seeded in each chamber of a 16-well chamberslide, and cells left to grow there for one day (70 % confluency); then cells were fixed with 1 % PFA/ PBS for 15 min at 4 °C. Subsequently, unspecific staining was blocked with 1 % BSA/PBS and then cells were stained for KLK7 protein expression analysis with an antibody from Arexis (stock concentration: 1.36 mg/ mL; Arexis AB, Molndal, Sweden) diluted 1:500 in 1 % BSA/PBS for 1 h at RT. Subsequently, and after washes with PBS, the fluorescently-labeled Alexa-488 IgG (#A-11008; goat anti-rabbit, 1:1000, stock: 2 mg/ mL) was added to react for 30 min at RT in the dark. Finally, after washes, slides were subjected into confocal laser microscopy.

### 4.6. Digitization of histological images and automated image analysis

The Hamamatsu Nanozoomer HT system (Hamamatsu Photonics, Herrsching, Germany) was used to capture whole-slide digital images with 20 x or 40 x objectives. A Positive Pixel Count® algorithm (SlidePath®, Dublin, Ireland) was used to develop a qualitative scoring model for protein expression.

A workflow had been defined to allow high-throughput image analysis of digital slides:

1) Creation of a color definition file to identify positively stained tissue (DAB+, brown color)
2) Selection of algorithm preferences adjusted to the individual ovarian cancer cohort samples under analysis. Settings were tested on field of view images and validation took place through application in multiple test areas. Once test results were confirmed, the modified algorithm module was applied on all digital images for a high throughput analysis.
3) Results from the algorithm include measurements of modal staining intensity (mode value) for positive pixels, and staining concentration within the tissue. Staining intensity

returns values between 0 and 255. A value of '0' represents zero intensity (black) whereas a value of '255' represents maximum intensity (white) in a grayscale intensity range. This output is the modal value of a grayscale intensity histogram of the positively stained pixels.

Staining concentration is the measure of the concentration of the stain within the tissue sample. The staining concentration is calculated using the following formula:

$$\boldsymbol{Concentration} = \frac{\sum_{\boldsymbol{i=0}}^{\boldsymbol{i=31}} [\boldsymbol{h(i)} * \boldsymbol{absorbance(i)}]}{\boldsymbol{Total\ Tissue\ Pixels}} * \mathbf{10000}$$

$$\boldsymbol{Absorbance(i)} = \boldsymbol{ln} \frac{(\boldsymbol{i\ x\ 8 + 4})}{\boldsymbol{Tissue\ threshold}}$$

where:

- **i** is an intensity bin number from 0 to 31
- **h(i)** is the number of positive pixels with intensity i
- **absorbance(i)** is the absorbance at intensity i
- **Total Tissue Pixels** is the total number of tissue pixels in the image
- **Tissue Threshold** is the input tissue threshold intensity
- **% Positive Pixels in Tissue**- Values range between 0 % – 100 %. This output is the percentage of positive pixels in the tissue {SlidePath, 2008 #536}.

Another output is the product of the staining intensity multiplied by the number of pixels stained on the tissue (positivity) (SlidePath 2008). This is comparable with the modified Remmele score (IRS), which was used for the manual scoring by the pathologist.

Operator's decision on the color shading was determinant. Multiple customization options allow exclusion of artifacts and establishment of a more precise evaluation method, based on optical quantification via digital processing.

For automated image analysis of KLK7 staining in ovarian cancer tumor tissue specimens, the software product OpTMA (SlidePath®, Dublin, Ireland) was employed. OpTMA facilitates high-throughput automated image analysis, utilizing positive pixel algorithms; results are presented as quantitative data. The software fully automates the dearraying process of TMAs,

and then automatically associates tissue spots with intensity data. From each tumor sample two to three cores were evaluated, and the mean score values (KLK7-AV) of the readings used for all statistical calculations.

### 4.7. Western blotting

The cell line extracts (20 µg/lane), tissue culture supernatants (30 µg/lane) and tissue extracts (25 µg/lane) as well as recombinant proteins (100 ng/lane) are heated and either reduced (5 min, 95 °C) in the presence of 3 x sample buffer (2 % (w/v) SDS and 5 % (v/v) β-mercaptoethanol) or not reduced (no β-mercaptoethanol). The samples are immediately put into the slots of the stacking gel and separated by 10 % SDS-polyacrylamide gel electrophoresis at 100-150 V. For assessment of the relative molecular mass of the separated proteins, a prestained Protein IV-Marker set (#27-2111, PeqLab; Erlangen, Germany) ranging from 11 to 170 kDa was used.

**Staining of separated proteins in polyacrylamide gels (Coommassie)**

After electrophoresis, gels were incubated for at least 10 min in fixation buffer (5 parts ethanol, 5 parts $H_2O_{dist}$ and 1 part 10 % acetic acid) and then in Coomassie stain solution (0.1 % Coomassie *Brilliant blue* in 10 % (v/v) acetic acid) for 1 h at RT. Next, the gels were washed twice in $H_2O_{dist}$ and then destained in 10 % acetic acid until the protein bands were clearly visible and the background almost colorless. Gels were dried between cellophane sheets for storage.

**Silver staining**

Gels were kept for 30 min in fixation buffer (see § above). After 2 x washes for 5 min in $H_2O_{dist}$, they were treated with Farmer's Reducer for 5 min (20 mL of solution/ gel) followed by several washes with $H_2O_{dist}$. Afterwards, the gels were incubated for 30 min in 0.1 % $AgNO_3$ and then washed for 30 seconds in $H_2O_{dist}$. Gels were left in development buffer for 3 to 10 min (20 mg/ mL) and the reaction stopped by addition of 10 % acetic acid. Finally, the gels were left for 10 min in glycerol buffer, then wrapped with gelatin sheets and left to dry.

**Reducing buffer (Farmer's Reducer)**
16 g $Na_2S_2O_3$ dissolve 10 mg in 100 mL $H_2O_{dist}$ just before use
10 g $K_3F_3(CN)_6$

**Developing buffer**▪
2,5 % $Na_2CO_3$ up to 1 L $H_2O_{dist}$
Add 1 ‰ volume formaldehyde 37 % just before use **-toxic!**

**$AgNO_3$ 0.1 %**
Add 1 g $AgNO_3$ in 1L $H_2O_{dist}$ -***protect from light***

## Western blotting and immunodetection

Proteins, separated by SDS-PAGE, were transferred onto a polyvinylidene fluoride membrane (PVDF, PALL; Dreieich, Germany; 3 h at 75 mA/membrane), applying a semi-dry transfer device (Whatman Biometra; Göttingen, Germany). After transfer, membranes were blocked with 5 % skimmed milk powder (#70166, Fluka; Munich, Germany) in PBS-0.1 % Tween-20 (pH 7.4, 1 h, RT). Subsequently, blots were incubated overnight at 4 °C with different primary antibodies against either His-Tag (anti$(His)_5$, 0.1 µg/mL), Tag-100 (anti-Tag100, 0.1 µg/mL) or the target protein, diluted in incubation buffer, and then washed three times (10 min, RT) with PBS-0.1 % Tween-20. Antigen-antibody complexes were visualized using HRP-conjugated goat anti-rabbit IgG (Jackson ImmunoResearch; #111-035-003, Dianova, Hamburg, Germany), HRP-conjugated rabbit anti-mouse IgG (Dianova; #315-035-045, Hamburg, Germany) or HRP-conjugated rabbit anti-chicken IgG (#A-9046; Sigma-Aldrich, Munich, Germany), diluted 1:10,000 in 5 % skimmed milk powder in PBS-0.1 % Tween-20, followed by chemiluminescent reaction (ECL, Amersham Biosciences; Little Chalfont, UK). Glyceraldehyde-3-phosphate dehydrogenase (GAPDH) was used as an internal control. The same blots were incubated with mouse anti-GAPDH (#MAB374; Chemicon, Billerica, MA, USA), after stripping the membranes in 1.5 % w/v glycine, 0.1 % w/v SDS, and 1 % Tween-20; pH 2.2, for 1 h at RT.

## Immunoprecipitation of KLK7 from cell and tissue extracts

For the enrichment of KLK7 from cell lysates or tissue extracts, the extracts were pre-cleared by incubation with protein G-agarose beads (Roche Diagnostics GmbH, Mannheim, Germany) overnight at 4 °C and after centrifugation the supernatant incubated with goat-anti-KLK7 (#AF2624, R&D Systems, Abingdon, UK) or rabbit-anti-KLK7 (#Tagena+Domino, Arexis AB, Molndal, Sweden), 2 h, 4 °C at 2.72 µg/mL. Subsequently, protein G-agarose beads were

added, and then the suspension incubated overnight at 4 °C with gentle agitation. After extensive washing of the beads with RIPA buffer, attached KLK7 proteins were eluted from the beads by boiling in SDS-PAGE sample buffer, followed for separation by SDS-PAGE and detection by western blotting, using KLK7-directed rabbit- and goat antibody, respectively.

### 4.8. Enzyme-linked immunosorbent assay (ELISA)

KLK7 antigen concentrations were determined in the supernatant using a non-commercial in-house ELISA test format (Paliouras and Diamandis 2006). For this, polyclonal capture antibodies and detection antibodies to KLK7 immunogen were generated by immunizing mice with recombinant human KLK7. Detection limits of the KLK7-ELISA: 0.2–10 ng/mL (Paliouras and Diamandis 2006). In this ELISA format, no cross-reactivity with any other member of the human tissue kallikrein family was detected. KLK7 antigen values were expressed as ng/mg of protein, which was determined in the tissue extracts by the Pierce BCA method (Kuhn 1999).

**Assessment of KLK7**

To test for binding capacity of KLK7-directed antibodies, microtiter plates Nunc (#456537, Nunc-Immuno-F96 Maxisorp, Thermo Fischer Scientific, Langenselbold, Germany) were coated with various concentrations of recombinant KLK7 diluted in TBS (American Diagnostica Inc., Pfungstadt, Germany)/ 1 % BSA (Sigma, Munich, Germany). Plates were incubated overnight at 4 °C, washed with TBS/ 0.1 % Triton X-100/ 0.05 % Tween-20 and then blocked with TBS/ 2 % BSA. Subsequently, horseradish peroxidase-conjugated rabbit-anti-mouse-IgG (Dianova, Hamburg, Germany) or mouse-anti-goat IgG (Jackson Immunoresearch (Dianova), Hamburg, Germany) or mouse-anti-rabbit-IgG (Jackson Immunoresearch (Dianova), Hamburg, Germany) was added to the wells (45 min, 20-21 °C) and reaction visualized by use of the chromogenic substrate TMB (3, 3', 5, 5'-tetramethylbenzidine) (#50-76-03, KPL, Gaithersburg, MD, USA). The reaction was stopped by addition of 2 N $H_2SO_4$ and absorption recorded at 450 nm.

### 4.9. DNA extraction

The isolation of total genomic DNA from cultured cell lines followed the respective protocol included in the QIAamp DNA Mini and Blood Mini Handbook (version November 2007) and it

was performed by use of the QiaCube microcentrifuge. Briefly, 5 x $10^6$ cells were harvested and resuspended with 200 µL PBS. Then, 20 µL proteinase K were added and subsequently 200 µL of buffer AL with 15 seconds of vortexing. The samples were incubated for 10 min at 56 °C and placed in the Qiacube according to manufacturer's instructions. The procedure in QiaCube is based on a set of lysis and wash buffers through sequential spinnings of filter columns.

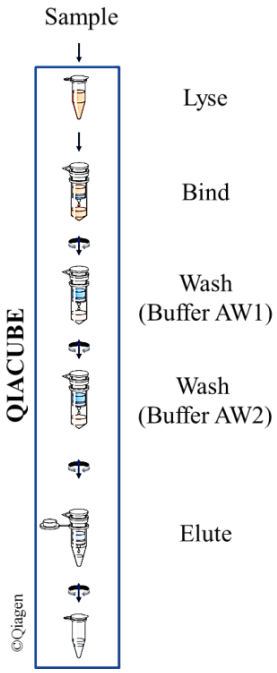


**Figure 6:** Graphic representation of the fully automated DNA purification procedure by use of QiaCube. The procedure is highly based on sequential spinnings of filter columns, on which the samples are loaded. Special lysis and wash buffers complete the procedure.

DNA from tissue samples (TNBC collective) was prepared from nuclear fractions of ultracentrifuge spins obtained from these tumor tissues using the QIAamp DNA Mini Kit (Qiagen, Germany), in a similar pattern as for the cells.

### 4.10. RNA extraction

Total RNA was isolated from human cancer cell lines (HaCaT, MCF-7, MDA-MB-435, OV-MZ-6, OVCAR-3), using the *RNeasy Mini Kit* (Qiagen, Hilden, Germany) following the manufacturer's instructions. Briefly, cells (max. $10^7$) grown in monolayer were detached from the flask surface using 0.05 % EDTA/PBS and collected as a pellet. Pelleted cells were disrupted by adding the appropriate volume of RLT buffer and homogenized by passing the

lysates at least 5 times through a blunt 20-gauge needle fitted to an RNase-free syringe. One volume of 70 % ethanol was added to the homogenate and the sample transferred after mixing to an RNeasy spin column and centrifuged for 15 seconds at 8,000 x g. As a next step, 700 µL RW1 buffer was added and the samples centrifuged once more for 15 seconds at 8,000 x g. Subsequently, 500 µL RPE buffer was added to the RNeasy spin column which was then centrifuged for 15 seconds at 8,000 x g to wash the spin column membrane. This step was performed twice. Lastly, the RNeasy spin column was placed in a 1.5 mL collection tube, 30–50 µL RNase-free water was directly added to the spin column membranes which were centrifuged for 1 min at 8,000 x g to elute the RNA.

Purity and concentration of RNA was determined by measuring the A260/A280 ratio in a Nanodrop device.

### 4.11. PCR-based amplification of DNA

Before proceeding with the real-time quantitative PCR, the set of primers designed to detect the KLK7 gene (as well as the neighboring KLK6 and KLK8 genes) was tested using different cancer cell lines as the starting material. The same cell samples were also analyzed for expression of the housekeeping gene HPRT. For amplification of DNA fragments (100 ng template) recombinant Taq DNA polymerase (#10342-053; Invitrogen GmbH, Darmstadt, Germany) was used.

| | **Step** | **Duration** | **Temperature** |
|---|---|---|---|
| | Initial denaturation | 3 min | 94.0 °C |
| **40 cycles** | Denaturation | 30 sec | 94.0 °C |
| | Annealing | 1 min | 58.0 °C |
| | Elongation | 1 min | 72.0 °C |
| | Final elongation | 8 min | 72.0 °C |
| | Cooling down | infinite | 4.0 °C |

**Primers**

**KLK7_last exon:**
Primer_F TCTCCGGCTCTATTCCCTCT
Primer_1_R GCGATGCTTTTTCATGGTGT
**KLK6_last exon**
Primer_1_F TCTTTCCTGCAGGGTGATTC
Primer_1_R GTCACTTGGCCTGAATGGTT
**KLK8_last exon**
Primer_3_F GAAGCTCCCCAGGCTCTAGT
Primer_3_R AGCAGGAACATCCACGTCTT

**e-PCR selected:**
Forward primer: ATGCACAGGAGTGAGGACG
Reverse primer: GATTGGTTTATCAACAGGGCA
**HPTR1:**
Forward primer: TATTGTAATGACCAGTCAACAG
Reverse primer: GGTCCTTTTCACCAGCAAG

**Amplicon sizes**: KLK7 (175 bp), KLK6 (167 bp), KLK8 (377 bp), eKLK7 (100 bp), HPRT1 (1435 bp)

**Mastermix** (for one reaction)

| | **Volume** | **Final concentration** | **Company** |
|---|---|---|---|
| 10 x PCR buffer (-$MgCl_2$) | 5 µL | 1 x | Invitrogen |
| $MgCl_2$ (50 mM) | 1.5 µL | 1.5 mM | Invitrogen |
| dNTPs (10 mM) | 1 µL | 0.2 mM | Invitrogen |
| primer F (10 µM) | 1 µL | 0.2 µM | Metabion |
| primer R (10 µM) | 1 µL | 0.2 µM | Metabion |
| Taq polymerase (5 U/µL) | 0.4 µL | 2 units | Invitrogen |
| Template DNA | 100 ng | | Invitrogen |
| Autoclaved $H_2O_{dist}$ | up to 50 µL | | |

**PCR PROTOCOL FOR HPRT**

| | **Step** | **Duration** | **Temperature** |
|---|---|---|---|
| | Initial denaturation | 3 min | 94.0 °C |
| **40 cycles** | Denaturation | 30 sec | 94.0 °C |
| | Annealing | 1 min | 57.0 °C |
| | Elongation | 1 min | 72.0 °C |
| | Final elongation | 8 min | 72.0 °C |
| | Cooling down | Indefinite | 4.0 °C |

**Primers**

HPRT1 forward: 5'-tat tgt aat gac cag tca aca-3'
HPRT1 reverse: 5'-ggt cct ttt cac cag caa g-3'

**Amplicon size**: 192 bp

## 4.12. DNA agarose gel electrophoresis

DNA fragments were separated electrophoretically on horizontal agarose gels (peqGOLD agarose; PEQLAB Biotechnology GmbH, Erlangen, Germany). The concentration of agarose gels was 1.5-2 % in TAE buffer including 10 µL of ethidium bromide (stock solution 10 mg/mL) in 100 mL. The DNA samples were mixed with 5 x DNA loading buffer (0.1 M EDTA; 50 % w/v saccharose; 0.1 % w/v bromophenol blue and 0.1 % v/v xylenecyanol FF in $H_2O_{dist}$, pH 8.0) and applied to the gel that was subsequently run at 9 $V/cm^2$ in TAE buffer. The fragments were visualized and documented upon UV illumination using UV solo (Biometra, Göttingen, Germany) peqGOLD 100 bp DNA ladder served as a marker (PEQLAB Biotechnology GmbH, Erlangen, Germany).

## 4.13. Taqman technology

### Bisulfite DNA conversion

The Bisulfite conversion procedure took place according to manufacturer's guidelines (Qiagen Epitect, Qiagen, Hilden, Germany). Briefly, in aliquots of Bisulfite Mix, 800 µL RNase-free water were added. Then bisulfite reactions in 200 µL PCR tubes were prepared, where the combined volume of DNA solution and RNase-free water was 20 µL (DNA solution 1 ng-2 µg and the rest water), 85 µL of Bisulfite mix and 35 µL of DNA Protect Buffer, in a total volume of 140 µL per reaction tube. After mixing, the DNA Protect Buffer should turn from green to blue. The bisulfite DNA conversion was then performed using a thermal cycler:

| Step | Duration | Temperature |
|---|---|---|
| Denaturation | 5 min | 99 °C |
| Incubation | 25 min | 60 °C |
| Denaturation | 5 min | 99 °C |
| Incubation | 85 min (1h 25 min) | 60 °C |
| Denaturation | 5 min | 99 °C |
| Incubation | 175 min (2h 55 min) | 60 °C |
| Hold | Indefinite (∞) | 20 °C |

Once the bisulfite conversion was complete, the PCR tubes containing the bisulfite reactions were centrifuged and then transferred into 1.5 mL microcentrifuge tubes. Using the DNA-clean-up program of the Qiacube, bisulfite-converted DNA was cleaned via subsequent cycles of buffer washes (carrier DNA buffer, wash buffer, desulfonation buffer, and elution buffer) and centrifugations.

### Realtime methylation- specific-PCR

Bisulfite-converted DNA was analyzed in duplicates by the MethyLight technique as described previously (Eads 2000), employing the ABI PRISM 7000 Sequence Detection System instrument and software (Applied Biosystems, Inc., Foster City, CA, USA). The process has been previously described (Napieralski 2007). Briefly, methylation-specific realtime PCR for the metastatic genes uPA and PAI-1 was performed in a final volume of 20 µL including 10 µL 2 x Quantitect Probe mastermix (Qiagen), 2 µL bisulfite-treated DNA, and assay-defined primer and probe concentrations. For normalization of input of bisulfite-converted DNA, an Alu1 reference system was used, containing a DNA-methylation status-independent consensus

sequence of the most common Alu1 repeat families. The experiment included a no-template control and a positive control with known DNA-methylation status. SssI-treated human chromosomal DNA (Qiagen) was used as a reference for fully methylated cytosine status, defining 100 % methylated reference (PMR) values for the normalization of samples. With Quantitect Buffer the cycle conditions were:

| | Step | Duration | Temperature |
|---|---|---|---|
| | Taq activation | 15 min | 95 °C |
| **45 cycles** | Denaturation | 15seconds | 95 °C |
| | Annealing | 1 min | 60 °C |

**Table 14:** Set of primers and probes employed for DNA methylation studies.

| Gene primer and probe | Sequence 5'-3' | PCR product | Reference Sequence | Reference |
|---|---|---|---|---|
| **uPA** | | 74 bp | X02419.1 791-717 | (Pakneshan 2005) |
| **Forward** | TTGTAAGATAGGGGAGGGAGT | | | |
| **Reverse** | ACICCTACTCTATATCAAAACCC | | | |
| **Probe** | FAM-CGTCGGGGCGGGTT-BHQ1 | | | |
| **PAI-1** | | 81 bp | X13323.1 871-952 | (Gao 2005) |
| **Forward** | GTAGTTGAATTTTTGTAGTTTAGTAGT | | | |
| **Reverse** | TCTACATCCTAAAATTCTCAAAAATAC | | | |
| **Probe** | FAM-TTAGAGTAGGACGAATCGTTAATCGT – BHQ1 | | | |
| **Alu 1** | | 98 bp | Consensus sequence | (Weisenberger 2005) |
| **Forward** | GGTTAGGTATAGTGGTTTATATTTGTAATTTTAGTA | | | |
| **Reverse** | ATTAACTAAACTAATCTTAAACTCCTAACCTCA | | | |
| **Probe** | VIC-CCTACCTTAACCTCCC-MGB | | | |

**Note:** Primer and probe concentrations were as follows: uPA, 600 nmol/L primer/200 nmol/L probe; PAI-1, 600 nmol/L primer/200 nmol/L probe; and Alu1, 300 nmol/L primer/100 nmol/L probe.
**Abbreviations:** BHQ: Black Hole Quencher; MGB: Minor Groove Binder

Results were analysed using the Relative Quantitation (ΔΔCt) method (Livak and Schmittgen 2001). Relative quantification determines the changes in steady-state mRNA levels of a gene across multiple samples and expresses it relative to the levels of an internal control RNA. Calculations are based on the comparison of the distinct cycle determined by threshold values (Ct) at a constant level of fluorescence (difference between threshold values, **ΔCt**):

$$\mathbf{R = 2^{-\,[\Delta Ct\ sample\ -\ \Delta Ct\ control]} = 2^{-\,\Delta\Delta Ct}}$$

Difference between treated with demethylated agent (Decitabine) cell lines versus untreated is symbolized by the difference in their multiplication threshold values ($\Delta\Delta$**Ct**).

**Relative quantification (qRT-PCR) of KLK7 –Lightcycler (Holzscheiter 2006)**

Total RNA from tissue samples was isolated with the RNeasy Mini Kit (Qiagen, Hilden, Germany) according to the manufacturer's protocol. For quantification of KLK7 mRNA, we established a highly sensitive QPCR assay applying the LightCycler technology (Roche Diagnostics, Penzberg, Germany; software Ver. 3.5). On the basis of the cDNA sequence of KLK7 (GenBank accession no. L33404), we designed the following gene-specific primers (amplicon length, 108 bp): forward primer, 5-GGA AAC TGC AGG AGA AGA AGC-3; reverse primer, 5-TGG AGC TGA TTG CCA CTG A-3.

Real-time monitoring of PCR was performed with hybridization probes with the following sequences: 5- GGT GGG AGC CTC TTG CAC ATG G-fluorescein-3; 5-LC Red640-CGC CAT CAA TAA TCT TGT CAC CCTG-phosphate-3.

We obtained primers and hybridization probes from TIB Molbiol (TIB Molbiol Berlin, Germany). Reverse transcription-PCR was performed with an optimized master mixture containing 4.5 mM $MgCl_2$, 0.5 μM each primer, and 0.2 μM each hybridization probe in a total volume of 20 μL. The amplification program started with pre-denaturation at 95 °C for 10 min, followed by 45 cycles of amplification (denaturation for 10 seconds at 95 °C, annealing for 10 seconds at 64 °C, and elongation for 6 seconds at 72 °C). To verify the results of the QPCR measurements, randomly selected samples were run on 1.5 % agarose gels and sequenced after purification. We generated 5-log-range calibration curves for each PCR run by use of 8 glass capillaries coated with defined numbers of linearized plasmid molecules carrying the KLK7 cDNA (pRcRSV-KLK7). The plasmid molecule numbers had been exactly determined by HPLC calibration (Roboscreen, Leipzig, Germany). The glass capillaries were coated with 10, 20, 50, 100, 1,000, 5,000, 10,000, and 100,000 copies, respectively.

We selected human glucose-6-phosphate dehydrogenase (h-G6PDH) for normalization of the data. The h-G6PDH Housekeeping Gene Set (Roche Diagnostics, Penzberg, Germany) was used according to the manufacturer's protocol (amplicon length 123 bp). All further

calculations and statistical analyses were carried out with the relative mRNA expression ratios (zmol KLK7/amol h-G6PDH).

**High resolution melting (HRM) analysis and Multiplex Ligation-dependent Probe Amplification (MLPA) (Gross 2011)**

After DNA extraction and bisulfite conversion (Epitect Bisulfite Kit, Qiagen), the promoter region of *BRCA1* was amplified by specific primers (forward: 5'-TATTTTGAGAGGTTGTTGTTTAG-3'; reverse: 5'-TATCTAAAAAACCCCACAACCTATC-3') covering a region earlier described by Esteller et al. (Esteller 2000). The methylation status was quantified by methylation-specific high resolution melting (MS-HRM) analysis (Epitect HRM PCR Kit, Qiagen) by use of Lightcycler 480-instrument (Roche, Penzberg, Germany). Melting curves were generated and analysed with the Gene Scanning software module. Normalized melting curves of the tumor samples were compared to serial dilutions of fully methylated and bisulfite converted control DNA (Epitect Control DNA, Qiagen), while unmethylated DNA from blood lymphocyte DNA of a healthy donor was employed for diluting the methylated control DNA.

The detection of *BRCA1* mutations was performed by HRM analysis of the entire coding region of the *BRCA1* gene on a Lightcycler 480 instrument. Forty-one (41) M13-tagged PCR primer pairs (van der Stoep 2009) were employed, data analysis was accomplished by use of the Gene Scanning module and normalized melting curves were visualized as Difference Plots. Samples with differences were subsequently subjected into sequencing analysis.

MLPA (Multiplex Ligation-dependent Probe Amplification) is a multiplex PCR method detecting abnormal copy numbers of up to 50 different genomic DNA or RNA sequences, which is able to distinguish sequences differing in only one nucleotide. The MLPA for BRCA1 (MRC-Holland, Amsterdam, The Netherlands) contains 25 probes for *BRCA1*, and 9 control probes specific for DNA sequences outside of *BRCA1*. MLPA was performed as described before (Schouten 2002). The relative peak area was calculated by dividing the mean of the peak areas of the control probes of each sample, by the mean of the peak areas of the control probes of all the samples. Subsequently, the relative peak area of each *BRCA1* probe was divided by the average relative peak area of this probe in all the tumor samples. In unaffected control

individuals this will result in a value of 1 (100%) representing two copies of the target sequence in the sample.

## 4.14. Protein array technology

### Deparaffinization and Protein Extraction from Slide-Mounted FFPE Sections

The method was performed according to the manufacturer's guidelines (Qproteome FFPE, Qiagen, Hilden, Germany). Briefly, slides were transferred into a staining dish containing xylene and incubated for 10 min at RT (2 x). Subsequently, slides passed through an alcohol-degraded row, namely 100 % ethanol, 96 % ethanol and 70 % ethanol. The deparaffinization process ends with $H_2O_{dist}$ immersion for 30 seconds. Areas of interest were excised from the slide and transferred into 1.5 mL collection tubes. Addition of 100 µl of extraction buffer (EXB), vortexing and incubation on ice for 5 min were followed by incubation on a heating block at 100 °C for 20 min and incubation at 80 °C for 2 h with agitation at 750 rpm using a Thermomixer. Finally, tubes were exposed to 4 °C for 1 min and then centrifuged for 15 min at 14,000 x g at 4 °C. The extracted proteins were isolated in the supernatants.

### Reverse phase protein microarrays (RPMA)

RPMAs are immobilized protein spots utilized for quantitative immunochemical detection. This allows a very accurate determination of the amount of protein. The protein lysates of interest were spotted on a nitrocellulose-coated glass slide, followed by incubation with the primary antibody. Detection was carried out by an enzyme-coupled secondary antibody together with its target substrate. Samples were immobilized and detected on a tape strap. Per lysate a 6-fold dilution curve in 4 replicates was spotted. For normalization of the antibody signals the slide was stained with a total protein detection reagent, SYPRO® Ruby stain. Subsequently, the detection antibody was applied. Fluorescence emitted from the reaction is measured and normalized to the total protein pre-stained slide by use of a specifically developed algorithm (Malinowsky 2010).

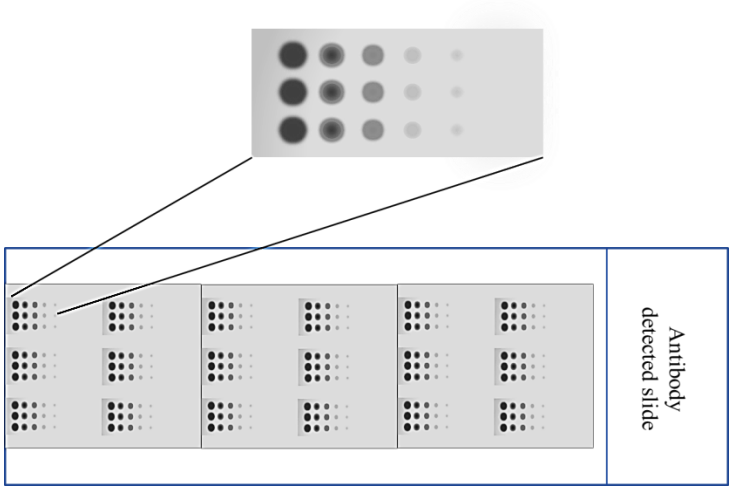


**Figure 7**: Protein lysates as spotted on nitrocellulose-coated glass slides. Proteins can be detected by an antibody assay similar to a western blot analysis. Each sample is spotted in triplicate and in a six-step dilution series to ensure the quantitative measurement of the target protein in the linear detection range.

## 4.15. Xcelligence technology

### Principle

Xcelligence is a cell-based assay system (Roche Diagnostics, Penzberg, Germany), which takes advantage of the impedance phenomenon to quantify cell populations in real time. The principle is clearly described in the manufacturer's guidelines. Briefly, cell chambers with electrodes attached are placed in the incubating device, which supplies the system with electricity. The presence of the cells on top of the electrodes affects the local ionic environment at the electrode/solution interface, leading to an increase in the electrode impedance. The more cells are attached to the electrodes, the larger the increases in electrode impedance. Thus, electrode impedance, which is displayed as cell index (CI) values, can be used to monitor cell viability, number, morphology, and adhesion degree in a number of cell-based assays. When cells are not present or are not well adhered to the electrodes, the CI is zero. Under the same physiological conditions, when more cells are attached to the electrodes, the CI values are larger. Thus, CI is a quantitative measure of cell number present in a well. Additionally, change in a cell status, such as cell morphology, cell adhesion, or cell viability will lead to a change in CI.

**Proliferation assay**

All the cells used in this study were the same as mentioned in Table 5 and maintained in a 37 °C incubator with 5 % $CO_2$ saturation. Cells were maintained in DMEM media containing 5 % FCS, HEPES and aminoacids.

For each cell type, the indicated number of cells/well (10,000 cells) was seeded untreated into 100 µL of media in 16 x well microtiter plates (E-Plate) and let grow for 5 h. Then, half of the cells were treated with Decitabine (1 µL + 29 µL fresh medium). The attachment, spreading and proliferation of the cells were monitored every 30 min using the RTCES® system. Cell proliferation was monitored for 50 h for two separate experiments.

# 5. Results

## 5.1 Use of specific antibodies to determine KLK7 protein expression by

KLK7 has been assessed by many researchers by use of various methods. In breast cancer by RT-PCR (Talieri 2004; Holzscheiter 2006), in cervical cancer by RT-PCR and by IHC (Santin 2004a; Tian 2004), in lung cancer by RT-PCR and by ELISA (Planque 2005; Planque 2008b), in brain cancer by RT-PCR (Prezas 2006b), in oral squamous cell carcinoma by IHC (Zhao 2011), in pancreatic cancer by RT-PCR (Johnson 2007) and in colorectal cancer by RT-PCR and by IHC (Talieri 2009b).

There are several methods employed in the literature to investigate KLK7 protein expression in ovarian cancer collectives (ELISA (Kyriakopoulou 2003; Shan 2006), immunofluorescence (Psyrri 2008)), but never by use of traditional immunohistochemistry. It was, therefore, crucial to discover the appropriate immunohistochemical tools for a thorough study on KLK7 expression in ovarian cancer.

Control assays help us to investigate the capability of an antibody to reveal protein expression. It is, however, of high significance to evaluate our biochemical tools before concluding on antibody performance. Recombinant proteins and antibodies were subjected into numerous conditions by means of Western blotting in order to simulate the actual microenvironment conditions of the formalin-fixed paraffin-embedded tissue specimens. Our goal was to obtain finally those performance indications leading to robust antibodies for immunohistochemical assessment. A reliable immunohistochemical score would contribute an additional biological parameter in the clinical study of KLK7 role in ovarian cancer patients.

KLK7 protein is essential as a reference for IHC and other assays , a fact that led us to evaluate appropriate tools (antibodies) available on the market, but also to generate own antibodies by immunization of rabbits.

### Recombinant KLK7 structure

Recombinant KLK7, harboring an N-terminal $(His)_6$-tag followed by an EK site, was expressed in E. coli and purified as described previously for KLK4 (Debela 2006a). Briefly, for the production of recombinant KLK7, the sequence encoding the mature protease (excluding the

signal- and the activation peptides) was amplified from cDNA originating from keratinocytes and fusion gene were generated encoding a synthetic pro-form of KLK7 with an N-terminally located histidine-tag followed by an enterokinase cleavage site. Transformed E. coli cells, induced with IPTG, produced high amounts of recombinant (nonglycosylated) protein. Recombinant KLK7 protein was purified under denaturing/ slightly reducing conditions and refolded subsequently in decreasing concentrations of urea, ranging from 8 until 2 M (Debela 2006b; Debela 2008).

In addition, expression plasmids encoding native pro-forms of KLK proteases (KLK2 to KLK15) plus an N-terminally located histidine-tag and a C-terminal Tag100 epitope were generated and used for production for the respective recombinant pro-forms.

Expressed (nonglycosylated) proteins were purified via their histidine-tag by nickel-nitrilotriacetic acid agarose affinity chromatography (Qiagen, Hilden, Germany) under denaturing/slightly reducing conditions. Subsequently, refolding procedures were employed, using reduced and oxidized glutathione as redox reagents (Sigma, Deisenhofen, Germany) in order to promote protein renaturation.

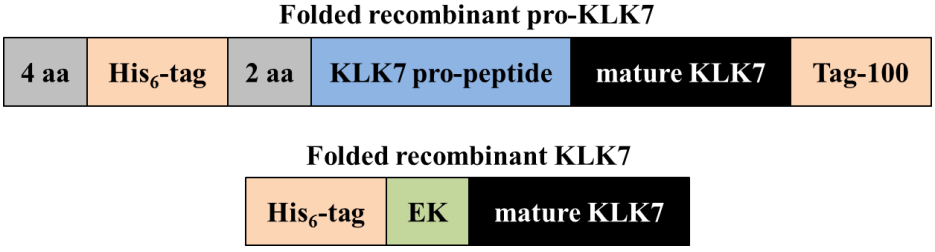


**Figure 8:** Graphic representation of the folded recombinant pro-KLK7 and of the folded recombinant KLK7, used for the evaluation of the antibodies. Their major structural differences are (a) the missing pro-peptide in the KLK7 structure, which is replaced by an enterokinase cleavage site for potential activation and (b) the additional tag in the pro-form, the Tag-100.The Tag-100 epitope is a sequence from mammalian MAP kinase 2 consisting of 12 amino acids. The $His_6$-tag allows immobilization of the proteins to $Ni^{2+}$-NTA columns. The orientated immobilization of the protein means that the Tag-100, which is positioned at the opposite end of the protein, is easily accessible and readily detected by the Tag-100 antibody (#34680, Qiagen, Hilden, Germany) which recognizes the Tag-100 epitope.

**Western blotting under reducing/non-reducing conditions**

It was crucial to initially determine the expected size of our in-house produced recombinant proteins as well as their optimum loading concentration. Silver staining was, therefore, selected, while SDS-PAGE comparing preforms to mature forms under reducing versus non-reducing conditions provided a clear image of the recombinant protein detection by the antibodies directed to KLK7.

Recombinant KLKs were subjected to classical Western Blot testing as a first step for concentration estimation, before evaluating the KLK7 antibodies. Silver staining was selected for its higher sensitivity to conclude on the appropriate protein concentration loading. Starting from a concentration of 500 ng/well, we were able to detect clear bands under reducing conditions with the proform located at 25 to 35 kDa, whereas folded recombinant KLK7 was detected at a lower band level (around 25 kDa). When proteins were subjected at the non-reducing setting (without β-mercaptoethanol), a faint signal was detected only.

A second control step referred to the original structural design of the recombinant proteins. A mouse antibody directed to $(His)_5$, the pentamer located only in the proform, was employed as part of the immunoblotting procedure and indicated indeed the presence of the pentamer (reducing conditions). The same situation occurred when a mouse antibody directed to the Tag-100 was employed at the same setting, only proforms revealed its presence. As far as non-reducing conditions are concerned, no proform was detected, possibly because the secondary protein structure hinders the binding of the antibody.

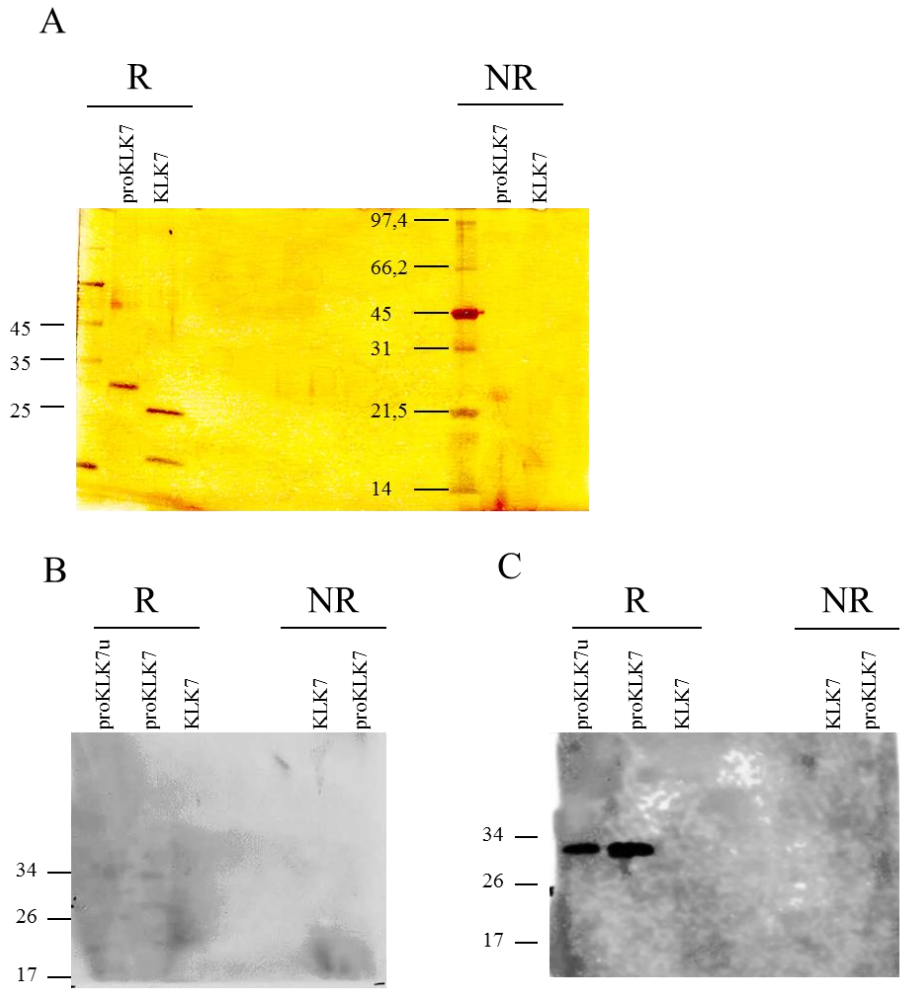


**Figure 9**: Silver stained blots **(A)** where higher sensitivity allowed 500 ng/ well loading. This fact permitted a rough estimation of the recombinant proteins' concentration under reducing and non-reducing conditions. Under reducing conditions, proKLK7 is located around 27 kDa, whereas KLK7 displays a band around 25 kDa. Under non-reducing conditions, faint bands reveal presence of proKLK7 at 25 kDa, but no clear presence for KLK7. **(B)** Immunoblotting with an anti-$(His)_5$ (0.1 μg/mL) or **(C)** with an anti-Tag-100 (0.1 μg/mL) revealed the presence of the Tag-100 only in the proforms. The anti-His detected all forms- faint bands between 20 and 30 kDa. Antibodies did not react under non-reducing conditions. First lanes from the left display the proKLK7 in denatured form, maintained in urea, whilst second lanes represent proteins left to refold. Protein samples loaded for **(B)** and **(C)** 100 ng/well. Chemiluminescent radiography, film exposure 6 min. Legend: R=reducing conditions, NR= non-reducing conditions.

All eight antibodies directed to KLK7 were subjected to immunoblotting at the following setting: a KLK7 proform, a KLK7 proform left to refold in urea and an enzymatically active KLK7 form (**Figure 10**). All proteins were tested under reducing and non-reducing conditions. Results revealed that best performing antibodies were able to detect all forms in every setting.

This refers to four antibodies, i.e. ABR , R&D, Arexis and one of the antibodies received from Diamandis' lab (Tanimoto 1999). The anti-KLK7 clone 83-1/Diamandis (mouse) recognizes only the active enzyme under non-reducing conditions and from the three antibodies purchased from Santa Cruz, E-16 (goat) recognizes the proform and the active enzyme only under reducing conditions and H-50 (rabbit) recognizes the proform under non-reducing conditions. This has been the third step to identify the best performing antibodies. Active forms, however, display an additional lower band (app. 20 kDa) under reducing conditions, potentially a degradation product. Degradation might be the result of higher temperature or changes in pH.

**Table 15** summarizes reactivity results for every antibody tested.

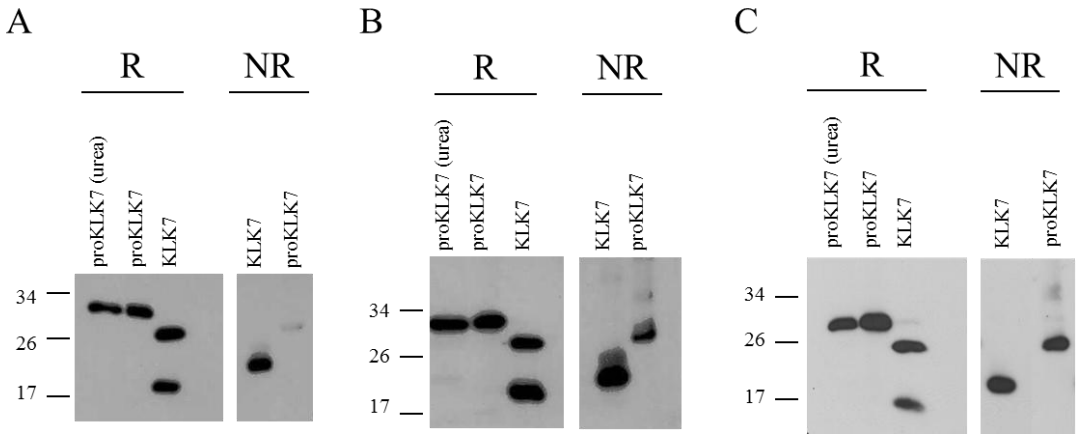


**Figure 10**: Immunoblotting of KLK7 antibodies to recombinant KLK7 protein forms. **(A)** Affinity Bioreagents, **(B)** R&D systems and **(C)** Arexis antibody. Under reducing conditions, proKLK7 (left to refold slowly in urea) was used together with the refolded proform and the active KLK7 enzyme. In all cases, the antibodies were able to detect all KLK7 forms under reducing conditions. Active KLK7 reveals a degradation product at a lower position of 20 kDa due to non-reducing conditions. All samples 100 ng/well. Chemiluminescent radiography, film exposure 13 min. Antibody concentration: ABR PA1-8435 0.5 µg/mL, R&D AF2624 0.2 µg/mL, Arexis Tagena+Domino 0.68 µg/mL. Legend: R= reducing conditions, NR= non-reducing conditions.

This kind of evaluation, testing varying conditions, was prerequisite before employing antibodies for immunohistochemical assessment. Tissue specimens may display change in conformation due to formalin fixation; therefore, antibodies were tested under these conditions.

**Table 15**: Antibodies directed to different KLK7 forms tested under reducing and non-reducing conditions in Western blot. Legend: R= reducing conditions, NR= non-reducing conditions.

| Antibody | Source | Species | Reactivity with pro-KLK7 (R) | Reactivity with KLK7 (R) | Reactivity with pro-KLK7 (NR) | Reactivity with KLK7 (NR) |
|---|---|---|---|---|---|---|
| **H-50** | Santa Cruz | rabbit | - | - | + | - |
| **C-15** | Santa Cruz | goat | - | - | - | - |
| **E-16** | Santa Cruz | goat | + | + | - | - |
| **AF2624** | R&D | goat | + | + | + | + |
| **PA1-8435** | Affinity Bioreagents | rabbit | + | + | + | + |
| **clone 83-1** | Diamandis | mouse | - | - | - | + |
| **In-house** | Diamandis | rabbit | + | + | + | + |
| **Tagena+Domino** | Arexis | rabbit | + | + | + | + |

**Evaluation of various KLK7 antibodies by means of Western blot**

Eight antibodies directed to KLK7 constituted a panel of evaluated reagents in our effort to assess KLK7 at protein level. After the initial control assays on reactivity to KLK7 recombinant forms, all recombinant proteins that comprise the KLK family of proteases were blotted in order to identify any potential cross-reactivity. The fact that, this family of proteases displays high similarity (Pavlopoulou 2010), allows assumptions on antibodies, which cross-react and thus identify more than one type of KLK. It is, therefore, crucial to check whether these antibodies cross-react.

Before employing the antibodies directed to KLK7, it was crucial to confirm the structure of the recombinant proKLKs to be used for the cross-reactivity control. Coommassie-stained gels (**Figures 9A** and **9B**) revealed valuable information about the expected position of each one of the recombinant proKLK (3-15) protein on the prospective blot. An irrelevant to KLK family protein, Tissue Factor fragment 1-214$^{aa}$, was added as additional control to cross-reactivity. SDS-PAGE for the detection of the $His_5$-tag (**Figure 9C**) confirmed the reliability of the method since all recombinant proKLKs were synthesized by use of the same expression system (pQE-30, Qiagen, Hilden, Germany) containing the $His_5$-tag. SDS-PAGE for the detection of the Tag-100 differentiated proKLKs from the Tissue Factor protein, since Tag-100 is contained only in the pro-KLKs.

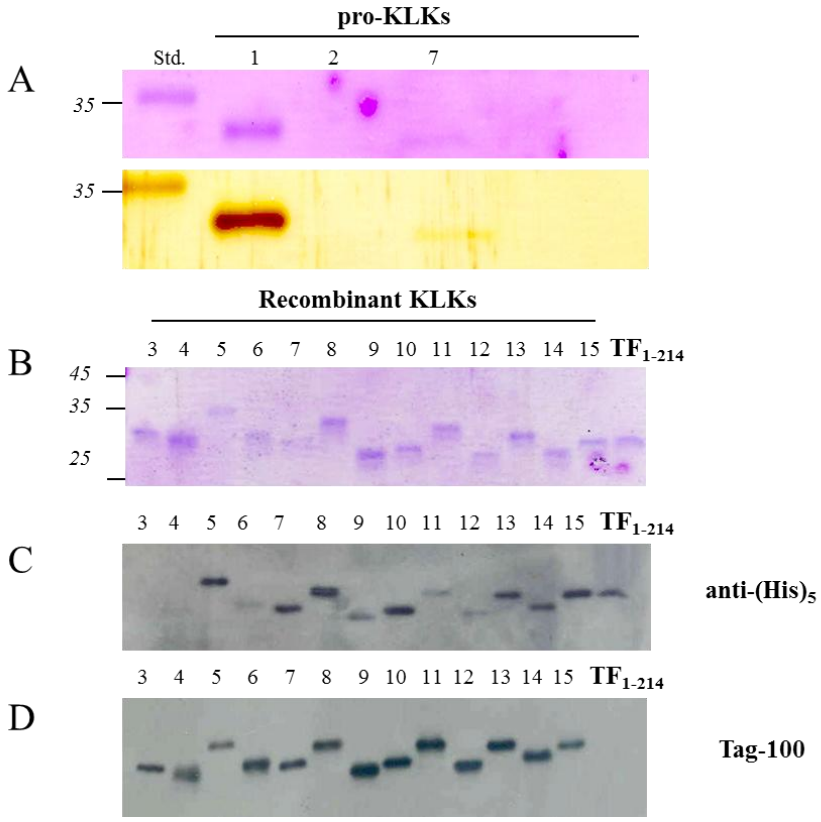


**Figure 11:** **(A, B)** Coommassie staining for all the KLKs blotted (all samples 1 μg/well). Actual protein location on the blot and therefore molecular weight is apparent. **(C)** anti-$His_5$ 0.1 μg/mL and **(D)** anti-Tag-100 0.1 μg/mL, samples 100 ng/well. Chemiluminescent radiography, film exposure 5 min.

The antibodies selected for evaluation came from different sources (**Table 15**). Blots were constructed with KLKs 1 to 8 at the top level and 7, 9-15 at the bottom level. KLK3-15 were in-house constructed, whereas KLK1-2 were a gift by Prof. Diamandis' lab. Again, the antibodies from Arexis, R&D systems and ABR revealed strong signal and absence of cross-reactivity. Not all of the antibodies reacted with the recombinant KLK proteins; only five out of eight reacted and from these five, one displayed severe crossreactivity with other KLKs and another one was of low reactivity. This analysis led us to judge five out of eight antibodies as inappropriate for immunohistochemical assessment where robust, non-crossreacting antibodies are needed for detection. As shown on **Table 16**, the antibodies used differed in terms of immunogenic production and they were specifically selected to cover a complete panel of potential epitopes. Natively expressed KLK7 isoforms (tissue specimens) might vary.

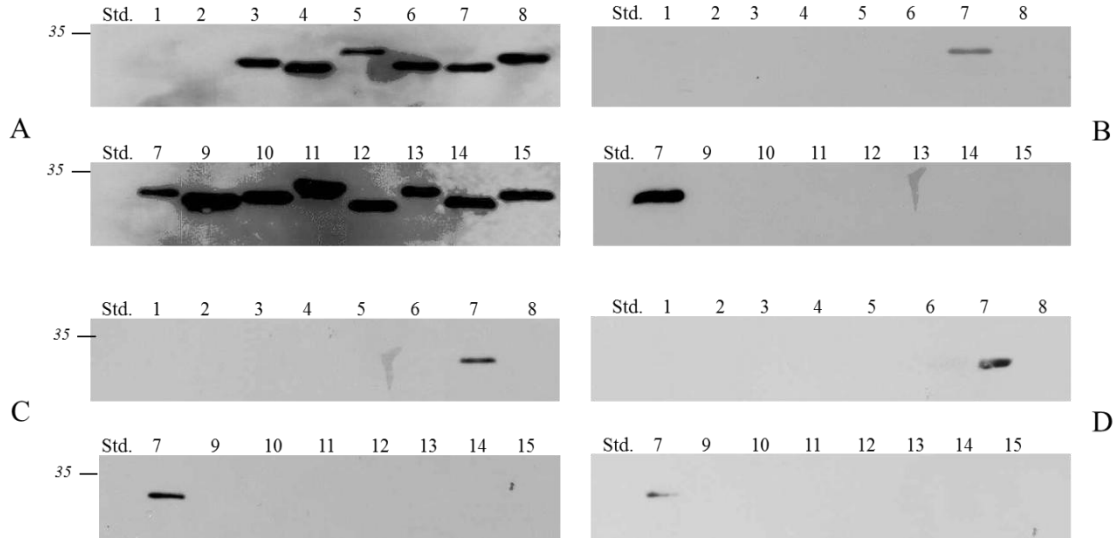


**Figure 12:** Immunoblotting with proform KLKs 1 to 15 blotted and anti-Tag100 (A, 0.1 µg/mL), anti-KLK7 Arexis (B, 0.68 µg/mL), R&D (C, 0.2 µg/mL) and ABR (D, 0.5 µg/mL). Chemiluminescent radiography, film exposure 12 min.

**Table 16**: Antibodies to KLK7 employed for detection of recombinant KLK7. The table summarizes the overall performance of the antibodies in Western blot control assays, including cross-reactivity with other KLKs check.

| Antibody | Source | Species | Immunogen | Strength of WB signal | Cross-reactivity with other KLKs |
|---|---|---|---|---|---|
| H-50 | Santa Cruz | *rabbit* | aa 154-203 mapping near the C-terminus of KLK7 | + | No cross-reactivity |
| C-15 | Santa Cruz | *goat* | Peptide mapping within an internal region of KLK7 | - | - |
| E-16 | Santa Cruz | *goat* | Peptide mapping within an internal region of KLK7 | - | - |
| AF2624 | RnD systems | *goat* | rhKLK7, aa 23-252 (proenzyme) | ++ | No cross-reactivity |
| PA1-8435 | Affinity Bioreagents | *rabbit* | Synthetic peptide within the kallikrein loop area of KLK7 | ++ | No cross-reactivity |
| clone 83-1 | E.P. Diamandis | *mouse* | Unknown (Kishi 2004) | - | - |
| In-house | E.P. Diamandis | *rabbit* | Unknown (Tanimoto 1999) | ++ | KLK9, KLK10 |
| H-50 | Santa Cruz | *rabbit* | 154-203 aa mapping near the C-terminus of KLK7 | + | No cross-reactivity detectable |
| Tagena + Domino | Arexis | *rabbit* | Unknown | +++ | Very low with KLK3, KLK6, KLK8 |

**Microtiter plate measurements of the reactivity of the antibodies directed to KLK7**

Microtiter plate measurements were performed to check the antibodies' binding capacity to their antigen. These types of assays reveal much of information about the sensitivity and specificity of the antibodies. Following the same principle as in ELISA, recombinant KLK7 coated the plate in different concentrations and it was incubated with different concentrations of all eight antibodies to KLK7. Subsequently, they were detected with a labeled secondary antibody. Besides that, a second assay, a reverse ELISA, where the plate was first coated with the antibodies in different concentrations and then KLK7 was detected via its binding to the antibody, was performed.

Immunoassays of this type are a matter of antibody concentration (Engvall and Perlmann 1972; Smith 1974; Svenson and Larsen 1977) and affinity (Ahlstedt 1974; Butler 1978). Especially a matter of affinity, since in these experiments same concentrations were tested and most antibodies were polyclonal (reagents with different affinity).

Antibody affinity is the strength of the reaction between a single antigenic determinant and a single combining site on the antibody. Most antibodies have a high affinity for their antigens. The higher the affinity of the antibody for the antigen, the more stable will be the interaction.

Avidity is a measure of the overall strength of binding of an antigen with many antigenic determinants and multivalent antibodies. Avidity is more than the sum of the individual affinities and applies certainly to polyclonal antibodies.

Specificity refers to the ability of an individual antibody combining site to react with only one antigenic determinant or the ability of a population of antibody molecules to react with only one antigen. In general, there is a high degree of specificity in antigen-antibody reactions.

Comparing all eight antibodies in two different set-ups as abovementioned (see **Appendix 11.1**), Diamandis's mouse antibody and all SantaCruz antibodies display low affinity to the antigen as clearly proved by the shallow curves when the recombinant protein or the antibody is coated. On the other hand, the other half of the antibodies reaches a certain standard represented by steep curves indicating that low antibody concentrations achieve already strong binding. In this respect, ABR antibody, R&D, Arexis and the Diamandis's polyclonal (all affinity-purified) demonstrate better binding potential, thus better quality for our purposes.

The original set-up of the microtiter plate measurement for the R&D antibody is shown on **Table 17** and **Figure 13**.

**Table 17:** Original set-up for the microtiter plate measurement (R&D antibody). Serial dilutions of the recombinant proKLK7 and the R&D anti-KLK7 in a 96-well plate (Nunc Maxisorp).

| | | Antigen (KLK7) (µg/mL) | | | | | |
|---|---|---|---|---|---|---|---|
| | | 2.50 | 1.25 | 0.60 | 0.30 | 0.15 | 0 |
| **R&D antibody (µg/mL)** | 2 | 3.389 | 3.391 | 3.370 | 3.410 | 3.133 | 0.098 |
| | 1 | 3.369 | 3.360 | 3.250 | 3.072 | 2.576 | 0.078 |
| | 0.5 | 3.305 | 3.259 | 3.016 | 2.587 | 1.814 | 0.073 |
| | 0.25 | 2.948 | 2.698 | 2.366 | 1.852 | 1.230 | 0.068 |
| | 0.125 | 2.156 | 1.821 | 1.522 | 1.146 | 0.760 | 0.072 |
| | 0.0625 | 1.377 | 1.188 | 0.927 | 0.672 | 0.455 | 0.068 |
| | 0.03 | 0.841 | 0.705 | 0.528 | 0.413 | 0.278 | 0.070 |
| | 0 | 0.081 | 0.070 | 0.073 | 0.071 | 0.069 | 0.068 |

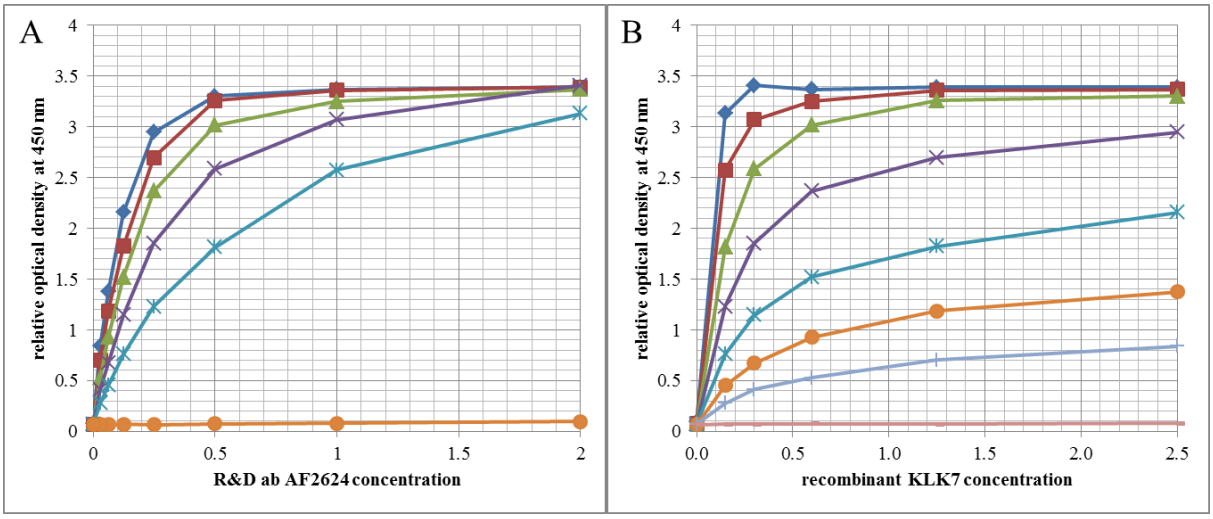


**Figure 13:** Photometric curves for mictotiter plate measurements. (**A**) Relative optical density at 450 nm. Antibody directed to KLK7 (R&D AF2624) coated and recombinant KLK7 added to bind. (**B**) Recombinant KLK7 coated, R&D AF2624 added to bind, relative optical density at 450 nm.

### Immunohistochemistry controls

The positive control was a tissue section fixed and processed like the test section and known to bear the target molecule, e.g. skin as the native expresser of KLK7 and kidney at least at gene level (Yousef and Diamandis 2001). The same sections were used for every different antibody tested (all eight). All slides were subjected to the same epitope retrieval and blocking procedures (Miller 2001a; Taylor 2009). HaCaT cells were the positive control for cytospins

(Brinkhuis 1995). The term ‘negative’ control refers typically to the omission of the primary antibody on a parallel tissue section that otherwise is treated identically. This is the way it was used here and this practice was followed repeatedly at every single staining session.
The primary antibody must employ positive and negative controls through all of the titration and validation procedures, to achieve optimal working dilutions of primary antibody and detection system reagents (Taylor 2009).

### 5.1.1 Cell lines for KLK7 assessment

**Pretreatment conditions on cell cytospins**

Cell lines (tumor and immortalized) offer a chance for target protein localization, especially if they correspond to the respective normal or malignant tissues, e.g. HaCaT cell line (immortalized keratinocytes) for skin tissue. This analogy allows researchers to obtain indications from cells before using up valuable FFPE tissue sections as well as to produce supportive data for the actual patient material.

Cell cytospins have been employed for long in cytology (Noack 2000; Oertel and Huhn 2000). They offer a clear advantage over cell clots since they avoid additional processing with clotting reagents.

In order to achieve optimal working conditions for the antibodies directed to KLK7, reactivity was assessed in two different parameters: (a) fixation conditions and (b) staining methodology.

Despite the fact that tissue blocks are in practice prepared as formalin-fixed paraffin-embedded (FFPE) and this process is commonly accepted as appropriate to preserve cell and tissue morphology, we needed to explore the level of effect of such preparation on the antigenicity of target proteins. Fixation is a chemical process which strongly affects proteins located on tissue (it might even destroy unique epitopes), but on the other hand it maintains secondary protein structure and secures its compartmental position (Taylor 2009). This etiology has led scientists to intensify their control tests in order to optimize conditions for fair antibody reactivity (Cornett 1985; Baum 1994). This signifies a fixation route maybe other than formalin. In reality, our antibodies were checked under dozens of conditions (see table 16), in order to identify optimal setting. In scientific literature, organic solvents such methanol, ethanol and acetone, and cross-linking reagents, such as paraformaldehyde, were common fixatives for

cell/tissue populations under different concentrations, temperatures and incubations times. Organic solvents remove lipids and dehydrate the cells, while precipitating the proteins on the cellular architecture. Cross-linking reagents form intermolecular bridges through free amino groups, thus creating a network of linked antigens. The target cell/tissue type as well as the antibody type defined the fixation protocol.

**Table 18:** Cell cytospins (HaCaT and OV-MZ-6) were produced under numerous individual variables, all combinations crossed. Set of variables included ± antigen retrieval, ± blocking, 14 different fixation alternatives (MeOH, EtOH, formalin, PFA and acetone under variable consistency, temperature and incubation time) and 25 different permeabilization alternatives (saponin and digitonin).

| Method | Enzyme | Chromogen | Antigen retrieval | Block | Dilutions |
|---|---|---|---|---|---|
| **LSAB** | Peroxidase | $DAB^+$ | +/- | +/- streptavidin-biotin block | |
| **APAAP** | Alkaline phosphatase | Fast Red | pressure cooking | levamisole | |
| **Fixation** | | | **Permeabilization** | | |
| **a) MeOH 100 % / 10 min, 4 °C**<br>**b) MeOH 100 % / 30 min, 20 °C**<br>**c) MeOH 70 % / 10 min, 4 °C**<br>**d) MeOH 70 % / 30 min, 20 °C**<br>**e) EtOH 96 % / 5 min, 4 °C**<br>**f) EtOH 96 % / 10 min, -20 °C**<br>**g) EtOH 70 % / 5 min, 4 °C**<br>**h) EtOH 70 % / 10 min, -20 °C**<br>**i) Formalin 4 % unbuffered, 30 min, 4 °C**<br>**j) Formalin 4 % buffered (PBS), 30 min, 4 °C**<br>**k) PFA 1 % unbuffered, 30 min, RT**<br>**l) PFA 1 % buffered, 30 min, RT**<br>**m) Acetone, 5 min, 4 °C**<br>**n) Acetone, 10 min, -20 °C** | | | 1. Saponin 0.025 % / 30 min, RT<br>2. Digitonin 10 µM / 5 min, on ice<br>3. Digitonin 10 µM / 10 min, on ice<br>4. Digitonin 10 µM / 15 min, on ice<br>5. Digitonin 10 µM / 5 min, RT<br>6. Digitonin 10 µM / 10 min, RT<br>7. Digitonin 10 µM / 15 min, RT<br>8. Digitonin 100 µM / 5 min, on ice<br>9. Digitonin 100 µM / 10 min, on ice<br>10. Digitonin 100 µM / 15 min, on ice<br>11. Digitonin 100 µM / 5 min, RT<br>12. Digitonin 100 µM / 10 min, RT<br>13. Digitonin 100 µM / 15 min, RT<br>14. Digitonin 1 mM / 5 min, on ice<br>15. Digitonin 1 mM / 10 min, on ice<br>16. Digitonin 1 mM / 15 min, on ice<br>17. Digitonin 1 mM / 5 min, RT<br>18. Digitonin 1 mM / 10 min, RT<br>19. Digitonin 1 mM / 15 min, RT<br>20. Digitonin 10 mM / 5 min, on ice<br>21. Digitonin 10 mM / 10 min, on ice<br>22. Digitonin 10 mM / 15 min, on ice<br>23. Digitonin 10 mM / 5 min, RT<br>24. Digitonin 10 mM / 10 min, RT<br>25. Digitonin 10 mM / 15 min, RT | **Range: 1.36 µg/mL- 13.6 µg/mL (Arexis anti-KLK7)** |

Permeabilization reagents, such as saponin and digitonin, act by creating small pores in cell membranes allowing antibodies to access intracellular structures in intact cells. This is most of the times necessary when cells are fixed with a cross-linking reagent and normally unnecessary when using a solvent, because the cholesterol targeted by saponin is vanished by the solvent. At

any case, even unorthodox combinations such MeOH-saponin were tested in order to confirm hypothesis. Freshly harvested HaCaT cells (immortalized keratinocytes) and OV-MZ-6, as the ovarian cancer representative, were the test cell lines. These findings can help to develop a preliminary protocol for tissue staining.

Test results were largely diversified, as assumed. Although cell fixation protocols vastly employ methanol and ethanol, in our case these two fixatives heavily damaged or totally vanished cells mounted on cytospins. Added to this, saponin was less harmful on cells than digitonin, which created cracks on cell surface and falsified therefore staining results. Saponin is preferred by other researchers too (Sander 1991). Temperature affected cell morphology to a certain extent: higher temperatures preserved structures adequately in contrast to -20 °C, which disrupted cells. Generally, increasing the temperature increases speed of fixation, so slower fixation (-20 °C) harms cell structures. Finally, 1 % PFA diluted in PBS demonstrated more accurate cell morphology and perhaps better staining result than 1 % PFA diluted in $H_2O_{dist}$. This might be due to greater stability of polyclonal antibodies (rabbit Arexis Tagena + Domino) in higher salt concentrations (Hayat 2002). Further testing continued with qualified settings including 4 % formalin, 1% PFA and acetone. Detection method varied from APAAP until LSAB.

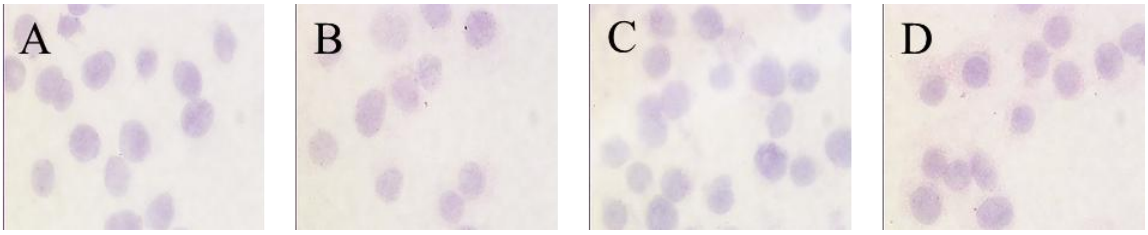


**Figure 14:** **(A)** Negative control with the omission of the primary antibody. HaCaT cytospins fixed with 1 % PFA in $H_2O_{dist}$ for 10 min on ice and stained by use of the APAAP method with the addition of alkaline phosphatase blocking agent levamisole, no antigen retrieval included. **(B)** Same setting as **(A)** with the addition of the anti-KLK7 (Tagena + Domino, Arexis, 13.6 μg/mL). **(C)** Negative control with the omission of the primary antibody. Setting without levamisole and fixation for 5 min instead of 10. **(D)** Same as **(C)** with the primary anti-KLK7 (Tagena + Domino, Arexis, 13.6 μg/mL). Blue for nucleus (hematoxylin), red for antigen (Fast Red). Magnification x 400. Faint granular red staining is observed in **(B)** and **(D)**.

After the initial condition screening, HaCaT cell line was chosen as the natively producing KLK7 cell line plus MCF-7 and MDA-MB-231 cell lines expressing low values of KLK7

mRNA (Holzscheiter 2006) that served as controls. The immunohistochemical detection method used was EnVision method with chromogen $DAB^+$ (after numerous tests with all commercially available staining techniques, this technique qualified). Each antibody had an optimal dilution. At the beginning, testing was restricted to four antibodies (Arexis Tagena + Domino, Santa Cruz E16, ABR PA1-8435, R&D AF2624) on one cell line (HaCaT) with the following variables to be examined: cross-linking fixative (4 % formalin or 1 % PFA), permeabilization factor (saponin 0.025 %, yes or no), HIER (yes or no). Small differences characterized cell staining when employing the Arexis Tagena + Domino, with saponin not offering any crisper image. Formalin fixation was affected (higher intensity) by HIER, in contrast with PFA, especially without saponin. When Santa Cruz E-16 was employed, saponin promoted a shift from membrane to cytoplasmic staining, whereas HIER caused the adverse effect when ABR was employed (cytoplasmic to nuclear). Finally, R&D antibody staining without the use of saponin was more distinct and HIER was always a prerequisite for successful color product development. These experiments demonstrate that saponin addition facilitates antibody reactivity when a cross-linking reagent is used. Consequently, it was used therefore in the standard protocol.

**Table 19:** Four different antibodies directed to KLK7 are subjected into diverse immunocytochemical assessment in terms of fixation (4 % formalin or 1 % PFA) and antigen retrieval (yes or no). HaCaT cell line serves as standard KLK7 producing cell line. Legend: C= cytoplasmic, M= membrane, Ø= without

| | **HaCaT** | | | | | | | | **Comments** |
|---|---|---|---|---|---|---|---|---|---|
| **Fixative** | **4 % Formalin** | | | | **1 % PFA** | | | | |
| **Saponin** | yes | | no | | yes | | no | | |
| **HIER** | yes | no | yes | no | yes | no | yes | no | |
| **Arexis Tagena + Domino** | ++ | + C M | + | ++ C M | + | + C M | ++ | ++ C M | More pronounced and distinct Ø saponin. HIER stronger signal, shift to cytoplasm and nucleus |
| **SC E-16** | ++ | ++ | + | + | + | ++ | ++ | + | Shift from cell membrane to cytoplasmic by staining with saponin |
| **ABR PA1-8435** | ++ | + | + | + | + | + | ++ | + | Both fixation method groups displayed nuclear next to cytoplasmic staining. HIER cytoplasmic to nuclear and cytoplasmic staining |
| **R&D AF2624** | ++ | - | + | - | + | - | ++ | - | HIER plus/either fixation method revealed granular cytoplasmic staining Ø saponin more pronounced and distinct immunostaining |

Integration of saponin in the staining procedure was essential under cross-linking fixation conditions (1 % PFA). Apart from PFA (1 % PFA/ 0.025 % saponin; 30 min; 4 °C), acetone also qualified from the group of the organic solvent fixatives (acetone; 5 min; 4 °C) for a final test on (a) three different cell types employing the prominent Arexis Tagena + Domino antibody to minimize intercellular variance (HaCaT, MCF-7, MDA-MB-231) and (b) HaCaT exclusively employing eight antibodies directed to KLK7.

(a) For HaCaT, 1 % PFA displayed crisper staining than using acetone. For MCF-7, HIER induced stronger staining for both fixatives. Similarly for the MDA-MB-231, the application of HIER resulted in case of acetone fixed cells in strong cytoplasmic staining and in case of 1 % PFA-fixed cells in massive cytoplasmic and nuclear membrane staining.

These results contradict Holzscheiter et al., where quantitative RT-PCR revealed no copies of KLK7 in MCF-7 and MDA-MB-231. On the other hand, Q-RT-PCR may not always correlate well with the level of protein expression, since protein presence depends on translational factors, post-synthetic modifications and protein degradation.

**Table 20:** Three different cell lines tested for KLK7 antibody reactivity employing two different fixation settings and two different antigen retrieval settings.

| | **HaCaT** | | | | **MCF-7** | | | | **MDA MB 231** | | | |
|---|---|---|---|---|---|---|---|---|---|---|---|---|
| **Fixative** | **Acetone** | | **1 % PFA + saponin** | | **acetone** | | **1 % PFA + saponin** | | **acetone** | | **1 % PFA + saponin** | |
| **HIER** | ✕ | ✔ | ✕ | ✔ | ✕ | ✔ | ✕ | ✔ | ✕ | ✔ | ✕ | ✔ |
| **Arexis Tagena + Domino** | - | N M | ++ | M | +/++ C M | +++ C/ N M | +/++ C M | +++ C/ N M | ++/+++ C M | +++ C | ++/+++ C M | +++ C/ N M |
| **ABR PA1-8435** | + | Hetero-genous pattern | ++ | N | **Legend**<br>N = nucleus<br>M = membrane<br>C = cytoplasm<br>G = granular<br>+ = weak<br>++ = moderate<br>+++ = strong<br>- = negative | | | | **Best dilution for HaCaT**<br>**Arexis; 1:100**<br>**ABR; 1:100**<br>**R&D; 1:500**<br>**SC H50; 1:100**<br>**SC C15; 1:100**<br>**SC E16; 1:100**<br>**Diam mab; 1:300**<br>**Diam rab; 1:100** | | | |
| **R&D** | - | + G | - | ++ G | | | | | | | | |
| **SC H50** | - | + C | - | ++ C | | | | | | | | |
| **SC C15** | + C | ++ G | + C | + C | | | | | | | | |
| **SC E16** | - | C | ++ G C | G C | | | | | | | | |
| **Diam mab 83-1** | + C | + C +++ N | ++ C | + C prtly N | | | | | | | | |
| **Diam rab** | ++ C M | +++ N ++ C | ++ C M | +++ N ++ C | | | | | | | | |

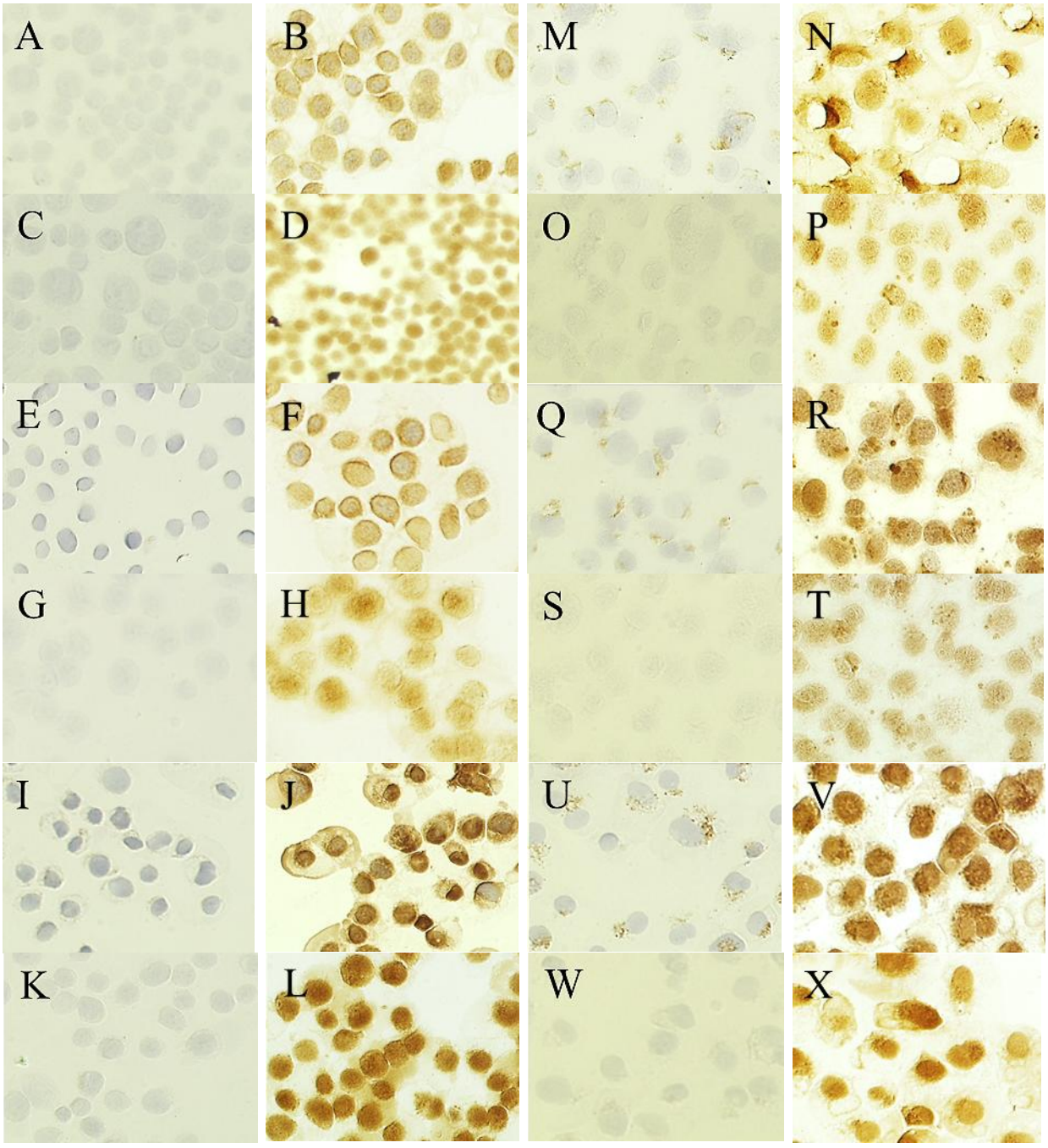


**Figure 15:** Comparison between two different cell lines, HaCaT (A-L) and MDA-MB-231 (M-X) under acetone fixation at 4 °C (A-D, M-P), -20 °C (E-H, Q-T) and 1 % PFA / 0.025 % saponin (I-L, U-X), without HIER (A-B, E-F, I-J, M-N, Q-R, U-V) or with HIER (C-D, G-H, K-L, O-P, S-T, W-X). Cell cytospins stained with Arexis Tagena + Domino (13.6 µg/mL). Brown for KLK7 ($DAB^+$), blue for nuclei (hematoxylin). Magnification x 200.

(b) Concerning the fixative comparison among eight antibodies directed to KLK7, the 1 % PFA/ 0.025 % saponin setting demonstrated similar but somewhat better results than acetone. There was, however, significant difference in staining pattern from antibody to antibody under

the same fixation. As mentioned previously, not all antibodies displayed specificity by means of Western blotting and thus staining homogeneity or overstaining might be due to cross-reactive elements.

Another general remark is the influence of HIER, which produces a predominant shift from cytoplasmic to nuclear staining.

**Staining methodology**

The second issue about the optimization of immunocytochemistry is the staining technique. Significant variance can be observed due to the choice of a detection kit. In order to achieve optimal immunohistochemical staining protocols, different immunohistochemical detection systems using multiple different chromogens were assessed. Differences were noted in the staining intensity, the duration of staining procedure, and the practicability.

Staining techniques were at the beginning applied on tissue specimens and soon results validated and adjusted on cell cytospins. HIER was excluded from the final protocol, as it produced less reliable results with the finally selected technique for use (Dako EnVision).

Staining protocol establishment is analyzed in detail in the "Tissues" section.

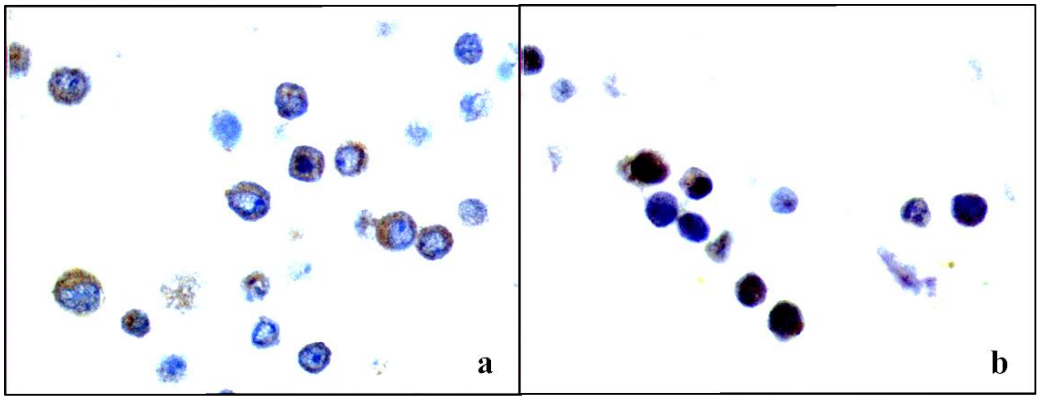


**Figure 16:** Ovarian cancer cell line transformed to overexpress KLK7 (OVMZ-6 RSV-KLK7) stained for KLK7 with **(a)** Arexis Tagena + Domino (1.36 μg/mL) and **(b)** R&D AF2624 (0.2 μg/mL). Brown for KLK7 ($DAB^+$), blue for nuclei (hematoxylin). Dako Envision method employed. Magnification x 200.

#### 5.1.1.1 Cell extract & supernatant KLK7 protein expression assessment by means of Western blot and immunoprecipitation

Cell lines often serve as tumor models (Prezas 2006a), analogs that offer valuable information about the behavior of studied molecules in hypothetical conditions. Tumor cell lines, transfected and immortalized, represent smaller entities to be examined before employing experimental procedures onto valuable patient tissue material. It is, moreover an additional proof or supporting evidence to achieve similar results on cell lines.

In order to study the KLK7 expression, specific cell lines as mentioned in the "Methods" section were chosen and subjected to Western blot analysis. As in most control and preliminary studies two antibodies qualified as best (Arexis and R&D), those two were employed to examine in a semi-quantitative mode whether pre-selected cell lines express KLK7. These cell lines were HaCaT, as the native expressers, breast cancer cell lines MCF-7 and MDA-MB-231 as control and ovarian cancer cell line OV-MZ-6 plus its transfected with KLK7 gene insert clone and the vector clone. The remaining slots were covered by in-house produced recombinant KLK7 and its preform. Triton-X-100 extracts and cell culture supernatants (conditioned medium) served as primary culture products, so that in case of native KLK7 presence there would be no chance to miss it (supernatant=secreted KLK7, Triton-X-100=intracellular compartment).

Cell extracts collected from cultivated HaCaT, MDA-MB-231, MCF-7, OV-MZ-6 WT, OV-MZ-6 pRc RSV and OV-MZ-6 pRc RSV/KLK7 together with recombinant proteins were blotted together and protein content was detected employing either the Arexis or the R&D antibody. R&D specifically recognized the intacellular KLK7 of HaCaT, and so did Arexis with the exception of another signal of the MDA-MB-231. This is probably false positive, since this particular cell was supposed not to express any KLK7, at least at the mRNA level (Holzscheiter 2006). Only shades of expression were marked for the other cell lines. Supernatants (conditioned medium) from the same passage used for blotting, revealed bands in every lane at the expected level, but also at a higher level, probably due to binding of an endogenous protein.

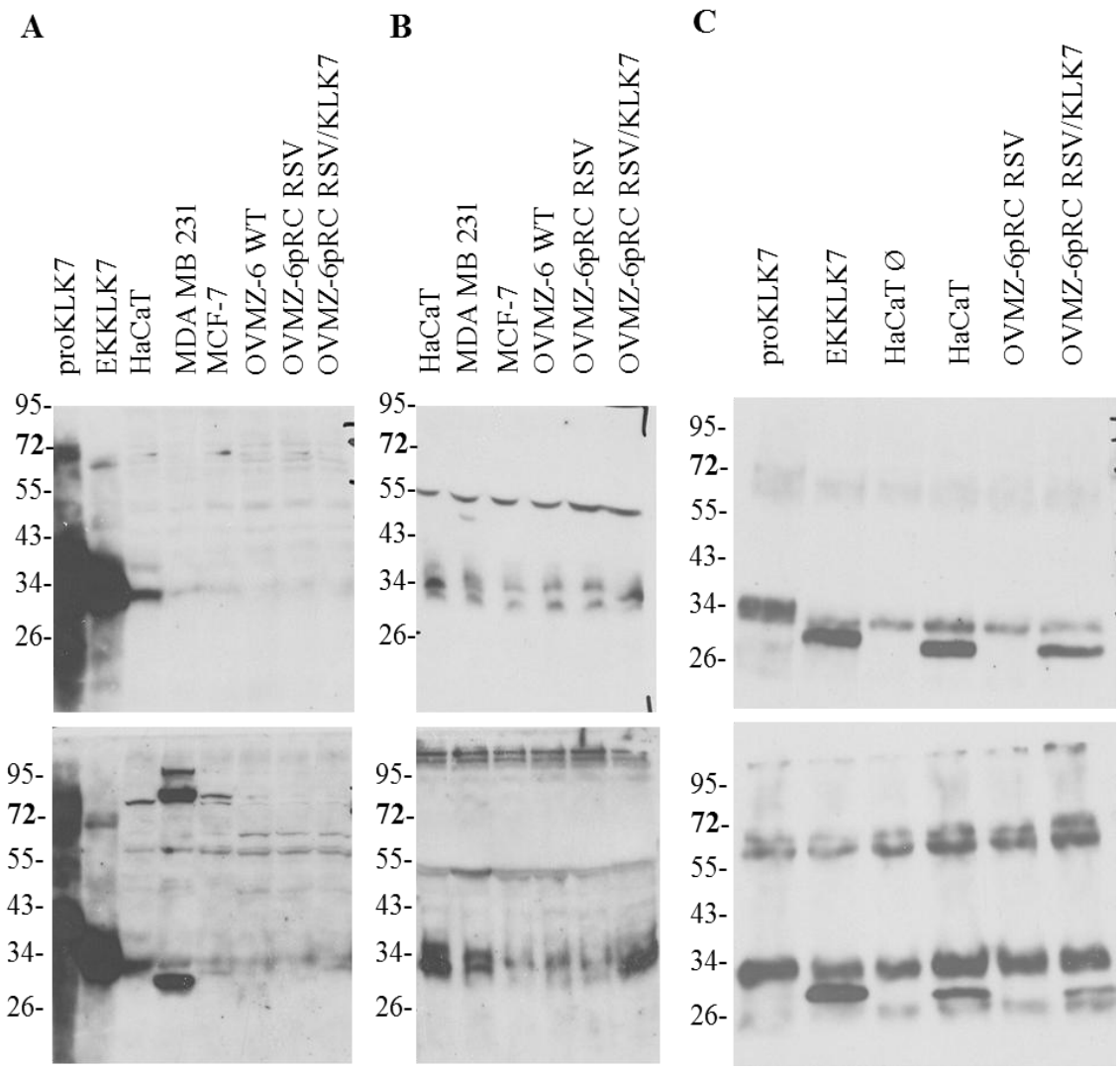


**Figure 17:** **(A)** Cell extracts, 20 μg per lane, recombinant proteins 100 ng, **(B)** supernatants 30 μg per lane. **(A), (B) top,** R&D AF2624 (0.2 μg/mL). **(A), (B) bottom**, Arexis Tagena + Domino (1.36 μg/mL). Chemiluminescent radiography, film exposure 30 min. **(C)** Supernatants subjected into immmunoprecipitaton. Recombinant proteins 0.5 μg in cell culture medium, supernatants 1.5 mL/reaction. Chemiluminescent radiography, film exposure 5 min. **(C) top**, Arexis for detection, R&D for precipitation, **(C) bottom**, R&D for detection, Arexis for immunoprecipitation. Non-specific binding of other proteins either to the Protein A or G beads or to the antibodies might be responsible for the presence of a strong unspecific band in every lane at the level just above the expected KLK7 position.

Since conditioned medium contains myriads of protein which can easily distract our blot, conditioned media from cell lines HaCaT, OV-MZ-6 pRc RSV and OV-MZ-6 pRc RSV/KLK7 were subjected once more to WB analysis. Employing a second antibody for immunoprecipitation (Arexis) we were able to detect strong bands for the recombinant proteins

(proKLK7 and EKKLK7) and for the HaCaT and the OV-MZ-6 pRc RSV/KLK7. The OV-MZ-6 pRc RSV displayed no reactivity as expected. Control cell line HaCaT without immunoprecipitant antibody was negative for KLK7.

Results confirm the presence of KLK7 in its secreted form in the conditioned medium of the native expressers (HaCaT) and of the overexpressing transfected cell line (OV-MZ-6 pRc RSV/KLK7) for both antibodies employed. Moreover, HaCaT seems to contain an intracellular fraction, as shown in the cell extract blot.

In contrast to the cellular environment, where enzymatic degradation of proteins is highly controlled, extra cellular proteases is the cause of uncontrolled protein degradation. The result of the proteolytic attack may vary from complete hydrolysis, single breaks within the peptide chain, or loss of a few N- or C-terminal amino acid residues. Proteolytic enzymes are released to the medium because of cell death, mechanical stress or induced cell lysis (L&K-Biosciences 2009).

#### 5.1.1.2 Cell microarrays (CMAs)

In parallel with the immunoprecipitation assay, cell microarrays constructed in-house were subjected to immunocytochemistry in order to investigate KLK expression and localization. The purpose of using CMAs is to gain protein localization information on cellular and subcellular levels, and to achieve relative quantification results. Cell microarrays are constructed to allow simultaneous analysis of protein expression in a multitude of cell samples. Their main advantage is that method variability is significantly reduced, since all cells are mounted on one single slide. Additionally, they are constructed as blocks, so they can be used in a similar manner as paraffin-embedded tissues. Finally, this is a fast way to investigate the expression of the target molecule.

Cell microarrays include various tumor cell lines as well as normal blood cells.

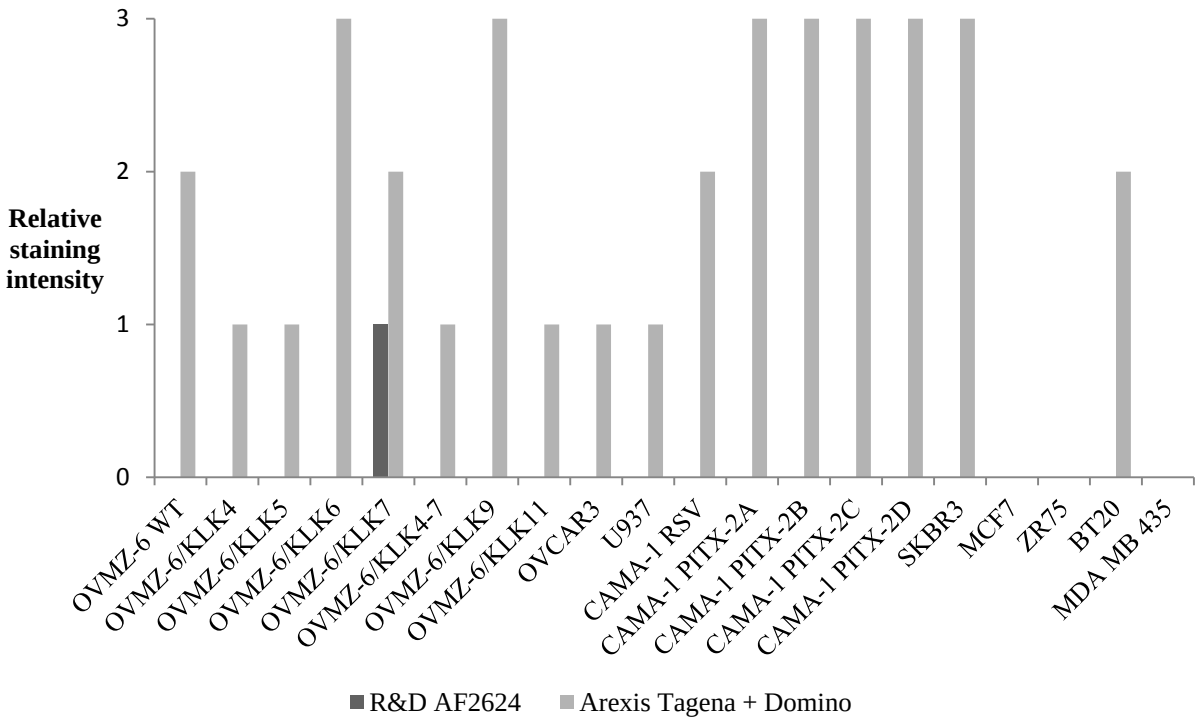


**Figure 18:** Graph displaying the quantified KLK7 signal from three series of CMAs produced as cell clots from cultivated cell lines. Arexis Tagena + Domino antibody recognizes epitopes in almost all tested cell lines, whereas R&D AF2624 confirms its reliability with only one positive result, the KLK7 overexpressing cell line.

Except for in-house cell lines, numerous other tumor cell lines were examined for KLK expression employing again two different antibodies to KLK7. One of the two antibodies tested (Arexis), showed higher staining intensity with the cells than the other one (R&D), but always in the same context. In reality, R&D showed remarkable positivity only for OVCAR-3 (ovarian cancer) and Mia-PaCa-2 (pancreatic cancer). This implies once more that either Arexis antibody somehow overreacts, whereas R&D recognizes consistently the correct epitopes, or that Arexis recognizes additional epitopes, perhaps neo-epitopes, which R&D fails to detect. Mia-PaCa-2 positivity is supported by the fact that numerous publications implicate KLK7 with pancreatic cancer (Johnson 2007; Ramani and Haun 2008a; b; Ramani 2008).

For immunocytochemistry, a staining protocol developed for tissue specimens and adjusted for cells was used, see “Tissues” section below.

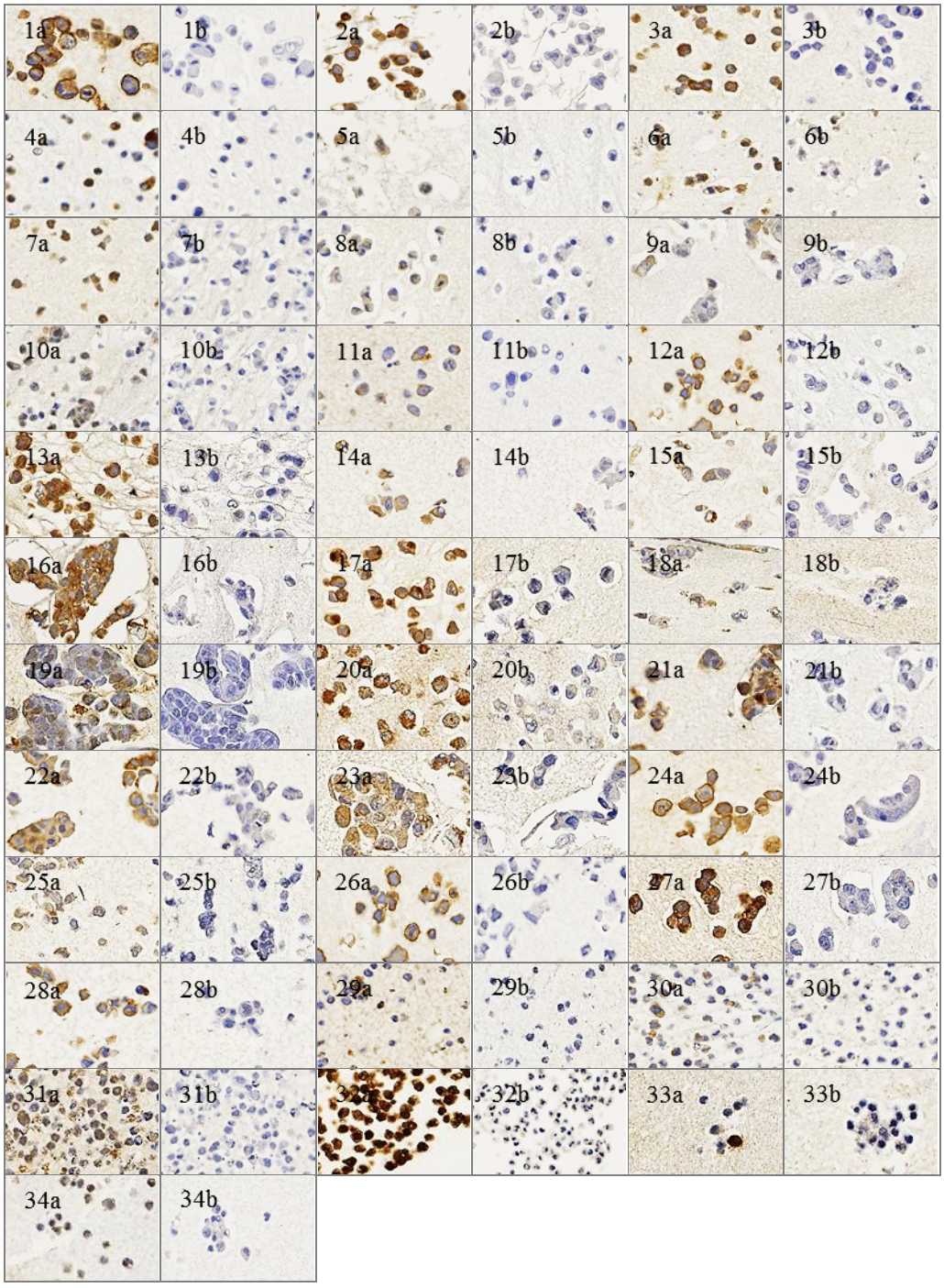


**Figure 19:** Thirty-four different cell types consisting a cell microarray. Letter (a) stands for Arexis Tagena + Domino (1.36 µg/mL) and (b) for R&D AF2624 (0.2 µg/mL). **(1)** SK-BR-3, **(2)** BT-20, **(3)** MCF-7, **(4)** MD-MB-435, **(5)** ZR-75-1, **(6)** OVCAR-3, **(7)** OV-MZ-6, **(8)** OV-MZ-10, **(9)** OV-MZ-15, **(10)** OV-MZ-19, **(11)** HeLa, **(12)** EJ-28, **(13)** RT-112, **(14)** Caki-1, **(15)** DU-145, **(16)** LnCAP, **(17)** PC-3, **(18)** CaCo-2, **(19)** SW-480, **(20)** Mia PaCa-2, **(21)** PaTu-II, **(22)** Cal 27, **(23)** BHY, **(24)** FaDu, **(25)** U-2 OS, **(26)** SaOS-2, **(27)** HT-1080, **(28)** SNB-19, **(29)** Raji, **(30)** U-937, **(31)** HL-60, **(32)** granulocytes, **(33)** lymphocytes, **(34)** trophoblasts. KLK7 brown ($DAB^+$), nuclei blue (hematoxylin). DAKO EnVision method employed. Magnification 200 x.

**CLSM and cytofluorometry on cell lysates for KLK7 protein expression assessment**

Multiple reactivity tests revealed that KLK7 deposition is mostly cytoplasmic, with some shifts occurring when HIER is applied. Fluorescence-based immunocytochemistry is superior to chromogenic, since detection signal is stronger and more precise. Another way to discover the exact location of a protein deposited intracellularly is the dissection by means of confocal laser microscopy (CLSM) (Noack 2000). Using freshly harvested instantly fixed with 2 % PFA, the cell lines HaCaT, MCF-7, MDA-MB-231, OV-MZ-6 plus its transfected with KLK7 gene insert clone and the vector clone, and the Arexis antibody for detection, we were able to localize KLK7 in the cytoplasmic compartment. Arexis was used for its robust properties. The aim of this experiment was among others to provide supporting data for KLK7 localization besides Western blot, ICC, Q-RT-PCR (Holzscheiter 2006).

CLSM provided us with precise pictures and enabled profound insight in cell morphology. HaCaT tend to form keratinized colonies in cell culture, each individual cell promotes cytoplasmic extensions to reach the neighboring ones. In our hands, HaCaT displayed clear staining in the cytoplasmic compartment and the merged image confirms the finding morphologically. MCF-7 did not reveal any expression, and so did the OV-MZ-6 pRc RSV as expected. The overexpressing cell line showed fluorescence, clear and distinct. The only dissonance was the superficial staining of the wild type cell line, although not anticipated.

Cytofluorometric analysis was additionally performed to discover how many cells expressed KLK7 protein, and how much of it they expressed. It allows staining of intracellular proteins, such as KLK7, at least the amount of KLK7 that remains intracellularly before secretion. It already known that KLK7 is synthesized as an inactive precursor with a 22-aa signal peptide, followed by a 7-aa activation peptide and a 226-aa catalytic domain. After cleavage of the signal peptide, the proenzyme is activated extracellularly (Caubet 2004). We expect, therefore, to detect the pre-pro-form of KLK7.

Cytofluorometric analysis proved to be rather inappropriate to distinguish KLK7 expression, as stained cell populations seemed to be low in fluorescence intensity. Since supporting evidence from cytofluorometric data was weak, results are not included.

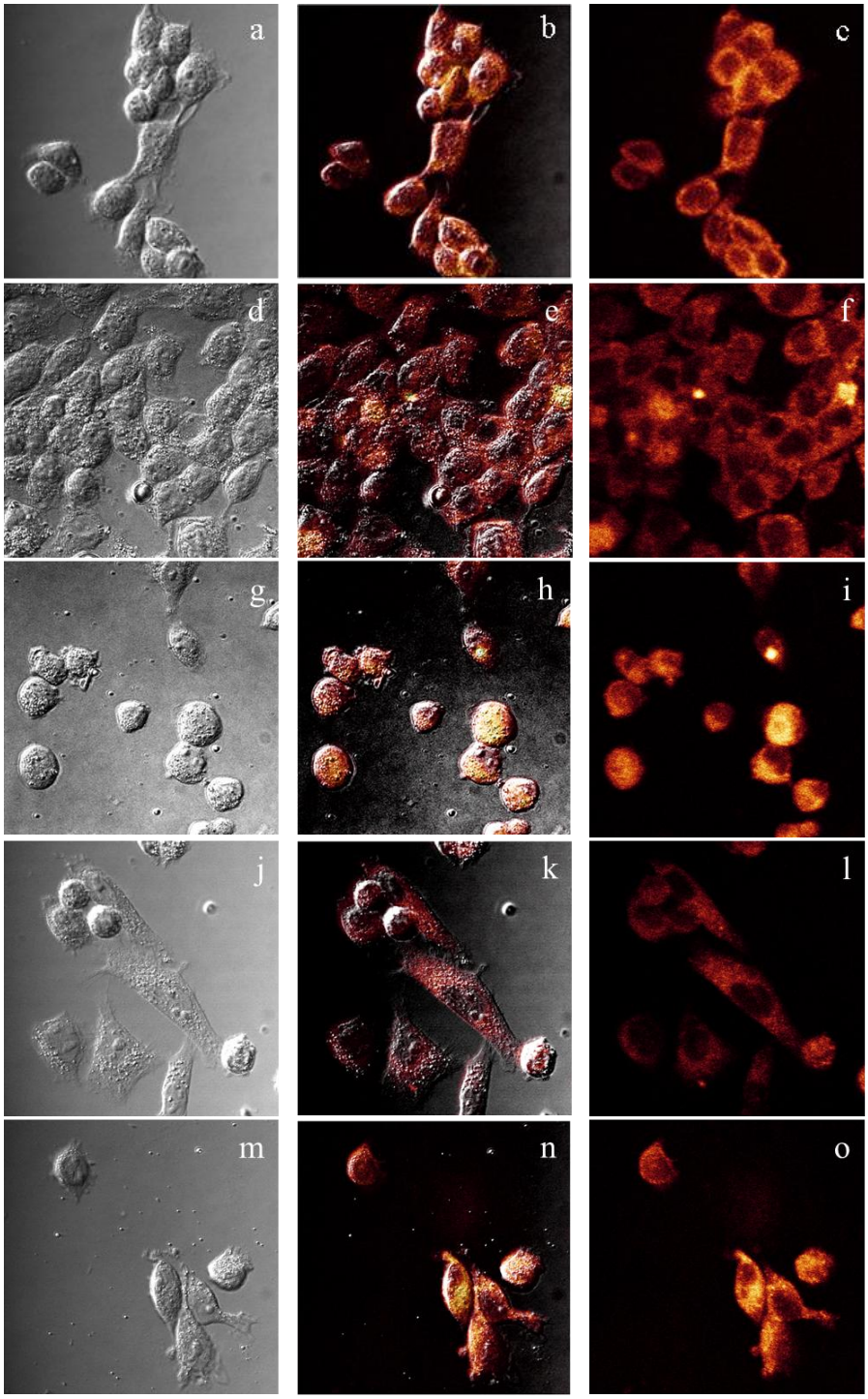


**Figure 20:** **(a, b, c)** HaCaT, **(d, e, f)** MCF-7, **(g, h, i)** OV-MZ-6 WT, **(j, k, l)** OV-MZ-6 pRc RSV, **(m, n, o)** OV-MZ-6 pRc RSV/KLK7. Left column represents the confocal image, right the fluorescent and middle the overlay image. Cells stained for KLK7 protein (Arexis Tagena + Domino, 0.68 µg/mL). Secondary detection antibody Alexa488 (2 µg/mL) Magnification x 400, brighter color represents increased in fluorescence intensity. Look-up table, see **Appendix 11.3**.

Starting from a previous study by Holzscheiter et al., where several cell lines (HaCaT, MCF-7, MDA-MB-231, OV-MZ-6 WT, OV-MZ-6 pRc RSV and OV-MZ-6 pRc RSV/KLK7) were tested for KLK7 presence by means of quantitative RT-PCR, we investigated the KLK7 localization by means of additional methods as Western Blot (WB)/ Immunoprecipitation (IMP), immunocytochemistry (ICC), confocal laser microscopy (CLSM) and cytofluorometry (FACS).

**Table 21:** Summarizing table of all cell lines and techniques used to investigate cellular KLK7 expression. (*) Data from Holzscheiter et al. 2006. Mark in parentheses signifies a borderline result. N/A= not available.

| | HaCaT | MCF-7 | MDA-MB-231 | OV-MZ-6 WT | OV-MZ-6 pRc RSV | OV-MZ-6 pRc RSV/KLK7 |
|---|---|---|---|---|---|---|
| **Q-RT-PCR*** | + | - | - | N/A | - | + |
| **WB/IMP** | + | N/A | N/A | N/A | - | + |
| **ICC** | + | - | - | - | - | + |
| **CLSM** | + | - | N/A | (+) | - | + |
| **FACS** | (+) | - | - | - | - | (+) |

By all means used to investigate cellular KLK7, findings agree in the vast majority of cases that differential expression of KLK7 among cell lines does exist. Native expressers (HaCaT) and overexpressing cell line (OV-MZ-6 pRc RSV/KLK7) pronounce in comparison with the rest of the cell lines, which actually served as controls. These results confirm the initial hypothesis, that KLK7 forms are present intracellularly. The amount always varies depending on the cell cycle phase (unsynchronized cell lines), so it might be case that KLK7 is actually released extracellularly before captured by the antibodies selected. Nevertheless, cell assays provide indications on cellular KLK7 expression and useful points for further investigation on tissue sections.

### 5.1.2 Tissues for KLK7 assessment

**Establishment of immunohistochemical techniques on test tissues (skin, kidney)**

Immunocytochemical protocol was the pilot procedure to achieve an optimized protocol for tissue section staining. For the optimization of immunohistochemical staining protocols, different immunohistochemical detection systems employing multiple different chromogenic reagents were assessed on normal skin and kidney specimens, the commonly accepted positive controls for KLK7 expression (Yousef and Diamandis 2001).

Indirect labeling methods, such as POX-avidin-biotin-based methods, such as ABC and LSAB, and enzymatically enhanced methods such as PAP and APAAP underwent examination. A chain polymer-based method (Dako Envision) was also examined.

**Table 22:** List of staining techniques employed for KLK7 detection. Legend: POX=peroxidase, ABC= avidin-biotin complex, PAP=peroxidase anti-peroxidase, APAAP= alkaline phosphatase anti-alkaline phosphatase, LSAB= labeled streptavidin biotin, $DAB^+$= 3,3'-Diaminobenzidine.

| Technique | Indirect-POX | ABC | PAP | APAAP | LSAB | Envision | Envision double staining |
|---|---|---|---|---|---|---|---|
| **Technology** | Indirect labeling | Avidin-biotin | Enzyme anti-enzyme | Enzyme anti-enzyme | Streptavidin-biotin | Dextran polymer chain | Dextran polymer chain |
| **Enzyme** | Horseradish peroxidase | Horseradish peroxidase | Alkaline phosphatase | Alkaline phosphatase | Horseradish peroxidase | One or the other | Both |
| **Number of steps** | 6 | 7 | 7 | 7 | 7 | 9 | 12 |
| **Chromogen** | $DAB^+$ | $DAB^+$ | Red chromogens like Fast Red | Red chromogens like Fast Red | $DAB^+$ | $DAB^+$ | Red chromogens e.g. Fast Red/DAB+ |
| **Sensitivity** | + | ++ | ++ | ++ | +++ | +++ | +++ |

POX, ABC and PAP did not qualify due to inconsistencies and method instability. APAAP, LSAB and Envision provided reproducible results for each one of the eight primary antibodies employed. Consistency through variable antibodies characterized an identical color deposition in cell as well as in structure units. The only differences were observed in the staining intensity and the duration of staining procedure. Envision detection system, which does not rely on the avidin-biotin signal amplification, proved to provide the most pronounced staining results without background staining. Added to this, Envision functions with reduced steps in staining procedure, a fact that minimizes intra- and inter-individual differences.

In chromogenic reagent category, $DAB^+$ compared to red chromogens provided superior quality in results. Stability (alcohol-insoluble, light stable), color contrast to greyish tissue, minimal background and specific product precipitation are the characteristics which qualified $DAB^+$ over red chromogens like Fast Red, Permanent Red or AEC.

**Table 23:** Comparative table of staining techniques and available chromogens

| | APAAP (#K5000, DAKO) | LSAB (#K0679, DAKO) | Envision system (#K5361, DAKO) |
|---|---|---|---|
| **Fast Red** | Insoluble vibrant, red reaction product, slight pink structure | | |
| **Permanent Red** | Red-colored, permanent reaction product at the site of the target antigen, granular structure **Greater intensity than with Fast Red** | | |
| **DAB$^+$** | | Develops into a brown precipitate and forms a permanent reaction product. **Greater intensity than with AEC** | -most distinct staining results with barely no background staining. -does not rely on avidin-biotin interaction to localize marker enzyme of antigen. -no need of blocking of endogenous biotin -easy to use two-step method. Intra- and inter-individual differences during staining procedure are minimized -assay time and workload are reduced. |
| **AEC** | | Brick-red stain product is soluble in organic solvents | |

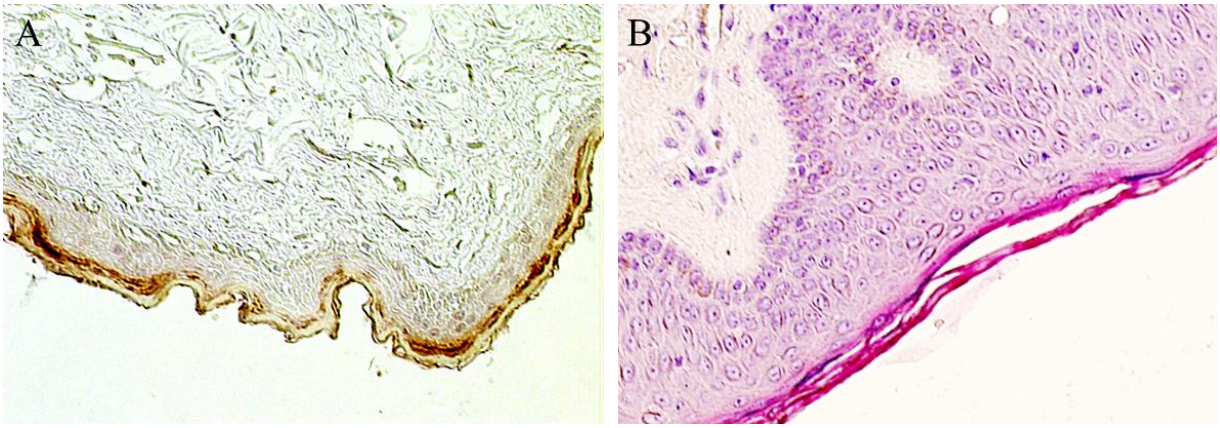


**Figure 21:** Skin tissue stained for KLK7 (Arexis Tagena + Domino, 4.5 µg/mL) employing the Dako Envision method with the addition of **(A)** DAB$^+$ chromogenic reagent (brown for KLK7, blue for nuclei) or **(B)** Permanent Red chromogenic reagent (pink red for KLK7, blue for nuclei). Magnification x 200.

## Antigen retrieval methods

Archived tissue specimens have undergone chemical changes due to fixation and paraffinization. Although there are formalin-resistant epitopes, some others will face this kind of changes that demand use of an antigen retrieval technique for unmasking and antibody manipulation (Miller 2001a; Taylor 2009). Antigen retrieval is not a selective method; it can potentially generate neo-epitopes which result in false-positive staining results. On the other side, some epitopes may never show up resulting in false-negative results.

There are two major types of antigen retrieval in the literature, Heat-Induced Epitope Retrieval (HIER) and Proteolysis-Induced Epitope Retrieval (PIER), as well as numerous combinations and variations of them. Proteolytic retrieval fails when overdigestion destroys target epitopes. HIER is inconsistent if an autoclave (too much of pressure), as waterbath (no pressure) or microwaves (no consistent heat induction). After initial testing, pressure-cooking qualified as the most reliable method, because it results in unmasking epitopes with the least tissue damage.

HIER follows deparaffinization of slides and precedes immunohistochemistry, with the aim of reversing cross-linking effects and epitope conformational changes induced by formalin fixation. The effect of HIER caused a shift in staining intensity of epidermal layers when specific primary antibodies were employed. Different structures were pronounced when HIER was applied, always compared to untreated specimens. Added to that, a shift from cytoplasmic to nuclear staining was observed. Without HIER, immunoreactivity was restricted to cytoplasmic compartment, while using HIER, reactivity was often localized in cell nuclei.

**Table 24:** Staining results for eight antibodies to KLK7 in every antigen retrieval setting for the test tissues skin and kidney. SC: stratum corneum, SL: stratum lucidum, SG: stratum granulosum, SS: stratum spinosum, SB: stratum basale; G: glomeruli, DT: distal tubuli, PT: proximal tubuli, ECM: extracellular matrix. Scale: - for negative, + weak, ++ moderate, +++ strong, * nuclear staining.

| | Skin | | | | | | | | | | Kidney | | | | | | | |
|---|---|---|---|---|---|---|---|---|---|---|---|---|---|---|---|---|---|---|
| | HIER | | | | | NO HIER | | | | | HIER | | | | NO HIER | | | |
| | SC | SL | SG | SS | SB | SC | SL | SG | SS | SB | G | DT | PT | ECM | G | DT | PT | ECM |
| ABR | +++ | - | - | - | - | - | +++ | +++ | - | + | - | +++ | +++ | - | - | ++ | ++ | - |
| Arexis | +++* | | +++ | +++ | +++ | - | +++ | +++ | ++ | ++ | + | +++ | +++ | - | - | +++ | +++ | + |
| R&D | +++* | | * | * | * | +++ | - | - | - | - | - | ++ | - | - | - | ++ | - | - |
| SC H50 | +++ | | * | * | * | - | +++ | +++ | + | + | | | | - | - | + | - | - |
| SC E16 | +++ | - | - | - | - | - | - | - | +++ | - | - | - | - | - | - | - | - | - |
| SC C15 | + | - | - | - | - | ++ | ++ | ++ | ++ | ++ | - | + | | - | - | ++ | ++ | - |
| D. mab | N/A | N/A | N/A | N/A | N/A | - | +++ | +++ | +++ | +++ | +++ | +++ | +++ | - | ++ | ++ | ++ | - |
| D. rab | N/A | N/A | N/A | N/A | N/A | - | + | ++ | ++ | ++ | ++* | ++* | ++* | - | +++ | +++ | +++ | +++ |

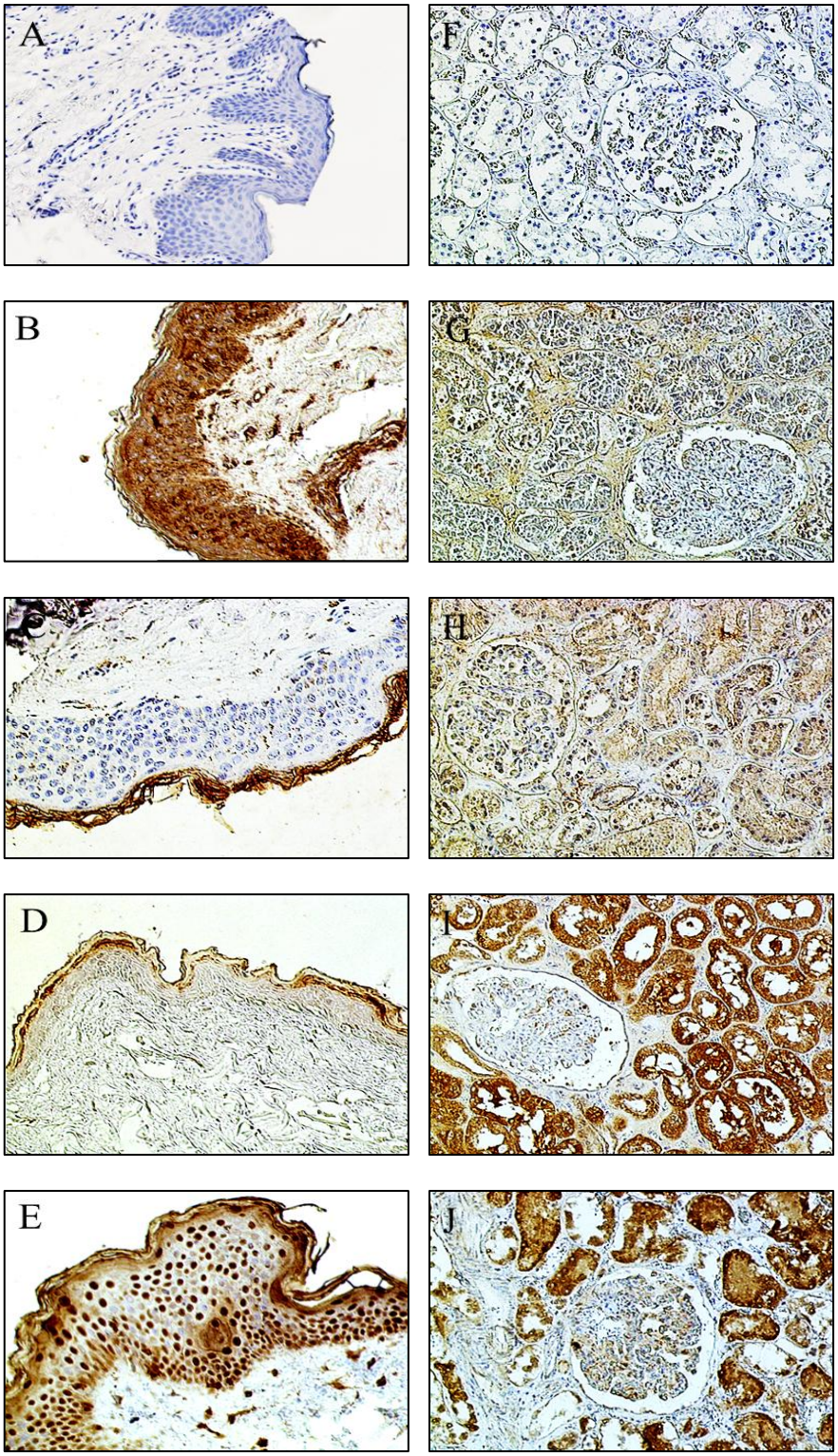


**Figure 22:** Effect of HIER on test tissue staining. Skin and kidney tissues stained for KLK7 protein expression with **(B, C, G, H)** SC-15 (40 µg/mL) or **(D, E, I, J)** Arexis Tagena + Domino antibody (2.72 µg/mL).**(A, F)** negative controls, with the omission of the primary antibody. **(B, D, G, I)** no HIER, **(C, E, H, J)** with HIER. Brown for KLK7 ($DAB^{+}$), blue for nuclei (hematoxylin). Magnification x 200.

As previous studies describe, KLK7 protein in human skin is located in the upper epidermal layers in a cytoplasmic distribution (Egelrud 1993b; Petraki 2006b). Our observations by use of HIER suggest that there is generation of neo-epitopes or epitope exposure. Staining patterns change thoroughly after HIER application, most obviously in skin test tissue, where different consecutive epidermal layers allow us to observe, for example, increased stratum corneum color deposition in the treated section (Arexis, ABR, SC H50, SC E16). This fact indicates the scale of effect of HIER on the tissue. On the other hand, the R&D primary antibody demonstrated antigen retrieval resistance, although nuclear staining appeared after HIER application. Stratum corneum and stratum lucidum layer borders are indiscrete, sometimes stratum lucidum is absent from skin tissue, so remarks on differential staining are almost on the edge.

HIER affected kidney tissue sections less than skin sections. No distinct differences were observed. Nevertheless, it demonstrated once more that certain antibodies are not useful for immunohistochemistry, since they actually produce false positive results. For example, while most antibodies tested do not stain glomeruli, the antibodies produced in Diamandis's laboratory react with these structures.

**Testing of eight antibodies to KLK7 in IHC**

The panel for evaluation consisted of eight primary antibodies directed to KLK7. Slides were mounted with normal skin and normal kidney samples, which served as positive control cases. To achieve optimal staining results, the Dako EnVision method was employed, with $DAB^{+}$ as the chromogenic reagent.

By means of immunohistochemistry, it is possible to define protein distribution in different cell types, independently of its average quantity in tissue. Tumor cell immunohistochemical scoring, for example, might produce totally different results compared to whole cell lysates assays (e.g. ELISA) due to specific protein localization, which is not distinguished by means of ELISA. Of course, quantitative methods like ELISA detect native or recombinant proteins in contrast to immunohistochemistry, where proteins pass through fixation process. The change of protein epitopes is a serious drawback in this method, although new immunohistochemical techniques shorten procedure time and steps in order to harm epitopes least possible. Of course,

despite the fact that results in IHC can be objective and reproducible, quantitative methods as ELISA are considered as the golden standard in protein quantitation.

The antibodies demonstrated variable behavior when tested on skin and kidney tissues. There were differences in cell and structure detection pattern. It was confirmed, however, that highest levels of KLK7 were found in cornified layer of skin (Sondell 1994; Petraki 2006b; Emami and Diamandis 2008) and that KLK7 protein in kidney is confined to the tubuli epithelium, while glomeruli remained unstained (Petraki 2006b).

**Table 23** summarizes the antibodies performance and reaction pattern in Western blot and immunohistochemistry as well as their specificity to KLK7.

**Table 25:** Antibodies to KLK7 performance as assessed by IHC and Western blot. Nopc: no pressure-cooking, +pc: pressure-cooking applied, SC: stratum corneum, SL: stratum lucidum, SG: stratum granulosum, SS: stratum spinosum, SB: stratum basale; G: glomeruli, DT: distal tubuli, PT: proximal tubuli, ECM: extracellular matrix. Scale: - for negative, + weak, ++ moderate, +++ strong, * nuclear staining.

| Antibody source | Immunogen | IHC Expression | | WB Strength of signal | Cross-reactivity |
|---|---|---|---|---|---|
| | | Skin | Kidney | | |
| **Diamandis, clone 83-1 mouse** | Unknown | nopc: SL pronounced, SC free (1:100)<br>+pc: SC stained, intensive nuclear staining in whole epidermis (1:500) | nopc: tubuli stained, gloms mostly free (1:100)<br>+pc: tubuli intensively stained, gloms mostly free (1:500) | - | - |
| **Affinity Bioreagents, rabbit** | Synthetic peptide based on the kallikrein loop area of KLK7 | nopc: epidermis slightly stained, SL pronounced (1:1000)<br>+pc: only SC clearly stained (1:1000) | nopc: very faint staining (1:1000)<br>+pc: tubuli + collective ducts pronounced staining, gloms negative (1:1000) | ++ | No cross-reactivity |
| **Arexis, Tagena + Domino rabbit** | Unknown | nopc: SL stained, SC free (1:300)<br>+pc: nuclear staining in all layers of epidermis (1:300) | nopc: tubuli strong staining, gloms free, ECM stained<br>+pc: tubuli strong staining, gloms positive, ECM negative | +++ | very low (KLK3, KLK6, KLK8) |
| **Diamandis, rabbit** | Unknown | nopc: whole epidermis stained, SL slightly pronounced, SC free (1:100)<br>+pc: SC pronounced, intensive nuclear staining in all layers of epidermis (1:200) | nopc: tubuli stained, gloms fainter (1:100)<br>+pc: tubuli stained, gloms fainter (1:200) | ++ | KLK9, KLK10 |

| Antibody source | Immunogen | IHC Expression | | WB Strength of signal | Cross-reactivity |
|---|---|---|---|---|---|
| | | Skin | Kidney | | |
| **Santa Cruz, H-50 rabbit** | aa 154-203 mapping near the C-terminus of KLK7 | nopc: SL pronounced, epidermis clearly stained, SC clear (1:100)<br>+pc: faint, nuclear staining partly in epidermis, SC faint staining (1:100) | nopc: very faint staining of tubuli (1:100)<br>+pc: tubuli stained, gloms free (1:100) | + | No cross-reactivity |
| **Santa Cruz, C-15 goat** | Peptide mapping within an internal region of KLK7 | nopc: all epidermal layers stained (1:500)<br>+pc: SC stained, melanocytes apparent (1:200) | nopc: tubuli more intense than gloms(1:500)<br>+pc: tubuli slightly stained, gloms free (1:200) | - | - |
| **Santa Cruz, E-16 goat** | Peptide mapping within an internal region of KLK7 | nopc: strong staining of all layers<br>+pc: strong staining of SC, no staining for the others | nopc: weak staining of all structures, ECM stronger<br>+pc: weak staining of all structures, no ECM staining | - | - |
| **R&D systems, AF2624 goat** | rhKLK7, aa 23-252 (proenzyme) | nopc: SL stained, rest of epidermis + SC faint staining (1:1000)<br>+pc: SC stained, nuclear staining in SG, SS (1:1000) | nopc: tubuli stained, gloms free (1:500)<br>+pc: tubuli slightly stained, gloms mostly clear (1:1000) | ++ | No cross-reactivity |

#### 5.1.2.1 Selection of antibodies directed to KLK7 and establishment of an immunohistochemical protocol.

**Table 25** indicates that Arexis Tagena + Domino, Affinity Bioreagents PA1-8435, and R&D AF2624 antibodies demonstrated comparable distribution patterns in skin and kidney test samples. The reaction color product was deposited into the cells of interest in a heterogeneous fashion, with cell staining pattern differentiating from each other. This signifies a true-positive staining (Miller 2001b; Taylor 2009). This is in agreement with results produced by others (Egelrud 1993b). The quality of the three antibodies was incomparable to the rest of the panel. Especially, the R&D and ABR performed in a very similar way; Arexis tended to more intensified staining. ABR discontinued the production of the specific to KLK7 antibody, so our study continued with the Arexis and the R&D. The other antibodies tested directed to KLK7 demonstrated questionable and often inconsistent staining patterns in terms of product localization, intensity and distribution, no compartmental confinement (nuclear staining co-resided with cytoplasmic). There were cases, for example, where granular cytoplasmic staining characterized homogenous color distribution with diverse cell categories stained. Often, in this pattern, cells of interest remained unstained. Antibodies displaying high levels of cross-

reactivity by means of Western Blot, e.g. the rabbit antibody from Diamandis' lab, they often resulted in homogenous immunohistochemical patterns, indicating detection of other KLKs besides KLK7.

What properties lead to antibody differentiation in staining? We definitely need to go back to the antibody design, production and purification procedures. This refers, for example, to the immunogenic KLK7 protein part recognized by the antibody: if this is not well-exposed in the FFPE tissue microenvironment, the antibody might not detect it. Not to mention the actually high probability that epitopes change during the hard processes of fixation, rehydration or dehydration, a fact leading to insufficient binding (Miller 2001b; Taylor 2009).

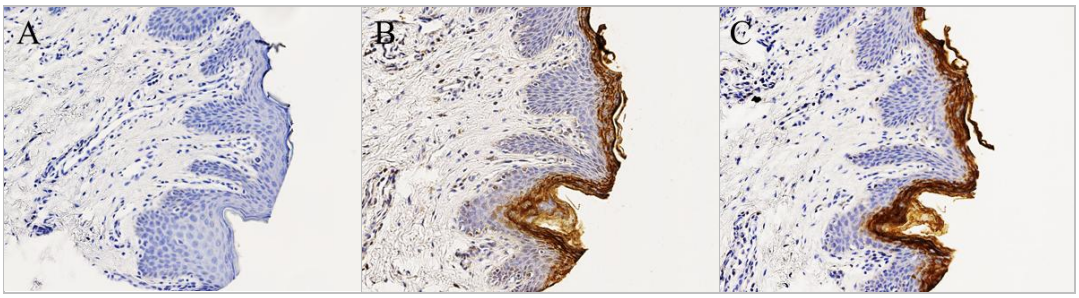


**Figure 23:** Skin, test tissue, consecutive sections. **(A)** negative control, **(B)** stained with Arexis Tagena + Domino (2.72 μg/mL) or **(C)** R&D AF2624 (0.4 μg/mL). Brown for KLK7 ($DAB^+$), blue for nuclei (hematoxylin). Envision method employed. Magnification x 100.

## Fixation

In the context of controlling antibody reactivity in various conditions, we created fixation settings beyond standards. Apart from commonly used buffered formalin (BF), tissue specimens fixed with Bouin's solution (BO) or a newly marketed fixative, Z-Fix (ZF) (Anatech, Battle Creek, MI). Buffered formalin is the cheapest, reliable and most widely utilized fixation buffer in Pathology Departments all over the world. On the other hand, Bouin's solution was used long before buffered formalin, which means that valuable archives might exist fixed this way. Recent publications assume that there might be a direct correlation among results received from the abovementioned fixatives (Gagnon 2010). Z-fix is an alcoholic zinc-based formalin solution (new generation of fixatives based on zinc and not on mercury, thus milder) which in our hands produced a crisp and clear staining. Picking an example from the tissue panel of **Figure 24**, ovarian cancer tissue was fixed under neutral buffered formalin, Bouin's solution or Z-fix and stained for three different primary antibodies to KLK7 (Arexis,

R&D and ABR). Bouin's solution generated tissue cracks and the staining was predominantly on the cell membrane for both antibodies, characteristic never observed previously. Buffered formalin produced similar results, with Arexis demonstrating high positivity while R&D did not exceed 10 %. Nevertheless, z-fix produces crisper images.

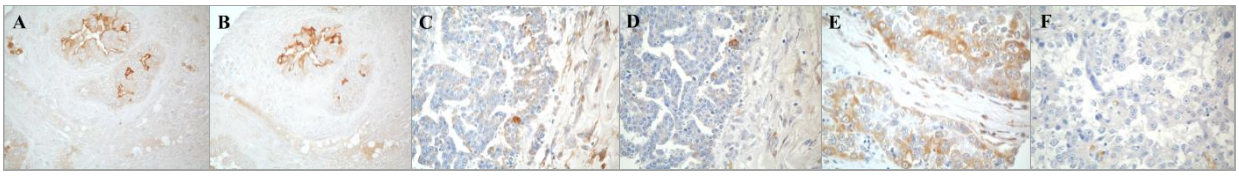


**Figure 24:** Ovarian cancer tissues stained for KLK7 with anti-KLK7 Arexis Tagena + Domino (2.72 µg/mL) **(A, C, E)** and R&D AF2624 (0.4 µg/mL) **(B, D, F)**. Tissues in **(A)**, **(B)** fixed with Bouin's solution, **(C)**, **(D)** with buffered formalin and **(E)**, **(F)** with Z-fix. Brown: KLK7. Blue: nuclei. Magnification x 400

Bouin's solution damaged tissues and provided a misleading image of the staining. Z-fix displayed crisp and clear staining, result comparable with the golden standard of buffered formalin. Arexis antibody seemed to overreact or to recognize different (and numerous) epitopes. On the other side, R&D and ABR demonstrated positive signal in a fixative-dependent manner and less intensely at every case than Arexis.

There are many discussions in the literature whether there is a tissue-dependent fixation; in other words, if certain fixatives perform better than others on specific tissues. Scientific articles provide a critical comparison between NBF and zinc formalin and details on probable mechanisms (Jones 1981; Mugnaini and Dahl 1983; Banks 1985; Herman 1988; Tome 1990; Abbondanzo 1991; Dapson 1993; L'Hoste 1995). Bouin's solution consists of picric acid, formaldehyde and acetic acid. The primary use of Bouin's fixative is for lymph nodes, prostate biopsies and kidney biopsies. However, it can also be used for decalcifying bones with the addition of formic acid (Crookham 1991; Carson 1992 ). Certainly, Bouin's is proposed for specific purposes, a fact which signifies a potential preference for tissues. On the other side, zinc-formalin is always directly compared to neutral buffered formalin as a candidate alternative product, and does not seem to perform differently with various tissues. Antibodies behavior was influenced by fixation in case of Bouin's solution (membrane staining, identical positivity), whereas zinc-formalin and neutral buffered formalin demonstrated similar reactivity; Bouin's seems to influence the R&D AF2624 more than the Arexis, a fact that manifested the latter to be more robust. In conclusion, the fixative testing procedure

demonstrated that the selected antibodies on a buffered formalin-fixed tissue produce similar results with the premium zinc-containing fixative (Z-fix), thus they are suitable for staining archived tissue specimens.

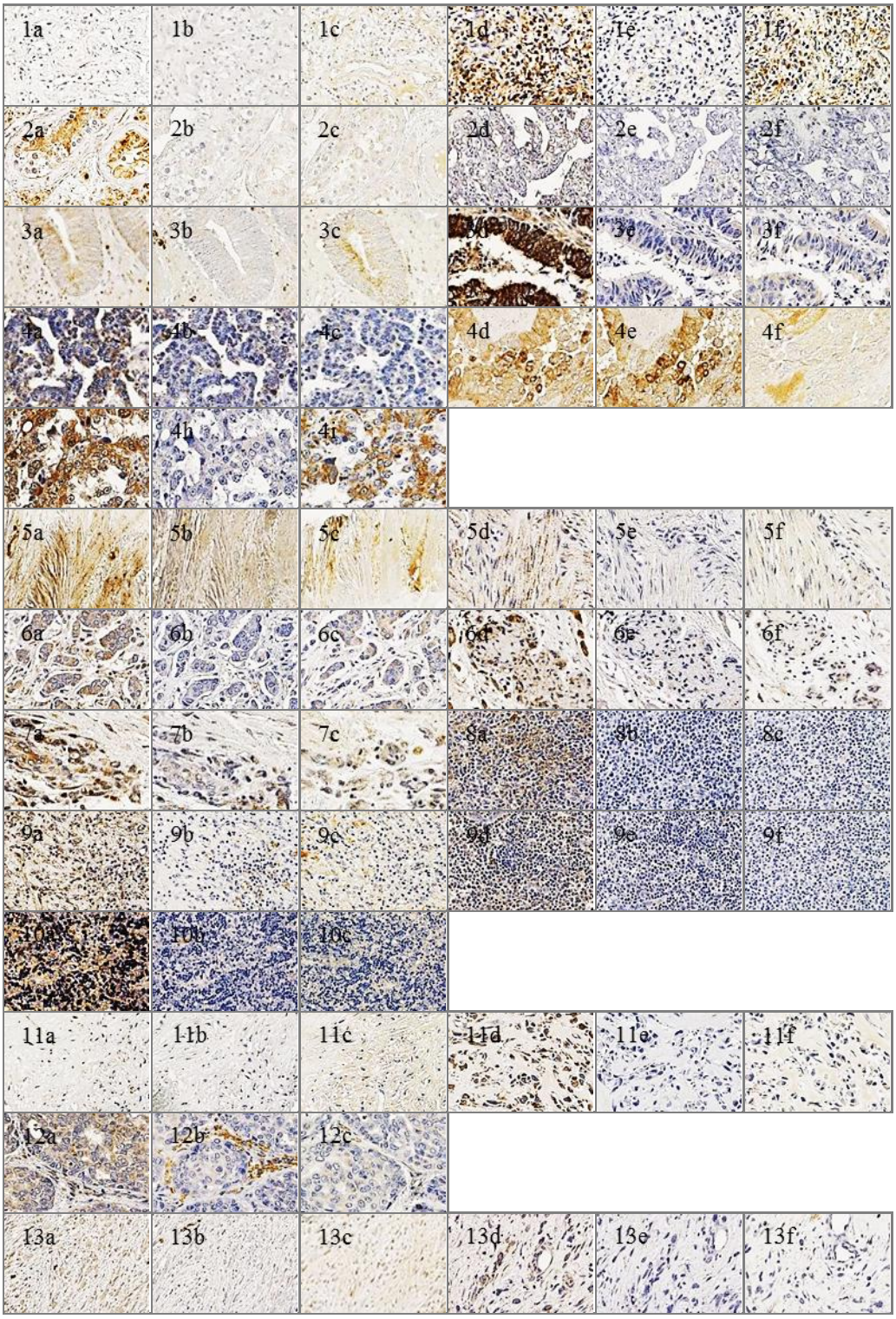

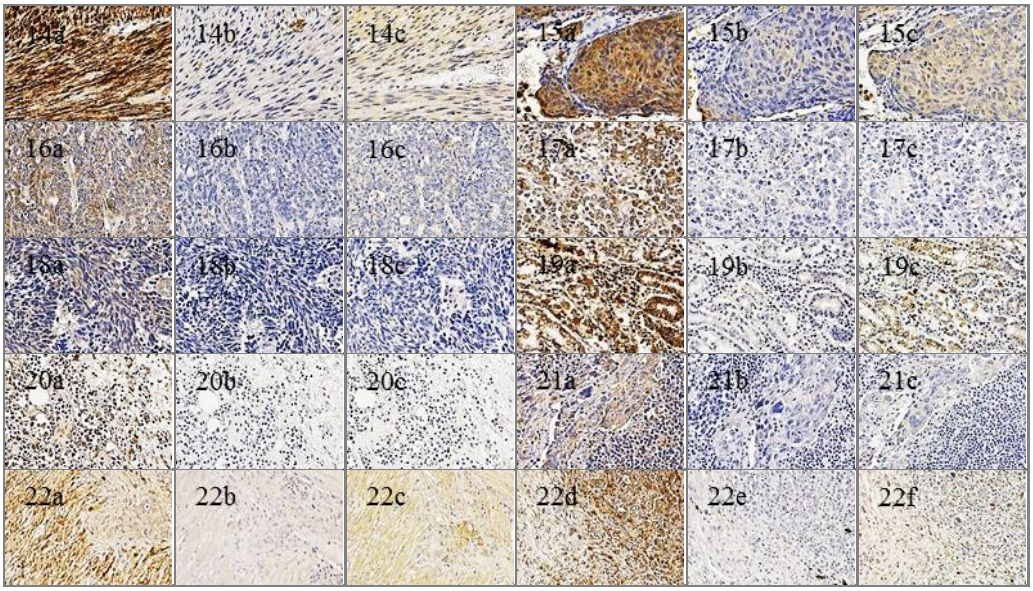


**Figure 25:** Comparison of three antibodies‘ performance in detection of KLK7 on various tumor tissues fixed under various conditions. Antibodies Arexis Tagena + Domino (2.72 µg/mL), R&D AF2624 (0.4 µg/mL) and ABR PA1-8435 (1 µg/mL). Brown for KLK7 ($DAB^+$), blue for nuclei (hematoxylin). Magnification x 50. Legend for the images, see **Table 26**.

**Table 26**: Type of cancer, type of fixation and antibody employed. Table corresponds to **Figure 25**

| No | Type of tumor | fixation | | | | | | | | |
|---|---|---|---|---|---|---|---|---|---|---|
| | | BO | | | ZF | | | BF | | |
| | | Arexis | R&D | ABR | Arexis | R&D | ABR | Arexis | R&D | ABR |
| 1 | Renal cancer | 1a | 1b | 1c | 1d | 1e | 1f | | | |
| 2 | Testis, mixed germ cell tumor | 2a | 2b | 2c | 2d | 2e | 2f | | | |
| 3 | Colon cancer | 3a | 3b | 3c | 3d | 3e | 3f | | | |
| 4 | Ovarian cancer | 4d | 4e | 4f | 4g | 4h | 4i | 4a | 4b | 4c |
| 5 | Leiomyoma (uterus) | 5a | 5b | 5c | 5d | 5e | 5f | | | |
| 6 | Breast cancer | | | | 6d | 6e | 6f | 6a | 6b | 6c |
| 7 | Endometrial cancer | | | | | | | 7a | 7b | 7c |
| 8 | NHL small cleaved cells LN | | | | 8a | 8b | 8c | | | |
| 9 | NHL node | | | | 9d | 9e | 9f | 9a | 9b | 9c |
| 10 | Thymoma | | | | 10a | 10b | 10c | | | |
| 11 | Sarcoma | | | | 11d | 11e | 11f | 11a | 11b | 11c |
| 12 | Mesothelioma | | | | 12a | 12b | 12c | | | |
| 13 | Testis (Sertolli cell tumor) | 13a | 13b | 13c | 13d | 13e | 13f | | | |
| 14 | Leiomyosarcoma | | | | 14a | 14b | 14c | | | |
| 15 | Squamous cervical carcinoma | | | | 15a | 15b | 15c | | | |
| 16 | Esophageal cancer | | | | | | | 16a | 16b | 16c |
| 17 | NSCLC | | | | 17a | 17b | 17c | | | |
| 18 | SCLC | | | | | | | 18a | 18b | 18c |
| 19 | Gastric cancer | | | | | | | 19a | 19b | 19c |
| 20 | NHL | | | | 20a | 20b | 20c | | | |
| 21 | Ovarian cancer (Hartmann) | | | | 21a | 21b | 21c | | | |
| 22 | Jejunum lymphoma | 22a | 22b | 22c | 22d | 22e | 22f | | | |

**Table 27:** Positivity for KLK7 of various carcinomas located on a tissue microarray collection.

| No | Type of tumor | fixation | | | | | | | | |
|---|---|---|---|---|---|---|---|---|---|---|
| | | BO | | | ZF | | | BF | | |
| | | Arexis | R&D | ABR | Arexis | R&D | ABR | Arexis | R&D | ABR |
| 1 | Renal cancer | - | - | (+) | ++ | - | ++ | | | |
| 2 | Testis, mixed germ cell tumor | ++ | + | + | + | - | - | | | |
| 3 | Colon cancer | ++ | - | - | +++ | + | + | | | |
| 4 | Ovarian cancer | ++ | ++ | - | +++ | + | +++ | +++ | ++ | + |
| 5 | Leiomyoma (uterus) | ++ | ++ | - | + | - | + | | | |
| 6 | Breast cancer | | | | ++ | + | + | +++ | - | + |
| 7 | Endometrial cancer | | | | | | | ++ | + | + |
| 8 | NHL small cleaved cells LN | | | | ++ | - | - | | | |
| 9 | NHL node | | | | + | - | - | ++ | (+) | + |
| 10 | Thymoma | | | | +++ | (+) | + | | | |
| 11 | Sarcoma | | | | +++ | - | (+) | ++ | - | - |
| 12 | Mesothelioma | | | | +++ | + | + | | | |
| 13 | Testis (Sertolli cell tumor) | ++ | (+) | + | ++ | - | - | | | |
| 14 | Leiomyosarcoma | | | | +++ | (+) | ++ | | | |
| 15 | Squamous cervical carcinoma | | | | +++ | + | ++ | | | |
| 16 | Esophageal cancer | | | | | | | +++ | - | + |
| 17 | NSCLC | | | | +++ | - | - | | | |
| 18 | SCLC | | | | | | | + | - | - |
| 19 | Gastric cancer | | | | | | | +++ | - | + |
| 20 | NHL | | | | +++ | - | - | | | |
| 21 | Ovarian cancer (Hartmann) | | | | ++ | - | ++ | | | |
| 22 | Jejunum lymphoma | ++ | + | ++ | ++ | - | + | | | |

### Ovarian cancer tissue extracts assessment by means of Western blot

Ovarian cancer was our target of study from the beginning. Cell experiments may have provided us with indications and hints on KLK7 content, but ovarian cancer tissue extracts would allow a direct comparison of employed methods. In order to question if previously published data (Dorn 2006; Dorn 2007) based on ELISA measurements from a predefined cohort of patients correspond to intensity of signal in Western blot, we randomly selected tissue extracts (2 x “high” ELISA value, 2 x “medium” ELISA value, 2 x “low” ELISA value). Despite the fact that Western blot is a semi-quantitative method, it actually contributes valuable sets of information to an extent that strength of signal can be correlated with the protein quantity. Whatever substrate is used, the intensity of the signal should correlate with the presence of the antigen on the blotting membrane (Bjerrum 1988; Ursitti 1995; Bollag 1996; Gallagher 1996).

Two antibodies were employed for detection, R&D AF2624 and Arexis Tagena + Domino, and GAPDH mouse antibody for normalization. We observed reactivity of the R&D antibody with

a protein duplet of an apparent molecular weight of about 30 and 32 kDa, respectively. These two bands may well correspond to pro-KLK7 and activated KLK7, respectively. The intensity of the two bands corresponds well with the classification high, medium, and low by ELISA (although ELISA antibodies were very different). Many KLK proteases contain one or more surface-associated loop(s), which are readily accessible and cleaved by proteolytic attack (Blaber 2007). This may be true also for KLK7 and thus can explain the about 15 kDa-band in the KLK7 high expressing protein extracts.

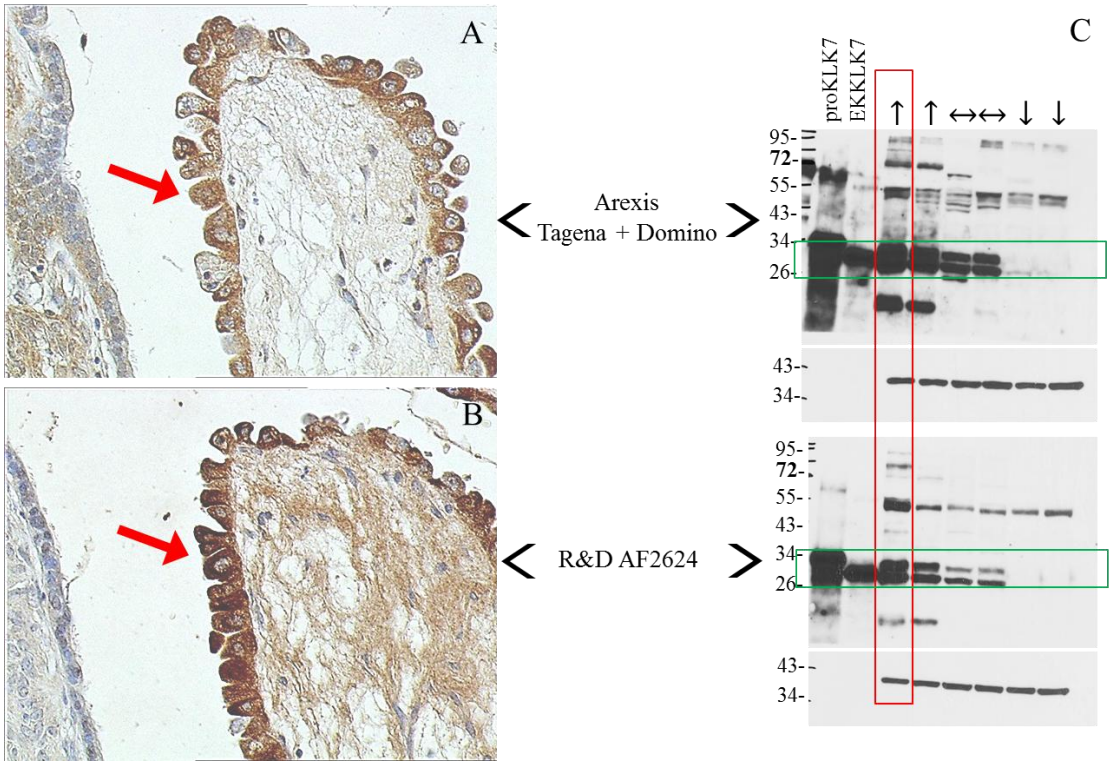


**Figure 26:** (a, b) Immunohistochemical image of a selected case corresponding to an extract from the blot. (a) Arexis Tagena + Domino (2.72 µg/mL) employed or (b) R&D AF2624 (40 µg/mL). Six randomly selected ovarian cancer cases categorized as couples of high, medium and low ELISA values (marked with arrowhead on the top, left-right and right respectively). Anti-GAPDH (20 ng/mL, #MAB374, Chemicon) on corresponding lanes below each main blot. proKLK7 and EKKLK7 100 ng/lane. Extracts 25 µg/lane. Blot on the top: KLK7 protein detected with Arexis Tagena + Domino (1.36 µg/mL), blot on the bottom detected with R&D AF2624 (0.2 µg/mL). Green frames indicate the position of the protein, between 26 and 34 kDa bands. Chemiluminescent radiography, film exposure 20 min. Red frame corresponds to a high ELISA value, which in turn matches with the immunohistochemical image deriving from the same tissue specimen. ELISA values highly correlate with band intensity as well as immunohistochemical intensity. Red arrows on immunohistochemical images indicate malignant ovarian epithelium, highly expressing KLK7 protein.

Employing the established immunohistochemical protocol for detecting KLK7 protein in tissue specimens, the corresponding cases were stained. Results confirm the already matching ELISA- Western blot data, as strong staining (+++) characterized the ovarian cancer tissue specimens with high ELISA values, and respectively the rest cases. This is an additional indication that (a) KLK7 is localized in malignant ovaries, (b) all techniques employed work adequately and produced results correlate perfectly.

Control studies, cell experiments, method cross-control and preliminary tissue extracts/specimen data all indicate the potential of a thorough immunohistochemical study including a follow-up of patients' clinical data on the basis of KLK7 expression levels.

**Staining of tissue microarrays employing the established immunohistochemical protocol**

Tissue microarray technology allows examination of a large number of samples at the same time, diminishing interindividual variance and decreasing technical time (Kononen 1998; Nocito 2001). For validation purposes, the antibodies directed to KLK7 were employed for assessment of normal multi-organ microarrays consisting of various benign tissue samples.

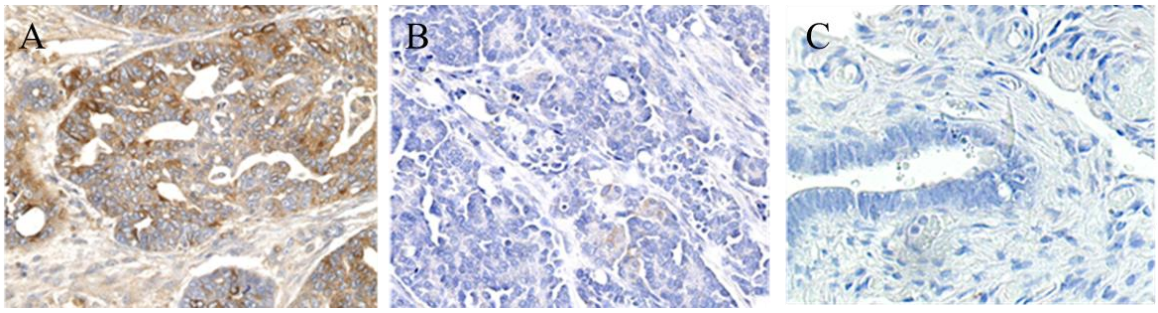


**Figure 27:** Expression of KLK7 antigen in ovarian cancer tissues. **(A-C)** Tissue microarray sections were stained with R&D AF2624 employing the Dako EnVision method. In **(A)** and **(B)**, paraffin-embedded, formalin-fixed ovarian cancer tissue samples either displaying a high **(A)** or a low **(B)** KLK7 antigen content as determined in detergent-released tissue extracts by KLK7-ELISA were stained for KLK7 antigen expression by immunohistochemistry. A high KLK7 antigen content **(A)** matches with pronounced cytoplasmic staining within tumor cells and moderate stromal staining whereas a low KLK7 antigen content **(B)** as determined by KLK7-ELISA is compatible with a faint cytoplasmic staining of tumor cells and absence of stromal cell staining (original magnification x 200). Benign ovary tissue (ovarian cystoma, 3915/96) **(C)** displays almost no KLK7 antigen.

Antibodies displayed different but constant results in diverse benign tissues as well as cytoplasmic staining. Immunostaining of luminal cells in case of prostate and placenta can be

interpreted as an indication for KLK7 being a secreted protein. In the same context of previously published data, cytoplasmic staining of tumor cells was revealed (Tanimoto 1999; Shigemasa 2001; Dong 2003). The immunostained TMAs were analyzed by pathologists according to a modified Remmele score. The results reveal a general trend of higher levels of KLK7 protein in malignant ovarian tissue compared to benign ovarian tissue. These results may suggest a potential role of KLK7 protein as tumor biological marker in ovarian cancer.

**Immunohistochemical evaluation -modified IRS**

For evaluation of KLK7 immunostaining intensity and tissue location, a quantitative score based on staining intensity and percentage of positive cells was created by inspecting at least two 0.6 mm tissue cores from each case. KLK7 staining intensity was classified on a scale of 0 to 3 (0 - no staining; 1 – weak staining; 2 – moderate staining; 3 – strong staining).

**Table 28:** Scoring scales for immunohistochemical assessment

| **R** | | | | | |
|---|---|---|---|---|---|
| **Intensity** | | **Positivity** | | **IRS** | |
| | **Score** | **%** | **Score** | | **Score** |
| - | 0 | ≤10 | 1 | negative | 0-2 |
| + | 1 | 11-50 | 2 | weak positive | 3-4 |
| ++ | 2 | 51-80 | 3 | moderate positive | 6-8 |
| +++ | 3 | >80 | 4 | strong positive | 9-12 |

| **$R_{10}$** | | | | **$R_4$** | | | |
|---|---|---|---|---|---|---|---|
| **Intensity** | | **Positivity** | | **Intensity** | | **Positivity** | |
| | **Score** | **%** | **Score** | | **Score** | **%** | **Score** |
| - | 0 | 0-10 | 1 | - | 0 | 0-25 | 1 |
| + | 1 | 11-20 | 2 | + | 1 | 26-50 | 2 |
| ++ | 2 | 21-30 | 3 | ++ | 2 | 51-75 | 3 |
| +++ | 3 | 31-40 | 4 | +++ | 3 | 76-100 | 4 |
| | | 41-50 | 5 | | | | |
| | | 51-60 | 6 | | | | |
| | | 61-70 | 7 | | | | |
| | | 71-80 | 8 | | | | |
| | | 81-90 | 9 | | | | |
| | | 91-100 | 10 | | | | |

The percentage of positively stained cells was scored by cell count on a scale of one to ten with grade 1: staining of <10 % of cells and grade 10 with >91 % of positive cells. Based on these scores, a final immunoreactivity score (IRS) was created by multiplication of the intensity score

values with the cell positivity score values for each, tumor cells (KLK7-RT) and stromal cells (KLK7-RN). In addition, an overall score was created by adding up the KLK7-RT and KLK7-RN score values (KLK7-RT+RN). Evaluation of immunostaining scores was performed independently by two examiners who basically agreed with the results of the analyses. In order to examine every potential, even hidden, this cohort could provide, we generated two artificial scores utilizing a different scale, as shown on **Table 28**. Briefly, these scores follow a different categorization pattern in positivity, namely a 10 % border and a 25 % border respectively. Statistics were applied for all three scores. The pattern and intensity of immunostaining of core punches on the TMA was comparable to that of whole tissue sections which have been evaluated in a preliminary study using the R&D antibody. Whereas benign ovary tissue sections displayed, if at all, a very low staining, in ovarian cancer tissue we observed staining of tumor cells and much less staining of stromal cells. The KLK7 immunostaining pattern varied from case to case.

### 5.1.3 Digitization and image analysis

Significant differences in appearance can occur among slides, despite the same processing. This discrepancy renders the slide unsuitable for statistical assessment. Artifacts may also cause variations among slides in terms of staining quality (aberrant staining, air bubbles). So, consistency in this respect is the challenge (Leong and McGee 2001).

Among the benefits of digitization is the archiving advantage in comparison with the millions of tissue blocks stored in Pathology institutes. Handling digitized slides is easier, less time-consuming and anytime accessible via computers.

Machines used for digitization are called slide-scanners and they are hybrid devices, as they combine the common image scanning principles with laser microscopes to achieve high-detail images. For the purposes of the ovarian cancer cohort, two different devices i.e. Hamamatsu Nanozoomer and Aperio Scanscope were employed to produce images of the tissue specimens, mostly of the tissue microarrays. They both take advantage of the line-scanning technology to compress large amounts of detail into one single image.

There are only a limited number of vendors that provide full-face and TMA high-throughput analysis, for example, SlidePath® and Aperio® (Conway 2008). In our case, the software

qualified for use was the one by SlidePath®, after thorough examination of the market (**Figure 29**).

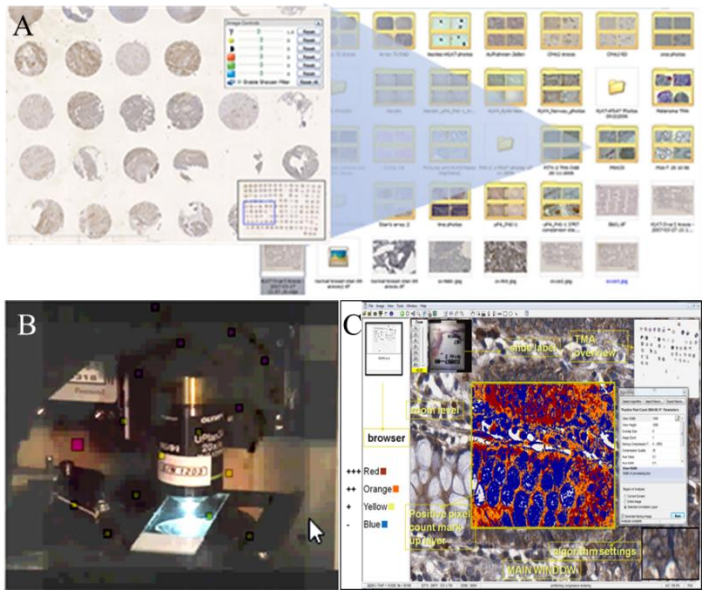


**Figure 28:** **(A)** Unique advantage of archiving with digitized slides. **(B)** Procedure of line scanning. **(C)** Image analysis module.

A high-detailed immunohistochemical image paves the way for further investigation, such as analysis of the scanned specimen. Image analysis is performed can be performed in multiple ways, such as in cognition principle or by employing algorithms (morphological and spatial).


**Figure 29:** Comparative alignment of image analysis software available in market. Green shade indicates tested software. The rest of the marketed software was approached with seminar or webinar sessions. There are only a limited number of vendors that provide full-face and TMA high-throughput analysis, for example, SlidePath® and Aperio®.

Positive Pixel Count® (PPC), an algorithm that quantifies the detection colored signal with use of layer masks, proved quite reliable. Average staining concentration, a measure which derives from the equation mentioned in the "Methods" section, provided us with a biological parameter straight comparable with the immunoreactive score (IRS) as assessed by the pathologist. In the "Statistics" section, average staining concentration is involved in correlation studies with clinicopathological parameters and other biological parameters, such as ELISA values. This underlines the significant properties of image analysis and provokes the already established manual evaluation by pathologists at the level of objectivity. Image analysis still lacks the human factor of comparative judgment (e.g. discrimination of tumor cells) but meets up the standards at simpler tasks, like staining quantification.

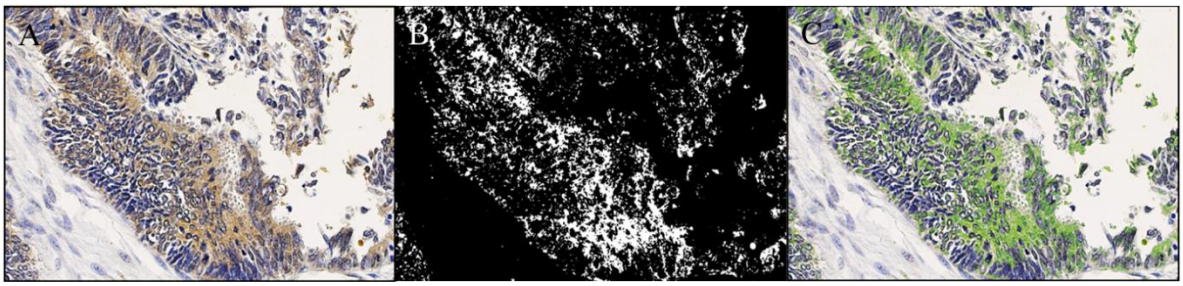


**Figure 30:** Proof-of-principle for SlidePath®'s Positive Pixel Count® algorithm. **(A)** Original ovarian cancer tissue stained with brown color ($DAB^+$). **(B)** Mask layer where color is subtracted and all the rest is blackened. **(C)** Green color artificially replaced the gaps (pseudocolor). Identical position of color proves the efficacy of the method. Magnification x 200.

### 5.1.4 Statistical analysis of KLK7 assessment in the ovarian cancer collective

For the assessment of clinical value of KLK7 in ovarian cancer, tumor biological and clinicopathological parameters were analyzed. KLK7 immunoscore derived from the immunohistochemical evaluation and represented as tumor cell score (RT-10), stromal cell score (RN-10) and combined score (RT+RN10). KLK7-Average concentration represented the automated analysis of the immunohistochemical staining, while KLK7 and CA125 were assessed by means of ELISA. Finally, age, stage, nuclear grade, residual tumor mass (RT), ascitic fluid volume, response to chemotherapy (CT) and lymph node contamination represented the panel of the clinicopathological factors.

#### 5.1.4.1 Correlation among the analyzed tumor biological factors

According to the statistical analysis, there is a strong, significant correlation between KLK7-RT10 and KLK7-RT+RN10 values ($r_s$=0.89, $P$<0.001) as well as between KLK7-RT+RN10 and KLK7-RN10 ($r_s$=0.70, $P$<0.001). Added to this, KLK7-Average concentration correlated significantly with either one of the KLK7-RT+RN10 ($r_s$=0.75, $P$<0.001) or KLK7-RT10 ($r_s$=0.74, $P$<0.001) and moderately with KLK7-RN10 ($r_s$=0.54, $P$<0.001). KLK7 protein content (ELISA) correlated weakly but significantly with all other factors: KLK7-RT10, KLK7-RN10, KLK7-RT+RN10 and KLK7-average concentration immunoscore values ($r_s$=0.39, $P$<0.001; $r_s$=0.30, $P$<0.01; $r_s$=0.30, $P$<0.001; and $r_s$=0.27, $P$<0.01). Additionally, we compared the CA125 levels in serum with the analyzed tumor biological factors. Here, we found a weak correlation with KLK7-RN10 ($r_s$=0.30, $P$<0.01), whereas in all other cases the $r_s$-value was below 0.2.

**Table 29:** Correlation ($r_s$) between tumor biological factors (n = 98)

| Parameter | KLK7-RT10 | KLK7-RN10 | KLK7-RT+RN10 | KLK7-Av. Conc. | KLK7 ELISA | CA125 (Serum) |
|---|---|---|---|---|---|---|
| RT10 | | | | | | |
| RN10 | 0.46 | | | | | |
| RT+RN10 | 0.89 | 0.70 | | | | |
| Av. Conc. | 0.74 | 0.54 | 0.75 | | | |
| KLK7 | 0.39 | 0.30* | 0.30* | 0.27* | | |
| CA125 | 0.13# | 0.30* | 0.12# | 0.10# | 0.06# | |

# n.s.; *$P$ < 0.01; all other: $P$ < 0.001

We grouped the values of all tumor biological factors into two categories (low and high) according to their median value and creating tertials. Alternatively, values were also grouped according to the 2/3 percentile (2 tertials; 66 %), defined as the optimal cut-off point for the group division into high (above the cut-off) or low (below the cut-off).

**Table 30:** Grouping of tumor biological factor values

| Parameter | n | median | high | low/high |
|---|---|---|---|---|
| KLK7 RT10 | 98 | 3.5 | > **5.01** | 68/30 (= 30.6% high) |
| KLK7 RN10 | 98 | 0 | > **0** | 74/24 (= 24.5% high) |
| KLK7 RT+RN10 | 98 | 5.0 | > **6.01** | 65/33 (=33.7% high) |
| KLK7 Average conc | 98 | 767.5 | > **1100** | 65/33 (=33.7% high) |
| KLK7 ELISA | 98 | 2.17 | > **4.0** | 65/33 (=33.7% high) |
| CA125 ELISA | 94 | 362.0 | > **800** | 63/31 (= 32.9% high) |

### 5.1.4.2 Association of KLK7 expression with clinicopathological parameters

The relationship between KLK7 immunoscore values and KLK7 antigen levels with relevant clinicopathological parameters of ovarian cancer patients is summarized in **Table 31**. A significant association was observed between KLK7-RT+RN10 score values and ascitic fluid volume for either categorization, zero values included in the low category or separated as a standalone category (*P*=0.004 and *P*=0.008, respectively). Furthermore, high levels of KLK7-RT10, KLK7-RT+RN10 and KLK7-Average concentration were related with residual tumor presence (*P*=0.033, P= 0.010 and *P*=0.018, respectively).Added to this, KLK7-Average concentration seems to be associated with the FIGO stage (P=0.034), KLK7-RN10 strongly with nuclear grade (P=0.004) and KLK7-ELISA with the response to chemotherapy (P=0.034). Weaker associations were found KLK7-RT10 with response to chemotherapy as well as for KLK7-ELISA with lymph nodes involvement (P= 0.052 and P=0.054 respectively) (**Table 31**).

**Table 31:** Association between clinical/histomorphologic characteristics of patients and tumor biological factors (n = 98)

| Clinicopathological parameters | No. patients | KLK7 RT10 low/high | KLK7 RN10 low/high | KLK7 RT+RN10 low/high | KLK7 Av. conc. low/high | KLK7 ELISA low/high |
|---|---|---|---|---|---|---|
| **Total** | **98** | 68/30 | 74/24 | 65/33 | 65/33 | 65/33 |
| Age | | *P* = 0.463 | P = 0.738 | *P* = 0.597 | *P* = 0.929 | *P* = 0.727 |
| ≤ 60 years | 60 | 40/20 | 46/14 | 41/19 | 40/20 | 39/21 |
| > 60 years | 38 | 28/10 | 28/10 | 24/14 | 25/13 | 26/12 |
| **FIGO stage** | | *P* = 0.195 | *P* = 0.935 | *P* = 0.281 | *P* = **0.034** | *P* = 0.970 |
| I + II | 21 | 17/4 | 16/5 | 16/5 | 18/3 | 14/7 |
| III + IV | 77 | 51/26 | 58/19 | 49/28 | 47/30 | 51/26 |
| **Nuclear grade** | | *P* = 0.883 | *P* = **0.004** | *P* = 0.497 | *P* = 0.278 | *P* = 0.840 |
| G1 + G2 | 37 | 26/11 | 22/15 | 23/14 | 27/10 | 25/12 |
| G3 + G4 | 61 | 42/19 | 52/9 | 42/19 | 38/23 | 40/21 |
| **Residual tumor mass** | | *P* = **0.033** | *P* = 0.171 | *P* = **0.010** | *P* = **0.018** | *P* = 0.695 |
| 0 cm | 52 | 40/12 | 43/9 | 41/11 | 40/12 | 35/17 |
| > 0 cm | 41 | 23/18 | 29/12 | 22/19 | 22/19 | 26/15 |
| **Residual tumor mass** | | *P* = ***0.093*** | *P* = 0.371 | *P* = **0.026** | *P* = ***0.061*** | *P* = 0.761 |
| 0 cm | 52 | 40/12 | 43/9 | 41/11 | 40/12 | 35/17 |
| ≤ 10 mm | 22 | 13/9 | 16/6 | 13/9 | 12/10 | 13/9 |
| > 10 mm | 19 | 10/9 | 13/6 | 9/10 | 10/9 | 13/6 |

| | | | | | | |
|---|---|---|---|---|---|---|
| **Ascitic fluid volume** | | *P* = 0.271 | *P* = 0.237 | *P* = **0.004** | *P* = 0.878 | *P* = 0.759 |
| < 500 ml | 64 | 47/17 | 51/13 | 49/15 | 43/21 | 42/22 |
| > 500 ml | 32 | 20/12 | 22/10 | 15/17 | 21/11 | 22/10 |
| **Ascitic fluid volume** | | *P* = 0.308 | *P* = 0.404 | *P* = **0.008** | *P* = 0.513 | *P* = 0.448 |
| None | 30 | 24/6 | 25/5 | 25/5 | 18/12 | 22/8 |
| < 500 ml | 34 | 23/11 | 26/8 | 24/10 | 25/9 | 20/14 |
| > 500 ml | 32 | 20/12 | 22/10 | 15/17 | 21/11 | 22/10 |
| **Nodes involved** | | *P* = 0.390 | *P* = 0.752 | *P* = 0.178 | *P* = 0.438 | *P* = ***0.054*** |
| No | 34 | 25/9 | 27/7 | 26/8 | 24/10 | 26/8 |
| Yes | 45 | 29/16 | 37/8 | 28/17 | 28/17 | 25/20 |
| **Response to CT** | | *P* = ***0.052*** | *P* = 0.507 | *P* = 0.469 | *P* = 0.353 | *P* = **0.034** |
| No | 13 | 12/1 | 11/2 | 10/3 | 10/3 | 12/1 |
| Yes | 63 | 41/22 | 48/15 | 42/21 | 40/23 | 39/24 |

$Chi^2$ test (cut-off point: > 66% percentile).

### 5.1.4.3 Association of KLK7 expression and clinicopathological parameters with patient survival

The association of clinicopathological parameters and KLK7 protein expression with OS and PFS is presented in **Table 32**. All clinical variables included in the Cox model, except for age, such as FIGO stage III/IV vs. I/II, nuclear grade, RT presence, and ascitic volume were univariate predictors for OS in the ovarian cancer cohort. Likewise, in univariate analysis of PFS, all of the clinicopathological parameters, except the age and the FIGO stage categories, reached statistical significance (**Table 32**). The expression level of KLK7 in tumor cells or stromal cells as detected by immunohistochemistry and the combined, overall score KLK7-RT+RN10 were not associated with patients' outcome in univariate Cox's regression analyses (**Table 32**). In case of the KLK7-Average score a weak relationship was observed with overall survival (HR=1.53, 95 % CI=0.92-2.53, P= 0.098). Strikingly, in multivariate analysis, KLK7-ELISA values, in addition to the FIGO stage and the residual tumor mass, were significantly associated with both OS and PFS. Ovarian cancer patients with low KLK7-ELISA levels had a significantly, more than two-fold higher risk of death or relapse with a hazard ratio of 0.51 (95 % CI=0.29-0.90, P=0.019) and 0.42 0.47 (95 % CI= 0.25-0.91, *P*=0.024), respectively as compared to patients who displayed high KLK7-ELISA levels (**Table 33**).

**Table 32:** Univariate Cox regression analysis for disease survival in patients with ovarian cancer (n = 98)

| Factor | No. cases | Overall survival | | Progression-free survival | |
|---|---|---|---|---|---|
| | | HR (95% CI)[a] | *P* | HR (95% CI)[a] | *P* |
| Total number | 98 | | | | |
| Age | | | | | |
| ≤ 60 years | 60 | 1 | | | |
| > 60 years | 38 | 1.49 (0.91-2.42) | 0.109 | 1.26 (0.73-2.19) | 0.410 |
| FIGO stage | | | | | |
| I + II | 21 | 1 | | 1 | |
| III + IV | 77 | 4.89 (2.10-11.4) | **<0.001** | 7.98 (2.48-25.7) | **<0.001** |
| Nuclear grade | | | | | |
| G1 + G2 | 37 | 1 | | 1 | |
| G3 + G4 | 61 | 1.88 (1.10-3.18) | **0.020** | 1.64 (0.91-2.96) | 0.100 |
| Residual tumor mass | | | | | |
| 0 mm | 52 | 1 | | 1 | |
| > 0 mm | 41 | 5.69 (3.28-9.87) | **<0.001** | 5.30 (2.91-9.63) | **<0.001** |
| Ascitic fluid volume | | | | | |
| < 500 ml | 64 | 1 | | 1 | |
| > 500 ml | 32 | 3.35 (2.03-5.52) | **<0.001** | 2.85 (1.61-5.05) | **<0.001** |
| KLK7 RT10[b] | | | | | |
| Low | 68 | 1 | | 1 | |
| High | 30 | 1.36 (0.82-2.27) | 0.235 | 1.53 (0.87-2.69) | 0.140 |
| KLK7 RN10 | | | | | |
| Low | 74 | 1 | | 1 | |
| High | 24 | 1.02 (0.59-1.77) | 0.942 | 0.83 (0.42-1.61) | 0.578 |
| KLK7 RT10+RN10[b] | | | | | |
| Low | 65 | 1 | | 1 | |
| High | 33 | 1.50 (0.91-2.46) | 0.110 | 1.41 (0.80-2.48) | 0.234 |
| KLK7 Av.conc.[b] | | | | | |
| Low | 65 | 1 | | 1 | |
| High | 33 | 1.53 (0.92-2.53) | ***0.098*** | 1.39 (0.78-2.47) | 0.258 |
| KLK7 ELISA[b] | | | | | |
| Low | 65 | 1 | | 1 | |
| High | 33 | 0.71 (0.42-1.20) | 0.201 | 0.66 (0.36-1.20) | 0.171 |

[a]HR: hazard ratio (95% confidence interval) of univariate Cox regression analysis. [b] dichotomized in high and low levels by the 66% percentile (low: 0 – 66%, high: > 66% percentile).

**Table 33:** Multivariate Cox regression analysis for the association of tumor biological factors with disease survival in patients with ovarian cancer.

| Factor | No. cases | Overall survival | | Progression-free survival | |
|---|---|---|---|---|---|
| | | **HR (95% CI)[a]** | ***P*** | **HR (95% CI)[a]** | ***P*** |
| Total number | 91 | | | | |
| Age | | | | | |
| ≤ 60 years | 57 | 1 | | 1 | |
| > 60 years | 34 | 1.37 (0.81-2.30) | 0.240 | 1.16 (0.64-2.10) | 0.624 |
| FIGO stage | | | | | |
| I + II | 18 | 1 | | 1 | |
| III + IV | 73 | 2.57 (0.95-6.99) | ***0.064*** | 3.80 (1.10-13.2) | **0.035** |
| Nuclear grade | | | | | |
| G1 + G2 | 34 | 1 | | 1 | |
| G3 + G4 | 57 | 1.20 (0.69-2.08) | 0.524 | 0.92 (0.50-1.70) | 0.787 |
| Residual tumor mass | | | | | |
| 0 mm | 51 | 1 | | 1 | |
| > 0 mm | 40 | 3.59(1.75-7.35) | **<0.001** | 3.43(1.65-7.12) | **0.001** |
| Ascitic fluid volume | | | | | |
| < 500 ml | 63 | 1 | | 1 | |
| > 500 ml | 28 | 1.14 (0.60-2.15) | 0.693 | 1.15 (0.57-2.33) | 0.699 |
| KLK7 RT10[b] | | | | | |
| Low | 62 | 1 | | 1 | |
| High | 29 | 1.12 (0.65-1.93) | 0.673 | 1.21 (0.67-2.18) | 0.526 |
| KLK7 RN10 | | | | | |
| Low | 71 | 1 | | 1 | |
| High | 20 | 0.62 (0.32-1.21) | 0.162 | 0.58 (0.28-1.21) | 0.149 |
| KLK7 RT10+RN10[b] | | | | | |
| Low | 62 | 1 | | 1 | |
| High | 29 | 0.97 (0.56-1.68) | 0.912 | 1.02 (0.55-1.88) | 0.949 |
| KLK7 Av.conc.[b] | | | | | |
| Low | 61 | 1 | | 1 | |
| High | 30 | 1.37 (0.76-2.47) | 0.288 | 1.20 (0.63-2.26) | 0.579 |
| KLK7 ELISA[b] | | | | | |
| Low | 60 | 1 | | 1 | |
| High | 31 | 0.51 (0.29-0.90) | **0.019** | 0.47 (0.25-0.91) | **0.024** |

[a]HR: hazard ratio (95% confidence interval) of multivariate Cox regression analysis. Biological markers were **separately** added to the base model of clinical parameters: age, FIGO stage, nuclear grade, residual tumor mass, and ascitic fluid volume. [b] dichotomized in high and low levels by the 66% percentile (low: 0 – 66%, high: > 66% percentile).

#### 5.1.4.4 Association of KLK7 expression and clinicopathological parameters with survival of FIGO III/IV patients

Additionally, we have performed analyses in the subgroup of patients with advanced ovarian cancer (FIGO stage III/IV; n=90). Here, the clinical variables RT presence and ascitic volume, but not nuclear grade, were univariate predictors for both OS and PFS (**Table 34**). Age was significant only in overall survival. Additionally, we found a significant association between low KLK7 antigen levels in tumor tissue extracts and an increased risk of death for FIGO III/IV patients in univariate Cox regression analysis (HR=0.55, 95 % CI= 0.31-0.95, P=0.032). KLK7 immunoscore values were not significantly related with OS and PFS in FIGO III/IV ovarian cancer patients.

Concerning the clinical parameters, in multivariate Cox analysis, the residual tumor mass remained a strong, statistically significant parameter for both OS and PFS. KLK7-ELISA turned out to be strongly associated with OS and PFS in multivariate analysis (HR=0.40, 95 % CI= 0.22-0.73, P=0.003 and HR=0.45, 95 % CI=0.23-0.87, P=0.018, respectively) (**Table 35**). These findings were confirmed by Kaplan-Meier estimation, and the association of KLK7-ELISA levels with OS and PFS is visualized by the respective survival curves (**Figure 31**). All other analyzed clinical and histomorphological markers as well as biological factors were not significantly related with OS and PFS in FIGO III/IV ovarian cancer patients.

**Table 34:** Univariate Cox regression analysis for disease survival in FIGO III/IV ovarian cancer patients (n = 77)

| Factor | No. cases | Overall survival | | Progression-free survival | |
|---|---|---|---|---|---|
| | | HR (95% CI)[a] | *P* | HR (95% CI)[a] | *P* |
| Total number | 77 | | | | |
| Age | | | | | |
| ≤ 60 years | 48 | 1 | | | |
| > 60 years | 29 | 1.82(1.08-3.04) | **0.023** | 1.47 (0.83-2.62) | 0.186 |
| Nuclear grade | | | | | |
| G1 + G2 | 24 | 1 | | 1 | |
| G3 + G4 | 53 | 1.51 (0.86-2.66) | 0.151 | 1.18 (0.64-2.16) | 0.600 |
| Residual tumor mass | | | | | |
| 0 mm | 33 | 1 | | 1 | |
| > 0 mm | 41 | 4.30 (2.39-7.73) | **<0.001** | 3.60 (1.93-6.69) | **<0.001** |
| Ascitic fluid volume | | | | | |
| < 500 ml | 46 | 1 | | 1 | |
| > 500 ml | 30 | 3.06 (1.81-5.19) | **<0.001** | 2.62 (1.45-4.73) | **0.001** |
| KLK7 RT10[b] | | | | | |
| Low | 51 | 1 | | 1 | |
| High | 26 | 1.37 (0.81-2.32) | 0.244 | 1.44 (0.81-2.56) | 0.214 |
| KLK7 RN10[b] | | | | | |
| Low | 58 | 1 | | 1 | |
| High | 19 | 1.10 (0.62-1.95) | 0.746 | 0.91 (0.46-1.78) | 0.786 |
| KLK7 RT10+RN10[b] | | | | | |
| Low | 49 | 1 | | 1 | |
| High | 28 | 1.53 (0.91-2.57) | 0.106 | 1.46 (0.82-2.59) | 0.202 |
| KLK7 Av.conc.[b] | | | | | |
| Low | 47 | 1 | | 1 | |
| High | 30 | 1.40 (0.83-2.35) | 0.207 | 1.18 (0.66-2.10) | 0.588 |
| KLK7 ELISA[b] | | | | | |
| Low | 51 | 1 | | 1 | |
| High | 26 | 0.55 (0.31-0.95) | **0.032** | 0.56 (0.30-1.05) | ***0.071*** |

[a]HR: hazard ratio (95% confidence interval) of univariate Cox regression analysis.

[b] dichotomized in high and low levels by the 66% percentile (low: 0 – 66%, high: > 66% percentile).

**Table 35:** Multivariate Cox regression analysis for the association of tumor biological factors with disease survival in FIGO III/IV ovarian cancer patients.

| Factor | No. cases | Overall survival | | Progression-free survival | |
|---|---|---|---|---|---|
| | | HR (95% CI)[a] | *P* | HR (95% CI)[a] | *P* |
| | 73 | | | | |
| Age | | | | | |
| ≤ 60 years | 46 | 1 | | 1 | |
| > 60 years | 27 | 1.40 (0.81-2.42) | 0.221 | 1.07 (0.58-1.99) | 0.822 |
| Nuclear grade | | | | | |
| G1 + G2 | 24 | 1 | | 1 | |
| G3 + G4 | 49 | 1.16 (0.65-2.07) | 0.611 | 0.86 (0.46-1.62) | 0.635 |
| Residual tumor mass | | | | | |
| 0 mm | 33 | 1 | | 1 | |
| > 0 mm | 40 | 3.49 (1.68-7.22) | **<0.001** | 3.31 (1.59-6.90) | **0.001** |
| Ascitic fluid volume | | | | | |
| < 500 ml | 46 | 1 | | 1 | |
| > 500 ml | 27 | 1.20 (0.62-2.31) | 0.586 | 1.24 (0.60-2.54) | 0.561 |
| KLK7 RT10[b] | | | | | |
| Low | 47 | 1 | | 1 | |
| High | 26 | 1.23 (0.70-2.16) | 0.468 | 1.26 (0.69-2.30) | 0.450 |
| KLK7 RN10[b] | | | | | |
| Low | 56 | 1 | | 1 | |
| High | 17 | 0.65 (0.33-1.28) | 0.217 | 0.59 (0.28-1.25) | 0.168 |
| KLK7 RT10+RN10[b] | | | | | |
| Low | 47 | 1 | | 1 | |
| High | 26 | 1.04 (0.59-1.83) | 0.895 | 1.05 (0.56-1.95) | 0.888 |
| KLK7 Av.conc.[b] | | | | | |
| Low | 46 | 1 | | 1 | |
| High | 27 | 1.66 (0.89-3.07) | 0.109 | 1.32 (0.68-2.54) | 0.411 |
| KLK7 ELISA[b] | | | | | |
| Low | 47 | 1 | | 1 | |
| High | 26 | 0.40 (0.22-0.73) | **0.003** | 0.45 (0.23-0.87) | **0.018** |

[a]HR: hazard ratio (95% confidence interval) of multivariate Cox regression analysis.

Biological markers were **separately** added to the base model of clinical parameters in the **FIGO III/IV** subgroup: age, nuclear grade, residual tumor mass, and ascitic fluid volume. [b] dichotomized in high and low levels by the 66% percentile (low: 0 – 66%, high: > 66% percentile).

If tumor biological factors are added in the basis model of the clinicomorphological characteristics simultaneously, then KLK7-ELISA association with OS and PFS is similar to the previous analysis (HR= 0.48, 95 % CI= 0.26-0.87, P= 0.016 and HR= 0.47, 95 % CI= 0.24-0.92, P= 0.026, respectively), where factors were added separately (**Table 36** and **37**). For the total of the patients then, FIGO stage and residual tumor mass are significant for the OS and PFS HR= 0.35, 95 % CI= 0.18-0.66, 0.001 and HR= 0.43, 95 % CI= 0.22-0.86, P= 0.016, respectively). In the reduced group of FIGO III/IV patients, KLK7-Average concentration is significant for the OS, while residual tumor mass proved to be significant for both OS and PFS (data not shown).

**Table 36:** Multivariate Cox regression analysis for KLK7-ELISA (**all patients**). **All** tumor biological factors were added **simultaneously** to the base model (including **age).**

| **Factor** | **No. cases** | **Overall survival** | | **Progression-free survival** | |
|---|---|---|---|---|---|
| | | HR (95% CI)[a] | *P* | HR (95% CI)[a] | *P* |
| KLK7 ELISA | 91 | | | | |
| Low | | 1 | | 1 | |
| High | | 0.48 (0.26-0.87) | **0.016** | 0.47 (0.24-0.92) | **0.026** |

**Table 37:** Multivariate Cox regression analysis for KLK7-ELISA (**FIGOIII/IV patients**). **All** tumor biological factors were added **simultaneously** to the base model (including **age).**

| **Factor** | **No. cases** | **Overall survival** | | **Progression-free survival** | |
|---|---|---|---|---|---|
| | | HR (95% CI)[a] | *P* | HR (95% CI)[a] | *P* |
| KLK7 ELISA | 73 | | | | |
| Low | | 1 | | 1 | |
| High | | 0.35 (0.18-0.66) | **0.001** | 0.43 (0.22-0.86) | **0.016** |

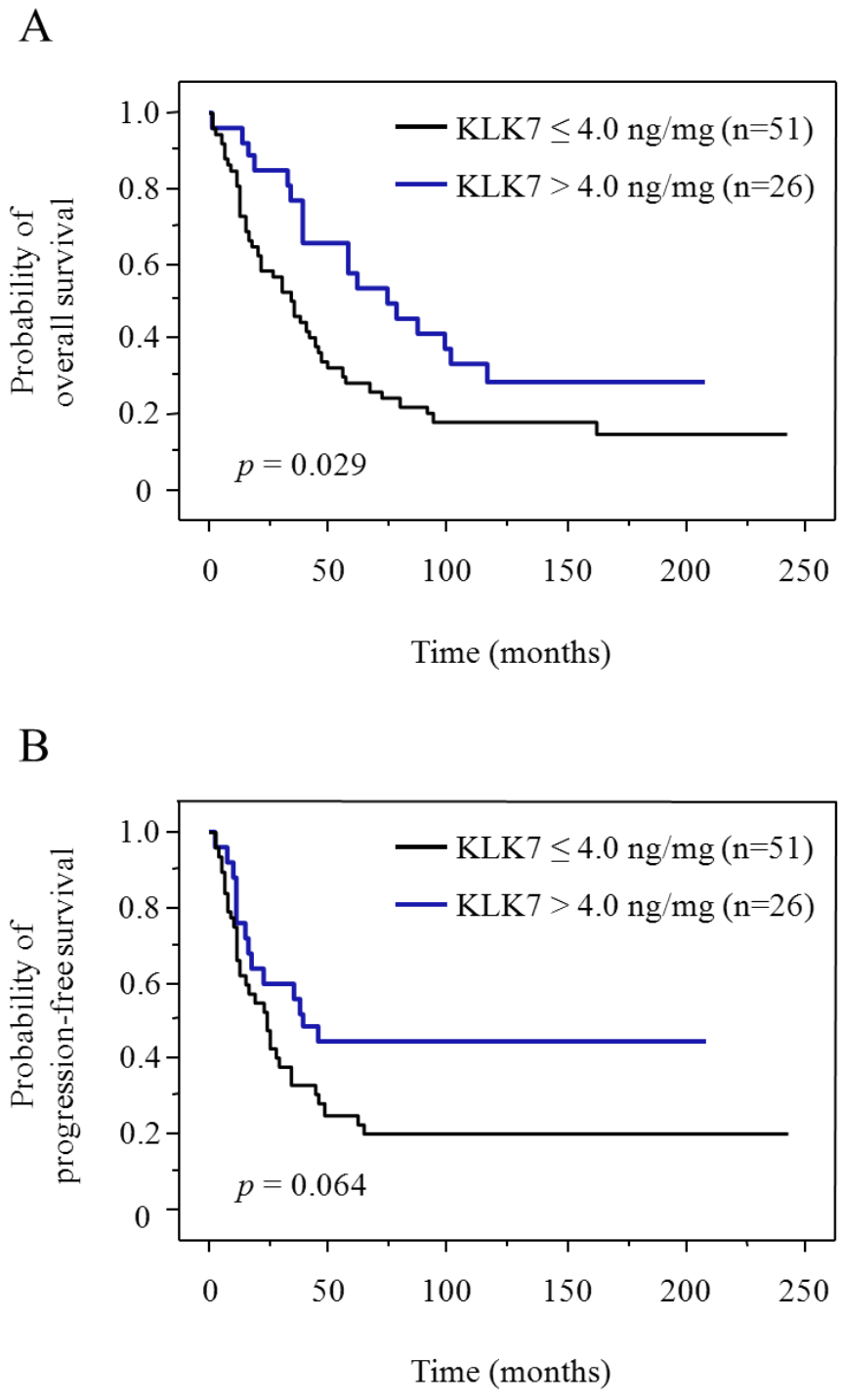


**Figure 31:** Prognostic significance of KLK7 antigen in advanced (FIGOIII/IV) ovarian cancer patients. Univariate Kaplan–Meier survival analysis revealed that patients with KLK7 status low (≤ 4.0 ng/mg protein, n= 51) display an increased risk of death (OS) (**A**) and progression (PFS) (**B**). P-values were calculated by use of Kaplan-Meier log rank test.

### 5.1.5 Ascitic fluid cells for assessment of KLK7 protein

Ovarian cancer is the third most common neoplasm of the female reproductive organs, but the leading cause of death from a gynecological malignancy (Cannistra 2004). Therefore, it is important to look for indications for early prognosis.

KLK7 seems to participate in skin desquamation, a process that is similar to detachment and dissemination of migrating cells in the process of metastasis (Brattsand 2005). KLK7 content was assessed by ELISA in biological fluids and found at highest concentrations in CVF, with lower concentrations in breast milk, seminal plasma, breast cancer cytosol, ascites, and saliva (Shaw and Diamandis 2007). Additionally, higher KLK7 and α5/β1 integrin levels in serous epithelial ovarian cancer cells from ascitic fluid were discovered by means of Western blot and immunohistochemistry; results which suggest a mechanism for the association of high KLK7 levels poor prognosis for serous ovarian cancer patients by promotion of peritoneal dissemination (Dong 2010). Independent data support the dissemination hypothesis, as serum and ascitic fluid from the same ovarian cancer patient cohort have been examined for KLK5 antigen content and confirm that significant amounts of KLK5 are released into the blood stream (Yousef 2003c; Dorn 2011). Since KLK5 and KLK7 co-participate in the skin desquamation process, this borrowed model implies that KLK7 might also play a role in the ovarian cancer cell dissemination.

Ascitic fluid cells potentially derive from the primary site and thus high KLK7 content in the malignant cell portion and/or the liquid fraction confirms hypothesis.

**Western blotting**

Ascitic fluid collected straight from the operation room was subjected into immediate centrifugation and fractions were divided into a cell pellet devoid of erythrocytes and a supernatant resulting from centrifugation. Five supernatants collected were tested for KLK7 presence using two antibodies for immunoprecipitation and detection, Arexis Tagena + Domino and R&D AF2624.

Generally, both antibodies reacted similarly, displaying strong reactivity with all ascitic fluid samples. This confirms the presence of KLK7 protein in the ascitic fluid. Despite strong cross-reactivity as result of the presence of many different proteins in ascitic fluid, KLK7 seems to be

present. Substances in sample bind non-specifically to unwanted proteins either agarose beads or antibodies, and this is not caused by high antibody concentrations or inadequate washing. At the same time, controls were clear of signal, fact that reassures the performance of the immunoprecipitation technique. Thus, non-specific binding to Protein G agarose beads can be excluded.

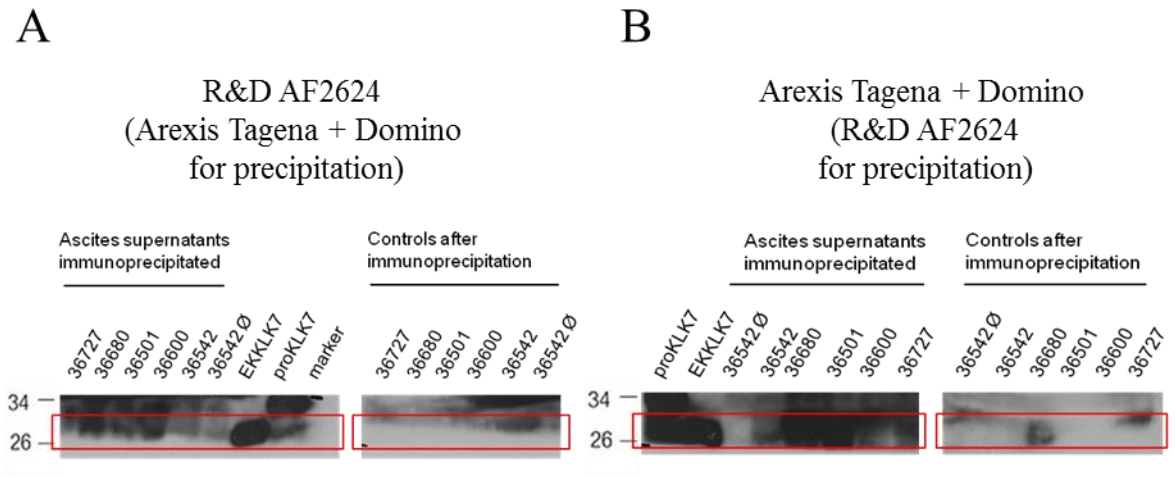


**Figure 32:** Ascitic fluid supernatants (collected after centrifugation) blotted together with recombinant KLK7 (100 ng) and the pro-form (100 ng), following an immunoprecipitation procedure with **(A)** Arexis Tagena + Domino (2 µg/mL) and detected with R&D AF2624 (0.2 µg/mL) or **(B)** with R&D AF2624 (2 µg/mL) and detected with Arexis Tagena + Domino (1.36 µg/mL). Chemiluminescent radiography, film exposed for 75 min. Controls marked with Ø lack immunoprecipitant antibody. Controls after immunoprecipitation represent the remaining solution after the procedure. Controls are clear at any case.

Samples used for immunoprecipitation were cleared from erythrocyte contamination. Different types of cells such as epithelial cells, macrophages and tumor cells reside in the samples. This means that the KLK7 origin is unknown, or at least it is not possible to identify epithelial origin or connect KLK7 to tumor cells. It is, however, a hint, supporting evidence that KLK7 is actually present in the extract together with other proteins which bind unspecifically and blur the total image of the blot.

Further, it is unclear from the blot if both forms of KLK7, proform and mature form, are detected. For sure that there is a band at the position of mature KLK7 (similar molecular weight), but one cannot confirm the same for the proform.

**CLSM and ICC**

Samples obtained from paramagnetic separation (MACS) were subjected to cytofluorometric and CLSM analysis. In these assays, Arexis Tagena + Domino detection antibody was employed to capture any potential native KLK7 epitope due to its broad spectrum, whereas FITC was used as fluorochrome.

Paramagnetic separation achieved to discriminate regular cell from debris, as well individual cells from cell clumps. EpCam antibody successfully selected the epithelial-origin cells, as this was visually confirmed by microscopy. On the contrary, cytofluorometry did not provide adequate evidence.

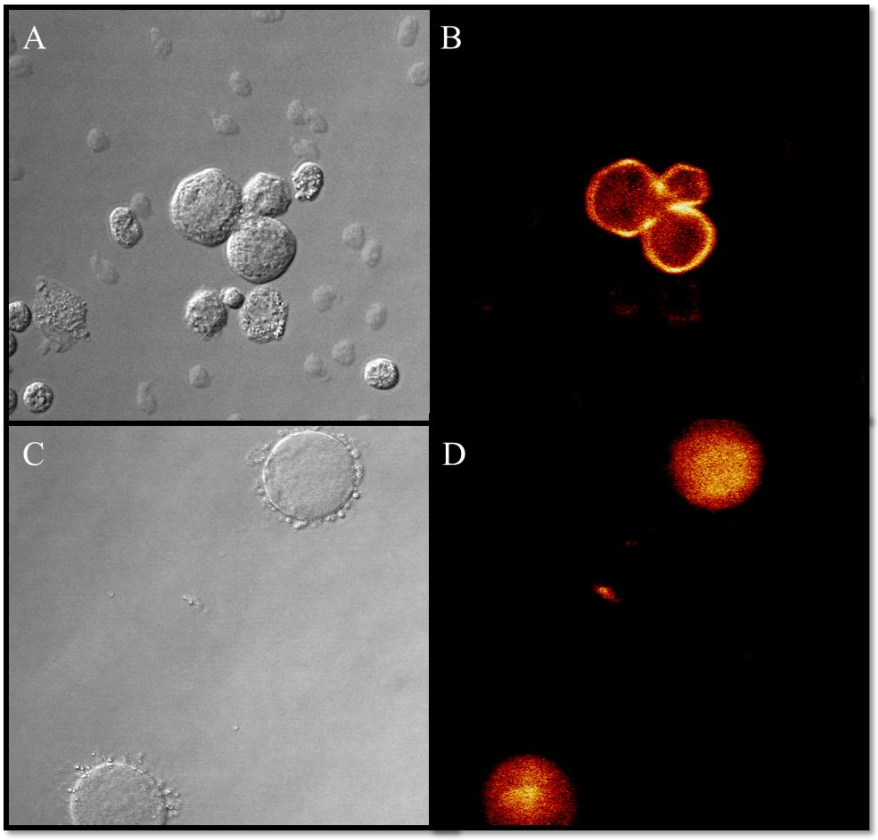


**Figure 33:** Ascitic fluid cells before **(A, B)** and after **(C, D)** magnetic separation. Color intensity, and thus protein content, increases as moving towards the yellow area (**Appendix 10.3**, look-up table). Only big epithelial-type cells could be detected with the FITC-conjugated antibody (#130-080-301, anti-EpCam-FITC, Miltenyi Biotec), in contrast with the unprocessed fraction, where smaller cells are also apparent. Magnification x 460.

While cell suspension is full of different types of cells, such as macrophages, lymphocytes and epithelial-type cells, as well as with cell debris before separation, this picture changes after paramagnetic force is applied. Images clearly demonstrate that only bigger cells (epithelial-type) express the EpCam antigen on their surface (CLSM images), while the rest seem to be dark. When $EpCam^{+}$-selected cells plus control samples (no paramagnetic enrichment) were deposited on a slide and subsequently stained for KLK7 with two different antibodies (Arexis and R&D), it was clearly demonstrated that the type of cells expressing the EpCam i.e. the bigger epithelial-type, it also expressed KLK7 cytoplasmically. Immunocytochemical images confirm the CLSM picture in terms of cell population and they additionally correlate epithelial-type cells with KLK7 expression.

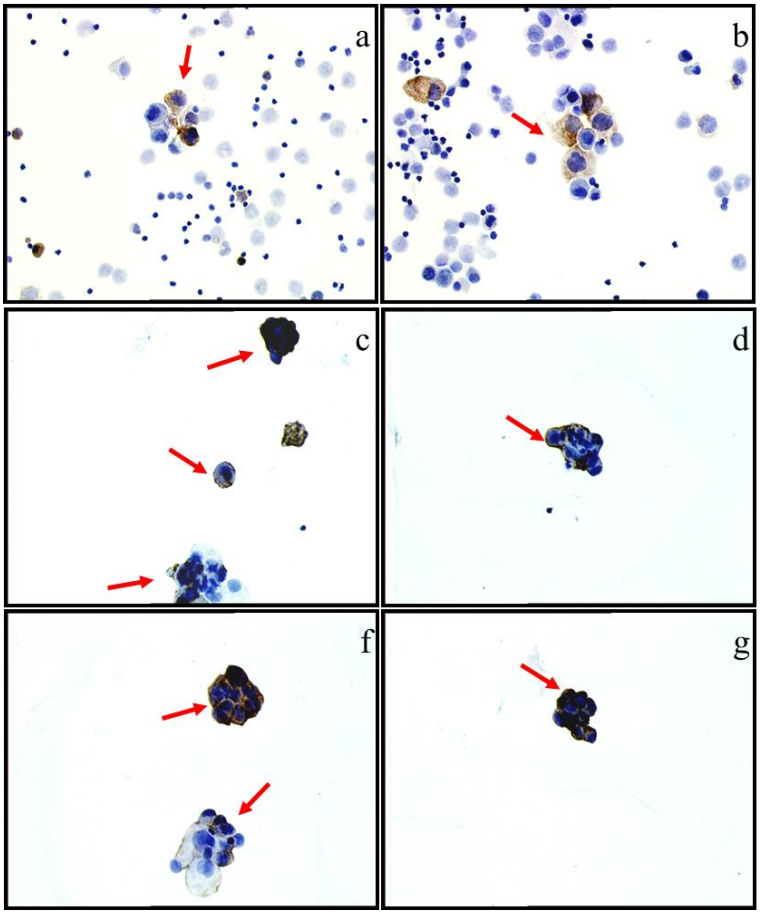


**Figure 34:** Ascitic fluid cell cytospins before **(a, b)** and after **(c, d, f, g)** magnetic separation. Cells stained for KLK7 with Arexis Tagena + Domino (1.36 μg/mL). Blue for nuclei (hematoxylin), brown for KLK7 antigen ($DAB^{+}$). Red arrows indicate stained cells. Clearly, magnetic separation discards cell debris and types other than epithelial cells. Positive staining characterizes epithelial cells at any case. Dako Envision method employed. Magnification x 200.

In this respect, it is important to know whether these stained cells of epithelial origin are tumor or normal cells. With the help of our cytopathologist, almost all paramagnetically selected samples stained with PAP and separately with Giemsa, revealed tumor cell populations mixed with normal cell populations.

Metastasis from an ovarian adenocarcinoma is the most common etiology for the presence of malignant cells in effusions in female patients. Tumor cells have disseminated to the peritoneal cavity already at diagnosis in two-thirds of ovarian carcinoma patients. Isolated malignant cells are often obscured by large mesothelial cell and macrophage populations in effusions. (Davidson 2004). These floating malignant cells are uniquely capable of proliferating, advancing and developing alternative means for acquisition of survival signals. The ascites of ovarian cancer itself has migratory properties on other cancer cell types and can contribute to additional MMP activation and invasion (Kassis 2005).

**Table 38:** Ascites cases studied, with diagnosis and cytology report included. The report confirms the presence of tumor cells in the ascitic fluid.

| Case | Diagnosis | Staining | Cytology report |
|---|---|---|---|
| 36542 | Ovarian cancer | PAP & Giemsa | Tumor cell clusters present |
| 36600 | Ovarian cancer | PAP & Giemsa | Tumor cell clusters present |
| 36501 | Ovarian cancer | PAP & Giemsa | Tumor cell clusters present, also normal mesothelial cells |
| 36680 | Ovarian cancer | PAP & Giemsa | Unclear/ undefined |

## Other tissues for assessment of KLK7

In order to expand the KLK7 panel of expression and get a hint of where this protease could harbor in physiological conditions, a tissue microarray consisting of multiple normal tissue cores was subjected into immunohistochemical analysis. KLK7 seems to reside in many tissues apart from the ones already mentioned in the literature (Shaw and Diamandis 2007), as aberrant levels could be observed in tissues like placenta, stomach and tonsils. No final conclusion can be extracted since this was just a small collection of tissues, but nevertheless our solid SOP for KLK7 indicates deposition especially in organs with secretory functions.

Analytically, skin outer layers expressed predominantly KLK7, a fact that is in accordance with the complete set of publications on skin physiology applying immunohistochemistry, but also by ELISA (Lundstrom and Egelrud 1991; Petraki 2006b; Shaw and Diamandis 2007). Arexis Tagena + Domino antibody produced a consistent and heterogeneous pattern, with distinct cell types stained. KLK7 in skin is considered to participate in protease activation pathways that lead in the physiological process of skin desquamation. In dermis, sweat glands are strongly stained, evidence supported by the secretory nature of kallikrein-related peptidases. In aorta, our immunohistochemical assessment revealed a weak to moderate staining in the smooth muscle of the tunica media, a finding that is not supported by any scientific reference by means of IHC or ELISA. On the other hand, heart muscle cells were moderately to intensively stained, in the same context with published ELISA data (Shaw and Diamandis 2007). All parts of the gastrointestinal tract demonstrated remarkable KLK7 localization. This might be not coincidental, since many peptic enzymes reside in the tract and KLKs could actually play the role of proteolytic activators. Appendix demonstrated KLK7 localization focally in mucosa and in crypts (all cell types) towards the luminal part, as Petraki et al. also noted. Added to that, colon was stained in all mucosa sites and crypts similarly to the appendix, in agreement with Petraki et al. but not with Shaw et al., where no KLK7 is detectable by means of ELISA. In small intestine, ileum is stained in the inner part of the cryptic mucosa and in the muscularis mucosa, while jejunum stained strongly in the inner mucosa of the epithelium (villi) and faintly in the outer part. Petraki also demonstrated expression in all epithelial-type cells; ELISA results indicate moderate expression for small intestine. In stomach, muscularis mucosae as well as chief cell layer of the mucosa are predominantly stained, again in agreement with Petraki et al. who underline that the gastric mucosa expressed KLK7 focally in all cell types (Petraki 2006b). Chief cells of the stomach secrete the digestive enzymes (pepsins) and have the typical appearance of serous-secretory epithelial cells. No KLK7 could be detectable by means of ELISA. Finally, esophagus was stained in the tunica mucosa, finding also supported by ELISA data.

**Table 39:** KLK7 protein expression in normal tissues, comparison with literature and potential link to physiologic role.

| Tissue | Findings and staining pattern | Literature findings | Reference | Potential link to physiology |
|---|---|---|---|---|
| **Skin** | Strongly stained outer layers/ Consistent and heterogeneous (distinct cell types stained) | Highest concentrations/ high KLK7 in cornified layers | (Lundstrom and Egelrud 1991) | Desquamation process |
| **Aorta** | smooth muscle of the tunica media; weak to moderate staining | Not present by ELISA | (Shaw and Diamandis 2007) | |
| **Appendix** | in mucosa and in crypts towards the luminal part; focally all cell types | All parts of the appendix showed IE in all cell types | (Petraki 2006b) | Activation of other enzymes |
| **Bone marrow** | Stained periphery of the adipose cells, sinusoids (endothelia) and erythrocytes | | | |
| **Cerebellum** | mostly in the white matter area with a faintly stained granular layer; Specific cell-type stained | | | |
| **Cerebral cortex** | pyramid cells of the granular layer remained unstained; Moderate staining | Gray- and white-matter neurons, as well as glial cells (astrocytes and oligodendrocytes), were weakly to moderately immunoreactive/ No KLK7 by ELISA. | (Petraki 2006b) (Shaw and Diamandis 2007) | Alzheimer's disease |
| **Colon** | all mucosa sites and crypts similarly to the appendix; Predominant staining (all epithelia-type cells) | No KLK7 by ELISA/ all cell types stained | (Shaw and Diamandis 2007) (Petraki 2006b) | Activation of other enzymes |
| **Heart muscle** | Heart muscle cells; moderately to intensively | High concentrations by ELISA | (Shaw and Diamandis 2007) | |
| **Jejunum** | stained strongly in the inner mucosa of the epithelium (villi) and faintly in the outer part | epithelial cells all intestine/ moderate expression by ELISA | (Petraki 2006b) (Shaw and Diamandis 2007) | Activation of other enzymes |
| **Esophagus** | stained in the tunica mucosa | High concentrations by ELISA/The non-keratinizing squamous epithelia of esophagus were negative. In contrast, the ductal epithelium of the submucosal glands expressed KLK7 | (Shaw and Diamandis 2007) (Petraki 2006b) | Location (perhaps secretion) of KLK7 in the submucosal glands |

| Tissue | Findings and staining pattern | Literature findings | Reference | Potential link to physiology |
|---|---|---|---|---|
| **Pancreas** | strongly positive in the glandular acinus but negative in the Langerhans islets. Distinctive staining | No KLK7 by ELISA/ In the exocrine pancreas, IE was observed in the medium- and small-sized pancreatic ducts, while acinar cells were negative. Strong positivity was found in cells of the islets of Langerhans. Scattered positive pancreatic acinar cells. | (Shaw and Diamandis 2007) (Petraki 2006b) | |
| **Placenta** | Placenta demonstrated strong staining of the villi, especially the outer membrane | KLK7 localized in the endothelia, calcifications of the villi, and 'X' cells, and focally in trophoblastic cells | (Petraki 2006b) | |
| **Prostate** | luminal secretory cells are positive, surrounding stroma (smooth muscle cells and connective tissue) faintly positive; Heterogeneous pattern | No KLK7 by ELISA/ In benign prostatic epithelium, the luminal secretory cells were stained. | (Shaw and Diamandis 2007) (Petraki 2006b) | |
| **Dermis (gland)** | sweat glands are strongly stained | | | |
| **ileum** | stained in the inner part of the cryptic mucosa and in the muscularis mucosa | Moderate expression by ELISA/ All parts of the small and large intestine showed IE in all cell types | (Shaw and Diamandis 2007) (Petraki 2006b) | Activation of other enzymes |
| **Stomach** | muscularis mucosae as well as chief cell layer of the mucosa are predominantly stained | No KLK7 by ELISA/ The gastric mucosa expressed KLK7 focally in all cell types | (Shaw and Diamandis 2007) (Petraki 2006b) | Chief cells of the stomach secrete the digestive enzymes (pepsins) |
| **Thymus** | the Hassal's corpuscles of the medulla are faintly stained whereas cortex is clear | No KLK7 by ELISA/ Characteristic positivity was only observed in Hassall's corpuscles of the thymus | (Shaw and Diamandis 2007) (Petraki 2006b) | |
| **Thyroid** | parafollicular cells, which secrete calcitonin, are stained positively. | Weak expression by ELISA/ Focal IE was revealed in follicular cells in the thyroid gland | (Shaw and Diamandis 2007) (Petraki 2006b) | |
| **Liver** | Hepatocytes are stained | Strong expression by ELISA/ Hepatocytes were negative | (Shaw and Diamandis 2007) (Petraki 2006b) | |
| **Lymph node** | Sparsely macrophages, sinusoids (endothelia). Heterogeneous pattern, specific cell types stained | | | |

| Tissue | Findings and staining pattern | Literature findings | Reference | Potential link to physiology |
|---|---|---|---|---|
| **Kidney** | glomeruli are not stained, while distal and proximal tubuli are | Moderate expression by ELISA/ Epithelium of tubuli showed IE, while glomeruli were negative | (Shaw and Diamandis 2007) (Petraki 2006b) | |
| **Breast** | ducts, lobes and luminal sections are stained | Negative by ELISA/ IE was identified in ductal and lobuloalveolar structures of the non-malignant breast. Luminal secretions were also positive | (Shaw and Diamandis 2007) (Petraki 2006b) | |
| **Skeletal muscle** | stained, but surrounding connective tissue clear | Moderate expression by ELISA | (Shaw and Diamandis 2007) | |

Pancreas was strongly positive in the glandular acinus but negative in the Langerhans islets, in a rather distinctive mode. This is in contrast with Petraki et al. who suggest that Langerhans islets are positive for KLK7 as well as with ELISA data, which do not indicate KLK7 expression. It seems that KLK7 is secreted in the exocrine gland (acinus) and not in the endocrine (Langerhans). Co-localization with KLK5 supports this finding as it reminds of the skin localization of the two proteases (Dong 2008). ELISA data contradict KLK7 pancreatic localization. Hepatocytes of liver are also stained, a result that agrees certainly with the published ELISA data. Since hepatocytes produce proteolytic enzymes, KLK7 presence there might play an activator role. In brain, cerebellum was stained mostly in the white matter area with a faintly stained granular layer, while in the cerebral cortex pyramid cells of the granular layer remained unstained. Petraki et al. state that gray- and white-matter neurons, as well as glial cells (astrocytes and oligodendrocytes), were weakly to moderately immunoreactive, although no KLK7 was detected by ELISA. KLK7 presence (downregulation) in brain has been previously speculated for dementia and Alzheimer's disease (Diamandis 2004b). Placenta demonstrated strong staining of the villi, especially the outer membrane, Petraki et al. contribute that KLK7 is localized in the endothelia, calcifications of the villi, and 'X' cells, and focally in trophoblastic cells. In prostate, luminal secretory cells are positive and surrounding stroma (smooth muscle cells and connective tissue) faintly positive. The staining pattern is distinctly heterogeneous. No KLK7 was detected by ELISA. In thymus, the Hassal's corpuscles of the medulla are faintly stained whereas cortex is clear (Petraki 2006b), whereas in thyroid gland, parafollicular cells, which secrete calcitonin, are stained positively. In kidney, glomeruli are not stained, while distal and proximal tubuli are. Moderate expression was captured by ELISA.

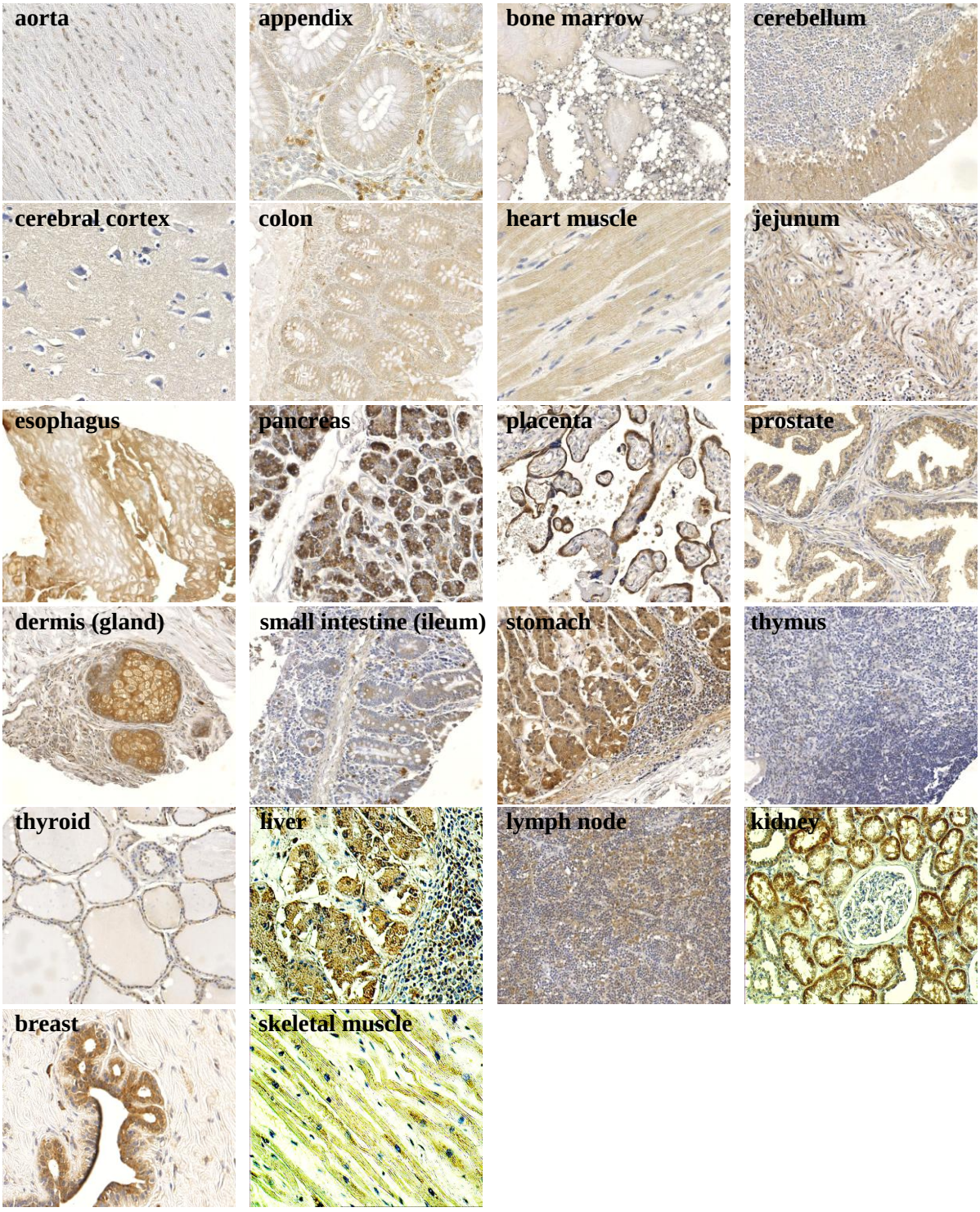


**Figure 35:** Various tissues stained for KLK7 protein with Arexis Tagena + Domino (2.72 µg/mL) employing the Envision method. Brown for KLK7 ($DAB^+$), blue for nuclei (hematoxylin). Magnification x 100. KLK7 protein is present in all secretory organ parts, but also in muscles and skin, a fact that indicates its proteolytic role in physiological processes.

In breast, ducts, lobes and luminal sections are stained but no expression is apparent by ELISA. Petraki et al. also provide evidence for all the above. In bone marrow, it seems that adipose cells in their periphery, sinusoids (endothelia) and erythrocytes are stained. In the breast lymph node, sparsely macrophages and also sinusoids are stained. Finally, skeletal muscle is stained, but surrounding connective tissue remains clear.

Apart from healthy FFPE tissue, immunohistochemical studies expanded in the malignant state and collectives of other types of cancer aligned with the ovarian cancer collective.

KLK7 is present in normal skin but downregulated in melanoma tissue. In our melanoma collective, tissue cores from >100 patients were included in a tissue microarray panel and arrays were stained for KLK7 (EnVision, Permanent Red). According to previously published data (Winnepenninckx 2006), KLK7 in melanoma was statistically significant and tended to underexpress in melanomatic nests. This was clearly indicated in our study, as 80 % of the cases demonstrated negativity in the same areas. KLK7 is overexpressed by ovarian tumor cells, but is not expressed by normal tissues. Elevated KLK7 expression in ovarian cancer tissue is associated with poorer prognosis of ovarian cancer patients, especially those with lower grade disease and those who have been optimally debulked (Tanimoto 1999; Shigemasa 2001; Dong 2003; Kyriakopoulou 2003; Yousef 2003d; Davidson 2004; Bondurant 2005; Bignotti 2006; Dorn 2006; Petraki 2006b; Shan 2006; Dorn 2007). KLK7 is expressed in normal breast and downregulated in breast cancer. Within breast cancer, high KLK7 expression is associated with good patient outcome (Yousef 2000d; Talieri 2004; Holzscheiter 2006). KLK7 is expressed in normal endocervical glands but elevated in cervical adenocarcinomas. No correlation was found between KLK7 expression and survival (Santin 2004a; Tian 2004). In non-small cell lung cancer, KLK7 expression is significantly lower expressed in adenocarcinoma than in matched non-malignant lung tissue (Planque 2005; Petraki 2006b). KLK7 is overexpressed in pancreatic adenocarcinomas over normal pancreatic tissue. Only about 15 % of the normal tissue specimens expressed the KLK7 protein (Johnson 2007). KLK7 is elevated in brain tumors over normal brain tissue. KLK7 mRNA expression is associated with shorter overall survival compared to patients with no KLK7 expression (Petraki 2006b; Prezas 2006b). KLK7 gene is up-regulated in colon cancer and its expression predicts poor prognosis for colon cancer patients (Talieri 2009b). In our colon cancer collective, tissue

specimens of 266 primary colon cancer patients were stained for KLK7 using two different antibodies. Colon cancer tissue specimens examined show an overall strong expression for KLK7. In oral cavity, cDNA microarray analysis revealed that KLK7 was upregulated in tumor samples versus normal controls. RT-qPCR analysis confirmed that KLK7 mRNA was most differentially regulated with a 5.3-fold increase. Immunohistochemical analysis demonstrated strong reactivity in and human OSCC tissues (Pettus 2009). In other experiments, KLK7 was expressed strongly in the majority of tumor cells in 68 of 80 cases: these were mostly moderately or poorly differentiated neoplasms. Staining was particularly intense at the infiltrating front. Patients with intense staining had significantly shorter overall survival ($p < .05$) (Zhao 2011).

**Table 40:** KLK7 expression in various carcinomas

| Type of cancer | Literature findings | References |
|---|---|---|
| **Ovary** | KLK7 is overexpressed by ovarian tumor cells, but is not expressed by normal tissues. Elevated KLK7 expression in ovarian cancer tissue is associated with poorer prognosis of ovarian cancer patients, especially those with lower grade disease and those who have been optimally debulked. | (Tanimoto 1999; Shigemasa 2001; Dong 2003; Kyriakopoulou 2003; Yousef 2003d; Davidson 2004; Bondurant 2005; Bignotti 2006; Dorn 2006; Petraki 2006b; Shan 2006; Dorn 2007) |
| **Breast** | KLK7 is expressed in normal breast and downregulated in breast cancer. Within breast cancer, high KLK7 expression is associated with good patient outcome. | (Yousef 2000d; Talieri 2004; Holzscheiter 2006) |
| **Cervix uteri** | KLK7 is expressed in normal endocervical glands but elevated in cervical adenocarcinomas. No correlation was found between KLK7 expression and survival. | (Santin 2004a; Tian 2004) |
| **Lung** | Non-small cell lung cancer: KLK7 expression is significantly lower expressed in adenocarcinoma than in matched non-malignant lung tissue. | (Planque 2005; Petraki 2006b) |
| **Pancreas** | KLK7 is overexpressed in pancreatic adenocarcinomas over normal pancreatic tissue. Only about 15 % of the normal tissue specimens expressed the KLK7 protein. | (Johnson 2007) |
| **Brain** | KLK7 is elevated in brain tumors over normal brain tissue. KLK7 mRNA expression is associated with shorter overall survival compared to patients with no KLK7 expression. | (Petraki 2006b; Prezas 2006b) |

| Type of cancer | Literature findings | References |
|---|---|---|
| **Skin** | KLK7 is present in normal skin but downregulated in melanoma tissue. | (Winnepenninckx 2006) |
| **Gastro-intestinal tract** | Colon: Semi-quantitative RT-PCR method showed that the KLK7 gene is up-regulated in colon cancer and its expression predicts poor prognosis for colon cancer patients.<br>Oral cavity: cDNA microarray analysis revealed that KLK7 was upregulated in tumor samples versus normal controls. RT-qPCR analysis confirmed that KLK7 mRNA was most differentially regulated with a 5.3-fold increase. Immunohistochemical analysis demonstrated strong reactivity in and human OSCC tissues.<br><br>KLK7 was expressed strongly in the majority of tumor cells in 68 of 80 cases: these were mostly moderately or poorly differentiated neoplasms. Staining was particularly intense at the infiltrating front. Patients with intense staining had significantly shorter overall survival ($p < .05$). | (Pettus 2009)<br>(Zhao 2011)<br>(Talieri 2009b) |
| **NHL node** | No information in the literature | |
| **Myoskeletal** | No information in the literature | |

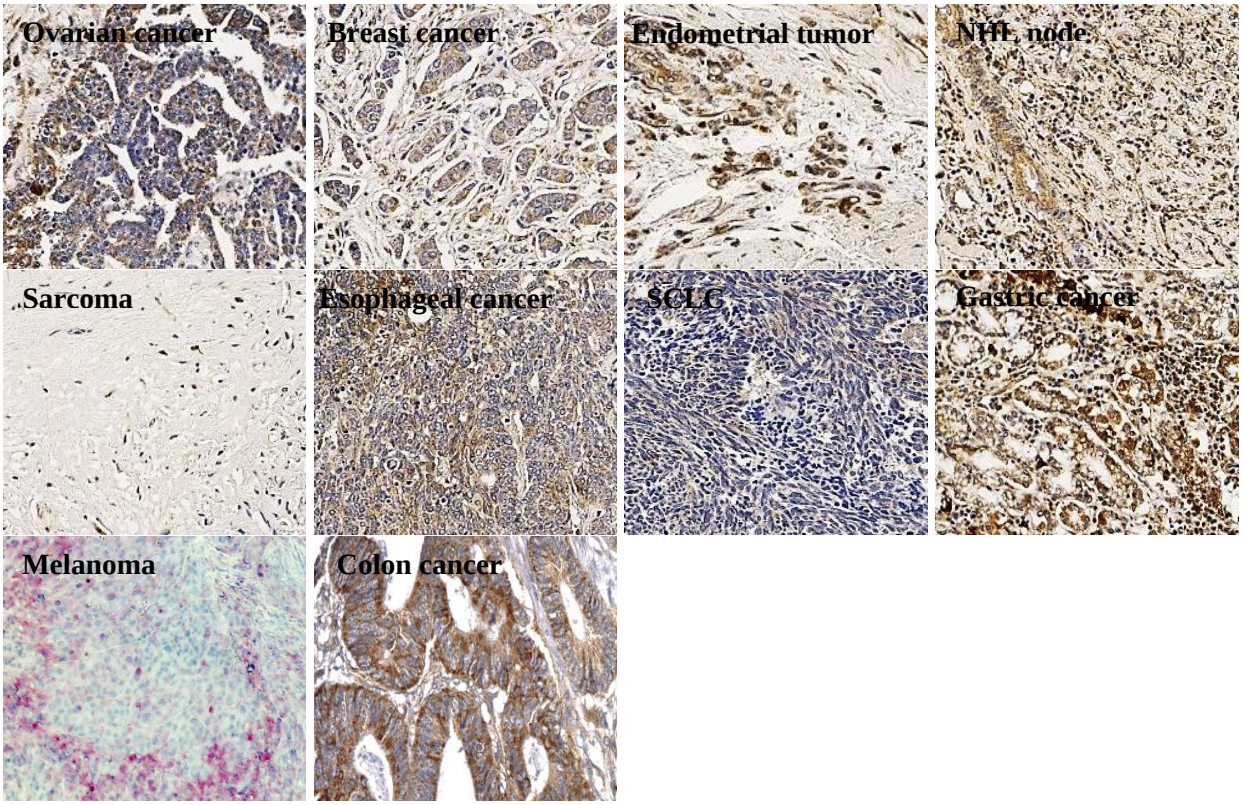


**Figure 36:** Various malignant tissues stained for KLK7 (Arexis Tagena + Domino, 2.72 µg/mL) employing the Envision method. Brown for KLK7 ($DAB^+$), blue for nuclei (hematoxylin). Magnification x 100. Melanoma stained by use of Permanent Red to avoid confusion with brown skin pigments. In most cases, malignant tissues demonstrate upregulated KLK7 levels over their healthy counterparts.

### 5.1.6 Antibodies directed to other KLKs

**KLK4 and KLK6**

The aim of the study was to generate polyclonal antibodies directed to KLK4 and KLK6, respectively, to develop novel tools for analysis of human KLK4 and 6-protein expression by immunohistochemistry, Western blot analyses and/or ELISA. This would be another cog in the wheel of creating the appropriate tools to study KLK4, KLK5, KLK6, KLK7 overexpression in ovarian cancer. For applications, in which the antigens are partly denaturated, e.g. in immunohistochemistry or Western blot analyses, it is preferable to employ antibodies directed to linear epitopes of the antigen (Seiz 2010). Therefore, short peptide sequences derived from the target protein are employed to generate anti-peptide antibodies (Harvey 2003).

The sequences encoding the mature forms of KLK4 and 6 (excluding the signal-sequence and the pro-peptides) were amplified from cDNA originating from ovarian cancer tissue and cloned into the bacterial expression plasmid pQE-30. The recombinant (non-glycosylated) proteins, carrying an N-terminal extension of 17 amino acids encompassing a histidine $(His)_6$-tag and an enterokinase (EK) cleavage site (DDDDK↓), were purified under denaturing and slightly reducing conditions, refolded and finally used for immunization of rabbits and chickens. Antibodies were purified by affinity chromatography by three different procedures: (a) against unique peptides of KLK4 or KLK6 to select for monospecific, polyclonal antibodies (fraction A); (b) by a "negative" purification using columns with immobilized peptides covering the tag of the recombinant proteins (corresponding to the His-tag [GSHHHHHHGS] and the EK cleavage site [HHHGSDDDDK]) and (c) against the immunogen (i.e. the recombinant protein; fraction C).

The antibodies were tested in microtiter plate-based assays ("one-sided ELISA"). Elution A shows strong reaction with both, the loop-derived peptide as well as the immunogen, whereas elution C does strongly react only with the immunogen but not at all with the respective synthetic peptide.

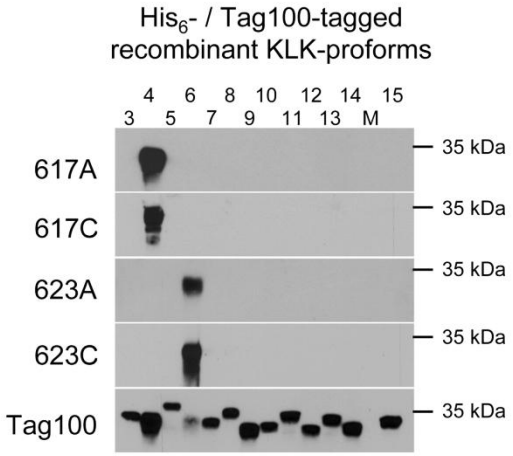


**Figure 37:** Western blot analysis for evaluation of KLK5. Specificity of the KLK4 (617A and 617C) as well as of the KLK6 (623A and 623C)-directed polyclonal antibodies. After separation by 12 % SDS-PAGE (A), His-tagged recombinant pro-forms of KLK3-15 (1 µg each), were blotted to a PVDF membrane and reacted with the antibodies. KLK3, 5, 7-15 did not react with the antibodies, only KLK4 in case of 617 and only KLK6 in case of 623, with an apparent molecular weight of 35 and 32 kDa respectively. Thus, no cross-reactivity of the antibodies with other KLKs except KLK4 or KLK6 was observed. Anti-Tag-100 confirmed the Tag-100 presence.

The produced antibodies were tested by Western blot analysis in order to detect any potential cross-reactivity with other members of the tissue kallikrein family. The experiment was performed under reducing conditions and the recombinant human tissue kallikreins, used as probes, were always loaded at a quantity of 100 ng/lane. The antibody fractions were found to be specific for KLK4 and KLK6, respectively, as there was no cross-reaction with all of the other tested KLK proteases, other His- and/or EK-tagged proteins, or the control peptides (e.g. see the Western blot analyses for chicken pAb 617A and C directed to KLK4 and rabbit pAb 623 A and C directed to KLK6 with different KLK pro-forms).

For the quantification of KLK4 and KLK6 proteins on FFPE tissue specimens, a modified protocol based on Dako EnVision method was followed (see **Appendix 11.6.2**).

**Table 41:** Comparison of in-house KLK4, 6 and 7 antibodies in Western blot and IHC.

| | | IHC | |
|---|---|---|---|
| | **Crossreactivity WB** | **Normal tissue** | **Malignant tissue** |
| **KLK4** | Chicken anti-KLK4 617A and C specific, whereas rabbit anti-KLK4 crossreact with several recombinant KLKs | Liver hepatocytes. Kidney renal tubular, but not in glomerular cells. Staining intensity in the renal cortex was higher as compared to renal medullary cells. | |
| | | Weak KLK4 staining in glandular luminal cells of non-malignant prostate tissue (Seiz 2010). | Distinct KLK4 immunostaining with 617A and 617C in malignant glandular epithelial cells, but not in the basal layer of surrounding normal tissue or fibromuscular stromal cells. Intense granular cytoplasmic staining of cancer glands was observed (Seiz 2010). |
| | | Employing 617A, a discrete immunoreactivity is detected in the "normal-appearing" mucosa, from patients with colon cancer, removed far from the neoplastic tissue. Similarly, in normal colonic samples from control patients, almost no staining was observed (Gratio 2010). | KLK4 in the mild dysplastic mucosa contiguous to a cancerous lesion. Staining in the columnar absorptive cells and in goblet cells with varying intensity from patient to patient. KLK4 is observed mainly in the cytoplasm of cancer cells (Gratio 2010). |
| **KLK6** | Both 622 and 623 no crossreactivity | Rabbit antibodies negative for prostate, kidney, skin and brain, whereas chicken antibodies specific for skin, kidney and brain. | |
| **KLK7** | Crossreactivity with other KLKs for all chicken, no signal for rabbit antibodies. Exception 583. | Not suitable for IHC | |

By immunohistochemical evaluation, both antibody fractions 617A and 617C were found to be suitable for detection of KLK4 in human tissues. Using a tissue microarray containing a variety of normal adult tissues, KLK4 was immunodetected with high frequency in liver hepatocytes and renal tubular, but not in glomerular cells. Staining intensity in the renal cortex was higher as compared to renal medullary cells. Other normal tissues such as colon, lung, skin or skeletal muscle were not immunoreactive for KLK4 with either of the antibodies.

Weak KLK4 staining in glandular luminal cells of non-malignant prostate tissue was observed (Seiz 2010), whereas distinct KLK4 immunostaining with 617A and 617C characterized malignant glandular epithelial cells, but not the basal layer of surrounding normal tissue or fibromuscular stromal cells. Intense granular cytoplasmic staining of cancer glands was noted (Seiz 2010).

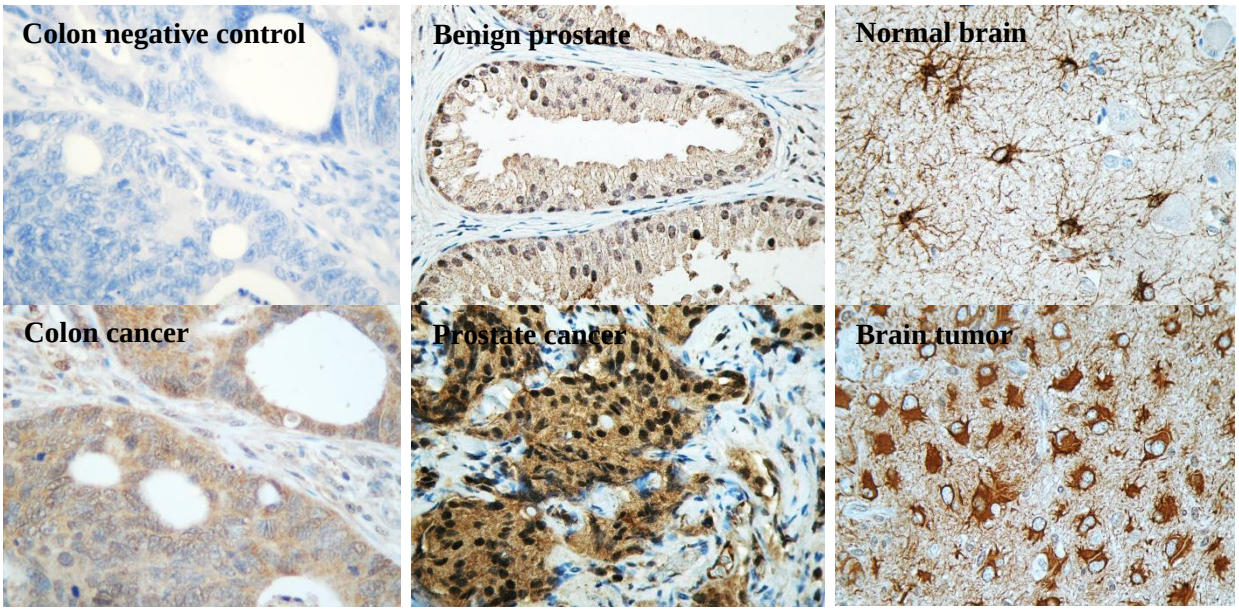


**Figure 38:** Examples of immunohistochemical assessment. KLK4 (617A, 0.57 µg/mL) is tested on colon cancer, where 20 x of immunogen excess control confirms antibody specificity and stained tissue demonstrates epithelial mucosa staining. Prostate cancer is remarkably stained in glandular epithelial cells in contrast with the moderate staining of the benign section. KLK6 (623A, 4.8 µg/mL) recognizes specifically astrocytes of the brain (Grebenchtchikov 2007). Brown for antigen ($DAB^+$), blue for nuclei (hematoxylin). Magnification x 400. Envision method employed, antigen retrieval by pressure-cooking.

Employing 617A, a discrete immunoreactivity was detected in the "normal-appearing" mucosa, from patients with colon cancer, removed far from the neoplastic tissue. Similarly, in normal colonic samples from control patients, almost no staining was observed (Gratio 2010). On the other hand, KLK4 was located in the mild dysplastic mucosa contiguous to a cancerous lesion. Staining characterized the columnar absorptive cells and goblet cells with varying intensity from patient to patient. KLK4 was observed mainly in the cytoplasm of cancer cells (Gratio 2010).

KLK6 antibodies produced in chickens seemed to perform quite well and displayed strong specificity for KLK6 in kidney, brain and skin. In brain, they specifically recognize the astrocytes of the cortex.

**KLK5**

In the context of collaboration between R&D Systems and our department, we received 23 antibodies, most of them not yet commercialized, directed to KLK7 and to KLK5 (12 and 11 respectively). The initial screening took place in IHC, where a range of dilutions where chosen to detect these proteins on test tissue specimens skin and kidney employing the DAKO EnVision method and modifying the original SOP. Our selection criteria were a) to find an antibody suitable for immunohistochemical practice, dilutions lower than 1:100 are actually inexpedient for daily use, b) to obtain a regular, specific staining pattern without background.

Applied immunohistochemistry was a fast and inexpensive way to screen all antibodies received. Five antibodies, three anti-KLK7 and two anti-KLK5, were selected for their performance in IHC, on test tissues but also on ovarian cancer specimens, employing the protocol previously established for KLK7 including antigen retrieval by pressure-cooking (Dako Envision/DAB$^+$, **Appendix 11.6.2** and **11.8**). To confirm specificity for corresponding antigens and exclude potential cross-reactivity with other proteases of the kallikrein-related peptidase family, these antibodies were employed to detect either KLK7 or KLK5 recombinant proteins on a blot where all recombinant KLK pro-forms KLK3-15 were present. Most of the five were negative, one displayed severe background and one provided a clear signal without any cross-reactivity with other KLKs. This antibody was the goat polyclonal anti-KLK5 AF1108 (R&D Systems).

By immunohistochemistry, KLK5 is most abundant in cornified skin layers to our findings, a fact which is in agreement with the sum of the scientific literature (Petraki 2006b; Shaw and Diamandis 2007). KLK5 is expressed in normal breast ductal epithelium and in the epithelium of the urinary tubuli of the normal kidney, while glomeruli remained unstained (Petraki 2006a). In heart muscle, moderate cytoplasmic staining of the cardiomyocytes is observed; ELISA levels correspond to this result (Shaw and Diamandis 2007). In pancreas, there is predominant localization of KLK5 in acinar cells suggesting role for this enzyme in digestion (Dong 2008). In liver, faint to moderate staining was confined to the hepatocytes, while in placenta,

erythrocytes were recognized by the antibody employed. Lung is also moderately stained in epithelium, as Planque et al. also noticed (Planque 2005). Neuron bodies in the peripheral nervous system, as well as connective fibers are moderately expressed for KLK5. Bone marrow is stained in erythrocytes and sinusoids (endothelia). Finally, in spleen, red pulp is faintly stained, so macrophages and blood cells that have not yet entered the venous sinuses. In conclusion, KLK5 in many cases co-resides with KLK7 (see chapter about KLK7), a fact which is explained by their interaction in proteolytic activation.

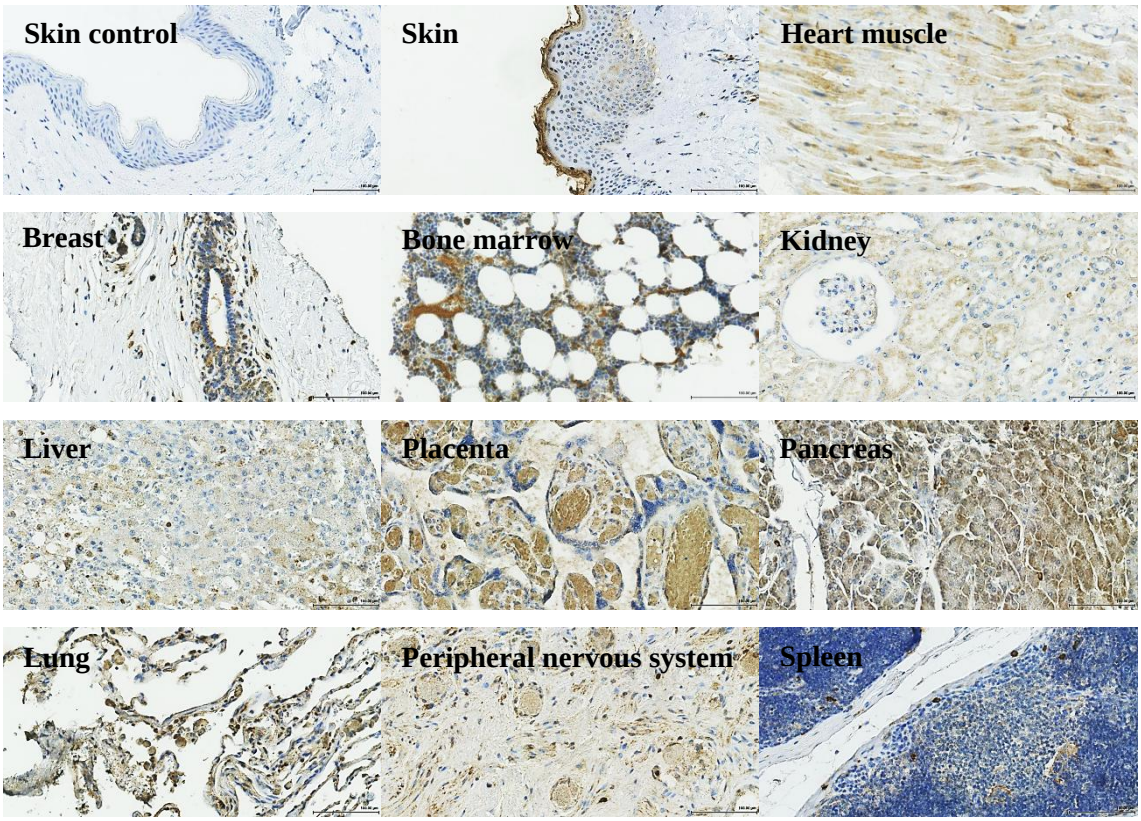


**Figure 39:** KLK5 protein expression as detected by R&D AF1108 (0.4 µL/mL) in various tissues. Negative control with the omission of the primary antibody (skin control). Dako Envision method employed. Blue for nuclei (hematoxylin), brown for KLK5 ($DAB^+$). Magnification x 200. KLK5 is most abundant in cornified skin, but also in kidney, lung, heart muscle and pancreas. The R&D AF1108 specifically reacts with erythrocytes in the placenta.

In ovary, a color deposit was observed in sparse cells in the stroma and in the surface ovarian epithelium. Epithelial ovarian tumors expressed a high percentage of KLK5, as shown in **Figure 40C**. Once the selection process was accomplished together with any necessary

competition experiments, ovarian cancer tissue extracts were randomly selected according to their ELISA values and subsequently subjected into Western blotting to check whether the signal intensity correlates with the antigen levels in ELISA. Added to this, tissue specimens from the corresponding cases were stained for KLK5 with the AF1108 (0.4 µg/ml).

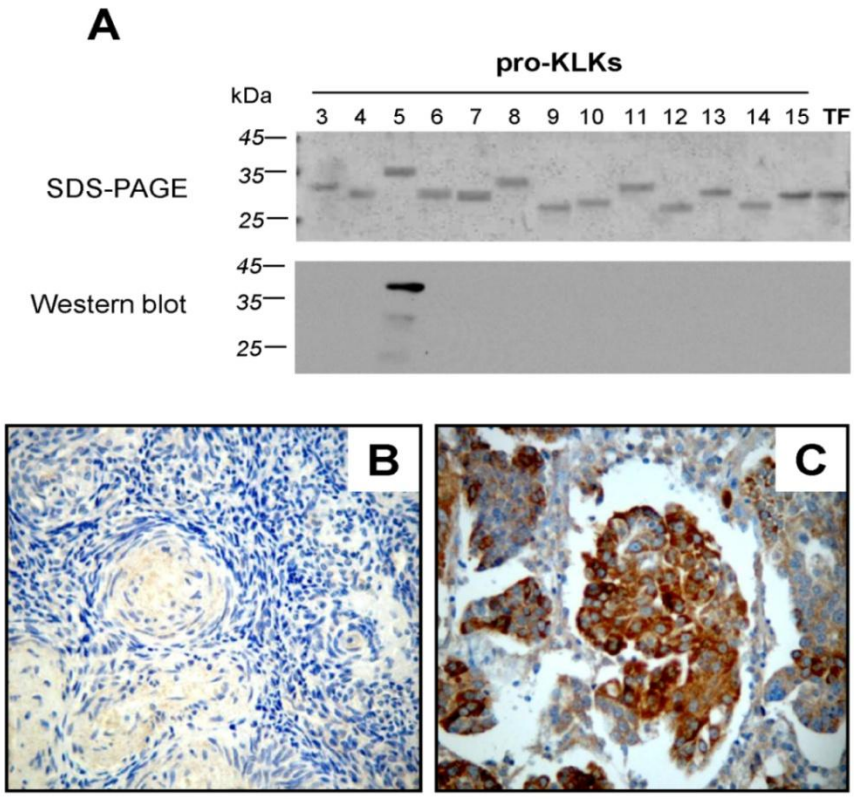


**Figure 40:** Immunohistochemical staining for presence of KLK5 in benign and malignant ovarian tumor tissues. Specificity of the KLK5-directed goat polyclonal antibody was tested by SDS-PAGE and Western blot analysis. After separation by 12 % SDS-PAGE **(A)**, His-tagged recombinant pro-forms of KLK3-15 (1 µg each), plus an irrelevant protein (His-tagged TF, tissue factor), were blotted to a PVDF membrane and reacted with polyclonal goat AF1108 antibody. KLK3, 4, 6-15 did not react with the antibody, only KLK5, with an apparent molecular weight of 40 kDa. Thus, no cross-reactivity of the AF1108 antibody with other KLKs except KLK5 was observed. Representative benign ovarian tumor **(B)** and ovarian cancer tissue **(C)** were stained with antibody AF1108 to KLK5. KLK5: brown color; nuclei: blue color. Magnification x 200. KLK5 protein expression is very low in benign tumor ovarian tissue (endometriosis cyst) of a 57-year old patient but high in ovarian cancer tissue and in cells of the extracellular matrix of 59-year old patient with serous ovarian carcinoma, FIGO IV, nuclear grade 3. Likewise, determined in tumor tissue extracts of the patients by KLK5-specific ELISA, antigen expression is low in the benign case and elevated in the tumor tissue of the ovarian carcinoma patient (Dorn 2011).

Ovarian cancer tissue microarrays, already constructed for KLK7 assessment, were used for a broad study of KLK5 levels and their correlation with clinicopathological data.

## 5.2 uPA/PAI-1 protein expression

### 5.2.1 uPA/PAI-1 immunohistochemical assessment

The antibodies employed for the uPA/PAI-1 assessment were already characterized for signal intensity and cross-reactivity by means of Western blot in previous publications (Kobayashi 1991; Costantini 1996). Adapting know-how methodology from kallikrein-related peptidases immunohistochemical assessments into the plasminogen field, we have been able to evaluate numerous parameters such as primary antibody incubation temperature, antibody concentration, antigen retrieval, blocking reagents, hematoxylin type, etc. and produce stable and repetitive protocols for manual and automatic mode. The latter refers to immunohistochemical assessment with use of autostainers, namely Dako Autostainer LINK 48 or Ventana Benchmark® XT.

Analytically, automatic staining was stronger than manual for tumor and stroma but in the same context. The staining, both in manual and automatic mode, follows a similar pattern, a finding which permits procedure automation without technical drawbacks. Similarly, both methods employed, LSAB and EnVision (also Ventana iVIEW® and ultraVIEW® respectively), produce similar results, so they are both recommended for staining. Moreover, there was no actual need for endogenous biotin block, since breast negative controls are really negative, while different protocols were generated for different temperature settings; Ventana Benchmark works only at 37 °C. Finally, antigen retrieval by pressure-cooking generally did not contribute any value to our stainings because pilot experiments with routinely FFPE control tissues (normal kidney) and breast cancer tissue sections revealed that pretreatment of tissue sections is not necessary for antigen retrieval. Just the opposite is true; monoclonal antibodies #3689, #ADG 25, #3785, and #3786 loose reactivity when HIER (Heat-Induced Epitope Retrieval) technique was used (steam cooking, steam pressure cooking). Also, PIER (Proteinase-Induced Epitope Retrieval) is lowering reactivity of the antibodies with the control and target tissues. Therefore, in the staining protocols developed, no HIER or PIER was applied before addition of the primary antibodies.

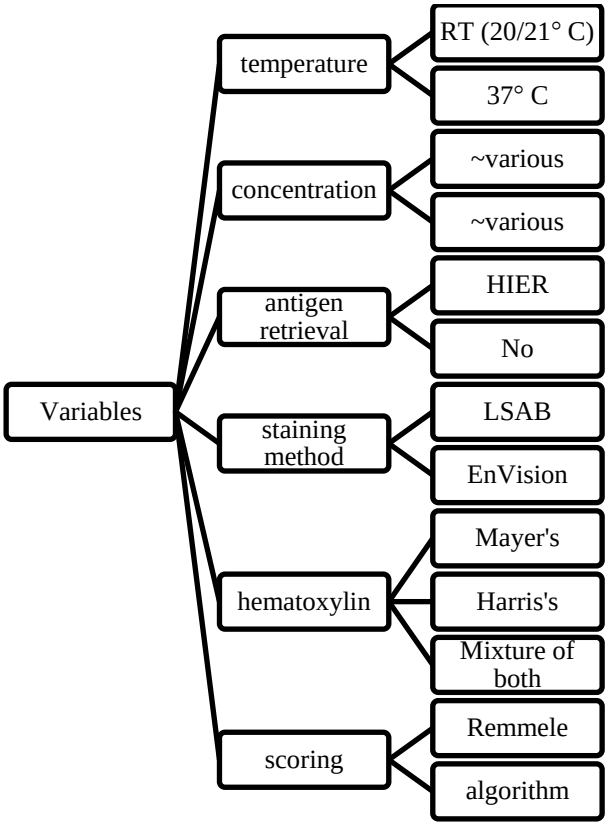


**Figure 41:** Graphical scheme demonstrating the numerous variable settings applied in immunohistochemical assessment. For each assay, test tissues skin and kidney as well as breast cancer tissue specimens were employed.

In different parts of the world, different hematoxylin mixtures are used. In Europe, Mayer's hematoxylin (stains mainly nuclei with light blue) is mainly used, while in USA mainly Harris' hematoxylin (stains nuclei and extranuclear structures, strong blue). Moreover, modifications of Mayer's or Harris's mixtures are known, such as Lillie's modification.

A valuable remark is that the differences among different cases (e.g. breast cancer) by immunohistochemical assessment as well as in protein content as assessed by ELISA (decimal subdivision) are pretty small for human eye to distinguish, therefore automatic scoring by use of algorithmic quantification software would be more efficient than manual evaluation by pathologist (Remmele score).

Testing all the abovementioned variables was a tedious procedure, which produced seven different SOP protocols:

**a)** Protocol to assess uPA/PAI-1 by immunohistochemistry (manual staining technique) in formalin-fixed, paraffin-embedded breast cancer tissue sections employing monoclonal antibodies #3689 (to uPA), #3785 (to PAI-1), #3786 (to PAI-1), and #ADG 25 (to PAI-1) using the LSAB/DAB$^+$-method (20 °C-21 °C)

**b)** Protocol to assess uPA/PAI-1 by immunohistochemistry (manual staining technique) in formalin-fixed, paraffin-embedded breast cancer tissue sections employing monoclonal antibodies #3689 (to uPA), #3785 (to PAI-1), #3786 (to PAI-1), and #ADG 25 (to PAI-1) using the LSAB/DAB$^+$-method (37 °C)

**c)** Protocol to assess uPA/PAI-1 by immunohistochemistry (manual staining technique) in formalin-fixed, paraffin-embedded breast cancer tissue sections employing monoclonal antibodies #3689 (to uPA), #3785 (to PAI-1), #3786 (to PAI-1), and #ADG 25 (to PAI-1) using the EnVision/DAB$^+$-method (20 – 21 °C)

**d)** Protocol to assess uPA/PAI-1 by immunohistochemistry (DAKO Autostainer Link48 automatic staining technique) in formalin-fixed, paraffin-embedded breast cancer tissue sections employing monoclonal antibodies #3689 (to uPA), #3785 (to PAI-1), #3786 (to PAI-1), and #ADG 25 (to PAI-1) and LSAB/DAB$^+$-method (20 – 21 °C)

**e)** Protocol to assess uPA/PAI-1 by immunohistochemistry (DAKO Autostainer Link48 automatic staining technique) in formalin-fixed, paraffin-embedded breast cancer tissue sections employing monoclonal antibodies #3689 (to uPA), #3785 (to PAI-1), #3786 (to PAI-1), and #ADG 25 (to PAI-1) and EnVision/DAB$^+$-method (20 – 21 °C)

**f)** Ventana Benchmark XT (working temperature: 37 °C) ultraVIEW®

**g)** Ventana Benchmark XT (working temperature: 37 °C) iVIEW®

Our findings in breast cancer tissue specimens as assessed by immunohistochemical means indicate that uPA protein content is upregulated in tumor cells (cytoplasmic and membrane compartment) and also myofibroblasts and stromal areas are stained mainly at the invasion front. This is in agreement with the proteolytic activity of uPA in tumor tissue, where other proteases are activated and ECM degradation is promoted. PAI-1 antibodies, acting similarly, demonstrated a pronounced expression in tumor cells, myofibroblasts, macrophages, endothelial cells and stromal areas.

**Table 42:** Antibody reactivity, findings and staining pattern of #3689, #3785, #3786 and #ADG25. Selected antibody concentration for each one of the seven worked-out protocols for immunohistochemical assessment in breast cancer tissue specimens. Characters (**a**), (**b**), (**c**), (**d**), (**e**), (**f**) and (**g**) correspond to the staining protocols mentioned above. For details, see **Appendix 11.7**. Concentrations always in μg/mL.

| | **Findings and staining pattern in breast cancer** | **Working concentration (in μg/mL) for protocol:** | | | | | | |
|---|---|---|---|---|---|---|---|---|
| | | **a** | **b** | **c** | **d** | **e** | **f** | **g** |
| **uPA #3689** | Pressure cooking plus citrate buffer does not improve staining results. Low dilution leads to background staining and blurry staining of tubules (kidney). High dilutions enough to stain even weak uPA-content cases. Tumor cells (cytoplasm and membrane) stained, myofibroblasts and stroma at invasion front. | 2 | 2 | 1.7 | 2 | 1.42 | 3.33 | 3.33 |
| **PAI-1 #3785** | Pressure cooking plus citrate buffer does not improve staining results. Stains cells plus ECM (moderate). Stained tumor, myofibroblasts, macrophages, endothelial cells and stroma. | 6.7 | 6.7 | 6.7 | 5 | 4 | 4 | 4 |
| **PAI-1 #3786** | Pressure cooking plus citrate buffer does not improve staining results Stained tumor, myofibroblasts, macrophages, endothelial cells and stroma. | 12 | 12 | 9.3 | 7 | 7 | 28 | 28 |
| **PAI-1 #ADG25** | Pressure cooking plus citrate buffer does not improve staining results. Stains cells plus ECM (weak). Stained tumor, myofibroblasts, macrophages, endothelial cells and stroma. | 48.6 | 48.6 | 11.3 | 13.6 | 13.6 | 56.6 | 56.6 |

Another observation is that the ELISA value is mainly an attribute of the size of the tissue extracted sample in relation to the concentration of the biomarker in question, expressed within this tissue. This is a hint from a preliminary study of twenty-nine (29) invasive breast carcinomas, where stromal cell, ECM and tumor cell staining intensity was also in agreement with the respective ELISA values.

Finally, stromal areas distant from the tumor site seem to be more stained than the ones close to the tumor, whereas tumor sites remain intense. This might be due to counterbalance effect, where adequate levels of protein are produced by the tumor cells, a phenomenon that keeps nearby stromal uPA/PAI-1 protein levels low.

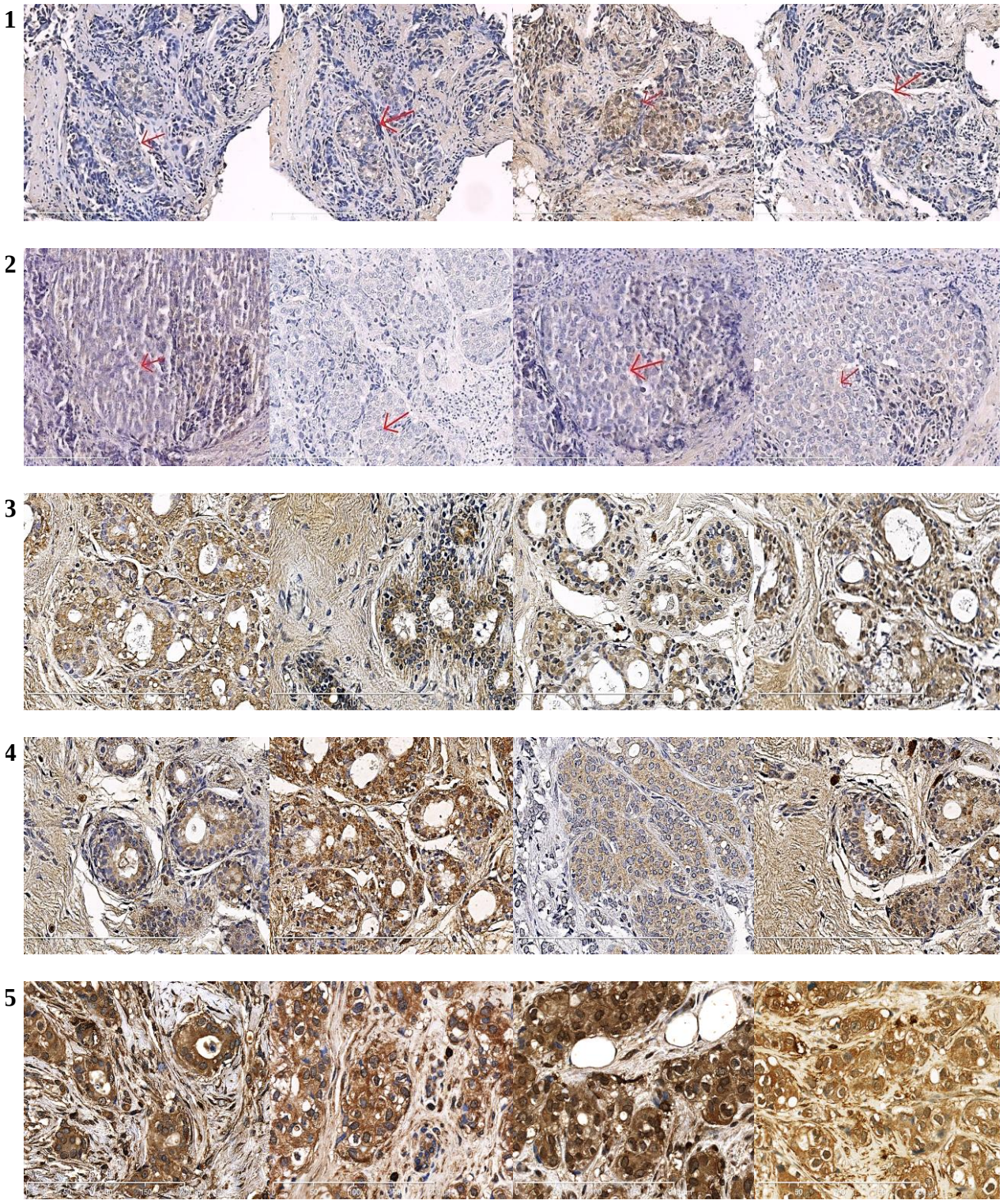
uPA #3689
PAI-1 #3785
PAI-1 #3786
PAI-1 #ADG25
1
2
3
4
5

6

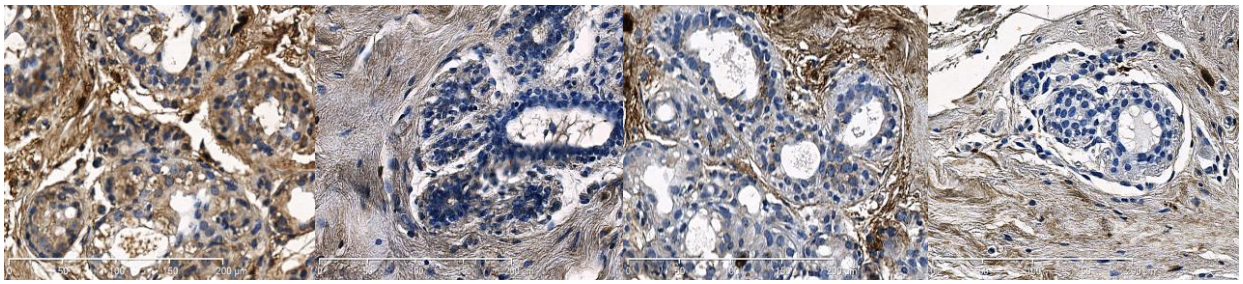

**Figure 42:** Lanes (**1)** and (**2)** represent manual staining of breast core biopsies (**1**) and primary breast tissue at the time of surgery (**2**) for every antibody used at RT setting by use of the LSAB method (#3689 2 μg/mL, #3785 6.7 μg/mL, #3786 12 μg/mL, #ADG25 48.6 μg/mL). Red arrows indicate tumor areas. Lane (**3)** represents immunohistochemical assessment with Dako Autostainer at RT by use of the LSAB method (#3689 2 μg/mL, #3785 5 μg/mL, #3786 7 μg/mL, #ADG25 13.6 μg/mL) whereas lane **(4)** represents the EnVision method (#3689 1.42 μg/mL, #3785 4 μg/mL, #3786 7 μg/mL, #ADG25 13.6 μg/mL). Lanes (**5)** and (**6)** display breast cancer tissue specimens stained by use of the Ventana Benchmark® XT, with the ultraVIEW® (#3689 3.33 μg/mL, #3785 4 μg/mL, #3786 28 μg/mL, #ADG25 56.6 μg/mL) and the iVIEW® (#3689 3.33 μg/mL, #3785 4 μg/mL, #3786 28 μg/mL, #ADG25 56.6 μg/mL) staining kit respectively. Blue for nuclei (hematoxylin), brown for antigen ($DAB^+$). Magnification x 200. Images captured with Hamamatsu Nanozoomer XT.

Once SOPs were established, these were followed by our laboratory, tissue specimens from a collective of breast cancer patients were stained. Scoring was performed either by an experienced pathologist or with use of algorithmic software (Positive Pixel Count®, SlidePath®).

## Immunofluorescence for uPA/PAI-1

A major drawback of the ELISA assessment is the inability to distinguish tumor from normal cells on the same tissue sample, and thus the actual cell origin of the protein content assessed. If ELISA fails to declare the origin of the protein content, immunohistochemistry follows the same blind pattern, since antibodies directed to uPA or to PAI-1 do not discriminate detected proteins. There is, therefore, need for additional reagent in the context of a double-staining procedure that could successfully recognize tumor cells together with the uPA/PAI-1 antibodies. Our efforts focused on combining the morphological advantages of regular immunohistochemistry with the amplified signal of immunofluorescence. A broad spectrum cytokeratin antibody (rabbit wide spectrum ab9377 Abcam, Cambridge, UK) was employed to

visualize tumor epithelia by use of green fluorochrome Alexa488 (#A-11008, goat anti rabbit, 2 µg/mL), while uPA #3689 detected protein signal by use of $DAB^{+}$.

Preliminary results confirmed uPA localization in tumor cells (cytokeratin-positive). Other scientists seem to appreciate the advantages of immunofluorescence for tissue quantification as well (Moeder 2009; Dolled-Filhart 2010).

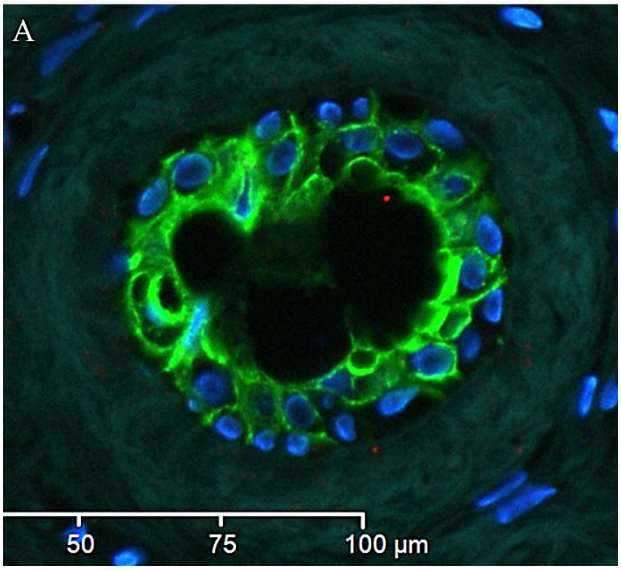


**Figure 43:** (**A**) Breast cancer tissue stained for cytokeratins (150 µg/mL, rabbit wide spectrum ab9377 Abcam, Cambridge, UK) and visualized with green fluorochrome goat Alexa488 (#A-11008, goat anti rabbit, 2 µg/mL), counterstained with DAPI (#S36939, Invitrogen SlowFade, 5 mg/mL stock), Envision method employed, no antigen retrieval. Magnification x 200. Respective images demonstrate the expression of uPA by the cytokeratin-positive cells.

### 5.2.2 Comparative method study for uPA/PAI-1 assessment by ELISA, IHC and RPMA

Complications in the uPA/PAI-1 protein assessment are well-known. ELISA is the golden standard for in vitro assessment but suffers from drawbacks such as (a) inability to distinguish individual cell morphology, (b) function with frozen or fresh-frozen tissue only. Immunohistochemistry, on the other hand, diminishes the material issue by use of FFPE sections, but (a) lacks objectivity, unless it is automatically quantified by use of algorithmic software, (b) first material is already processed by fixation, (c) in the case of uPA/PAI-1 detection, the two factors are expressed in both tumour tissue and surrounding stroma, thus making exact scoring quite difficult.

Formalin fixation is a routine standard, as it offers tissue stability by crosslinking of proteins and nucleic acids (Becker 2007), a procedure that is reversible and extraction successful by use of new methodological approaches (Ikeda 1998; Chu 2005; Shi 2006; Becker 2007; Becker KF 2008a; Becker KF 2008b; Chung 2008; Addis 2009; Nirmalan 2009).

A combination of the advantages of the two methods is presented by the protein arrays (Becker 2007; Blechschmidt 2007; Hipp 2008; Kroll 2008). This method exploits the practicability of the FFPE material to bring in the sensitivity of ELISA or Western blot. The FFPE material is primarily lysed and the protein lysates of interest are spotted on a nitrocellulose-coated glass slide, followed by incubation with the primary antibody. Detection is carried out by an enzyme-coupled secondary antibody together with its target substrate, a procedure which reminds of ELISA.

Based on the new technology of the protein arrays (RPMA), a collective of breast cancer tissues was employed to initiate a comparative study about different techniques on protein assessment. This is not the first time someone compared different assessment techniques for uPA/PAI-1 factors (Ferrier 1999; Janicke 2001; Sweep 2003). In Ferrier *et al*., it was shown that although a higher IHC score category was constantly associated with an increased median ELISA value, there was an overlap of ELISA values from different scoring classes. This indicates that the two techniques are not directly interchangeable (Malinowsky 2010). A comparison including protein array data has never been performed before.

Eighteen randomly selected different breast cancer cases disposed material for ELISA, immunohistochemistry and reverse phase protein microarray assessment (by Claudia Boellner). As ELISA and RPMA represent continuous variables, automated IHC replaced manual evaluation in this study, in order to obtain a direct comparison of the three biological parameters. Added to this, the differences among different cases in ELISA values are small, therefore an automatic scoring would be more efficient than a manual. Then it is easier and more representative to apply simple correlation formulas, such as Pearson's.

SlidePath®'s Positive Pixel Count® was employed to produce a quantified signal, with most representative property the average staining concentration.

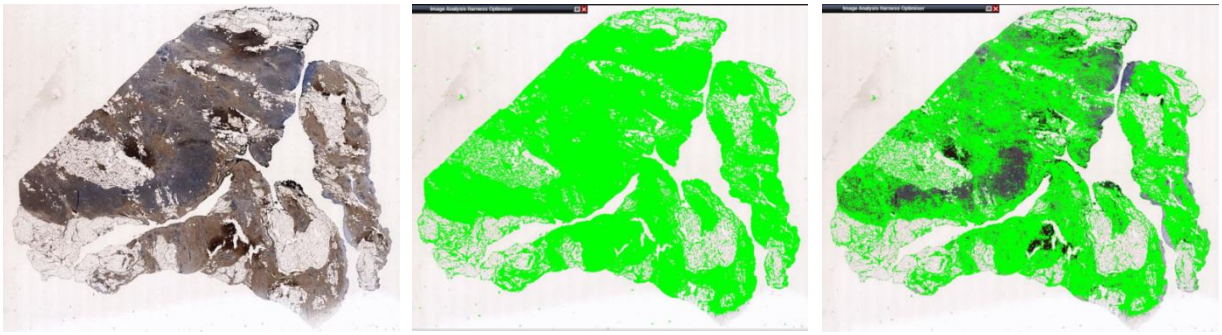

**Figure 44:** Breast cancer tissue slide stained for uPA with #3689 antibody (2 μg/mL). Blue for nuclei (hematoxylin) and brown for the antigen ($DAB^+$). Envision method employed, no antigen retrieval. Digitized image with Hamamatsu Nanozoomer RS, magnification x 250. Images represent original tissue the way it is scanned (**left**), after artificial tissue layer application (recognition of tissue areas)(**middle**) and after Positive Pixel Count® application (detection of brown color deposit)(**right**).

The antibodies employed for detection in each technique are different, a fact which alone produces result variation. Putting everything together, for PAI-1 we observe no correlation between IHC and ELISA as well as between IHC and the protein array. There is, however, a very strong correlation (0.84), between ELISA and the array, which signifies the RPMA as a good candidate to replace ELISA in protein levels assessment, even from FFPE material. Results were not promising for uPA, since no correlation was observed for any of the combinations examined.

| **Pearson correlation** | **IHC/ELISA** | **ELISA/Array** | **IHC/Array** |
|---|---|---|---|
| **PAI-1** | 0,21683309 | 0,84284465 | -0,20843335 |
| **uPA** | -0,05065469 | -0,05309439 | -0,3113154 |

These are preliminary, restricted in a small collective of 18 cases. It is recommended to expand this study by investigating a larger independent collective.

There is a clear advantage of protein array technology, since it combines benefits from two different methods, immunohistochemistry and ELISA. It is, however, still unclear whether this array approach signifies a third path; preliminary uPA comparison results are not in perfect agreement. On the other hand, the highly significant correlation for PAI-1 expression creates expectations for quantitation as sensitive as ELISA and simultaneously as practical as immunohistochemistry.

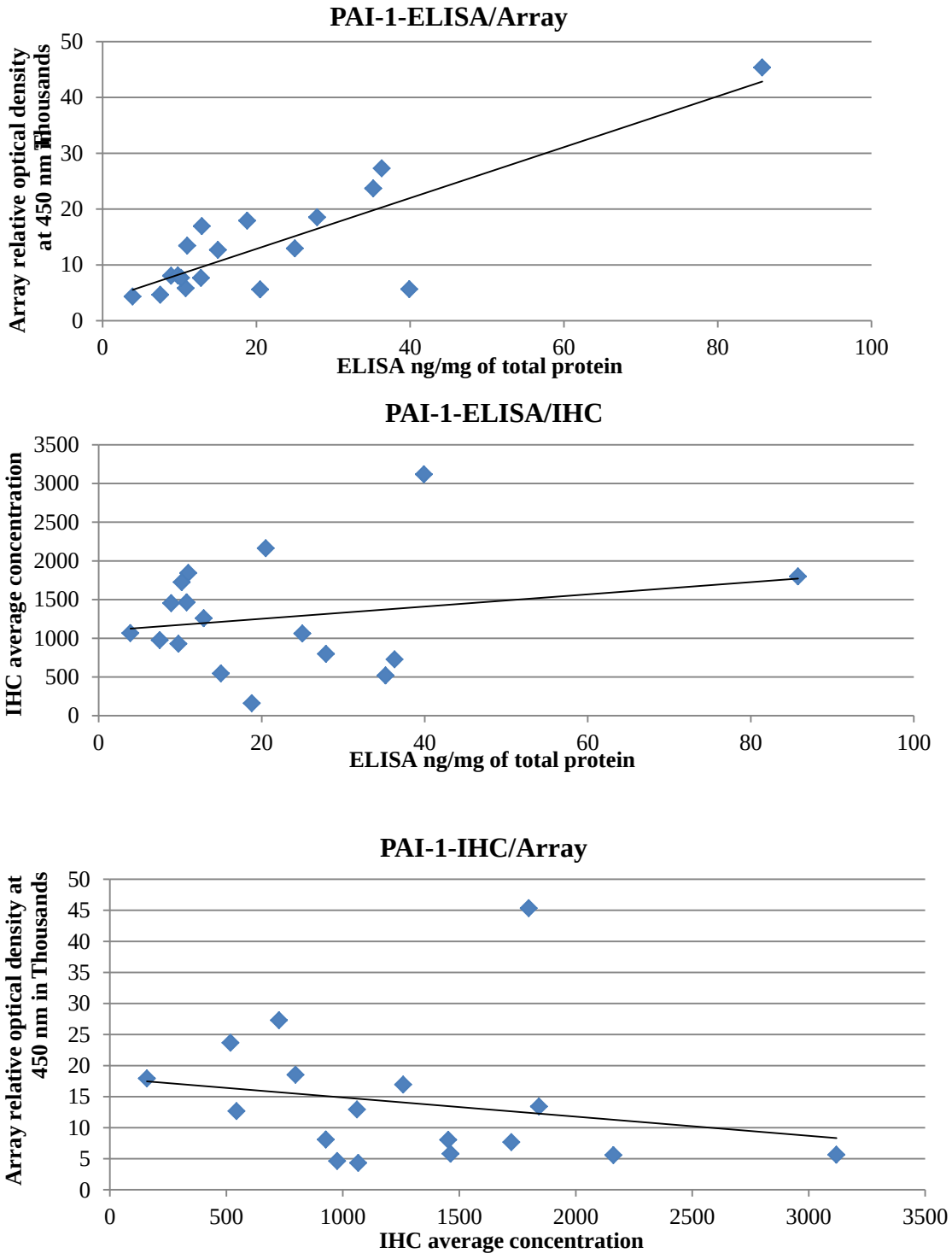


**Figure 45:** Graphical representation of the coupled correlations for PAI-1. ELISA assay Femtelle® uPA/PAI-1 kit (#899, American Diagnostica Inc., Pfungstadt, Germany), protein extraction by use of QProteome® FFPE tissue kit (#37623, Qiagen, Hilden, Germany) and binding detection at 450 nm, immunohistochemistry by use of Envision method (#3785, 1.7 µg/mL) and quantification by SlidePath® Positive Pixel Count® algorithm. Clearly, PAI-1 ELISA displays a strong correlation with protein array data.

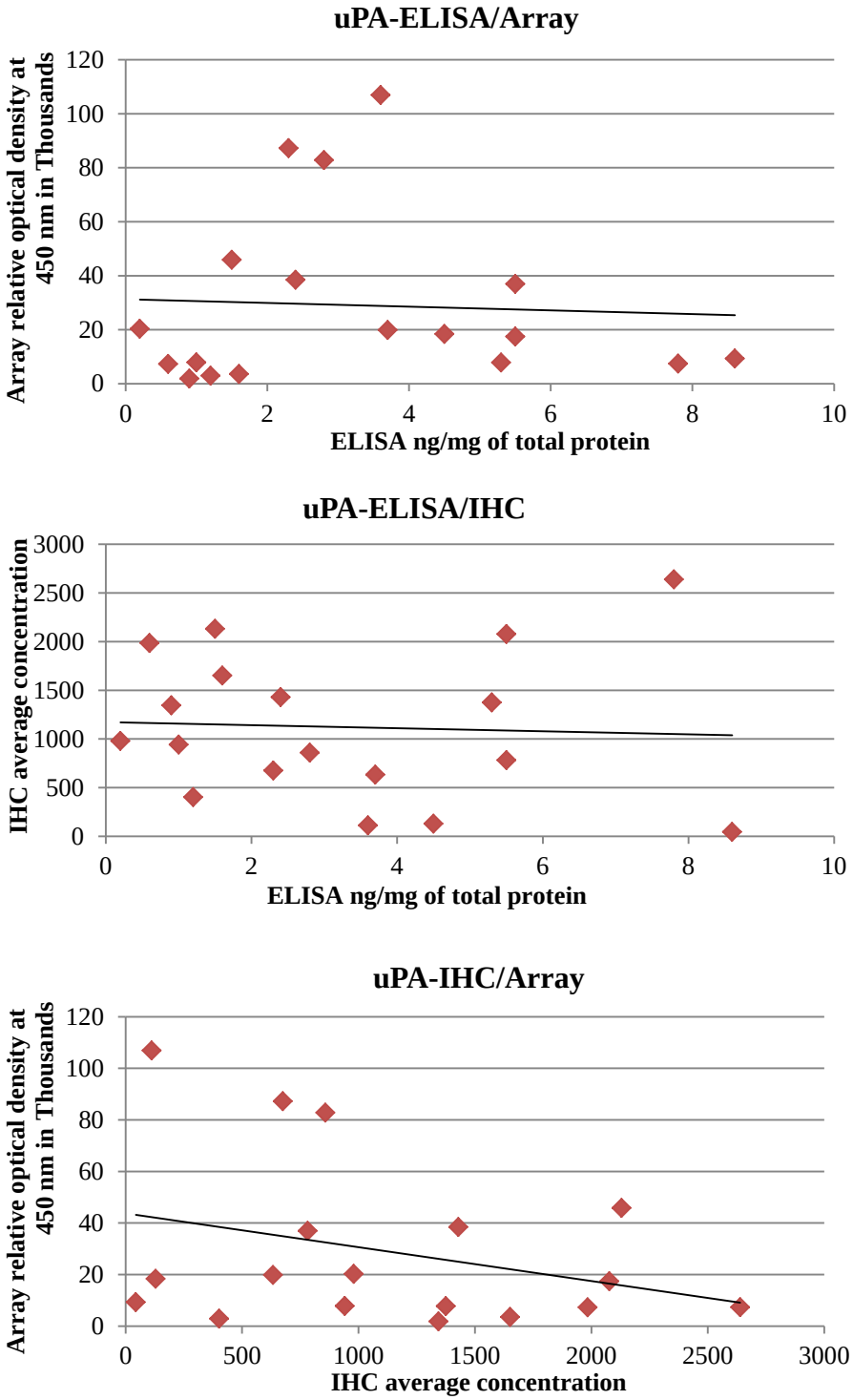


**Figure 46:** Graphical representation of coupled correlations for uPA protein. ELISA assay Femtelle® uPA/PAI-1 kit (#899, American Diagnostica Inc., Pfungstadt, Germany), protein extraction by use of QProteome® FFPE tissue kit (#37623, Qiagen, Hilden, Germany)and binding detection at 450 nm, immunohistochemistry by use of Envision method (#3689, 2 µg/mL) and quantification by SlidePath® Positive Pixel Count® algorithm. No correlation is observed.

## 5.3 DNA methylation

### 5.3.1 KLKs

Aim of this project was the characterization of epigenetic transcription control of KLK7 and subsequently other members of the KLK genomic loci. Although, *KLK7* gene locus contains a CpG-poor promoter region (Pampalakis 2009), regulation by DNA methylation might also occur (Jones and Baylin 2002).

The KLK7 genetic locus has already been characterized (Yousef 2000d). It has been shown, that transcription levels of KLK7 (by means of Q RT-PCR measurement) are associated with course of the disease in breast and ovarian cancer, whereby ovarian cancer high expression levels of KLK7 were associated with a patient outcome.

Therefore, determination of KLK7 transcription and specific DNA methylation levels in clinical samples (fresh frozen tissue, FFPE material, blood) may be valuable clinically relevant cancer biomarkers.

For this, seven different cell lines [breast: MCF-7, MDA MB 435 (*wild type*, RSV, KLK7), ovarian: OVMZ-6 *wild type*, OVCAR-3), keratinocytes (HaCaT)] were selected to study the expression of KLKs under different conditions of treatment. The demethylating agent Decitabine (5-aza-dC) was applied in the cell lines and our purpose was to investigate the change of the methylation status on DNA level, as well as expression changes in RNA and protein level.

**Standard point PCR**

In order to investigate whether KLK7 loci are present in cells under examination (HaCaT, MCF-7, OVMZ-6 WT, OVCAR-3), three different PCR systems specific for KLK7 and neighboring genes (*KLK6*, *KLK8*) were designed by use of CLC Sequence Viewer (version 6.3, CLC bio, Aarhus, Denmark) and Primer Express software (version 3.0, ABI, Foster City, USA). Amplification products confirmed the presence of these genes in the cell lines under investigation as well as in whole blood extracted DNA, which served as control. HPRT-1 (hypoxanthine phosphoribosyltransferase 1) a well-studied housekeeping gene, was used for

normalization purposes. The findings exclude the possibility that the gene loci are not present in the cellular genome due to gene deletion.

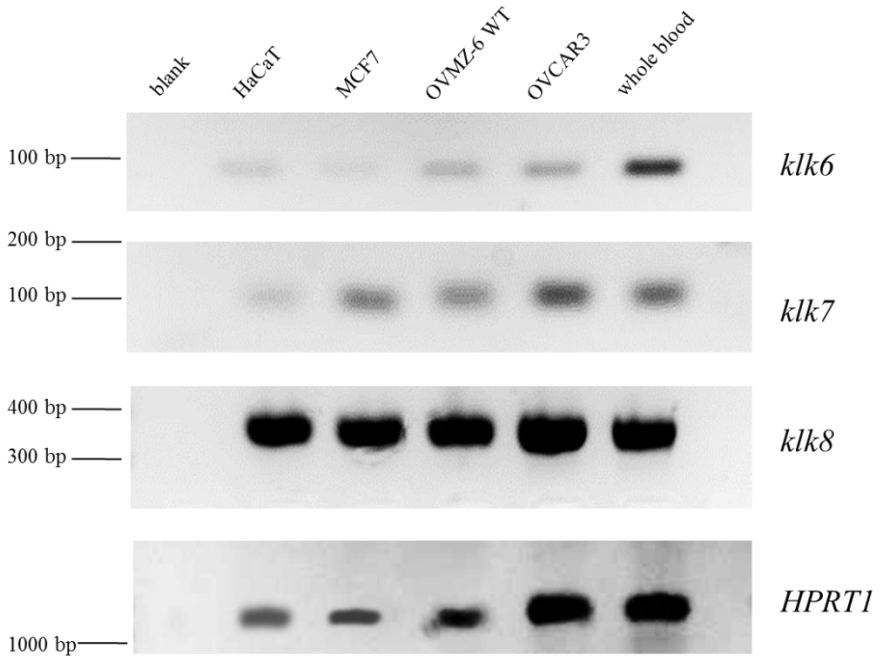


**Figure 47:** Gel electrophoresis. Standard point PCR for detection of the *KLK6, KLK7, KLK8* genes on cultivated cell lines HaCaT, MCF7, OVMZ-6 WT, OVCAR-3 and whole blood DNA as control. *KLK6* is expected at 167 bp, *KLK7* at 175 bp and *KLK8* at 350-400 bp. HPRT1 serves as the housekeeping gene for normalization at 1435 bp (40 cycles). No gene deletion is apparent for *KLK7* or neighboring genes (*KLK6, KLK8*).

**5-aza-dC-treated vs. untreated cell extracts by ELISA assessment**

Since the group of kallikrein-related peptidases originally studied together included KLK4, KLK5, KLK6 and KLK7 (Prezas 2006a) in the frame of ovarian cancer, it was meaningful to expand it to the transcription level and find out if these genes are influenced by methylation status. Despite the lack of CpG-rich regions, KLK6 and KLK7 might also be of interest, next to CpG-rich KLK4 and KLK5 (Pampalakis 2006).

ELISA was selected as the appropriate tool to discover the effect of epigenetic regulation on the protein level. ELISA assays for kallikrein-related peptidases were already established and validated by Diamandis *et al.* (Diamandis 2003a; Diamandis 2003b; Kishi 2004; Obiezu 2005). KLKs are secreted proteases and therefore their content can be assessed by ELISA in the conditioned medium (supernatant) of a cell culture. On the other hand, a protein portion might be still in the cytosol, information that would be lost if not assessed by ELISA in a cytosolic

extract, which can be obtained by the treatment of cells with the Triton-X-100 detergent. It is crucial, to consider as complete KLK expression score, including the total amount coming from the supernatant and the cytosolic extract.

The second point is the comparison of demethylated cell lines versus the untreated ones. Results demonstrated a relatively low KLK4 and KLK6 expression, while KLK5 and KLK7are measured at higher scales.

In our experiments, KLK4 displayed very low levels, mostly deriving from the cytosolic extracts and untreated cells seemed to produce more protein than their demethylated counterparts. According to Pampalakis et al., in MDA-MB-231 breast cancer cell line, 5-aza-dC reactivated the expression of KLK6 and KLK4, while in ovarian cancer cell lines ES-2 and HTB-161, KLK4 was downregulated, a phenomenon which implies that specific epigenetic mechanisms underlie the regulation of KLK4 in breast compared to ovarian cancer (Pampalakis 2006).

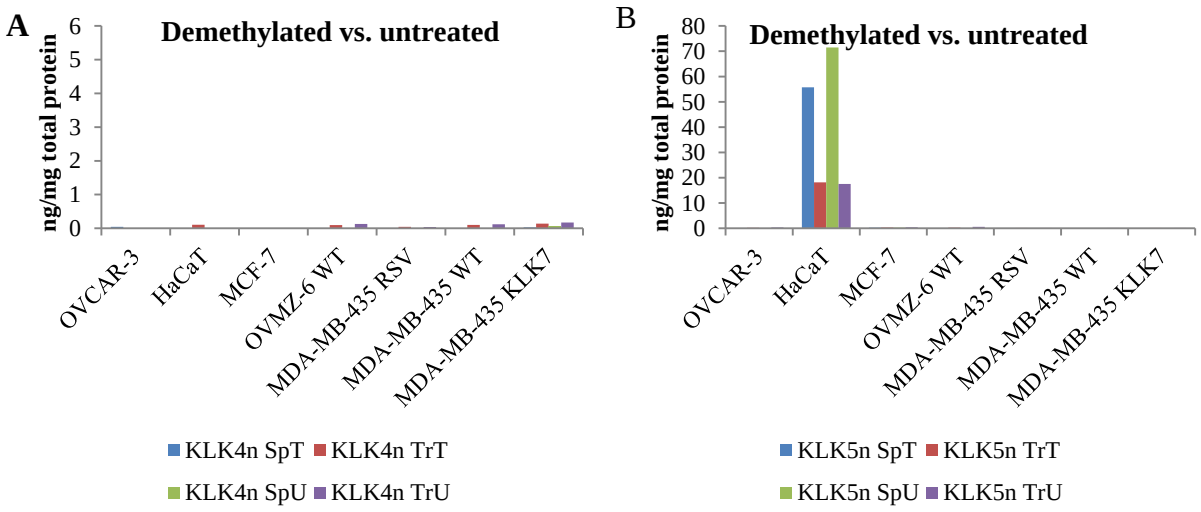

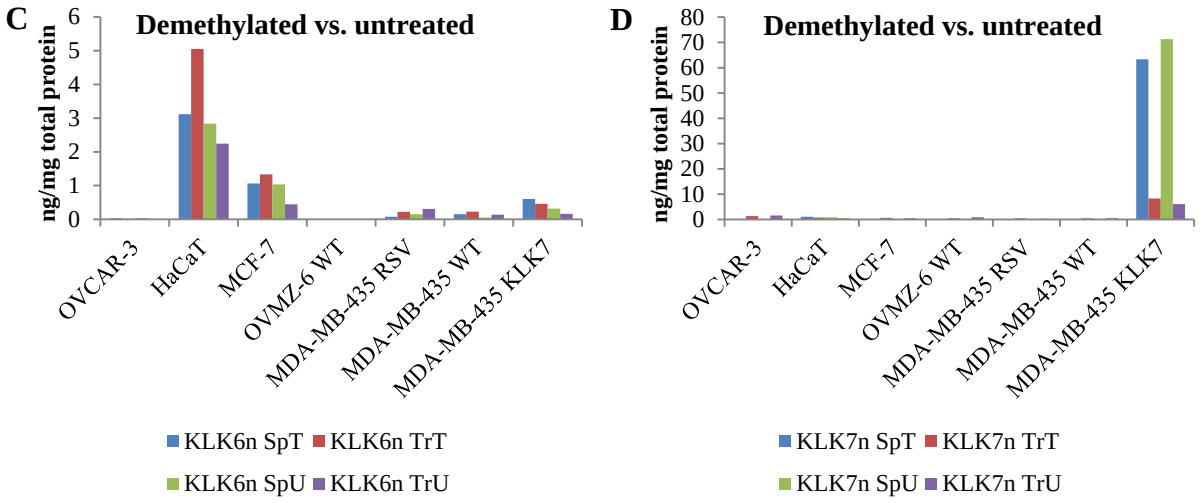


**Figure 48:** (**A**) KLK4 protein content levels as assessed by ELISA, normalized to cell number (n), for cell lines HaCaT, MCF-7, OVCAR-3, OV-MZ-6 *wild type*, MDA-MB-435 wild type, MDA-MB-435 pRc RSV and MDA-MB-435 pRc RSV/KLK7 in a comparison of demethylated (T) versus untreated (U) cell lines. Protein content levels available for supernatants (Sp) and for Triton-X-100 extracts (Tr). Similarly for (**B**) KLK5 protein content, (**C**) KLK6 protein content and (**D**) KLK7 protein content. Experiments always performed twice and graphs represent mean values. Differences in scaling allow beter comparison.

KLK6 expression, significantly higher than KLK4, is pronounced only in HaCaT and MCF-7, and follows a pattern where cytosolic extracts display higher levels than supernatants and demethylated cells produce more KLK6 than the untreated ones.

KLK5 expression is clearly pronounced in very high levels in HaCaT with demethylated cells showing lower expression than their untreated counterparts. This is in contrast with Pampalakis et al., where KLK5 remained unaffected in MDA-MB-231 and it was downregulated in the ovarian cancer cell line ToV-21G.

Finally, KLK7 is highly expressed in the transfected MDA-MB-435 pRC RSV/KLK7 cell line, a fact definetely anticipated, mostly secreted in the conditioned medium and less located in the cytosolic extracts. Moreover, methylation or demethylation does not seem to affect any expression, since no big difference among differentially treated cells is apparent.

To diminish any questions about inter-cycle variation, cells were also compared at cycle level. In other words, the expression levels of each kallikrein-related peptidase in the same aliquot (**Figure 48**). KLK5 dominated in the HaCaT, KLK7 in the overexpressing cell line, KLK6

demonstrated some expression in HaCaT and MCF-7, and KLK4 was very low or absent anywhere assessed.

KLK7 does not seem to be influenced by the demethylating agent Decitabine, whereas KLK5 and KLK6 seem to be somehow affected by the treatment. KLK5 levels are too low to extrapolate any conclusion.

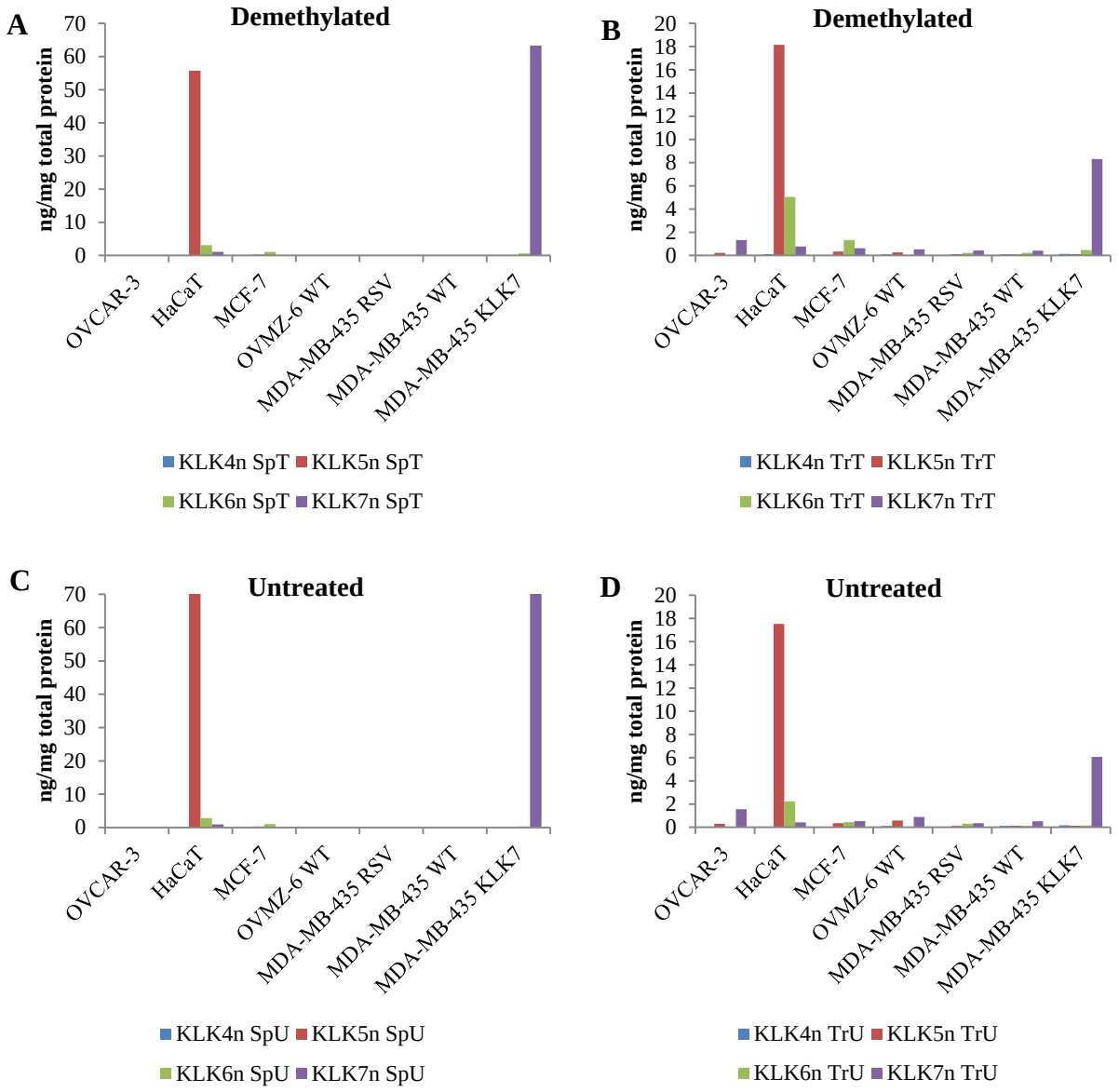


**Figure 49:** (**A**) KLK4-7 supernatant (Sp) and (**B**) Triton-X-100 (Tr) protein content levels as assessed by ELISA, normalized to cell number (n), for cell lines HaCaT, MCF-7, OVCAR-3, OV-MZ-6 *wild type*, MDA-MB-435 wild type, MDA-MB-435 pRc RSV and MDA-MB-435 pRc RSV/KLK7 after treatment with demethylating agent 5-aza-dC (T). (**C**) and (**D**) their untreated (U) counterparts, respectively.

If we focus on KLK7, clearly there is some sort of change in the expression in the transition from methylation to demethylation. Most cell lines demonstrate low KLK7 levels, so it is unclear whether changes are significant. In the MDA-MB-435 pRc RSV/KLK7, expression is high both in cytosolic extracts and in supernatants and the effect of demethylation significant. It is rather odd that although demethylated cells display lower KLK7 protein levels in the supernatant fraction, the Triton-X-100 fraction shows the opposite: demethylated cells have higher expression.

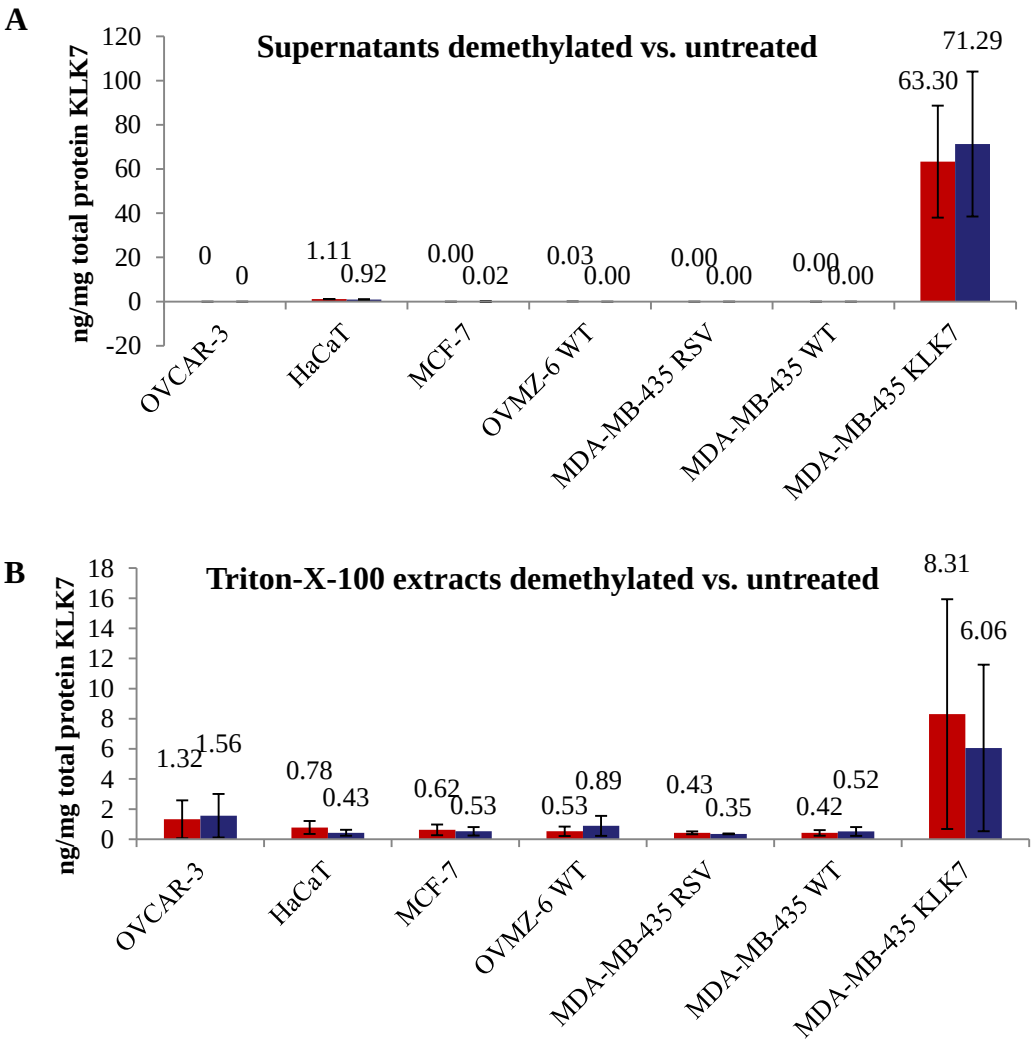


**Figure 50:** (**A**) KLK7 supernatant and (**B**) Triton-X-100 protein content levels as assessed by ELISA, normalized to cell number (n), for cell lines HaCaT, MCF-7, OVCAR-3, OV-MZ-6 *wild type*, MDA-MB-435 wild type, MDA-MB-435 pRc RSV and MDA-MB-435 pRc RSV/KLK7 in a comparison of demethylated (red) versus untreated (blue) cell lines.

This phenomenon may be an effect of diminished protein export. Added to this, the MDA-MB-435 pRc RSV/KLK7 are a transfected cell line with an artificial promoter, other than the original KLK7 promoter. This phenomenon implies that the demethylating agent affects the overall cell methylation status, maybe of a region that regulates KLK7 expression. It is though, unsafe to conclude on KLK7 regulation by methylation based on the presented results.

**Immunocytochemistry for treated and untreated cell lines (cell clots)**

Two clusters of cells, treated with the demethylating agent Decitabine and untreated, were grown until confluency and harvested to form a cell clot together with clotting agents such as fibrin, casein and thrombin. Paraffin-embedded material has the same properties as the regular FFPE tissue specimens, and thin slices can be used for immunocytochemistry in order to quantify the KLK7 protein acquisition. Protein signal would be directly correlated to change in protein production due to methylation regulation.

Clotting agents often cross-react with antibodies, a fact that bears high background. Antibodies are highly charged molecules and may bind non-specifically to components bearing reciprocal charges (e.g. collagen). Such non-specific binding may lead to localization of either the primary antibody or the labeled moiety (e.g. conjugate), producing "false-positive" staining of collagen (Dabbs 2010). Employing specific software by SlidePath®, the Positive Pixel Count® algorithm, we were able to obtain an objective and representative measure of quantified signal, the average concentration. After normalization for the cell number, differences in levels were obvious, especially in cell lines with higher KLK7 expression. Treated (demethylated) cell lines demonstrated significant overexpression of KLK7 over their untreated counterparts, for at least two cell types: the MDA-MB-435 pRc RSV/KLK7 and the corresponding wild type.
As far as the wild type is concerned, promoter region of KLK7 might be affected by Decitabine treatment and this could lead to an overexpression of the protein. On the other side, the overexpressing cell line, since it contains a high copy expression construct of KLK7 with an artificial promoter, might affect not in its native genome, but in its plasmid construct. Plasmid sequences can influence their expression activity in transfected cells since they are object of methylation due to a kind of host defense against virus (Bryans 1992; Kass 1993). For all other cell lines, low expression in general overlaps differences and no clear conclusions can be made.

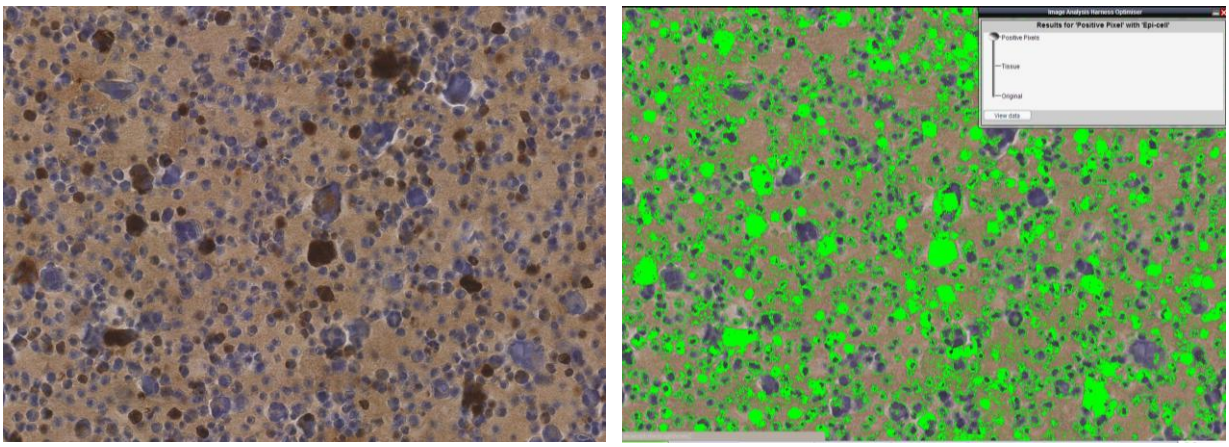

**Figure 51:** Example of ICC of the overexpressing cell line. (**A**) the digitized image before processing, (**B**) the positive pixel layer in green, which discriminates positive cells from the unspecific background. Brown for KLK7 ($DAB^+$), blue for nuclei (hematoxylin). EnVision method employed, no antigen retrieval. Magnification x 200.

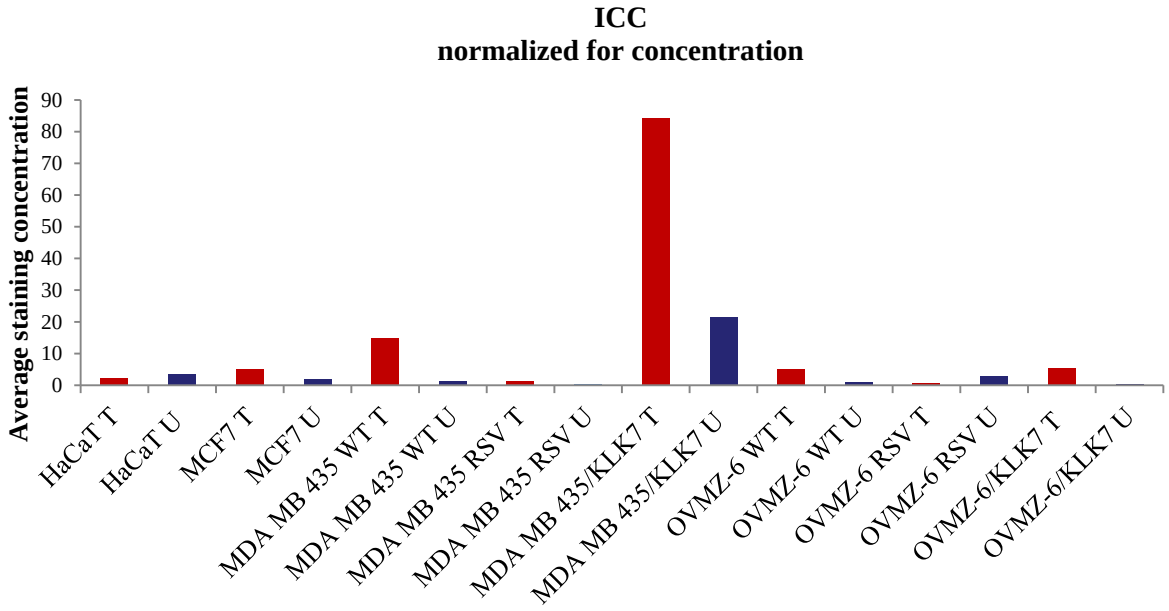


**Figure 52:** Average staining concentration (ICC) chart for cell lines HaCaT, MCF-7, OV-MZ-6 *wild type*, OV-MZ-6 pRc RSV, OV-MZ-6 pRc RSV/KLK7, MDA-MB-435 wild type, MDA-MB-435 pRc RSV and MDA-MB-435 pRc RSV/KLK7 in a comparison of demethylated (red) versus untreated (blue) cell lines with all cell lines, treated (demethylated) and untreated plotted. Red is for treated (T), blue for untreated (U).

The result reveals higher expression for the demethylated overexpressors and the HaCaT cell line over their untreated counterparts at the mRNA level. This result partly agrees with the ICC evaluation, where the overexpressing cell line clearly showed higher expression levels for the

demethylated cells. Elements connected with the KLK7 expression might be responsible for the increase despite the lack of a native promoter. Decitabine may influence expression status of other genes, e.g. involved in protein trafficking or protein degradation.

HaCaT acquired a small difference, sign that Decitabine changes cellular expression programme. For the rest of the cell lines, levels of expression were insignificant.

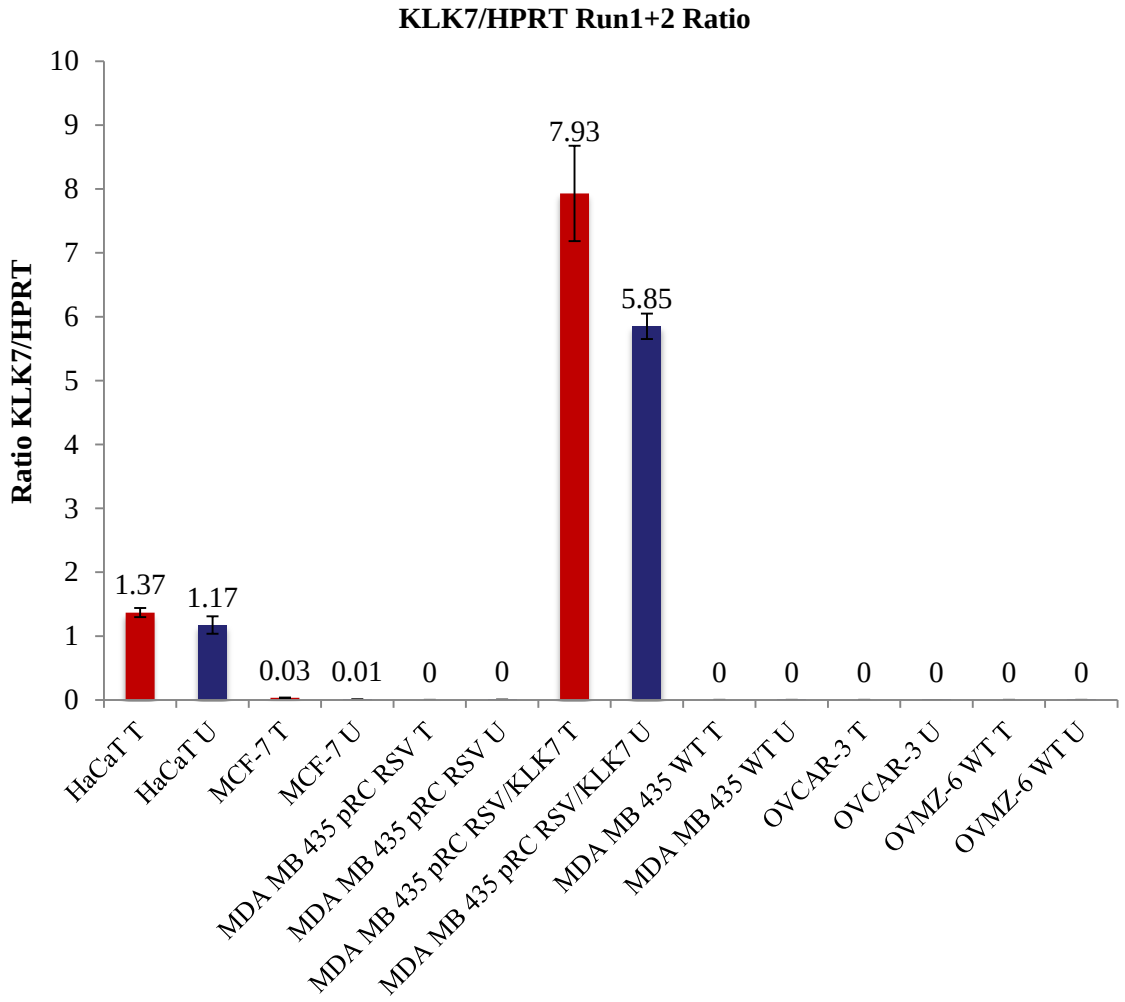


**Figure 53:** Q-RT-PCR results (two rounds) for cell lines HaCaT, MCF-7, OV-MZ-6 *wild type*, OV-MZ-6 pRc RSV, OV-MZ-6 pRc RSV/KLK7, MDA-MB-435 wild type, MDA-MB-435 pRc RSV and MDA-MB-435 pRc RSV/KLK7. Red is for treated (T), blue is for untreated (U) cell lines. This is a ratio of the KLK7 signal to the housekeeping gene (HPRT1) signal deriving from two amplification rounds.

## Correlations

In most cases, it is still unclear whether KLK7 is affected by the Decitabine treatment. **Table 43** summarizes results on the cell lines tested by every method assessed. For thorough comparison, Q-RT-PCR is listed with two independent runs and ELISA values represent two independent cycles of demethylation treatment. The absence of a clear-cut conclusion on the effect of methylation status on the KLK7 protein expression implies that KLK7 is either not regulated by methylation, at least not directly, or there is another kind of influence by 5-aza-dC application. For example, it could be that upregulation is either a downstream effect of 5-aza-dC, probably through the activation of a specific transcriptional activator, or that specific non-CpG island cytosines are involved in the regulation of transcription (Pampalakis 2006). Decitabine may influence many other proteins involved in KLK maturation. The difference in supernatant to cytoplasmic ratio indicates a participation of trafficking and /or degradation.

**Table 43:** Cells lines HaCaT, MCF-7, OVCAR-3, OV-MZ-6 *wild type*, OV-MZ-6 pRc RSV, OV-MZ-6 pRc RSV/KLK7, MDA-MB-435 *wild type*, MDA-MB-435 pRc RSV and MDA-MB-435 pRc RSV/KLK7 were subjected to 5-aza-dC demethylation treatment and assessed by Q-RT-PCR (mRNA level, rounds 1st and 2nd), ELISA (supernatant cycle 1- SP1, supernatant cycle 2- SP2, Triton-X-100 extract cycle 1- TR1 and Triton-X-100 extract cycle 2- TR2) and ICC (protein level). Red arrowheads represent downregulation in KLK7 expression, whereas green arrowheads represent upregulation in KLK7 expression. As shown in the comments, in most cases the role of methylation is rather unclear, with the exception of the transfected MDA-MB-435, where surprisingly there is an upregulation.

| Cell line | Q-RT-PCR | | ELISA | | | | ICC | Comments |
|---|---|---|---|---|---|---|---|---|
| | 1st | 2nd | SP 1st | SP 2nd | TR 1st | TR 2nd | | |
| HaCaT | ▼ | ▲ | ▲ | ▲ | ▲ | ▼ | ▼ | unclear |
| MCF-7 | ▲ | ▲ | ▼ | ---- | ▼ | ▲ | ▲ | unclear |
| OVCAR-3 | ▲ | ▲ | ---- | ---- | ▼ | ▼ | | unclear |
| OV-MZ-6 *wild type* | ▼ | ▲ | ▲ | ▲ | ▼ | ▼ | ▲ | unclear |
| OV-MZ-6 RSV | | | | | | | ▼ | |
| OV-MZ-6/KLK7 | | | | | | | ▲ | |
| MDA-MB-435 *wt* | ▲ | ▲ | ---- | ---- | ▼ | ▼ | ▲ | unclear |
| MDA-MB-435 RSV | ▼ | ▲ | ---- | ---- | ▲ | ▲ | ▲ | increase |
| MDA-MB-435/KLK7 | ▲ | ▲ | ▼ | ▼ | ▲ | ▲ | ▲ | increase |

It seems that MDA-MB-435 overexpressors are somehow influenced by the Decitabine treatment. Elements connected with the KLK7 expression might be responsible for the increase. There is still the native promoter in the cell lines, which may also be influenced epigenetically by the transfection of a high copy plasmid. Therefore, there can be still an effect on this native promoter as well as on the plasmid promoter. There are studies that speculate other mechanisms to co-operate in KLK regulation: from the production of multiple splice variants till the use of alternative promoters, as previously reported for KLK6 (Christophi 2004; Pampalakis 2004) and KLK11 (Nakamura 2001).

**Proliferation**

In the context of a thorough comparison between treated cell lines and their untreated counterparts, it was crucial to monitor changes in cell properties with the drug use. The use of cell-based assays is crucial for understanding the efficacy, specificity, permeability, solubility, stability and mechanism of drug interaction with target cells.

The Roche xCelligence® system utilizes an electronic readout by determination of changes of impedance to quantify cell proliferation and viability of the adherent cells in real-time. The cells were seeded in standard microtiter plates that contained microelectronic sensors. The cell-electrode impedance response that not only indicates cell viability but also correlates with the number of cells seeded in each well. The system used for this purpose, namely Roche xCelligence®, allows real-time, rather than end point measurements.

At the endpoint of approximately 50 hours after seeding (beginning of treatment with Decitabine at 5 hours), no apparent difference between treated and untreated cells was observed. Similar experiments for other KLKs demonstrated diminished proliferation rates when KLK10 protein was expressed (Lu 2009; Zhang 2011). Added to that, re-expression of KLK6 in non-expressing MDA-MB-231 breast tumor cells by stable cDNA transfection resulted in reversal of their malignant phenotype, manifested by lower proliferation rates and reduced cell motility (Pampalakis 2009).

Nevertheless, the triad of OV-MZ-6 (*wild type*, vector control and transfected with the KLK7 gene) provided an interesting finding: transfected cell lines demonstrated reduced proliferation rates in contrast with the *wild type*. Still RSV showed lowest expression rates in the two

experiments altogether. Transfected cells showed higher proliferation rates, so Decitabine induced even higher proliferation rates.

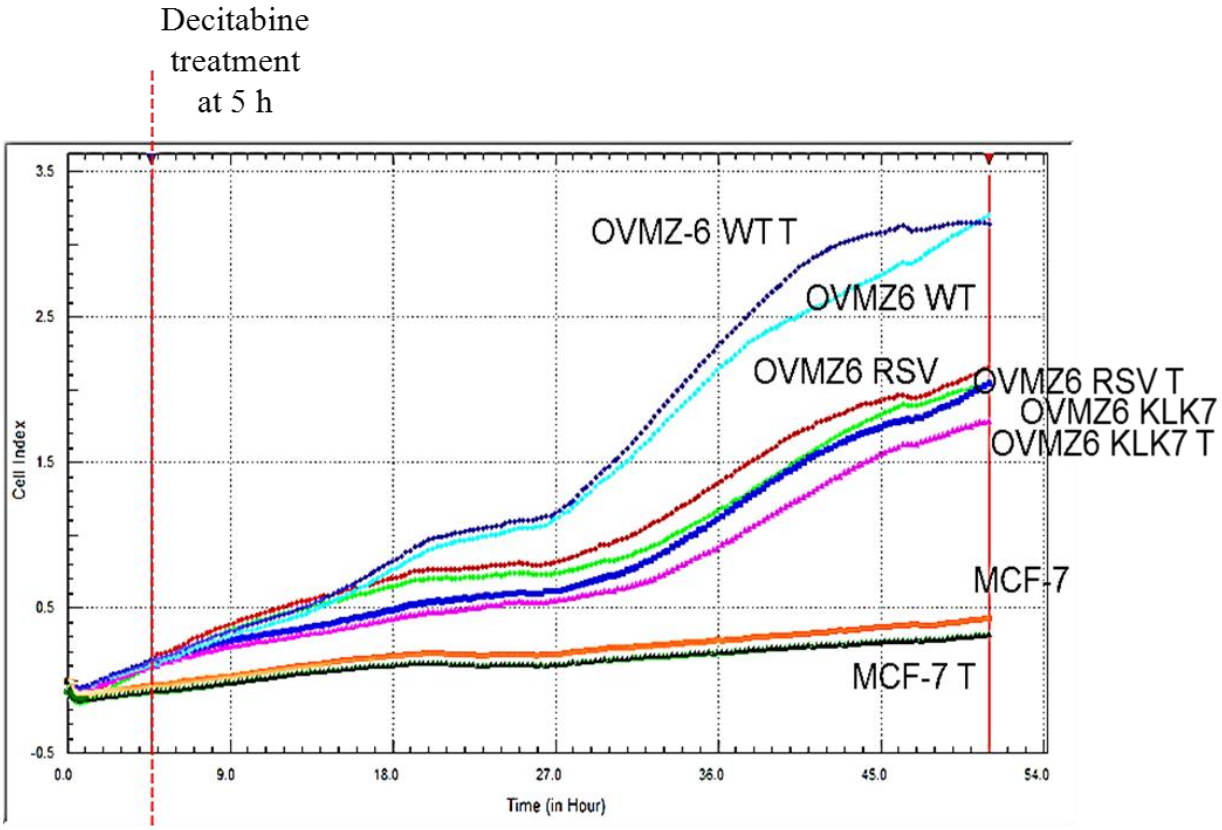


**Figure 54:** Example of proliferation curve (cell index versus time) for treated (T) and untreated cell lines MCF-7, OV-MZ-6 *wild type*, OV-MZ-6 pRc RSV, OV-MZ-6 pRc RSV/KLK7. Originally seeded cell population 10,000 cells in 16 x well microtiter plates (E-Plate, #05469830001, Roche, Penzberg, Germany). Cell impedance measured by use of RTCA® software (#05454433001, Roche, Penzberg, Germany). See also **Appendix 10.5**.

This is not the first time this kind of effect is reported. Cancer cell lines transfected with KLK3 cDNA have decreased proliferation rates and they give rise to tumors with decreased metastatic potential (Balbay 1999), while PC-3 cells expressing KLK4 had a decreased growth rate (Veveris-Lowe 2005). About KLK7, Mo et al., in contrast to our findings, did not discover any obvious differences in cell proliferation between cells overexpressing KLK7 and cells transfected with empty vector in the prostate cancer cell lines 22RV1 and DU-145 (Mo 2010).

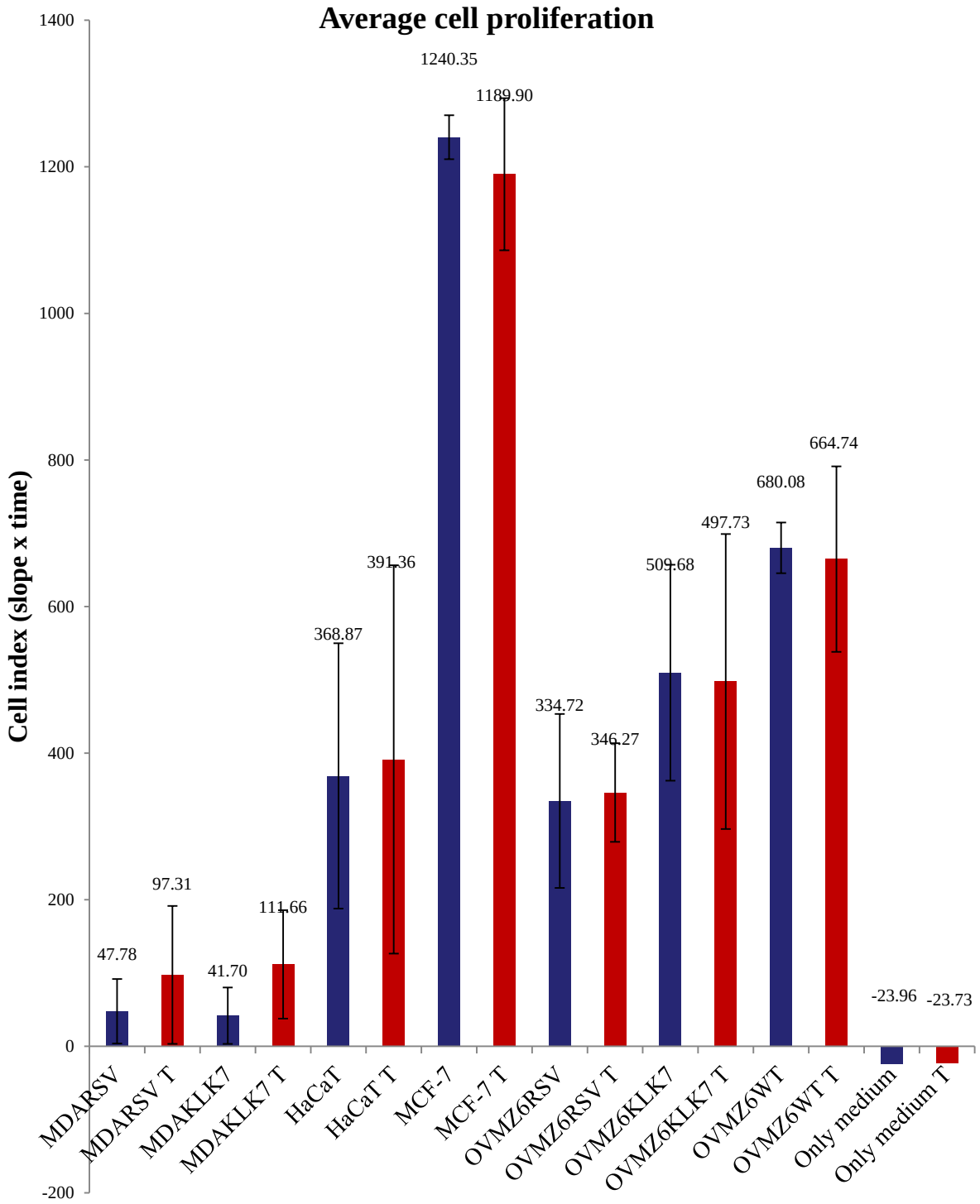


**Figure 55:** Cell proliferation for treated (T, red) versus untreated (blue) cells. Proliferation average from two individual experiments. Cell lines: HaCaT, MCF-7, OV-MZ-6 *wild type*, OV-MZ-6 pRc RSV, OV-MZ-6 pRc RSV/KLK7, MDA-MB-435 pRc RSV and MDA-MB-435 pRc RSV/KLK7. Controls are wells seeded with medium only and therefore they present negative values in proliferation. Experiments conducted with use of the xCelligence® system (Roche, Penzberg, Germany).

### 5.3.2 uPA/PAI-1

uPA displays expression differences due to methylation in four different cell lines, as it is assessed by methylation specific quantitative realtime PCR (Q-MS-PCR): in the MDA-MB-435 triad methylation decreases for the treated *wild type* and the treated overexpressing cell line, whereas it increases for the treated vector control, similarly to KLK7. On the other hand, MCF-7 treatment seems to increase the methylation. This finding is in contrast with Guo et al., where the combination of increased DNA methyltransferase activity with reduced demethylase activity contributed to the methylation and silencing of uPA expression in MCF-7 cells (Guo 2002). Estimation of total methylation content of Alu elements is useful for evaluation of the global genomic methylation status and level of homologous and non-homologous chromatin recombination in gene-rich regions . Global methylation status of repetitive genomic sequences such as long interspersed nuclear element 1 (LINE-1) and Alu sequences has been examined by comparison of treated with Decitabine cells versus their untreated counterparts. Demethylation occurs in every cell line as shown in **Figure 56** and **57**. This is an indication that the cell lines employed for these experiments are literally affected by demethylating agents.

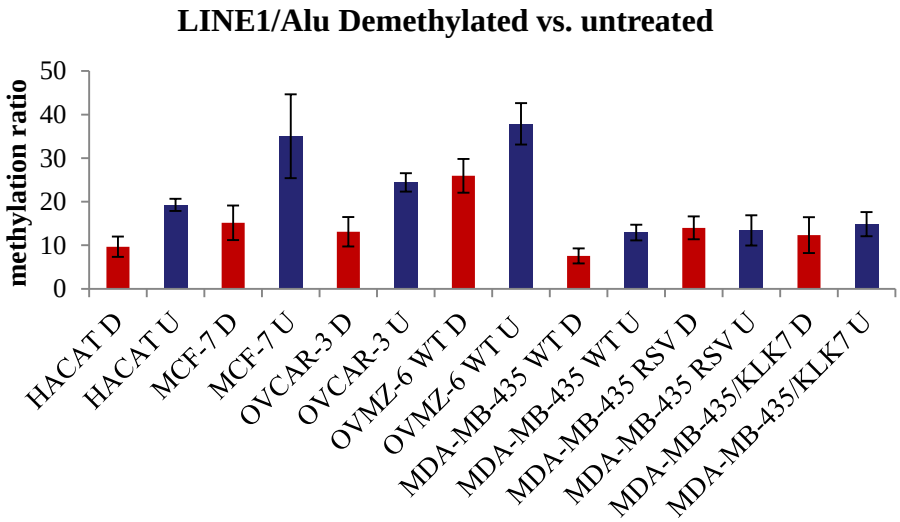


**Figure 56:** Global methylation status as affected by 5-aza-dC (Decitabine, #A3656, Sigma, Munich, Germany) treatment. Cells lines HaCaT, MCF-7, OVCAR-3, OV-MZ-6 *wild type*, MDA-MB-435 *wild type*, MDA-MB-435 pRc RSV and MDA-MB-435 pRc RSV/KLK7 were subjected to 5-aza-dC demethylation treatment. Extracted DNA was bisulfite-converted (introduction of specific changes in the DNA sequence) and amplified by use of TaqMan Q-RT-PCR assay. Here, LINE1 gene to Alu gene ratio gives an idea about the global DNA methylation content of the cell lines assessed. Demethylated cell lines are marked with (D), their untreated counterparts with (U).

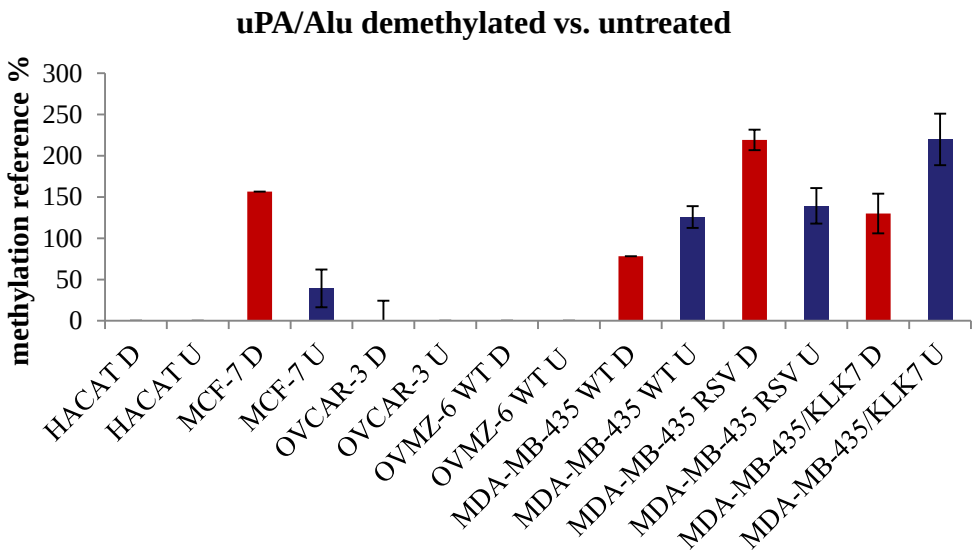


**Figure 57:** TaqMan Q-MS-PCR assay after bisulfite conversion of the treated (D, red) and the untreated (U, blue) cell lines for uPA gene. Cell lines HaCaT, MCF-7, OVCAR-3, OV-MZ-6 *wild type*, MDA-MB-435 *wild type*, MDA-MB-435 pRc RSV and MDA-MB-435 pRc RSV/KLK7. uPA methylation levels presented as a ratio to Alu1 repetitive element as reference.

Antigen levels (ELISA) for the same cell lines reveal higher expression of uPA for HaCaT, OV-MZ-6 and OVCAR-3 with significant change in expression after treatment only for OV-MZ-6 *wild type*, where hypomethylation causes decrease. uPA expression in HaCaT is confirmed by other studies (Krebs 1999). Obviously, cells affected at the gene level, do not produce much of uPA protein or many intermediate regulatory steps suppress any changes.

It makes sense at this point to go back and investigate whether untreated cell lines produce results that correlate to each other. In other words, if hypothetically there was no treatment, what would be the methylation status and what would be the levels of protein expression? Therefore, in a correlation study, where the two individual assessments, TaqMan Q-MS-PCR and ELISA are included, we obtain meaningful results. HaCaT, OV-MZ-6 and OVCAR-3 demonstrate the highest uPA protein levels, while at the same time their methylation status is lowest. Despite their hypomethylation, they seem to be affected by 5-aza-dC treatment so that uPA protein levels decrease.

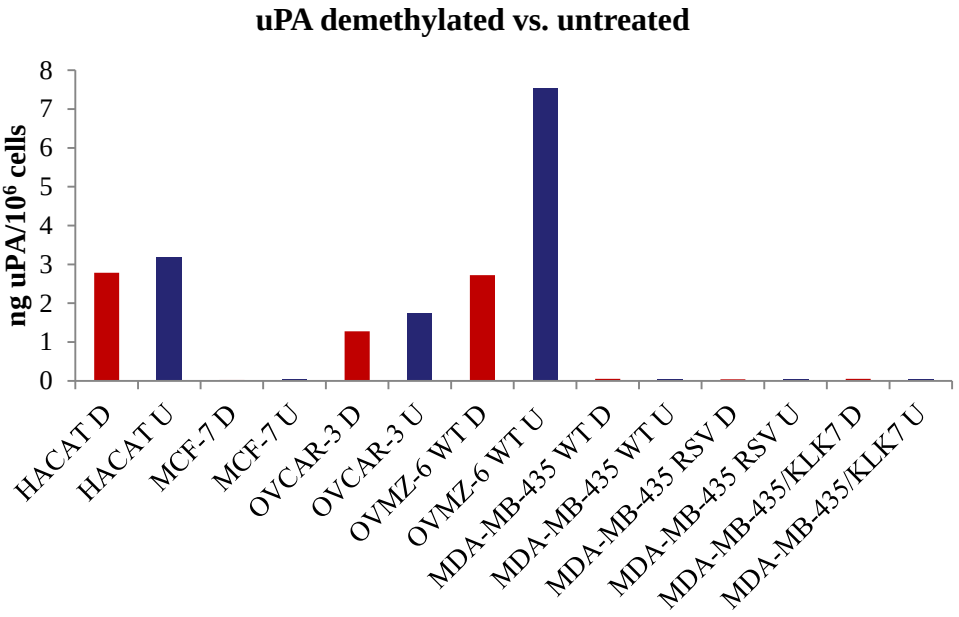


**Figure 58:** Cells lines HaCaT, MCF-7, OVCAR-3, OV-MZ-6 *wild type*, MDA-MB-435 *wild type*, MDA-MB-435 pRc RSV and MDA-MB-435 pRc RSV/KLK7 as assessed by ELISA for their uPA protein levels (Imubind #894, American Diagnostica Inc., Pfungstadt, Germany) and normalized to number of cells. Treated (D, red), untreated (U, blue).

For the other cell lines, methylation seems to be high in their untreated portion causing silencing of the gene. Demethylation, however, diminishes further RNA expression in the MDA-MB-435 wild type and the overexpressing KLK7, while it causes the adverse effect on the vector type.

What we learn from these findings is that at least for the untreated portion (**Figure 58**), high protein levels go along with low methylation status and vice versa.

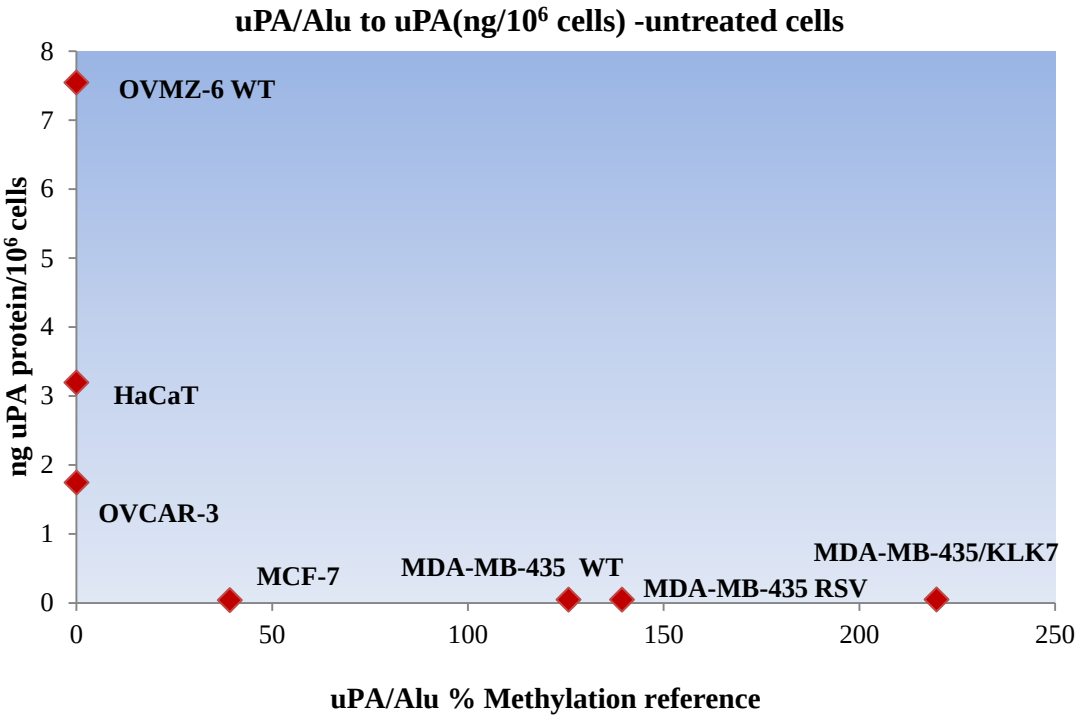


**Figure 59:** Correlation graph for uPA antigen levels versus TaqMan Q-RT-PCR. Cells lines HaCaT, MCF-7, OVCAR-3, OV-MZ-6 *wild type*, MDA-MB-435 *wild type*, MDA-MB-435 pRc RSV and MDA-MB-435 pRc RSV/KLK7.

As far as PAI-1 is concerned, the MDA-MB-435 displays exactly the same results as for the uPA, whereas there is an adverse effect for the MCF-7: this time hypomethylation goes along with treatment. We measured methylation levels, which should decline with Decitabine treatment (any DNMT-inhibitor) associated with an increase in mRNA expression levels and maybe protein levels. This finding is in similar to results of Gao *et al.*, where the methylation frequency was inversely correlated with PAI-1 mRNA level within its 20-fold range in MCF-7 and treatment with 5-aza-2'-dC led up to circa a 40-fold increase in the PAI-1 mRNA level (Gao 2005). At protein level, only MCF-7 and OVCAR-3 displayed significant levels of expression, with MCF-7 higher PAI-1 expression in demethylated populations.

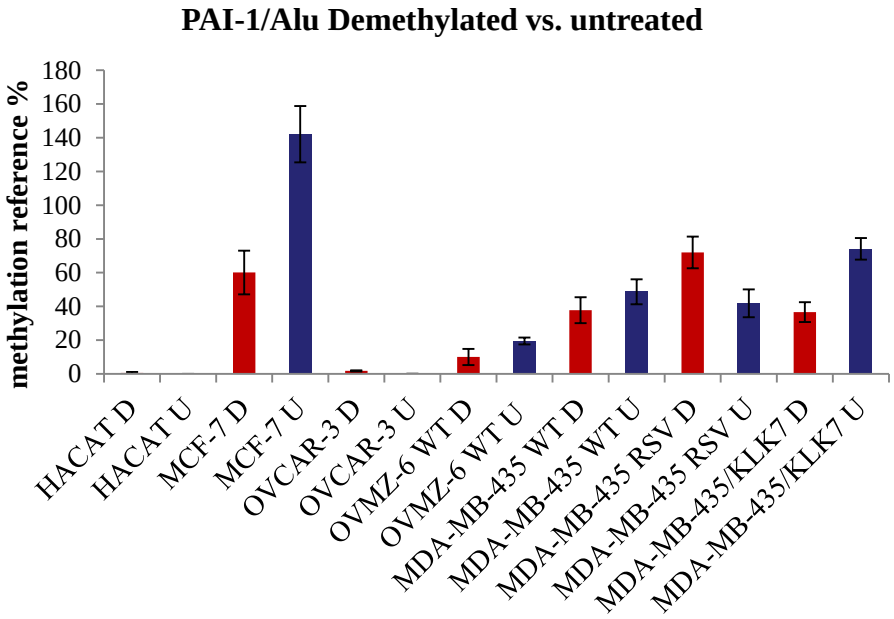


**Figure 60:** TaqMan Q-MS-PCR assay after bisulfite conversion of the treated (D, red) and the untreated (U, blue) cell lines for PAI-1 methylation status. Cells lines HaCaT, MCF-7, OVCAR-3, OV-MZ-6 *wild type*, MDA-MB-435 *wild type*, MDA-MB-435 pRc RSV and MDA-MB-435 pRc RSV/KLK7. PAI-1 methylation levels presented as a ratio to Alu1 repetitive element.

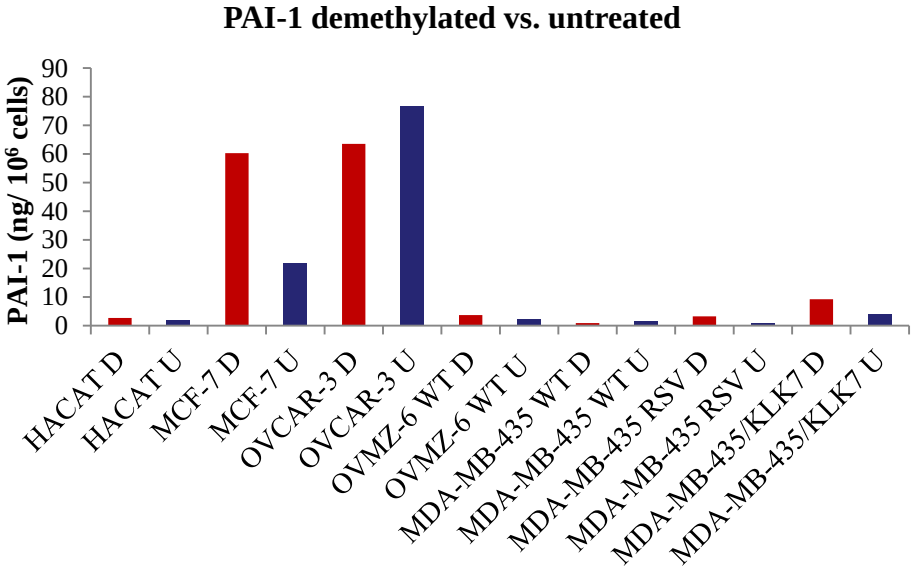


**Figure 61:** Cells lines HaCaT, MCF-7, OVCAR-3, OV-MZ-6 *wild type*, MDA-MB-435 *wild type*, MDA-MB-435 pRc RSV and MDA-MB-435 pRc RSV/KLK7 as assessed by ELISA for their PAI-1 protein levels (Imubind #894, American Diagnostica Inc., Pfungstadt, Germany) and normalized to millions of cells. Treated (D, red), untreated (U, blue).

Going back to the untreated population, it becomes clear that only OVCAR-3 and MCF-7 display high protein levels with either low or high methylation status, respectively. Of course, we would always await an rise of protein levels with decreased methylation levels, since methylation inhibits transcription and therefore probably in some way translation. Protein levels that normally decrease after treatment for OVCAR-3, they surprisingly rise in case of MCF-7, possibly due to an adverse effect. The rest of the cell lines displayed higher levels of methylated mRNA expression, but low protein expression.

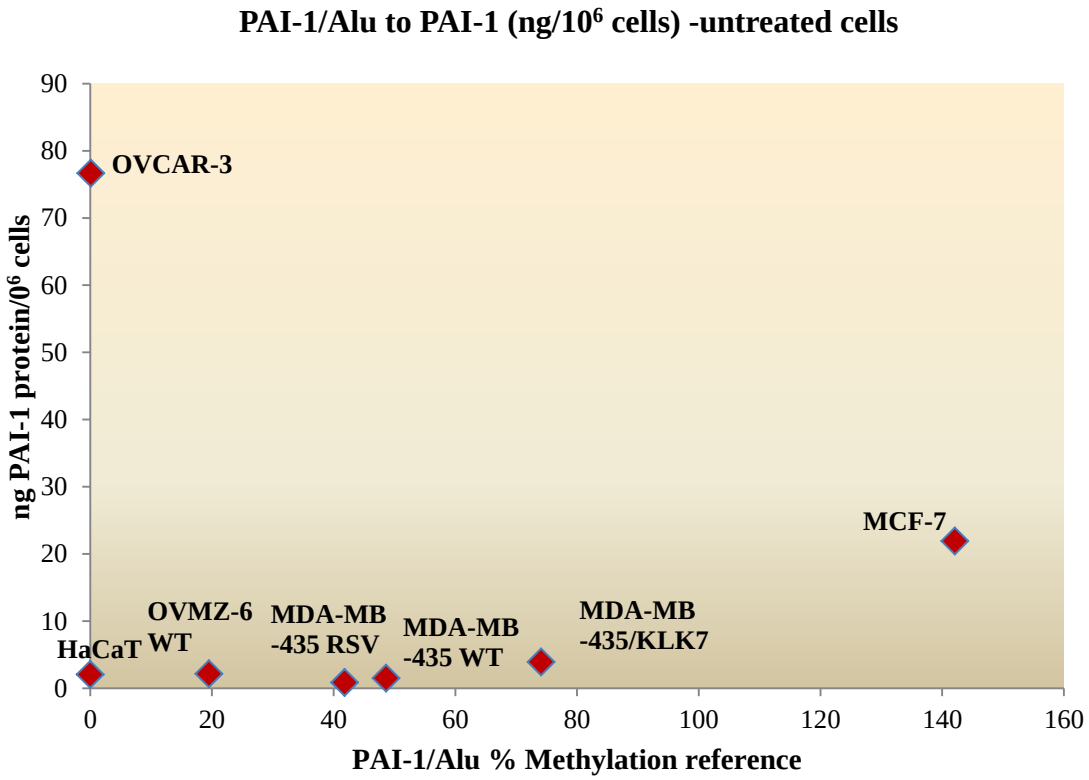


**Figure 62:** Correlation graph for PAI-1 antigen levels versus TaqMan Q-MS-PCR. Cells lines HaCaT, MCF-7, OVCAR-3, OV-MZ-6 *wild type*, MDA-MB-435 *wild type*, MDA-MB-435 pRc RSV and MDA-MB-435 pRc RSV/KLK7

Summarizing our findings, for uPA hypermethylation causes expression downregulation in HaCaT, MCF-7 and OVMZ-6, whereas demethylation causes expression upregulation in MDA-MB-435 wild type and overexpressing KLK7. Hypermethylation goes along with low expression for OVCAR-3.

**Table 44:** Summarizing results table displaying the effect of demethylation treatment on cell lines HaCaT, MCF-7, OVCAR-3, OV-MZ-6 *wild type*, MDA-MB-435 *wild type*, MDA-MB-435 pRc RSV and MDA-MB-435 pRc RSV/KLK7 as assessed by TaqMan Q-RT-PCR and ELISA. (D) stands for treated with 5-aza-dC samples, (U) for the untreated. Color-coding is explained below the table.

| Cell line | uPA/Alu | uPA (ng/$10^6$ cells) | Comments | PAI-1/Alu | PAI-1 (ng/$10^6$ cells) | Comments |
|---|---|---|---|---|---|---|
| HaCaT D | | | Hypermethylation causes expression downregulation | | | Hypermethylation goes along with high expression |
| HaCaT U | | | | | | |
| MCF-7 D | | | Hypermethylation causes expression downregulation | | | Demethylation causes expression upregulation |
| MCF-7 U | | | | | | |
| OVCAR-3 D | | | Hypomethylation goes along with low expression | | | Hypermethylation causes expression downregulation |
| OVCAR-3 U | | | | | | |
| OVMZ-6 WT D | | | Hypermethylation causes expression downregulation | | | |
| OVMZ-6 WT U | | | | | | |
| MDA-MB-435 WT D | | | Demethylation causes expression upregulation | | | Hypomethylation goes along with low expression |
| MDA-MB-435 WT U | | | | | | |
| MDA-MB-435 RSV D | | | | | | Hypermethylation goes along with high expression |
| MDA-MB-435 RSV U | | | | | | |
| MDA-MB-435/KLK7 D | | | Demethylation causes expression upregulation | | | Demethylation causes expression upregulation |
| MDA-MB-435/KLK7 U | | | | | | |

Upregulation-low signal

. Downregulation-low signal

Upregulation-medium/high signal

Downregulation-medium/high signal

For PAI-1, hypermethylation goes along with high expression for HaCaT and MDA/RSV. demethylation causes expression upregulation for MCF-7 and MDA-MB/KLK7. hypermethylation causes expression downregulation in OVCAR-3, whereas hypomethylation goes along with low expression in MDA-MB-435 wild type.

### 5.3.3 Triple negative breast cancer patients: assessment of BRCA1 status

**Overall survival and Time to progression in the patient cohort**

Within a follow-up period of up to 260 months (median follow up 76 months), 41 (26 %) patients showed recurrence of disease and 37 patients (23 %) died. The one-, two- and five year survival rates were estimated to 95 % ± 1.8 %, 90 % ± 2.4 % and 76 % ± 3.6 % respectively. In the univariate analysis, the clinically established parameters age, tumor stage, and nodal category revealed to be significantly associated with worse survival. Tumor stage and nodal category turned out to be the most predictive clinical parameters for the progression-free survival. (**Table 45** and **46**). The one-, two- and five year recurrence-free survival rates were estimated to 94 % ± 1.9 %, 84 % ± 2.9 % and 73 % ± 3.8 %, respectively. The majority of events related to disease recurrence occurred within the first 3-5 years.

**BRCA1 methylation status**

HRM analysis detected DNA methylation of the *BRCA1* promoter region in 47 of 171 TNBC tissue samples. Sequencing revealed that in methylated clones usually all potential CpG sites of the studied region were involved. Methylation in this region had been previously shown by others to cause loss of *BRCA1* transcripts (Esteller et al, 2000; Wei et al, 2005).

Patients showing at least 25 % methylation content within the tumor tissue (31 (18 %) out of 171) were in mean 6.4 years younger than individuals with less than 25 % methylation (52.5 vs. 58.9 years, 95 % CI mean difference: 0.83 to 12.0, $p$=0.025). Likewise, a positive methylation status occurred more frequently in premenopausal women ($p$=0.015).

Correlation with follow-up data (n=149) within the whole TNBC subgroup revealed that *BRCA1* promoter methylation (degree $\geq$ 25 %) was significantly associated with longer time to progression (**Table 45**). Accordingly, a hazard ratio (HR) of 0.11 [CI 0.02-0.80]; $p$=0.029, was determined for the risk of disease recurrence in the univariate analysis (**Table 46**). Moreover,

multivariable analysis by Cox regression analysis identified the methylation status as an independent prognostic factor for progression-free survival (HR=0.14 [CI 0.02-0.99]; *p*=0.049) among tumor stage (pT) and nodal category (pN) (**Table 47**). A tendency towards improved overall survival was seen as well (**Figure 63**), but the impact of *BRCA1* methylation did not reach statistical significance.

Since BRCA1 plays a major role in DNA repair, we next tested if the observed effect of the BRCA1 methylation status on TTP might rely on the patient group treated with DNA-intercalating/DNA-alkylating chemotherapeutic drugs such as anthracyclines and/or cyclophosphamide (n= 108). Indeed, similarly elevated recurrence-free times as described for the whole patient cohort with respect to a positive BRCA1 methylation status were observed: HR= 0.12 [0.02-0.87], *p*= 0.036.

**Table 45:** Predictive values of clinical and molecular-genetic factors for disease-free survival in patients with TNBC

| Variable | Valid cases | % | Univariate analysis[1] HR [95 % CI] | *p* |
|---|---|---|---|---|
| Age | 157 | | | |
| <50 | 53 | 33.8 | 1.00 | |
| ≥50 | 104 | 66.2 | 2.00 [0.96-4.20] | 0.066 |
| Tumor stage | 156 | | | |
| pT 1/2 | 135 | 86.5 | 1.00 | |
| pT 3/4 | 21 | 13.5 | 6.20 [3.18-12.12] | <0.001* |
| Nodal category | 153 | | | |
| pN 0/1 | 132 | 86.3 | 1.00 | |
| pN 2/3 | 21 | 13.7 | 4.88 [2.50-9.54] | <0.001* |
| Grade | 153 | | | |
| 1/2 | 36 | 23.5 | 1.00 | |
| 3 | 117 | 76.4 | 1.96 [0.89-4.30] | 0.094 |
| Therapy | 155 | | | |
| none | 33 | 21.3 | 1.00 | |
| CTX | 122 | 79.7 | 0.94 [0.43-2.04] | 0.876 |
| BRCA1 methylation status | 149 | | | |
| <25 % | 122 | 81.9 | 1.00 | |
| ≥25 % | 27 | 18.1 | 0.11 [0.02-0.80] | 0.029* |

[1] Cox regression analysis; * statistically significant

**Table 46:** Predictive values of clinical and molecular-genetic factors for overall survival in patients with TNBC

| Variable | Valid cases | % | Univariate analysis[1] HR [95 % CI] | *p* |
|---|---|---|---|---|
| Age | 157 | | | |
| <50 | 56 | 35.7 | 1.00 | |
| ≥50 | 101 | 64.3 | 3.25 [1.35-7.79] | 0.008* |
| Tumor stage | 156 | | | |
| pT1/2 | 135 | 86.5 | 1.00 | |
| pT3/4 | 21 | 13.5 | 8.21 [4.24-15.90] | <0.001* |
| Nodal category | 153 | | | |
| pN 0/1 | 132 | 86.3 | 1.00 | |
| pN 2/3 | 21 | 13.7 | 4.35 [2.16-8.77] | <0.001* |
| Grade | 153 | | | |
| 1/2 | 36 | 23.5 | 1.00 | |
| 3 | 117 | 76.4 | 2.04 [0.86-4.82] | 0.104 |
| Therapy | 155 | | | |
| none | 31 | 20.0 | 1.00 | |
| CTX | 124 | 80.0 | 0.43 [0.21-0.86] | 0.017* |
| BRCA1 methylation status | 150 | | | |
| <25 % | 121 | 80.7 | 1.00 | |
| ≥25 % | 29 | 19.3 | 0.49 [0.17-1.39] | 0.178 |

[1] Cox regression analysis; * statistically significant

**Table 47:** BRCA1 methylation status is an independent factor of PFS among tumor stage and nodal category

| **Multivariable Cox regression analysis of PFS** | | |
|---|---|---|
| **Variable** | **HR [95 % CI]** | **p** |
| Tumor stage (pT 1/2 vs pT 3/4) | 3.87 [1.75-8.55] | 0.001 |
| Nodal category (pN 0/1 vs pN 2/3) | 2.97 [1.40-6.33] | 0.005 |
| BRCA1 methylation status (<25 % vs ≥25 %) | 0.14 [0.02-0.99] | 0.049 |

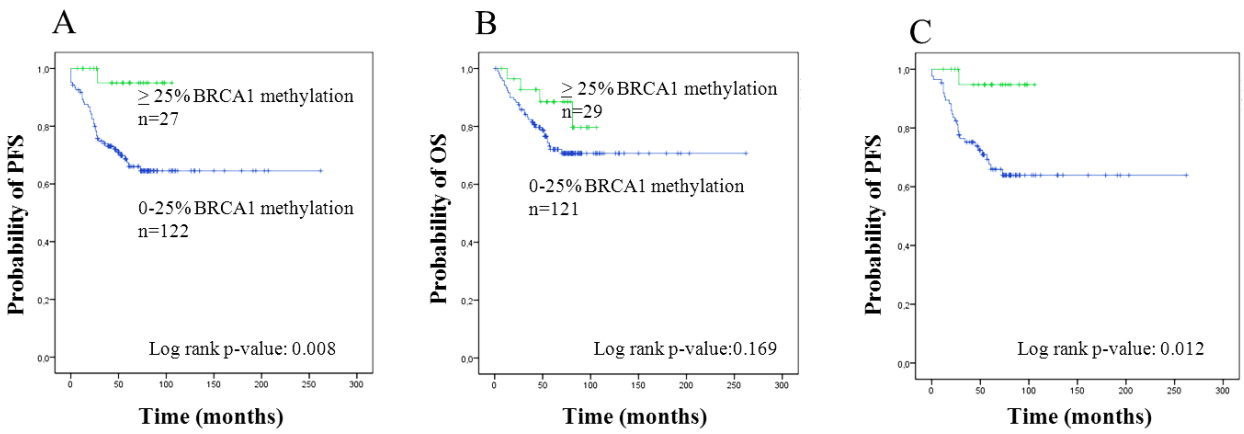


**Figure 63:** Effect of the *BRCA1* methylation status in TNBC on disease-free (**A**, **C**) and overall (**B**) survival rates.

# 6. Discussion

Late diagnosis and the heterogeneity of ovarian cancer and unidentified molecular pathways prohibit efficient individualized treatment strategies and result in high mortality rate. Shortage of clinical, histomorphological and tumor biological markers suitable for diagnosis, prognosis and therapy response prediction intensifies the critical state (Rosen 2005). Therefore, tumor risk predictors for cancer patients regarding disease recurrence, early death, or response to preoperative, adjuvant or palliative therapy are in demand.

Added to this, breast cancer is the most common class of cancer worldwide with more than one million cases diagnosed annually, followed by cancer of the lung and colon, making it the leading cause of cancer deaths in women with >400,000 deaths per year (Parkin 2005). Histological, immunohistochemical, mRNA expression, and genomic analyses have indicated that breast cancer is a heterogeneous disease that varies in morphology, biology, behavior, and response to therapy (Perou 2000; Sorlie 2001; Voduc and Nielsen 2008; Geyer 2009). Consequently, in breast cancer, specific biomarkers indicating the course of the disease and/or response to therapy are very much needed to help systemic treatment move from the current trial-and-error approach to more personalized cancer care.

Tumor-associated proteases may also serve as markers to portray cancer cell invasion and metastasis, also in ovarian cancer (Borgono and Diamandis, 2004; Kessenbrock 2010; López-Otín 2010; Blasi 2010; Lankelma 2010; Sotiropoulou 2009; Roy 2009; Cudic 2009). Of particular interest is the finding that several of the members of the serine protease-type kallikrein-related peptidase family of genes (KLK1-15), located on chromosome 19q13.4, may serve as diagnostic, prognostic, and/or predictive tumor biomarkers in ovarian cancer patients (Borgono and Diamandis, 2004).

KLKs are expressed in several tissues, at both mRNA and protein level. The parallel expression of many KLKs in the same tissue under physiologic and/or pathologic conditions implies potential participation in enzyme cascade reactions similar to those established for the processes of digestion, fibrinolysis, coagulation, complement activation, wound healing, angiogenesis, and apoptosis (Yousef and Diamandis 2002). The aberrant expression in human tissues reflects tissue-specific substrate specificity.

KLK4, 5, 6 and 7 were investigated for tumorigenic potential in ovarian cancer (Prezas 2006a) and this property generated the initial hypothesis that there might be certain association of these particular KLKs with the disease. Although the golden standard in protein quantification is the ELISA assay, there is a plethora of archived FFPE material which remains unexploited and could be useful in determination of additional factors in ovarian cancer. It would be, therefore, essential to establish tools (e.g. antibodies directed to KLKs) for the identification and immunohistochemical assessment of the KLK4, 5, 6 and 7.

Apart from KLK protease web, plasminogen activation system components (uPA and PAI-1) were subject of interest. By the end of the year 2007, the American Society of Clinical Oncology (ASCO) recommended two more widely evaluated cancer biomarkers to the list: uPA and PAI-1, whose clinical utilities were demonstrated at the highest level of evidence (LOE-I) (Hayes 1996; Harris 2007). No other cancer biomarker has ever achieved such high level of clinical evidence, serving as prognostic factors and predicting response to systemic adjuvant therapy (Hayes 1996; Harbeck 2002). The serine protease uPA, its inhibitor PAI-1, and the uPA receptor uPA-R (CD87) are controlling fibrinolysis, a feature associated with dissolution of blood clots and rearrangement of the extracellular matrix, also in cancer. In patients with primary invasive breast cancer, not only uPA and PAI-1 but also the receptor for uPA, uPA-R (CD87), are potential predictors of disease-free and overall survival (Grondahl-Hansen 1995; Foekens 2000; de Witte 2001). Knowledge of the clinical impact of uPA, PAI-1, and uPA-R, and associated factors, could be helpful to assess the individual risk of breast cancer patients, to select various types of adjuvant treatment and to identify patients who may benefit from uPA-R targeting therapies (Schmitt 1997; Schmitt 2008).

## 6.1 Assessment of performance of antibodies directed to KLKs and uPA/PA-1

KLK7 has been assessed by many researchers by use of various methods. In breast cancer by RT-PCR (Talieri 2004; Holzscheiter 2006), in cervical cancer by RT-PCR and by IHC (Santin 2004a; Tian 2004), in lung cancer by RT-PCR and by ELISA (Planque 2005; Planque 2008b), in brain cancer by RT-PCR (Prezas 2006b), in oral squamous cell carcinoma by IHC (Zhao 2011), in pancreatic cancer by RT-PCR (Johnson 2007) and in colorectal cancer by RT-PCR and by IHC (Talieri 2009b). Several methods have been employed in the literature to investigate KLK7 protein expression in ovarian cancer collectives (ELISA (Kyriakopoulou

2003; Shan 2006), immunofluorescence (Psyrri 2008)), but never by use of traditional immunohistochemistry. It was, therefore, crucial to discover the appropriate immunohistochemical tools for a thorough study on KLK7 expression in ovarian cancer.

The KLK7 antibodies' reactivity was initially assessed by means of Western blot under diverse conditions, namely reducing and non-reducing to simulate FFPE tissue microenvironment. Added to this, employing recombinant KLK7, signal strength and cross-reactivity with the other KLKs of this family were examined**.** The fact that, this family of proteases displays high similarity (Pavlopoulou 2010), allows assumptions on antibodies, which cross-react and thus identify more than one type of KLK. Third, microtiter plate measurements were performed to check the antibodies' binding capacity to their antigen. Immunoassays of this type are a matter of antibody concentration (Engvall and Perlmann 1972; Smith 1974; Svenson and Larsen 1977) and affinity (Ahlstedt 1974; Butler 1978).

For the antibodies directed to KLK4 and KLK6 a novel technique was established. Short peptide sequences derived from the target protein were employed to generate anti-peptide antibodies (Harvey 2003). The sequences encoding the mature forms of KLK4 and 6 (excluding the signal-sequence and the pro-peptides) were amplified from cDNA originating from ovarian cancer tissue and cloned into the bacterial expression plasmid pQE-30. The recombinant (non-glycosylated) proteins were purified under denaturing and slightly reducing conditions, refolded and finally used for immunization of rabbits and chickens. Antibodies were purified by affinity chromatography and tested by microtiter plate-based assays ("one-sided ELISA") and by Western blot analysis in order to detect any potential cross-reactivity with other KLKs. The antibody fractions were found to be specific for KLK4 and KLK6, respectively, as there was no cross-reaction with all of the other tested KLK proteases.

Additional KLK5 and KLK7 antibodies were obtained by R&D Systems and assessed by use of immunohistochemistry. Five antibodies, three anti-KLK7 and two anti-KLK5, were selected for their performance in IHC, on test tissues but also on ovarian cancer specimens, employing the protocol previously established for KLK7 including antigen retrieval by pressure-cooking. Additionally, three out of five were negative, one displayed severe background and one provided a clear signal without any cross-reactivity with other KLKs by means of Western blot. This antibody was the goat polyclonal anti-KLK5 AF1108 (R&D Systems).

The antibodies employed for the uPA/PAI-1 assessment were already characterized for signal intensity and cross-reactivity by means of Western blot in previous publications (Kobayashi 1991; Costantini 1996). This new panel of antibodies was selected for immunohistochemical assessment of these proteases. These antibodies had never been employed for this type of immunoassay before.

Cell lines were employed for target KLK7 protein localization, especially if they correspond to the respective normal or malignant tissues, e.g. HaCaT cell line (immortalized keratinocytes) for skin tissue. This analogy allows researchers to obtain indications from cells before using up valuable FFPE tissue sections as well as to produce supportive data for the actual patient material. Optimal working conditions for the antibodies directed to KLK7 were achieved in terms of (a) fixation conditions and permeabilization reagents under different concentrations, temperatures and incubations times and (b) staining methodology. PFA (1 % PFA/ 0.025 % saponin; 30 min; 4 °C). Observed staining homogeneity or overstaining in some cases might be due to cross-reactive elements. Additionally, cell extracts collected from cultivated HaCaT, MDA-MB-231, MCF-7, OV-MZ-6 WT, OV-MZ-6 pRc RSV and OV-MZ-6 pRc RSV/KLK7 and protein content was detected employing either the Arexis or the R&D antibody. R&D specifically recognized the intracellular KLK7 protein of HaCaT. Supernatants (conditioned medium) from the same passage used for blotting, revealed bands in every lane at the expected level while immunoprecipitation results confirmed the presence of KLK7 in its secreted form in the conditioned medium of the native expressers (HaCaT) and of the overexpressing transfected cell line (OV-MZ-6 pRc RSV/KLK7). Moreover, HaCaT seems to contain an intracellular fraction. Cell microarrays containing except for in-house cell lines, numerous other tumor cell lines were examined for KLK expression employing again two different antibodies to KLK7. Arexis antibody somehow overreacted, whereas R&D recognizes consistently the correct epitopes, or that Arexis recognized additional epitopes, perhaps neo-epitopes, which R&D fails to detect. By means of CLSM, it was demonstrated that HaCaT tend to form keratinized colonies in cell culture, each individual cell promotes cytoplasmic extensions to reach the neighboring ones. In our hands, HaCaT displayed clear staining in the cytoplasmic compartment and the merged image confirms the finding morphologically. The overexpressing cell line showed fluorescence, clear and distinct, probably the inactive KLK7 precursor with. After cleavage of the signal peptide, the proenzyme is activated extracellularly (Caubet 2004).

By all means used to investigate cellular KLK7, findings agreed in the vast majority of cases that differential expression of KLK7 among cell lines does exist (**Table 48**). Native expressers (HaCaT) and overexpressing cell line (OV-MZ-6 pRc RSV/KLK7) demonstrate higher expression levels in comparison with the rest of the cell lines, which actually served as controls. These results confirm the initial hypothesis, that KLK7 forms are present intracellularly.

**Table 48:** Summarizing table of all cell lines and techniques used to investigate cellular KLK7 expression. (*) Data from Holzscheiter et al. 2006. Mark in parentheses signifies a borderline result. N/A= not available.

| | HaCaT | MCF-7 | MDA-MB-231 | OV-MZ-6 WT | OV-MZ-6 pRc RSV | OV-MZ-6 pRc RSV/KLK7 |
|---|---|---|---|---|---|---|
| **Q-RT-PCR*** | + | - | - | N/A | - | + |
| **WB/IMP** | + | N/A | N/A | N/A | - | + |
| **ICC** | + | - | - | - | - | + |
| **CLSM** | + | - | N/A | (+) | - | + |
| **FACS** | (+) | - | - | - | - | (+) |

KLK7 seems to participate in skin desquamation, a process that is similar to detachment and dissemination of migrating cells in the process of metastasis (Brattsand 2005). Independent data support the dissemination hypothesis, as serum and ascitic fluid from the same ovarian cancer patient cohort skin desquamation process, this borrowed model implies that KLK7 might also play a role in the ovarian cancer cell dissemination. Therefore, ascitic fluid supernatant from five different patients was collected and tested for KLK7 presence using two antibodies for immunoprecipitation and detection, Arexis Tagena + Domino and R&D AF2624. Generally, both antibodies reacted similarly displaying strong reactivity with all ascitic fluid samples and this confirmed the presence of KLK7 protein in the ascitic fluid. Samples obtained from paramagnetic separation (MACS) were subjected to CLSM analysis where epithelial-origin cells (bigger) were successfully selected, as this was visually confirmed by microscopy. Immunocytochemical images confirm the CLSM picture in terms of cell population and they additionally correlate epithelial-type cells with KLK7 expression. With the help of our cytopathologist, almost all paramagnetically selected samples stained with PAP and separately with Giemsa, revealed tumor cell populations mixed with normal cell populations.

By means of immunohistochemistry, it is possible to define protein distribution in different cell types, independently of its average quantity in tissue. Tumor cell immunohistochemical

scoring, for example, might produce totally different results compared to whole cell lysates assays (e.g. ELISA) due to specific protein localization, which is not distinguished by means of ELISA. Of course, quantitative methods like ELISA detect native or recombinant proteins in contrast to immunohistochemistry, where proteins pass through fixation process. The change of protein epitopes is a serious drawback in this method, although new immunohistochemical techniques shorten procedure time and steps in order to harm epitopes least possible. Arexis Tagena + Domino, Affinity Bioreagents PA1-8435, and R&D AF2624 antibodies demonstrated comparable distribution patterns in a heterogeneous fashion, with cell staining pattern differentiating from each other. This signifies a true-positive staining (Miller 2001b; Taylor 2009). This is in agreement with results produced by others (Egelrud 1993b). The other antibodies tested directed to KLK7 demonstrated questionable and often inconsistent staining patterns in terms of product localization, intensity and distribution, no compartmental confinement (nuclear staining co-resided with cytoplasmic). This refers, for example, to the immunogenic KLK7 protein part recognized by the antibody: if this is not well-exposed in the FFPE tissue microenviroment, it might not be detected by the antibody. Not to mention the actually high probability that epitopes change during the hard processes of fixation, rehydration or dehydration, a fact leading to insufficient binding (Miller 2001b; Taylor 2009).

In order to question if previously published data (Dorn 2006; Dorn 2007) based on ELISA measurements from a predefined cohort of patients correspond to intensity of signal in Western blot, we randomly selected tissue extracts. Despite the fact that Western blot is a semi-quantitative method, it actually contributes valuable sets of information to an extent that strength of signal can be correlated with the protein quantity. Whatever substrate is used, the intensity of the signal should correlate with the presence of the antigen on the blotting membrane (Bjerrum 1988; Ursitti 1995; Bollag 1996; Gallagher 1996). We observed reactivity of the R&D antibody with a protein duplet of an apparent molecular weight of about 30 and 32 kDa, respectively. These two bands may well correspond to pro-KLK7 and activated KLK7, respectively. The intensity of the two bands corresponds well with the classification high, medium, and low by ELISA (although ELISA antibodies were very different). Employing the established immunohistochemical protocol for detecting KLK7 protein in tissue specimens, the corresponding cases were stained. Results confirm the already matching ELISA/ Western blot data, as strong staining (+++) characterized the ovarian cancer tissue specimens with high

ELISA values, and respectively the medium and the low cases. This is an additional indication that (a) KLK7 is localized in malignant ovaries, (b) all techniques employed work adequately and produced results correlate perfectly. The same procedures, i.e. ovarian cancer tissue extract assessment and immunohistochemical characterization were followed for the other anti-KLKs tested too. In the context of immunohistochemical evaluation, skin outer layers expressed predominantly KLK7, a fact that is in accordance with the majority of publications on skin physiology (Lundstrom and Egelrud 1991; Petraki 2006b; Shaw and Diamandis 2007). Arexis Tagena + Domino and R&D AF2624 antibodies produced a consistent and heterogeneous pattern, with distinct cell types stained. KLK7 in skin is considered to participate in protease activation pathways that lead in the physiological process of skin desquamation. In dermis, sweat glands are strongly stained, evidence supported by the secretory nature of kallikrein-related peptidases. In aorta, our immunohistochemical assessment revealed a weak to moderate staining in the smooth muscle of the tunica media, a finding that is not supported by any scientific reference by means of IHC or ELISA. Pancreas was strongly positive in the glandular acinus but negative in the Langerhans islets, in a rather distinctive mode. This is in contrast with Petraki et al. who suggest that Langerhans islets are positive for KLK7 as well as with ELISA data, which do not indicate KLK7 expression. It seems that KLK7 is secreted in the exocrine gland (acinus) and not in the endocrine (Langerhans). Co-localization with KLK5 supports this finding as it reminds of the skin localization of the two proteases (Dong 2008). ELISA data contradict KLK7 pancreatic localization.

KLK7 is present in normal skin but downregulated in melanoma tissue. In our melanoma collective, tissue cores from >100 patients were included in a tissue microarray panel and arrays were stained for KLK7 (EnVision, Permanent Red). According to previously published data (Winnepenninckx 2006), KLK7 in melanoma was statistically significant and tended to underexpress in melanomatic nests. This was clearly indicated in our study, as 80 % of the cases demonstrated negativity in the same areas. KLK7 is overexpressed by ovarian tumor cells, but is not expressed by normal tissues. Elevated KLK7 expression in ovarian cancer tissue is associated with poorer prognosis of ovarian cancer patients, especially those with lower grade disease and those who have been optimally debulked (Tanimoto 1999; Shigemasa 2001; Dong 2003; Kyriakopoulou 2003; Yousef 2003d; Davidson 2004; Bondurant 2005; Bignotti 2006; Dorn 2006; Petraki 2006b; Shan 2006; Dorn 2007). KLK7 is expressed in

normal breast and downregulated in breast cancer. Within breast cancer, high KLK7 expression is associated with good patient outcome (Yousef 2000d; Talieri 2004; Holzscheiter 2006). KLK7 is expressed in normal endocervical glands but elevated in cervical adenocarcinomas. No correlation was found between KLK7 expression and survival (Santin 2004a; Tian 2004). In non-small cell lung cancer, KLK7 expression is significantly lower expressed in adenocarcinoma than in matched non-malignant lung tissue (Planque 2005; Petraki 2006b). KLK7 is overexpressed in pancreatic adenocarcinomas over normal pancreatic tissue. Only about 15 % of the normal tissue specimens expressed the KLK7 protein (Johnson 2007). KLK7 is elevated in brain tumors over normal brain tissue. KLK7 mRNA expression is associated with shorter overall survival compared to patients with no KLK7 expression (Petraki 2006b; Prezas 2006b). KLK7 gene is up-regulated in colon cancer and its expression predicts poor prognosis for colon cancer patients (Talieri 2009b). In our colon cancer collective, tissue specimens of 266 primary colon cancer patients were stained for KLK7 using two different antibodies. Colon cancer tissue specimens examined show an overall strong expression for KLK7. In oral cavity, cDNA microarray analysis revealed that KLK7 was upregulated in tumor samples versus normal controls. RT-qPCR analysis confirmed that KLK7 mRNA was most differentially regulated with a 5.3-fold increase. Immunohistochemical analysis demonstrated strong reactivity in and human OSCC tissues (Pettus 2009). In other experiments, KLK7 was expressed strongly in the majority of tumor cells in 68 of 80 cases: these were mostly moderately or poorly differentiated neoplasms. Staining was particularly intense at the infiltrating front. Patients with intense staining had significantly shorter overall survival ($p < .05$) (Zhao 2011).

By immunohistochemical evaluation, both antibody fractions 617A and 617C were found to be suitable for detection of KLK4 in human tissues. Using a tissue microarray containing a variety of normal adult tissues, KLK4 was immunodetected with high frequency in liver hepatocytes and renal tubular, but not in glomerular cells. Staining intensity in the renal cortex was higher as compared to renal medullary cells. Other normal tissues such as colon, lung, skin or skeletal muscle were not immunoreactive for KLK4 with either of the antibodies. Weak KLK4 staining in glandular luminal cells of non-malignant prostate tissue was observed (Seiz 2010), whereas distinct KLK4 immunostaining with 617A and 617C characterized malignant glandular

epithelial cells, but not the basal layer of surrounding normal tissue or fibromuscular stromal cells. Intense granular cytoplasmic staining of cancer glands was noted (Seiz 2010).

Employing 617A, a discrete immunoreactivity was detected in the "normal-appearing" mucosa, from patients with colon cancer, removed far from the neoplastic tissue. Similarly, in normal colonic samples from control patients, almost no staining was observed (Gratio 2010). On the other hand, KLK4 was located in the mild dysplastic mucosa contiguous to a cancerous lesion. Staining characterized the columnar absorptive cells and goblet cells with varying intensity from patient to patient. KLK4 was observed mainly in the cytoplasm of cancer cells (Gratio 2010). KLK6 antibodies produced in chickens seemed to perform quite well and displayed strong specificity for KLK6 in kidney, brain and skin. In brain, they specifically recognize the astrocytes of the cortex.

**Table 49:** KLK4 expression in malignant tissues as present in the literature

| Type of cancer | Comments | References |
|---|---|---|
| **Ovary** | Ovarian carcinoma tissue cells express KLK4 which is lower in FIGO IV than FIGO III tumors. KLK4 expression is associated with progression of ovarian cancer, particularly late stage SER adenocarcinomas. In one study (Davidson 2005) KLK4 expression did not predict survival, in another (Obiezu, 2001) it was shown that ovarian tumor KLK4 expression is associated with an increased risk for relapse and death. KLK4 is suggested as a predictive marker for paclitaxel resistance. | (Dong 2001; Obiezu 2001; Xi 2004a; Davidson 2005; Obiezu 2005; Davidson 2007) |
| **Breast** | KLK4 protein is expressed in breast cancer tumor tissue. | (Davidson 2007) |
| **Prostate** | KLK4 protein is significantly overexpressed in malignant prostate compared with the normal prostate. The abundant prostatic expression of KLK4 is associated with mineralized tissues. There are two major isoforms of KLK4 (KLK4-254 and KLK4-205). KLK4-254 is cytoplasmically localized, while the N-terminal truncated KLK4-205 is in the nucleus of prostate cancer cells. | (Obiezu and Diamandis 2000; Obiezu 2002; Xi 2004a; Dong 2005; Obiezu 2005; Gao 2007; Klokk 2007) |
| **Mesothelioma** | KLK4 is frequently expressed in malignant mesothelioma, a non-hormonally regulated tumor. This finding provides support to the histogenetic link between mesothelial and epithelial cells. | (Davidson 2007) |

KLK4 displays trypsin-like activity (Debela 2006a; Debela 2006b) and can convert prourokinase- type plasminogen activator (pro-uPA) into active uPA, a key player in ECM remodeling, angiogenesis, wound healing, embryogenesis, tumor invasion and metastasis (Takayama 2001; Beaufort 2006). Low concentrations of KLK4 are present in a wide variety of fetal and adult tissues, e.g. the brain, breast, cervix, liver, prostate, salivary gland, skin, and

thyroid. KLK4 is secreted into seminal plasma, breast milk, and urine (Yousef 1999b; Komatsu 2003; Obiezu 2005; Shaw and Diamandis 2007). Overexpression of KLK4 mRNA has been demonstrated for prostate and ovarian cancer (Dong 2001; Xi 2004a), associated with progression and unfavorable prognostic outcome in ovarian cancer patients (Obiezu 2001) (**Table 49**).

**Table 50:** KLK6 expression in malignant tissues as presented in the literature

| Type of cancer | Comments | References |
|---|---|---|
| **Ovary** | KLK6 is absent in normal ovary tissue but expressed in ovarian cancer, also in early-stage and low-grade tumors. Elevated KLK6 was also found in benign epithelia coexisting with borderline and invasive tissues, suggesting that overexpression of KLK6 is an early phenomenon in the development of ovarian cancer. KLK6 levels have utility as an independent adverse prognostic marker. KLK6 is not found in serum of healthy women but at high concentration in serum of ovarian cancer patients. | (Diamandis 2000b; Tanimoto 2001; Hoffman 2002; Diamandis 2003b; Yousef 2003d; Ni 2004; Santin 2004a; Rosen 2005; Bignotti 2006; Davidson 2006; Dorn 2006; Petraki 2006b; Dorn 2007; Shan 2007) |
| **Breast** | KLK6 is expressed in normal breast ductal epithelium but is decreased in breast cancer tissue. | (Yousef 2004e; Obiezu and Diamandis 2005) |
| **Endometrium** | KLK6 is highly expressed in uterine serous papillary carcinoma and is released in the plasma and serum of these patients. KLK6 is considered a novel biomarker for uterine serous papillary carcinoma, for monitoring early disease recurrence and response to therapy. | (Santin 2005a; Santin 2005b; Petraki 2006b) |
| **Prostate** | KLK6 is expressed by normal prostatic epithelium, benign prostate, and prostatic intraepithelial neoplasia, but expression of KLK6 is decreased in neoplasia. Expression of KLK6 does not correlate with aggressiveness or prostate cancer prognosis. | (Petraki 2003a; Petraki 2006b) |
| **Urothelium** | Umbrella cells of the urothelium express KLK6, urothelial tumors do also express KLK6 which is suggested as a marker of urothelial differentiation and urothelial carcinogenesis. | (Petraki 2006b) |
| **Kidney** | In the normal renal parenchyma adjacent to the tumors, the renal tubular epithelium shows cytoplasmic expression of KLK6 whereas in renal cell carcinoma expression of KLK6 is decreased. KLK6 expression is negatively correlated with disease-specific survival. | (Petraki 2006b) |
| **Colon** | KLK6 is expressed in normal colon but expression is elevated in colon carcinoma. High expression of KLK6 correlates with serosal invasion, liver metastasis, advanced Duke's stage, and a poor prognosis in patients with colorectal cancer. | (Yousef 2004a; Ogawa 2005; Petraki 2006b) |
| **Stomach** | KLK6 is expressed in normal gastric tissue but expression is elevated in gastric carcinoma. Patients with elevated KLK experience poorer survival than those with low KLK6. | (Nagahara 2005) |
| **Pancreas** | KLK6 is expressed in normal pancreas and overexpressed in pancreatic cancer tissue. | (Yousef 2004a) |
| **Salivary gland** | KLK6 is expressed in salivary gland tissues and salivary gland tumors whereas KLK6 expression is downregulated in salivary gland tumors. | (Darling 2006; Petraki 2006b) |
| **Brain** | KLK6 is expressed in brain tumors. | (Petraki 2006b) |

KLK6 is most abundant in the brain and spinal cord. with moderate to high concentrations in the breast, prostate, fallopian tube, kidney, endometrium, lung, colon, bile ducts, gallbladder, and salivary gland. Low concentrations of KLK6 are found in a wide array of other adult and fetal tissues. KLK6 is secreted into breast milk, cerebrospinal fluid, cervicovaginal fluid; breast cyst fluid, saliva, seminal plasma, amniotic fluid, follicular fluid, and urine (Diamandis 2000b; Petraki 2001; Hutchinson 2003; Shaw and Diamandis 2007). KLK6 is absent in normal ovary tissue but expressed in ovarian cancer, also in early-stage and low-grade tumors.

Elevated KLK6 was also found in benign epithelia coexisting with borderline and invasive tissues, suggesting that overexpression of KLK6 is an early phenomenon in the development of ovarian cancer (**Table 50**). KLK6 levels have utility as an independent adverse prognostic marker. KLK6 is not found in serum of healthy women but at high concentration in serum of ovarian cancer patients (Diamandis 2000b; Tanimoto 2001; Hoffman 2002; Diamandis 2003b; Yousef 2003d; Ni 2004; Santin 2004a; Rosen 2005; Bignotti 2006; Davidson 2006; Dorn 2006; Petraki 2006b; Dorn 2007; Shan 2007).

By immunohistochemistry, KLK5 is most abundant in cornified skin layers to our findings, a fact which is in agreement with the sum of the scientific literature (Petraki 2006b; Shaw and Diamandis 2007). KLK5 is expressed in normal breast ductal epithelium and in the epithelium of the urinary tubuli of the normal kidney, while glomeruli remained unstained (Petraki 2006a). KLK5 in many cases co-resides with KLK7, a fact which is explained by their interaction in proteolytic activation. In ovary, a color deposit was observed in sparse cells in the stroma and in the surface ovarian epithelium. KLK5 expression in ovarian cancer tissues is significantly higher compared to their normal counterparts. Furthermore, a KLK5 variant (KLK5-SV1) was found in ovarian cancer tissues which is not present in their normal tissue counterparts. KLK5 expression is higher in FIGO III/IV than in FIGO I/II patient tissues. High levels of KLK5 are present in ascites fluid of metastatic ovarian cancer patients. As far as we know, KLK5 is enzymatically active, glycosylated and forms complexes with two protease inhibitors in ovarian cancer fluids (Yousef 2003b). KLK5 is an indicator of poor prognosis for patients with FIGO III tumors and with optimal debulking. Whereas KLK5 protein is almost undetectable in serum of normal female subjects, KLK5 protein is found in more than half of the ovarian cancer patients. Serum KLK5 is elevated in patients with late-stage, higher-grade disease and in

patients with serous histotype (Kim 2001; Diamandis 2003a; Dong 2003; Yousef 2003c; Yousef 2003d; Kurlender 2004; Yousef 2004c; Dorn 2006; Petraki 2006b; Dorn 2007).

**Table 51:** Expression of KLK5 in malignant tissue as presented in the literature.

| Type of cancer | Comments | References |
|---|---|---|
| **Ovary** | KLK5 expression in ovarian cancer tissues is significantly higher compared to their normal counterparts. Furthermore, a KLK5 variant (KLK5-SV1) was found in ovarian cancer tissues which is not present in their normal tissue counterparts. KLK5 expression is higher in FIGO III/IV than in FIGO I/II patient tissues. High levels of KLK5 are present in ascites fluid of metastatic ovarian cancer patients. KLK5 is an indicator of poor prognosis for patients with FIGO III tumors and with optimal debulking. Whereas KLK5 protein is almost undetectable in serum of normal female subjects, KLK5 protein is found in more than half of the ovarian cancer patients. Serum KLK5 is elevated in patients with late-stage, higher-grade disease and in patients with serous histotype. | (Kim 2001; Diamandis 2003a; Dong 2003; Yousef 2003c; Yousef 2003d; Yousef 2003e; Kurlender 2004; Yousef 2004c; Dorn 2006; Petraki 2006b; Dorn 2007) |
| **Breast** | KLK5 is expressed in normal breast ductal epithelium but is decreased in breast cancer tissue where it is found frequently in pre-/perimenopausal, node-positive and estrogen receptor-negative breast cancer patients. KLK5 is a prognostic factor in patients with large tumors and positive nodes, indicating unfavorable prognosis. Whereas KLK5 protein is almost undetectable in serum of normal female subjects, KLK5 protein is found in about half of the breast cancer patients. | (Yousef 2002d; Yousef 2003c; Yousef 2004c; Yousef 2004e; Obiezu and Diamandis 2005) |
| **Endometrium** | Focal KLK5 expression was observed in adenocarcinomas of the endometrium. | (Petraki 2006b) |
| **Prostate** | KLK5 expression in prostate cancer tissues is significantly lower compared to their normal counterparts, with lowest levels of expression in stage T3 tumors. Furthermore, a KLK5 variant (KLK5-SV1) was found which is also elevated in normal prostate tissues over their matched cancer tissue counterparts. | (Yousef 2002c; Kurlender 2004) |
| **Testis** | KLK5 expression is high in testis but KLK5 expression in testicular cancer is lower than in the normal counterpart. Immunohistochemical analysis of KLK5 expression in testicular germ cell tumors revealed weak positivity in seminomas and stronger positivity in embryonic carcinomas and teratomas. | (Yousef 2002b; Luo 2003b; Obiezu and Diamandis 2005; Petraki 2006b) |
| **Kidney** | KLK5 is highly expressed in the epithelium of the urinary tubuli of the normal kidney but downregulated in renal cell carcinoma. | (Petraki 2006a; Petraki 2006b) |
| **Urothelium** | Umbrella cells of the urothelium express KLK5, urothelial tumors do also express KLK5 which is suggested as a marker of urothelial differentiation and urothelial carcinogenesis. | (Petraki 2006b) |
| **Lung** | Non-small cell lung cancer: KLK5 expression is significantly more expressed in squamous cell carcinoma than in matched nonmalignant lung tissue. | (Planque 2005; Petraki 2006b) |
| **Salivary gland** | KLK5 is expressed in the epithelium of the excretory ducts of the major and minor salivary glands. Ductal epithelium of cystadenolymphomas and tumors derived from ductal epithelium expressed KLK5 as well. . | (Petraki 2006b) |
| **Brain** | KLK5 is expressed in brain tumors. | (Petraki 2006b) |

HMW-uPA converts the protein plasminogen to its proteolytically active form, the serine protease plasmin (Schmitt 1997). Plasmin, in turn, will act on cell-bound pro-uPA to effect conversion of pro-uPA to HMW-uPA. The broad-spectrum protease plasmin will then degrade fibrin and other constituents of the ECM, a feature known as fibrinolysis, to facilitate cell migration and dissemination **(Figure 64)**. Pro-uPA is produced and secreted by quite a range of cell types, such as endothelial cells, muscle cells, specific types of leukocytes, fibroblasts (e.g., subepithelial fibroblasts in the GI tract), granulosa cells in the follicles, several epithelial-like cell types including proximal and distal kidney tubule cells and bladder urothelium cells, trophoblast cells, migrating keratinocytes and cancer cells. uPA content in the bloodstream of healthy individuals is low. However, in case of inflammatory (also in arteriosclerotic vessels), infectious or malignant processes, uPA expression and secretion are often increased considerably (Schmitt 1997; Zorio 2008; Fevang 2009). uPA's main role as a protease is the cleavage of plasminogen to its proteolytically active form, plasmin, but substrates other than plasminogen are also known, such as $a_6$-integrin, fibronectin, fibrinogen, diphtheria toxin, HGF/scatter factor, uPAR and uPA itself. By its proteolytic activity, uPA influences cell signaling cascades, such as matrix metalloproteinase (MMP) activation, directly or by plasmin (Zhao 2008), growth-factor release from the ECM (by plasmin activation)(Matsuoka 2006) and chemotaxis by uPAR cleavage (Binder 2007). Besides its catalytic activity, uPA, in association with uPAR and/or its inhibitor PAI-1, is involved in several cell signaling cascades and can therefore impact cell adherence, cell migration, chemotaxis, anoikis, cell growth and cell survival. Interaction of uPA with uPAR leads to conformational changes in the complex, thereby enabling binding of the complex to integrins such as $a_vb_3$ and the ECM component vitronectin (VN) (Franco 2006; Tarui 2006; Binder 2007; Crippa 2007; Ulisse 2009).

Adapting know-how methodology from kallikrein-related peptidases immunohistochemical assessments into the plasminogen field, we have been able to evaluate numerous parameters such as primary antibody incubation temperature, antibody concentration, antigen retrieval, blocking reagents, hematoxylin type, etc. and produce stable and repetitive protocols for manual and automatic mode. The latter refers to immunohistochemical assessment with use of autostainers, namely Dako Autostainer LINK 48 or Ventana Benchmark® XT.

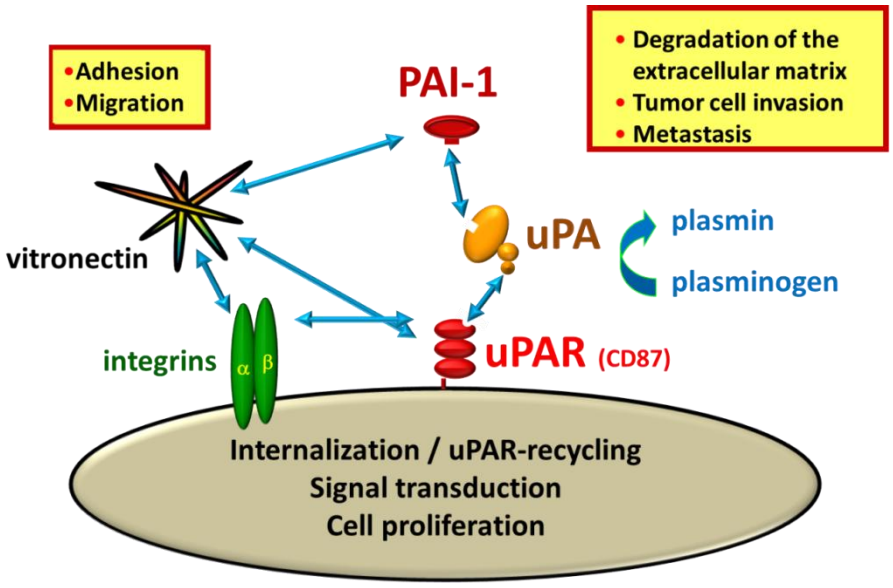


**Figure 64:** The multifunctional role of uPA, PAI-1, and uPAR in tumor growth, invasion and metastasis. In addition to pericellular proteolysis, many other tumor biologically important processes such as cell migration, adhesion, intracellular signaling, and proliferation are

Analytically, automatic staining was stronger than manual for tumor and stroma but in the same context. The staining, both in manual and automatic mode, follows a similar pattern, a finding which permits procedure automation without technical drawbacks. Similarly, both methods employed, LSAB and EnVision (also Ventana iVIEW® and ultraVIEW® respectively), produce similar results, so they are both recommended for staining. Moreover, there was no actual need for endogenous biotin block, since breast negative controls are really negative, while different protocols were generated for different temperature settings; Ventana Benchmark works only at 37 °C. Finally, antigen retrieval by pressure-cooking generally did not contribute any value to our stainings because pilot experiments with routinely FFPE control tissues (normal kidney) and breast cancer tissue sections revealed that pretreatment of tissue sections is not necessary for antigen retrieval. A valuable remark is that the differences among different cases (e.g. breast cancer) by immunohistochemical assessment as well as in protein content as assessed by ELISA (decimal subdivision) are pretty small for human eye to distinguish, therefore automatic scoring by use of algorithmic quantification software would be more efficient than manual evaluation by pathologist (Remmele score). Our findings in breast cancer tissue specimens as assessed by immunohistochemical means indicate that uPA protein content is upregulated in tumor cells (cytoplasmic and membrane compartment) and also myofibroblasts and stromal areas are stained mainly at the invasion front. This is in agreement with the proteolytic activity

of uPA in tumor tissue, where other proteases are activated and ECM degradation is promoted. PAI-1 antibodies, acting similarly, demonstrated a pronounced expression in tumor cells, myofibroblasts, macrophages, endothelial cells and stromal areas. Another observation is that the ELISA value is mainly an attribute of the size of the tissue extracted sample in relation to the concentration of the biomarker in question, expressed within this tissue. This is a hint from a preliminary study of twenty-nine (29) invasive breast carcinomas, where stromal cell, ECM and tumor cell staining intensity was also in agreement with the respective ELISA values. Finally, stromal areas distant from the tumor site seem to be more stained than the ones close to the tumor, whereas tumor sites remain intense. This might be due to counterbalance effect, where adequate levels of protein are produced by the tumor cells, a phenomenon that keeps nearby stromal uPA/PAI-1 protein levels low. Additionally and for comparison reasons, a collective of breast cancer tissues was employed and assessed by the new technology of the protein arrays (RPMA). Eighteen randomly selected different breast cancer cases disposed material for ELISA, immunohistochemistry and reverse phase protein microarray assessment (by Claudia Boellner). As ELISA and RPMA represent continuous variables, automated IHC replaced manual evaluation in this study, in order to obtain a direct comparison of the three biological parameters. Added to this, the differences among different cases in ELISA values were small, therefore an automatic scoring would be more efficient than a manual. The antibodies employed for detection were different in each technique, a fact which alone produces result variation. Putting everything together, for PAI-1 we observed no correlation between IHC and ELISA as well as between IHC and the protein array. There was, however, a very strong correlation (0.84), between ELISA and the array, which signifies the RPMA as a good candidate to replace ELISA in protein levels assessment, even from FFPE material.

**Other variables affecting immunostaining performance**

In the context of controlling antibody reactivity in various conditions, we created fixation settings beyond standards. Apart from commonly used buffered formalin (BF), tissue specimens fixed with Bouin's solution (BO) or a newly marketed fixative, Z-Fix (ZF) (Anatech, Battle Creek, MI). Antibodies behavior was influenced by fixation in case of Bouin's solution (membrane staining, identical positivity), whereas zinc-formalin and neutral buffered formalin demonstrated similar reactivity. The fixative testing procedure demonstrated that the selected antibodies on a buffered formalin-fixed tissue produce similar results with the

premium zinc-containing fixative (Z-fix), thus they are suitable for staining archived tissue specimens.

Dealing with protease immunohistochemical staining generates interpretation difficulties due to the diffuse nature of the staining pattern. Protease staining represents a continuous variable in contrast to other types of molecules which display zero variance patterns. Second to that, objective immunohistochemical scoring is limited by the pathologist's ability to score on a continuous scale, discriminate between subtle low-level staining differences, and accurately score expression within subcellular compartments (Camp 2002). Standardization of IHC interpretation can improve the quality of the data obtained from IHC studies. Automated software solutions allow increased sensitivity in scoring and provide a more reliable analysis of protein expression in situ. Improved image analysis technologies have the potential to bypass the pitfall of interpretation and intraobserver variability, offering the potential to develop objective automated quantitative scoring models for IHC. A deviation from the semiquantitative manual scoring models could lead to less variable results, to high throughput analysis and to the identification of new prognostic subgroups, probably masked with manual analysis (Cregger 2006).

## 6.2 Clinical impact of KLK7 on ovarian cancer

According to the statistical analysis, there is a strong, significant correlation among the different immunoscores as extracted by the manual immunohistochemical evaluation. Added to this, the automated analysis score correlated significantly with either one of the manual immunoscores. Values were also grouped according to the 2/3 percentile (2 tertials; 66 %), defined as the optimal cut-off point for the group division into high (above the cut-off) or low (below the cut-off). In comparison with another ovarian cancer collective as published by Psyrri *et al.*, there KLK7 protein expression, as quantified by immunofluorescence, demonstrated no association with clinicopathological variables including age, differentiation, histological type, histological grade, FIGO stage, residual disease and clinical response to chemotherapy (Psyrri 2008). A significant association, on the other hand, was observed in our collective between combined manual immunoscore and ascitic fluid volume. Furthermore, high levels of tumor cell score and combined score and automated analysis score were related with residual tumor presence. Finally, automated analysis score seems to be associated with the

FIGO stage, stromal cell immunoscore strongly with nuclear grade and KLK7-ELISA with the response to chemotherapy.

All clinical variables included in the Cox model, except for age, such as FIGO stage III/IV vs. I/II, nuclear grade, RT presence, and ascitic volume were univariate predictors for OS in the ovarian cancer cohort, a fact which applies also to the FIGO III/IV cohort, apart from the nuclear grade parameter. Likewise, in univariate analysis of PFS for the total number of patients, all of the clinicopathological parameters, except the age and the FIGO stage categories, reached statistical significance. Additionally, we found a significant association between low KLK7 antigen levels in tumor tissue extracts and an increased risk of death for FIGO III/IV patients in univariate Cox regression analysis. Consequently, **the expression level of KLK7 in tumor cells or stromal cells as detected by immunohistochemistry and the combined, overall score were not associated with patients' outcome in univariate Cox's regression analyses.** Psyrri *et al.*, on the other side, found that low KLK7 immunoscore was was associated with improved outcome for OS and DFS, respectively, having grouped patients by use of the X-tile cut-off in the uneven groups of KLK7 low expressers (n = 118), and KLK7 high expressers (n = 10). Our values were grouped according to the 2/3 percentile (2 tertials; 66 %), so the difference was much smaller. Strikingly, **in multivariate analysis, KLK7-ELISA values, in addition to the FIGO stage and the residual tumor mass, were significantly associated with both OS and PFS, either in the total number of the patients or the FIGO III/IV subgroup.** This is in accordance with Psyrri *et al.*, where low KLK7 level was significant predictor variable of OS (but not for PFS).

In conclusion, KLK7-ELISA levels of the FIGO III/IV patients seem to be predictors in univariate analysis, as well in multivariate analysis, where KLK7-ELISA values, in addition to the FIGO stage and the residual tumor mass, were significantly associated with both OS and PFS, either in the total number of the patients or the FIGO III/IV subgroup. Our results indicate that in contrast to earlier findings, high KLK7 antigen levels in tumor tissue extracts may be associated with a better prognosis of ovarian cancer patients.

## 6.3 Assessment of DNA methylation status for KLKs, uPA/PAI-1 and BRCA1

### 6.3.1 KLKs

Methylation of CpG islands of genes causes epigenetic changes in chromatin structure without altering DNA sequence to regulate transcription of these genes. This epigenetic regulation of gene expression plays an important role in the process of tumor invasion, growth and metastasis in malignancies (Pakneshan 2005). Global methylation status of repetitive genomic sequences such as long interspersed nuclear element 1 (LINE-1) and Alu sequences has been examined by comparison of treated with Decitabine cells versus their untreated counterparts. Demethylation occurs in every cell line. This is an indication that the cell lines employed for these experiments are literally affected by demethylating agents.

Accumulating evidence in the literature suggests that kallikrein-related peptidases are epigenetically regulated and that their expression is modified by specific hyper- or hypomethylation of their gene promoters. Sidiropoulos et al. noted that upregulation of (mRNA)*KLK10* levels, which was accompanied by an increase in secreted KLK10 protein concentration, was observed for a subset of breast, ovarian, and prostate tumor cell lines after 5-aza-2'-dC application (demethylating agent). Genomic sequencing of sodium-bisulfite-treated DNA demonstrated that CpG sites within the KLK10 gene exon 3 were highly methylated. Hypermethylation of exon 3 CpG regions was also detected in primary ovarian cancers. KLK6 was identified based on its transient upregulation in a primary breast tumor and its subsequent silencing in a metastatic tumor from the same patient. KLK6 can be reactivated in non-expressing breast cancer cells by treatment with 5-aza-2'-deoxycytidine (5-aza-dC), a compound causing DNA demethylation and its inactivation is associated with hypermethylation of specific CpG dinucleotides located in the KLK6 proximal promoter and overexpression with complete demethylation (Pampalakis 2006; Pampalakis and Sotiropoulou 2006; Pampalakis 2009).

Aim of this project was the characterization of epigenetic transcription control of KLK7 and subsequently other members of the KLK genomic loci. Although, *KLK7* gene locus contains a CpG-poor promoter region (Pampalakis 2009), regulation by DNA methylation might also occur (Jones and Baylin 2002). The KLK7 genetic locus has already been characterized (Yousef 2000d). It has been shown, that transcription levels of KLK7 (by means of Q RT-PCR

measurement) are associated with course of the disease in breast and ovarian cancer, whereby ovarian cancer high expression levels of KLK7 were associated with a patient outcome. Therefore, determination of KLK7 transcription and specific DNA methylation levels in clinical samples (fresh frozen tissue, FFPE material, blood) may be valuable clinically relevant cancer biomarkers. For this, seven different cell lines [breast: MCF-7, MDA MB 435 (*wild type*, RSV, KLK7), ovarian: OVMZ-6 *wild type*, OVCAR-3), keratinocytes (HaCaT)] were selected to study the expression of KLKs under different conditions of treatment. The demethylating agent Decitabine (5-aza-dC) was applied in the cell lines and our purpose was to investigate the change of the methylation status on DNA level, as well as expression changes in RNA and protein level.

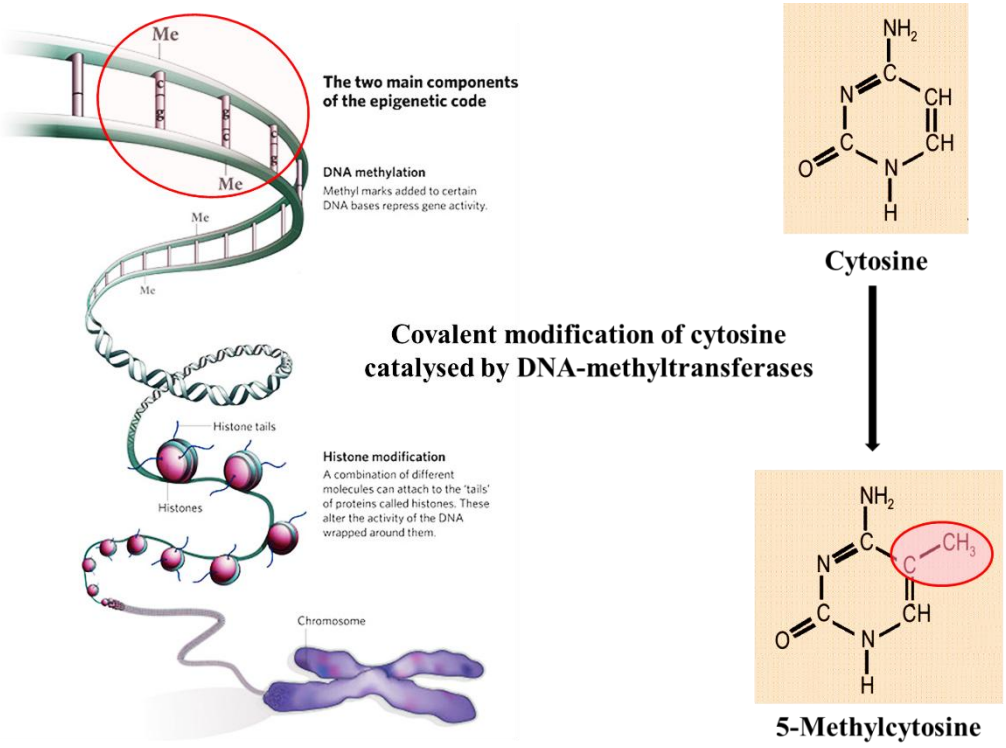


**Figure 65:** Covalent modification of cytosine as catalyzed by DNA-methyltransferases

KLK7 loci are present in cells under examination (HaCaT, MCF-7, OVMZ-6 WT, OVCAR-3), as three different PCR systems specific for KLK7 and neighboring genes (*KLK6*, *KLK8*) confirmed the presence of these genes in the cell lines. The findings exclude the possibility that the gene loci are not present in the cellular genome due to gene deletion. Added to this, established ELISA assays for kallikrein-related peptidases in the comparison of demethylated

cell lines versus the untreated ones demonstrated a relatively low KLK4 and KLK6 expression, while KLK5 and KLK7are measured at higher scales. In our experiments, KLK4 displayed very low levels, mostly deriving from the cytosolic extracts and untreated cells seemed to produce more protein than their demethylated counterparts. According to Pampalakis et al., in MDA-MB-231 breast cancer cell line, 5-aza-dC reactivated the expression of KLK6 and KLK4, while in ovarian cancer cell lines ES-2 and HTB-161, KLK4 was downregulated, a phenomenon which implies that specific epigenetic mechanisms underlie the regulation of KLK4 in breast compared to ovarian cancer (Pampalakis 2006). KLK6 expression, significantly higher than KLK4, is pronounced only in HaCaT and MCF-7, and follows a pattern where cytosolic extracts display higher levels than supernatants and demethylated cells produce more KLK6 than the untreated ones. KLK5 expression is clearly pronounced in very high levels in HaCaT with demethylated cells showing lower expression than their untreated counterparts. This is in contrast with Pampalakis et al., where KLK5 remained unaffected in MDA-MB-231 and it was downregulated in the ovarian cancer cell line ToV-21G. Finally, KLK7 is highly expressed in the transfected MDA-MB-435 pRC RSV/KLK7 cell line, a fact definetely anticipated, mostly secreted in the conditioned medium and less located in the cytosolic extracts. Moreover, methylation or demethylation does not seem to affect any expression, since no big difference among differentially treated cells is apparent.

To diminish any questions about inter-cycle variation, cells were also compared at cycle level. In other words, the expression levels of each kallikrein-related peptidase in the same aliquot. KLK5 dominated in the HaCaT, KLK7 in the overexpressing cell line, KLK6 demonstrated some expression in HaCaT and MCF-7, and KLK4 was very low or absent anywhere assessed. KLK7 does not seem to be influenced by the demethylating agent Decitabine, whereas KLK5 and KLK6 seem to be somehow affected by the treatment. KLK5 levels are too low to extrapolate any conclusion.

If we focus on KLK7, clearly there is some sort of change in the expression in the transition from methylation to demethylation. Most cell lines demonstrate low KLK7 levels, so it is unclear whether changes are significant. In the MDA-MB-435 pRc RSV/KLK7, expression is high both in cytosolic extracts and in supernatants and the effect of demethylation significant. It is rather odd that although demethylated cells display lower KLK7 protein levels in the supernatant fraction, the Triton-X-100 fraction shows the opposite: demethylated cells have

higher expression. This phenomenon may be an effect of diminished protein export. Added to this, the MDA-MB-435 pRc RSV/KLK7 are a transfected cell line with an artificial promoter, other than the original KLK7 promoter. This phenomenon implies that the demethylating agent affects the overall cell methylation status, maybe of a region that regulates KLK7 expression. It is though, unsafe to conclude on KLK7 regulation by methylation based on the presented results.

Finally, in immunocytochemical evaluation of clotted cells, differences in levels were obvious, especially in cell lines with higher KLK7 expression. Treated (demethylated) cell lines demonstrated significant overexpression of KLK7 over their untreated counterparts, for at least two cell types: the MDA-MB-435 pRc RSV/KLK7 and the corresponding wild type. As far as the wild type is concerned, promoter region of KLK7 might be affected by Decitabine treatment and this could lead to an overexpression of the protein. On the other side, the overexpressing cell line, since it contains a high copy expression construct of KLK7 with an artificial promoter, might affect not in its native genome, but in its plasmid construct. Plasmid sequences can influence their expression activity in transfected cells since they are object of methylation due to a kind of host defense against virus (Bryans 1992; Kass 1993). For all other cell lines, low expression in general overlaps differences and no clear conclusions can be made.

Following the same methodology as in (Holzscheiter 2006), a quantitative realtime PCR set-up was established to detect both full-length (mRNA)*KLK7* and the short splice variant. We evaluated the performance of the QPCR assay by assessing *KLK7* expression in treated and untreated cell lines. The result reveals higher expression for the demethylated overexpressors and the HaCaT cell line over their untreated counterparts at the mRNA level. This result partly agrees with the ICC evaluation, where the overexpressing cell line clearly showed higher expression levels for the demethylated cells. Elements connected with the KLK7 expression might be responsible for the increase despite the lack of a native promoter. Decitabine may influence expression status of other genes, e.g. involved in protein trafficking or protein degradation.

HaCaT acquired a small difference, sign that Decitabine changes cellular expression programme. For the rest of the cell lines, levels of expression were insignificant.

In most cases, it is still unclear whether KLK7 is affected by the Decitabine treatment. The absence of a clear-cut conclusion on the effect of methylation status on the KLK7 protein expression implies that KLK7 is either not regulated by methylation, at least not directly, or there is another kind of influence by 5-aza-dC application. For example, it could be that upregulation is either a downstream effect of 5-aza-dC, probably through the activation of a specific transcriptional activator, or that specific non-CpG island cytosines are involved in the regulation of transcription (Pampalakis 2006). Decitabine may influence many other proteins involved in KLK maturation. The difference in supernatant to cytoplasmic ratio indicates a participation of trafficking and /or degradation. It seems that MDA-MB-435 overexpressors are somehow influenced by the Decitabine treatment. Elements connected with the KLK7 expression might be responsible for the increase. There is still the native promoter in the cell lines, which may also be influenced epigenetically by the transfection of a high copy plasmid. Therefore, there can be still an effect on this native promoter as well as on the plasmid promoter. There are studies that speculate other mechanisms to co-operate in KLK regulation: from the production of multiple splice variants till the use of alternative promoters, as previously reported for KLK6 (Christophi 2004; Pampalakis 2004) and KLK11 (Nakamura 2001).

### 6.3.2 uPA/PAI-1

Urokinase type plasminogen activator (uPA), plus its inhibitor PAI-1, are associated with invasive and metastatic potential of malignancies. Added to this, novel serine proteases potentially playing a physiological role in these processes, such as KLK7, might be implicated in interactions with uPA. DNA methylation might be the regulatory mechanism of the uPA/PAI-1 system expression. It is already known in the literature, that demethylating drugs, such as Decitabine (Christman 2002), affect the expression of uPA in breast cancer cell lines by altering the methylation status of CpG island (Xing and Rabbani 1996; Rabbani and Xing 1998; Xing and Rabbani 1999; Guo 2002). Employing an established commercial uPA/PAI-1 methylation system (Hs_PLAU_1_SG QuantiTect Primer Assay (200), #QT00013426, Qiagen, Hilden, Germany), we set several tumor cell lines under investigation, including KLK7 overexpressing cells to check whether there is any correlation between uPA and KLK7 expression.

uPA displays expression differences due to methylation in four different cell lines, as it is assessed by methylation specific quantitative realtime PCR (Q-MS-PCR): in the MDA-MB-435 triad methylation decreases for the treated *wild type* and the treated overexpressing cell line, whereas it increases for the treated vector control, similarly to KLK7. On the other hand, MCF-7 treatment seems to increase the methylation. This finding is in contrast with Guo et al., where the combination of increased DNA methyltransferase activity with reduced demethylase activity contributed to the methylation and silencing of uPA expression in MCF-7 cells (Guo 2002).

Estimation of total methylation content of Alu elements is useful for evaluation of the global genomic methylation status and level of homologous and non-homologous chromatin recombination in gene-rich regions. Global methylation status of repetitive genomic sequences such as long interspersed nuclear element 1 (LINE-1) and Alu sequences has been examined by comparison of treated with Decitabine cells versus their untreated counterparts. Demethylation occurs in every tested cell line. This is an indication that the cell lines employed for these experiments are literally affected by demethylating agents.

Antigen levels (ELISA) for the same cell lines reveal higher expression of uPA for HaCaT, OV-MZ-6 and OVCAR-3 with significant change in expression after treatment only for OV-MZ-6 *wild type*, where hypomethylation causes decrease. uPA expression in HaCaT is confirmed by other studies (Krebs 1999). Obviously, cells affected at the gene level, do not produce much of uPA protein or many intermediate regulatory steps suppress any changes.

It makes sense at this point to go back and investigate whether untreated cell lines produce results that correlate to each other. In other words, if hypothetically there was no treatment, what would be the methylation status and what would be the levels of protein expression? Therefore, in a correlation study, where the two individual assessments, TaqMan Q-MS-PCR and ELISA are included, we obtain meaningful results. HaCaT, OV-MZ-6 and OVCAR-3 demonstrate the highest uPA protein levels, while at the same time their methylation status is lowest. Despite their hypomethylation, they seem to be affected by 5-aza-dC treatment so that uPA protein levels decrease. For the other cell lines, methylation seems to be high in their untreated portion causing silencing of the gene. Demethylation, however, diminishes further RNA expression in the MDA-MB-435 wild type and the overexpressing KLK7, while it causes

the adverse effect on the vector type. What we learn from these findings is that at least for the untreated portion high protein levels go along with low methylation status and vice versa.

As far as PAI-1 is concerned, the MDA-MB-435 displays exactly the same results as for the uPA, whereas there is an adverse effect for the MCF-7: this time hypomethylation goes along with treatment. We measured methylation levels, which should decline with Decitabine treatment (any DNMT-inhibitor) associated with an increase in mRNA expression levels and maybe protein levels. This finding is in similar to results of Gao *et al.*, where the methylation frequency was inversely correlated with PAI-1 mRNA level within its 20-fold range in MCF-7 and treatment with 5-aza-2'-dC led up to circa a 40-fold increase in the PAI-1 mRNA level (Gao 2005). At protein level, only MCF-7 and OVCAR-3 displayed significant levels of expression, with MCF-7 higher PAI-1 expression in demethylated populations.

Going back to the untreated population, it becomes clear that only OVCAR-3 and MCF-7 display high protein levels with either low or high methylation status, respectively. Of course, we would always await a rise of protein levels with decreased methylation levels, since methylation inhibits transcription and therefore probably in some way translation. Protein levels that normally decrease after treatment for OVCAR-3, they surprisingly rise in case of MCF-7, possibly due to an adverse effect. The rest of the cell lines displayed higher levels of methylated mRNA expression, but low protein expression.

Summarizing our findings, for uPA hypermethylation causes expression downregulation in HaCaT, MCF-7 and OVMZ-6, whereas demethylation causes expression upregulation in MDA-MB-435 wild type and overexpressing KLK7. Hypermethylation goes along with low expression for OVCAR-3. For PAI-1, hypermethylation goes along with high expression for HaCaT and MDA/RSV. demethylation causes expression upregulation for MCF-7 and MDA-MB/KLK7. hypermethylation causes expression downregulation in OVCAR-3, whereas hypomethylation goes along with low expression in MDA-MB-435 wild type.

### 6.3.3 BRCA1

Among the major breast cancer-relevant DNA repair genes, breast cancer susceptibility gene *BRCA1* is supposed to play a prominent role in the evolution and biology of at least a proportion of TNBCs. This has been previously demonstrated by the shared molecular profiles

between sporadic TNBCs and BRCA1-related breast cancer (Turner 2004). Moreover, the *BRCA1* status might be an excellent molecular marker predicting sensitivity to novel therapeutic agents which specifically target cancers deficient in DNA-double-strand-break repair such as PARP inhibitors (Anders 2010). Our aim was therefore to study the *BRCA1* status in a cohort of unselected patients with primary TNBC. Since knowledge about somatic *BRCA1* aberrations in this subtype was scarce, we were particularly interested in the contribution of epigenetic changes or intragenic rearrangements to the subset with an altered *BRCA1* status. In this study, we have identified a subpopulation of approximately two thirds of tumors with prominent promoter methylation.

While mutational inactivation of *BRCA1* contributes to a relatively small proportion of TNBCs, we observed a higher incidence of epigenetic alterations within *BRCA1*. Coincidently, two reports published very recently, suggested that CpG island hypermethylation of *BRCA1* might be predominantly associated with the TNBC subtype of the breast cancer disease (Singh 2010; Stefansson 2011). By using the novel HRM technology for investigating the extent of DNA methylation in the tumor samples, we found evidence for detectable methylation events in 41 of 171 TNBCs. The amount of methylation was confirmed by cloning and bisulfite sequencing of the respective DNA fragments and revealed good concordance of the method. Since most of the recurrences (7 of 8 events) observed with methylated tumors occurred below a degree of 25 % CpG island methylation, we set the cut-off value of a positive methylation status to $\geq$ 25 %.

The fact that 77 % of the tumors with *BRCA1* alterations also possessed large rearrangements affecting one allele of the *BRCA1* gene may reflect the classical two-hit hypothesis of tumorigenesis according to Knudson (Knudson 1971). Indeed, the majority of the methylated or mutated tumors indicated more complex, biallelic *BRCA1* aberrations which might be a prerequisite for the observed effects on patient outcome. Coincidence of *BRCA1* methylation and LOH had been previously reported in sporadic breast cancer (Wei 2005; Rhiem 2010).

Several studies investigated the effect of chemotherapy in TNBC and have described this subtype as a particularly chemosensitive entity (Carey 2007; Liedtke 2008). Moreover, we could reproduce the effect of a positive *BRCA1* methylation status on longer time to progression in a TNBC subpopulation which had been specifically selected for only anthracycline and /or cyclophosphamide-containing therapy. However, it cannot be excluded

yet that *BRCA1*-deficient cancers may be associated with better prognosis independent of chemotherapy due to an intrinsic property of the tumor itself.

In conclusion, our study strongly suggests that profound alterations in the *BRCA1* gene compatible with a somatic BRCA1 dysfunction are restricted to a subpopulation of TNBC. This subset of patients had favourable prognosis at standard anthracycline/cyclophosphamide-containing therapy and should further benefit from agents inducing DNA double-strand-breaks or from PARP inhibitors. Knowledge of the somatic BRCA1 status in patients with TNBC should therefore have implication for therapy decision. A challenge remains the treatment of chemoresistent and non-BRCA1-like TNBCs warranting the development of new therapeutic drugs.

# 7. Conclusions and outlook

Whilst there is broad consent that the cancer biomarkers uPA and PAI-1 are of clinical value in predicting the course of the disease and response to cancer therapy in breast cancer patients and other types of cancer (Schmitt 2010), information about the clinical utility of members of the family of kallikrein-related peptidases (KLK) is scarce and often not validated in a multicenter fashion. Most of the assays performed to assess expression of KLKs were performed by assessing mRNA expression or protein expression determined by ELISA, the same is true for uPA and PAI-1. Occasionally, immunohistochemical staining was undertaken, but often with in-house antibodies, with minimal information about the immunogen used or target and epitope specificity, respectively (Borgono 2004; Schmitt 2008). So far, these biomarkers have not been assessed thoroughly by immunohistochemistry in a multicenter fashion, a task mandatory before clinical use for prognosis or therapy response prediction.

Second to that, digitization of immunohistochemical staining has now reached a high technical standard, and elaborate software packages are in place to automatically analyze topical distribution and expression level of these biomarkers in archived, fixed tumor tissue specimens, even retrospectively. By such an approach, absence/low expression of other cancer biomarkers can be assessed as well and related to cancer subgroups at different stage of the disease. Immunohistochemistry offers also the possibility of combining with other histological detection methods. Examples for this are the novel two-dimensional mass spectrometry technology (MALDI-IMS) (Walch 2008), the proximity ligand assay allowing to pinpoint nearest neighborship of KLKs or uPA with inhibitors, acceptors, or receptor proteins (Aubele 2007), and the single-molecule detection of mRNA or DNA methylation in tumor tissue sections (Masand 2011).

Regarding heterogeneity of tumor tissue samples, larger numbers of well-defined tumor tissue specimens with sufficient follow-up should be available for testing to avoid any bias when conducting high-level statistical analyses. Needless to say that complete information about surgical procedures, radiotherapy, systemic (neo)adjuvant therapy, of the cancer patients and storage and fixation of the tissue samples has to be available as well.

uPA and KLKs may serve as targets for systemic therapy of cancer patients too, and such drugs have been developed and are in clinical testing (Felber 2006; Schmitt 2010). Nevertheless,

before testing, one should know about topical distribution of for instance KLKs or uPA in tumor tissues and that in normal healthy tissues to avoid severe, adverse side effects of the therapeutic drugs by targeting the proteases in both the tumor cells and the normal cells.

Epigenetic testing of the DNA-methylation status of CpG-islands within the promotor regions of cancer biomarker genes has emerged recently as an attractive approach to predict the course of the cancer disease or response to cancer drugs (Duffy 2009). Different than mRNA or protein, DNA is very stable and in general not modified by surgery or standard cancer drugs. High-quality DNA for methylation assays can be extracted from fresh, frozen or fixed tissues, and the methylation status defined for healthy tissues and tumor tissues. Drugs are available now for reversing the DNA-methylation status in patients, to either allow up- or downregulation of genes and thus modulation of protein expression.

In conclusion, standard-operating procedures have been provided, described in this thesis, to allow staining and quantitative assessment of staining intensity of tumor tissue samples, for both, KLKs and uPA/PAI-1. Comparison of immunohistochemical staining data with ELISA data, mRNA expression data, and DNA-methylation status is now possible. Screening the scientific literature, we have to admit that such correlations are missing for the KLKs and uPA/PAI-1, but not only for these cancer biomarkers. Such correlations are also missing for other cancer biomarkers and the clinical impact defined by multivariate analyses, also by integrating the KLKs/uPA/PAI-1 in the statistical analyses as well.

# 8. Summary

The present approach to systemic treatment of cancer is often referred to as "trial and error" or "one size fits all"; but this practice is inefficient and frequently results in inappropriate therapy and treatment-related toxicity. Conversely, personalized cancer treatment has the potential to increase efficacy and decrease toxicity. However, to achieve personalized treatment for cancer, we need meaningful biomarkers (signatures) for characterization of cancer subgroups, determining prognosis, predicting response to therapy, and predicting severe toxicity related to treatment.

Breast cancer is by far the most common form of cancer among women; ovarian cancer, on the other hand, is the most fatal gynecological cancer disease. Previous histological, immunohistochemical, mRNA expression, and genomic analyses have indicated that these cancer diseases are heterogeneous in nature, varying in morphology, biology, behavior, and response to therapy. Consequently, novel prognostic/predictive biomarkers / signatures indicating the course of these diseases and/or response to therapy are very much needed to help systemic treatment move from the current trial-and-error approach to more personalized cancer care. Therefore, principal objectives of the thesis were to explore at the gene and protein level the potential of novel cancer biomarkers, e.g. certain kallikrein-related peptidases (KLKs) and other coexpressing factors, in tumor tissues of patients afflicted with advanced ovarian or primary breast cancer.

For this, the thesis was divided into three different work packages, namely 1) Production, testing, and set-up of standard operating procedures for immunohistochemical localization and quantification of KLK-proteases and the protease uPA (urokinase) and its inhibitor PAI-1. 2) Validation of the clinical relevance of KLK7 protein expression to predict outcome in advanced ovarian cancer patients. 3) Exploration of the DNA-methylation status of KLKs, uPA/PAI-1 and the caretaker gene BRCA1.

In subproject 1 different antibodies to KLK3-15 were produced or selected from the literature or commercial vendors to be tested on a large number of different normal and diseased tissues fixed by different means. Standard operating procedures (SOP) for reliably working antibodies to a wide range of KLKs, especially KLK4,5,6,7, were established in parallel with SOPs for

tumor-associated uPA and PAI-1, to be applied to automatic staining instruments. Images were digitized and automated image analyses set-up for quantitative assessment of protein expression levels of these cancer biomarkers.

Subproject 2 centers on the clinical value of selected KLK7 in advanced ovarian cancer FIGO stage III/IV. Important result of this investigation is that KLK7 protein expression quantified by immunohistochemical staining is not a marker to predict the course of this disease. In opposition, determination of KLK7 in tumor tissue extracts by ELISA is of clinical value to predict the course of the disease. This result reflects findings obtained for uPA and PAI-1 since for these cancer biomarkers quantitation of protein expression by ELISA is recommended as well; similar to KLK7, immunohistochemistry is not a practicable option to evaluate their clinical relevance.

Subproject 3 addresses the question of epigenetic modification of KLKs, uPA/PAI-1, and the important tumor suppressor gene BRCA1. Preliminary study of tumor cell lines treated with demethylating agents revealed expression modifications as quantified by means of MS-PCR, ELISA and immunocytochemistry. Additionally, the investigation of BRCA1 gene alterations in the triple negative breast cancer (TNBC) patient subgroup revealed a CpG hypermethylation. Interestingly, these had favourable prognosis at standard chemotherapy.

# 9. Acknowledgements

I would like to express my deep gratitude to:

My doctoral father, Prof. Dr. Dr. h. c. Horst Kessler, who allowed me to conduct this thesis.

My supervisor, Prof. Dr. rer. nat. Dr. med. habil. Manfred Schmitt, who supported me from the very first moment and set the basis for my scientific career.

Prof. Dr. rer. nat. Viktor Magdolen, for his scientific stimuli in the kallikrein-related peptidase field.

Prof. Dr. rer. nat. Dr. med. habil. Ute Reuning for her continuous scientific advice.

Dr. rer. nat. Rudolf Napieralki for the memorable collaboration and his friendly attitude.

Prof. Dr. med. Markus Kremer of the Institut für Pathologie, Technische Universität München, whose precise evaluations inspired new scientific goals.

Dr. rer. nat. Matthias Kotzsch for his kind assistance in the statistics of my dissertation.

All the people who work in the Clinical Research Unit and assist in the realization of projects, such as Karin Mengele, Daniela Hellmann, Anita Welk, Alex Sturmheit, Elisabeth Schüren, Alex Stöckel, Sandra Baur, Anke Benge and Sabine Creutzburg.

Claudia Beutner, secretary to Prof. Schmitt, for meeting up with my everyday concerns.

Collaborators, such as Dr. Stan Krajewski (Sanford-Burnham Institute, La Jolla, US) and Prof. Eleftherios Diamandis (Mount Sinai Hospital, Toronto, Canada), who hosted me in their labs as guest scientist and constantly responded to my scientific questions.

Professionals that I worked with, such as Catherine Conway and Donal O' Shea, Erk Mennenga-Klopp, Richard Hart, Claudia Olenik and Michael Kramer.

Last but not least, my family and friends, who encouraged me to continue.

The work on clinical relevance of KLK7 in ovarian cancer is a team effort together with the colleagues of the Frauenklinik (TU Muenchen, Prof. Dr. Manfred Schmitt, Prof. Dr. Viktor Magdolen, Prof. Dr. Barbara Schmalfeldt) and with Dr. Matthias Kotzsch (Institut für

Pathologie der TU Dresden). The same applies for the BRCA-1 work on breast cancer, where the evaluation of the clinical relevance of BRCA-1 DNA methylation status is teamwork together with Dr. Eva Gross, Prof. Dr. Alfons Meindl and Prof. Dr. Manfred Schmitt.

## 10. List of own publications


1. Dorn J, Magdolen V, **Gkazepis A**, Gerte T, Harlozinska A, Sedlaczek P, Diamandis EP, Schuster T, Harbeck N, Kiechle M, Schmitt M. Circulating biomarker tissue kallikrein-related peptidase KLK5 impacts ovarian cancer patients' survival. Ann Oncol. 2011 Jan 27. [Epub ahead of print] PubMed PMID: 21273346.

2. Schmitt M, Mengele K, Napieralski R, Magdolen V, Reuning U, **Gkazepis A**, Sweep F, Brünner N, Foekens J, Harbeck N. Clinical utility of level-of-evidence-1 disease forecast cancer biomarkers uPA and its inhibitor PAI-1. Expert Rev Mol Diagn. 2010 Nov;10(8):1051-67. PubMed PMID: 21080821.

3. Mengele K, Napieralski R, Magdolen V, Reuning U, **Gkazepis A**, Sweep F, Brünner N, Foekens J, Harbeck N, Schmitt M. Characteristics of the level-of-evidence-1 disease forecast cancer biomarkers uPA and its inhibitor PAI-1. Expert Rev Mol Diagn. 2010 Oct;10(7):947-62. Review. PubMed PMID: 20964613.

4. Dorn J, Harbeck N, Kates R, **Gkazepis A**, Scorilas A, Soosaipillai A, Diamandis E, Kiechle M, Schmalfeldt B, Schmitt M. Impact of expression differences of kallikrein-related peptidases and of uPA and PAI-1 between primary tumor and omentum metastasis in advanced ovarian cancer. Ann Oncol. 2011 Apr;22(4):877-83. Epub 2010 Oct 5. PubMed PMID: 20924077.

5. Seiz L, Kotzsch M, Grebenchtchikov NI, Geurts-Moespot AJ, Fuessel S, Goettig P, **Gkazepis A**, Wirth MP, Schmitt M, Lossnitzer A, Sweep FC, Magdolen V. Polyclonal antibodies against kallikrein-related peptidase 4 (KLK4): immunohistochemical assessment of KLK4 expression in healthy tissues and prostate cancer. Biol Chem. 2010 Apr;391(4):391-401. PubMed PMID: 20180634.

6. Yfanti C, Mengele K, **Gkazepis A**, Weirich G, Giersig C, Kuo WL, Tang WJ, Rosner M, Schmitt M. Expression of metalloprotease insulin-degrading enzyme insulysin in normal and malignant human tissues. Int J Mol Med. 2008 Oct;22(4):421-31. PubMed PMID: 18813847.

7. Weirich G, Mengele K, Yfanti C, **Gkazepis A**, Hellmann D, Welk A, Giersig C, Kuo WL, Rosner MR, Tang WJ, Schmitt M. Immunohistochemical evidence of ubiquitous distribution of the metalloendoprotease insulin-degrading enzyme (IDE; insulysin) in human non-malignant tissues and tumor cell lines. Biol Chem. 2008 Nov;389(11):1441-5. PubMed PMID: 18783335.

8. Schmitt M, Mengele K, **Gkazepis A**, Napieralski R, Magdolen V, Reuning U, Harbeck N. Assessment of Urokinase-Type Plasminogen Activator and Its Inhibitor PAI-1 in Breast Cancer Tissue: Historical Aspects and Future Prospects. Breast Care (Basel). 2008;3(s2):3-10. Epub 2008 Oct 15. PubMed PMID: 20824007; PubMed Central PMCID: PMC2930995.

# 11. Appendix

## 11.1 Microtiter plate measurements full set-up. Schematic representation of the curves demonstrating epitope antibody-antigen binding.

| R&D AF2624 | | Arexis T + G | |
|---|---|---|---|
| 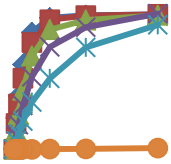 | 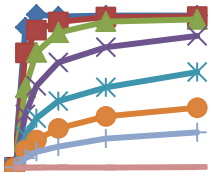 | 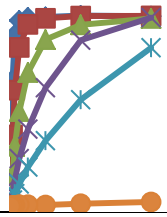 | 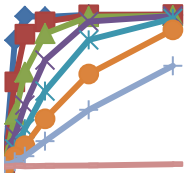 |
| Antibody concentration | Rec protein concentration | Antibody concentration | Rec protein concentration |
| **SC-E16** | | **SC-ABR** | |
| 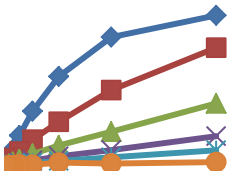 | 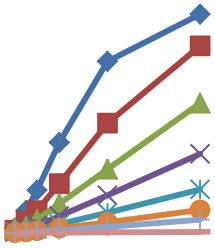 | 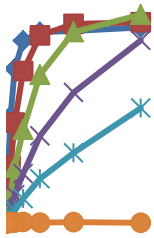 | 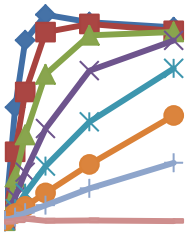 |
| Antibody concentration | Rec protein concentration | Antibody concentration | Rec protein concentration |
| **SC-H50** | | **SC-C15** | |
| 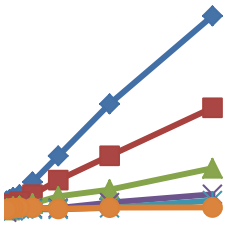 | 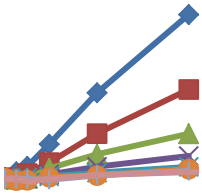 | 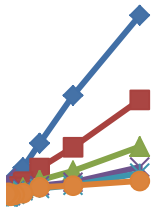 | 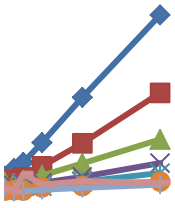 |
| Antibody concentration | Rec protein concentration | Antibody concentration | Rec protein concentration |
| **Diamandis rabbit** | | **Diamandis mouse** | |
| 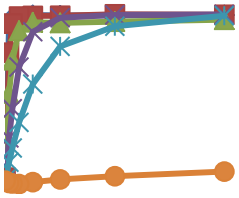 | 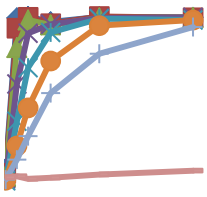 | 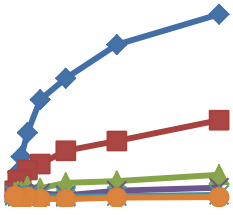 | 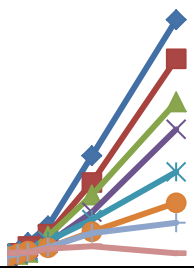 |
| Antibody concentration | Rec protein concentration | Antibody concentration | Rec protein concentration |

## 11.2 CMAs assessed for KLK7 protein expression by use of Arexis Tagena + Domino and R&D AF2624.

| *Cell line* | *Antibody* | |
|---|---|---|
| | *Arexis* | *R&D* |
| **SK-BR-3** | 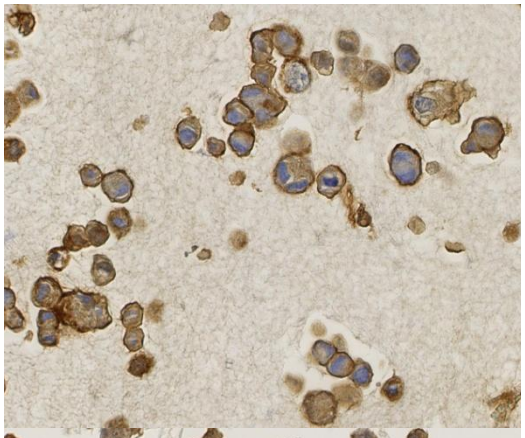 | 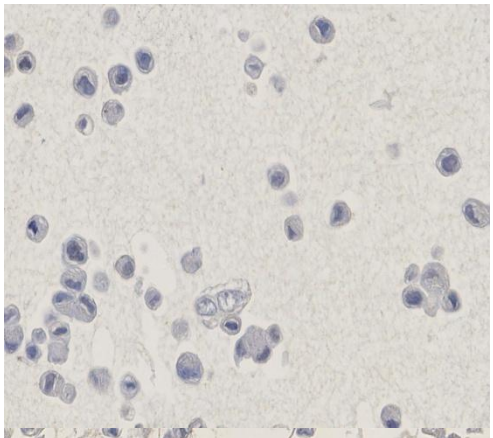 |
| **BT-20** | 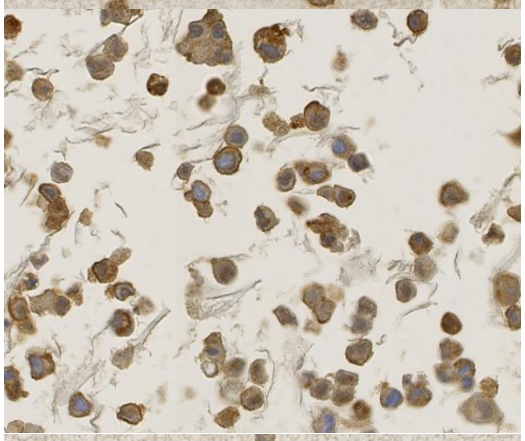 | 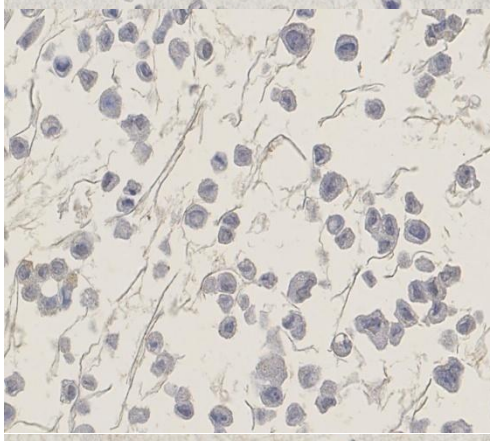 |
| **MCF7** | 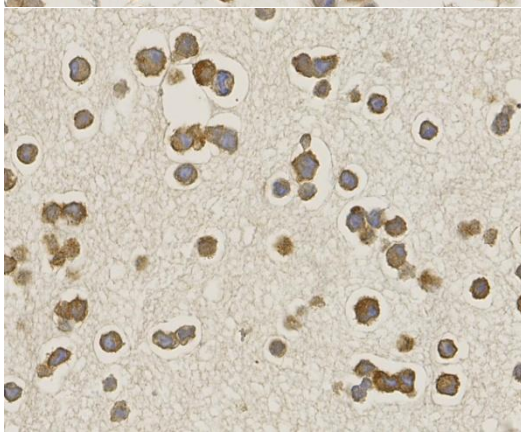 | 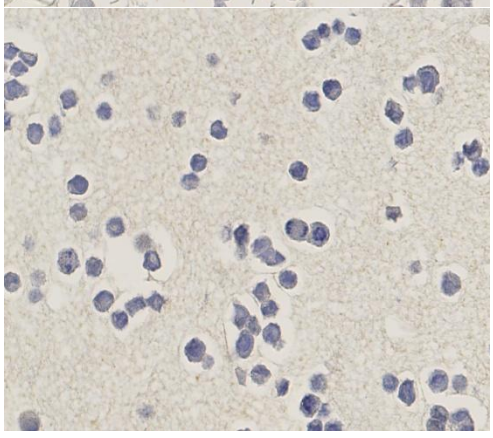 |

**MDA-MB-435**

**ZR-75-1**

**OVCAR-3**

**OVMZ6**

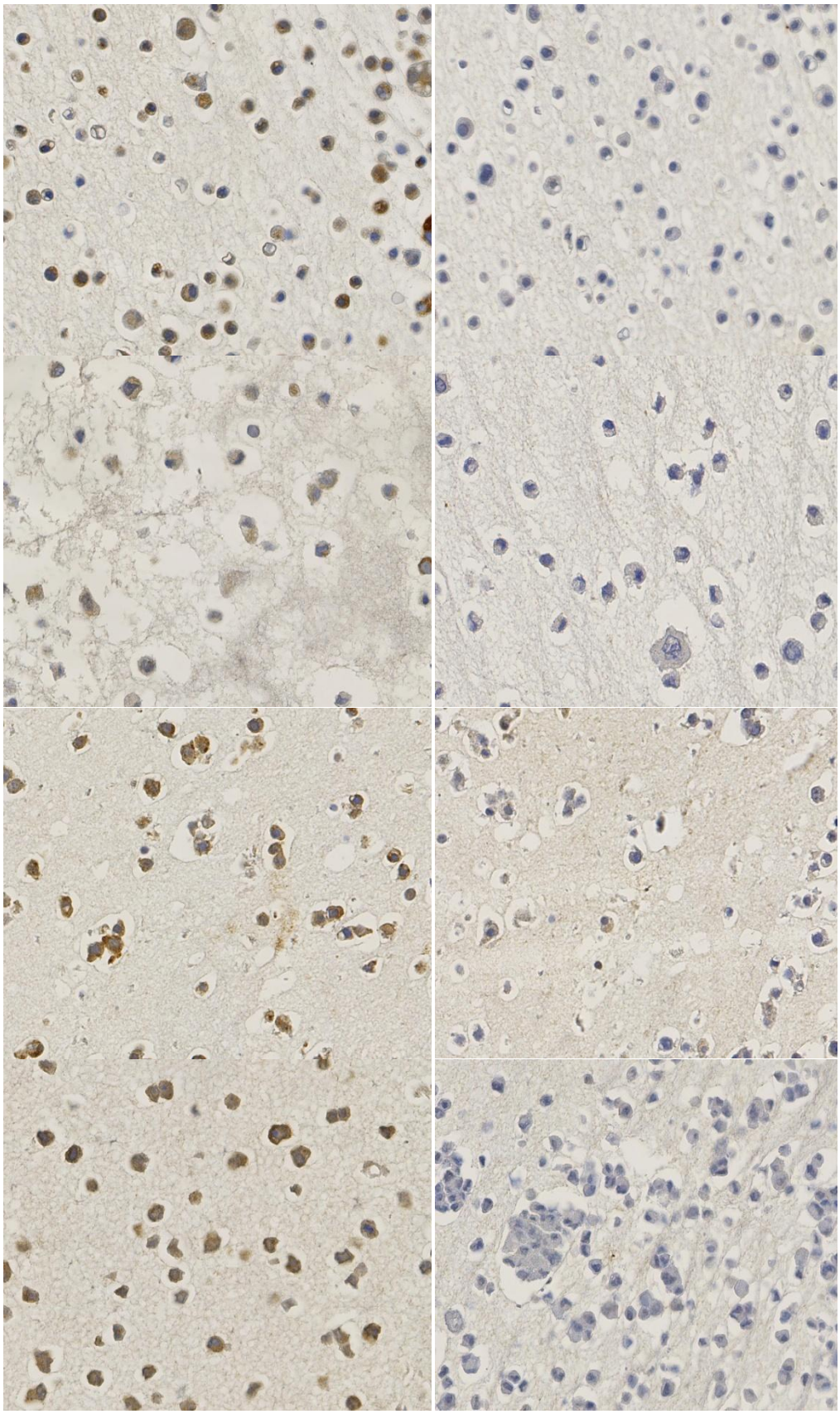

**OVMZ10**

**OVMZ15**

**OVMZ19**

**HeLa**

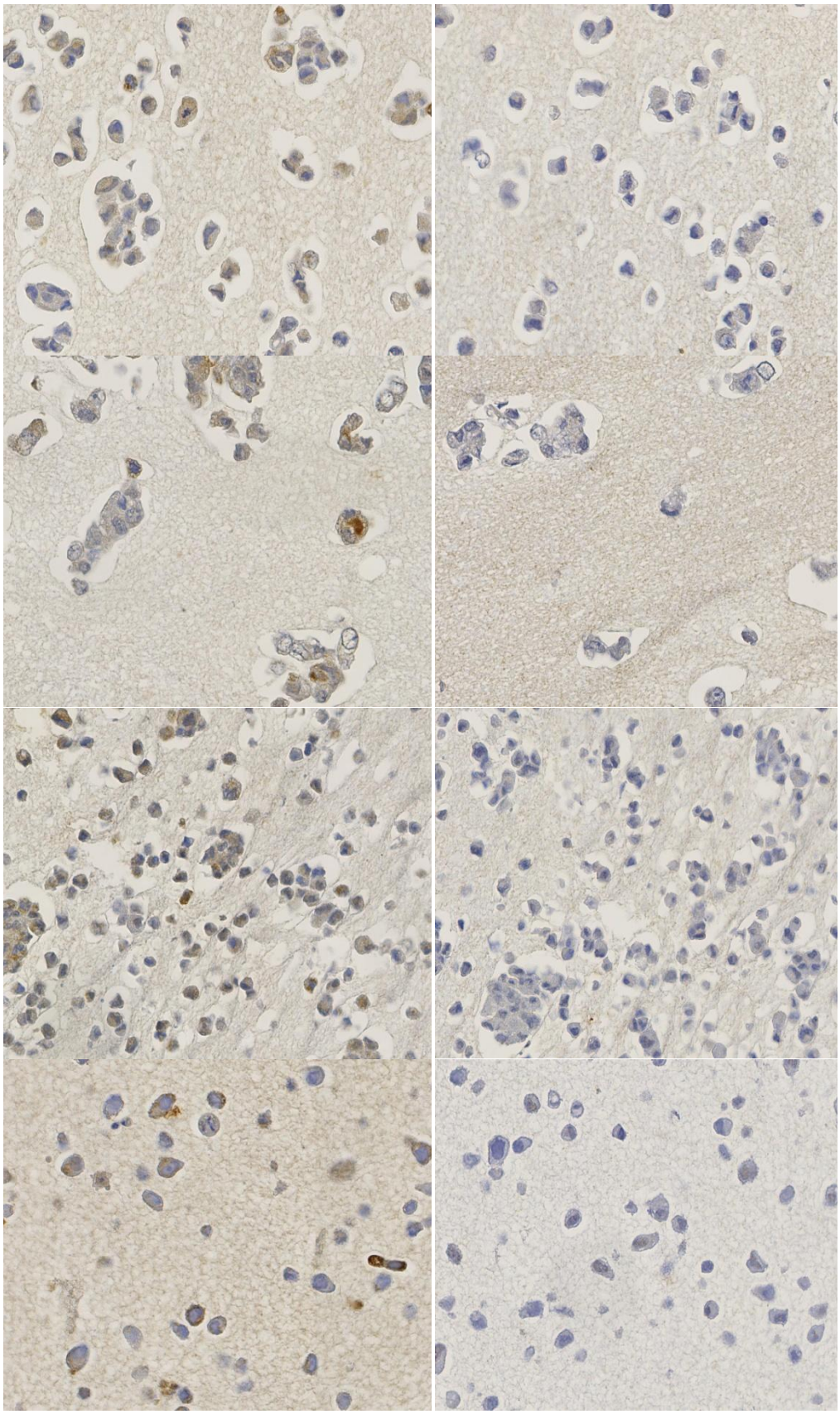

**EJ 28**

**RT-112**

**Caki-1**

**DU 145**

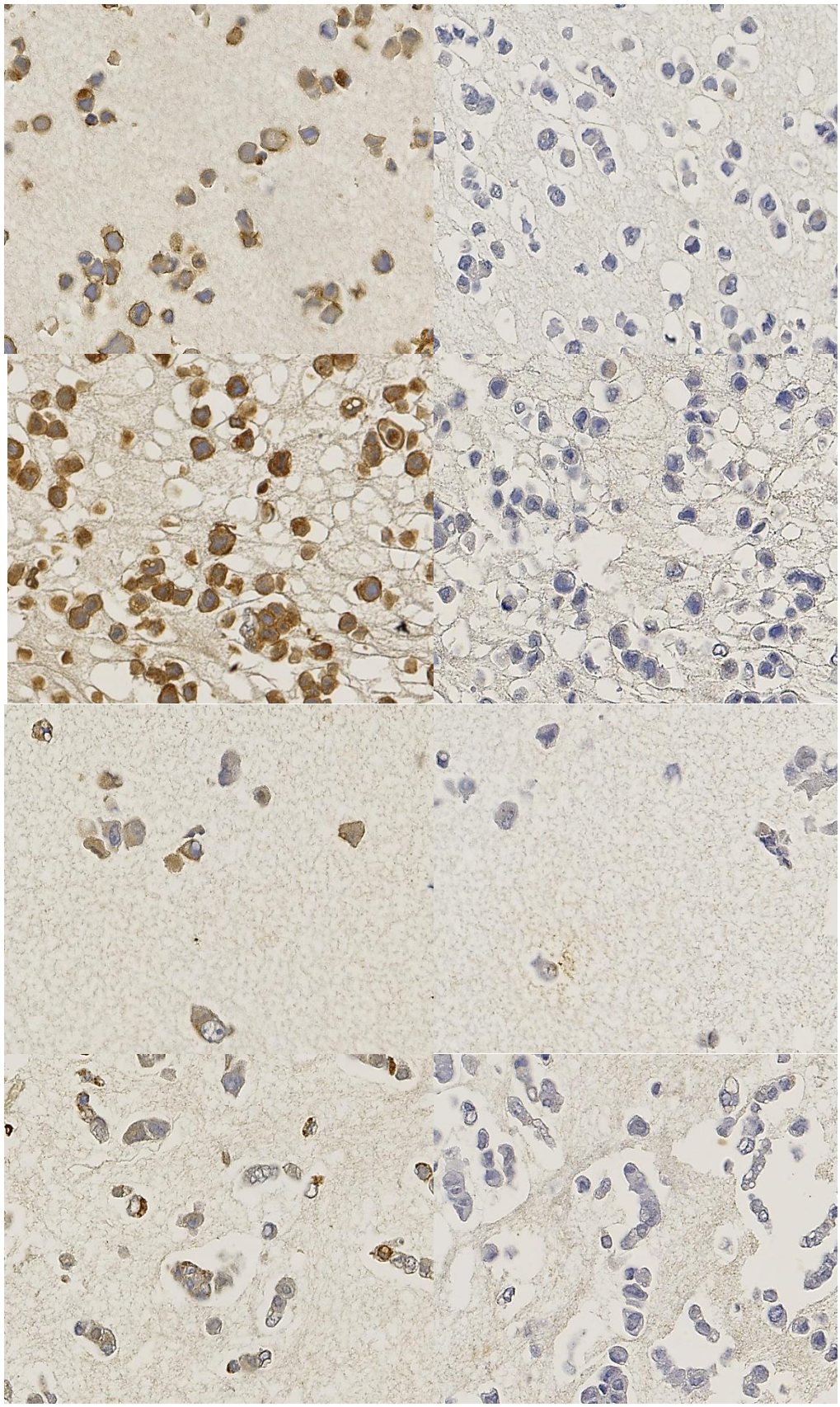

**LNCaP**

**PC-3**

**Caco-2**

**SW480**

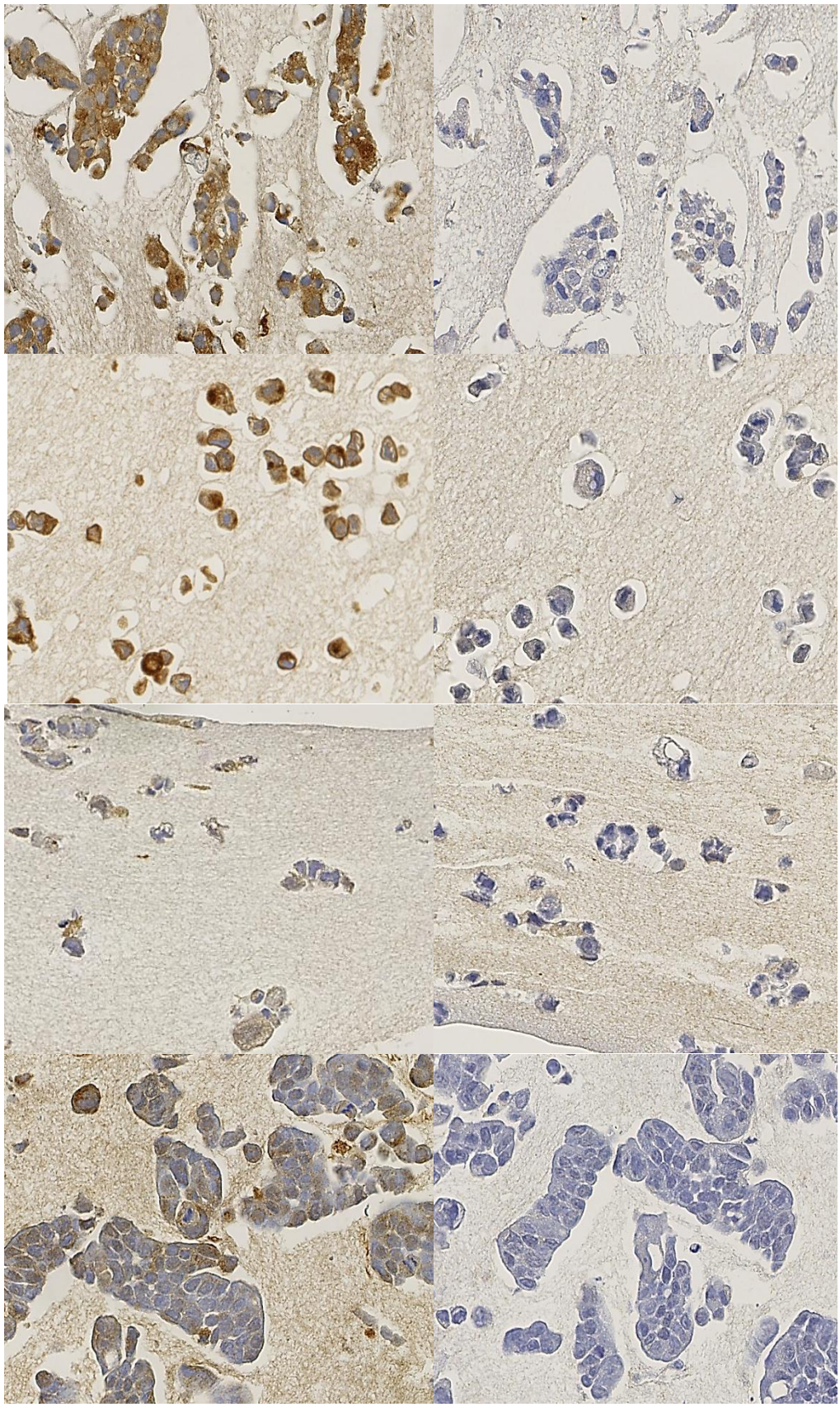

**MIA PaCa-2**

**PaTu-II**

**CAL 27**

**BHY**

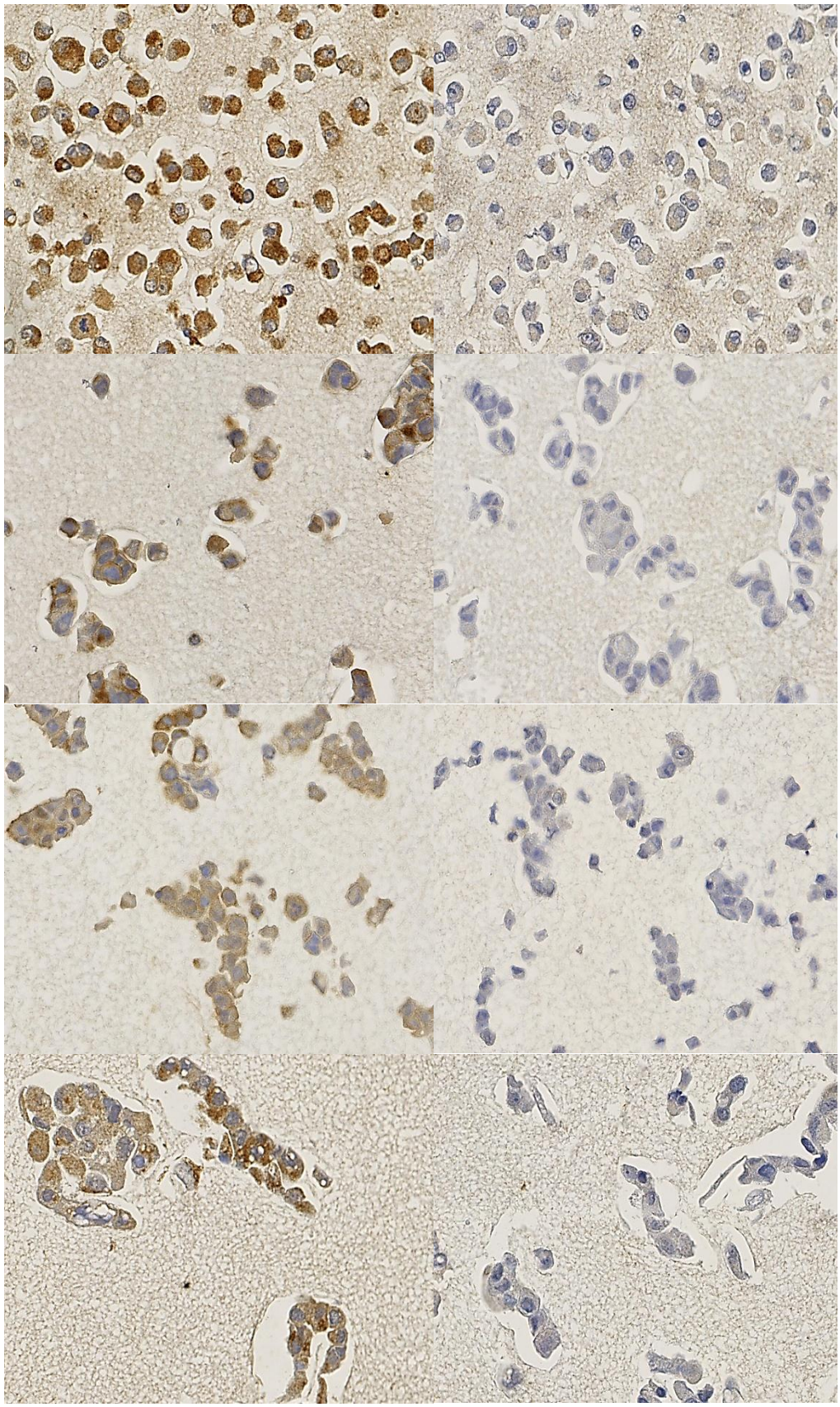

**FaDu**

**U-2 OS**

**Saos-2**

**HT-1080**

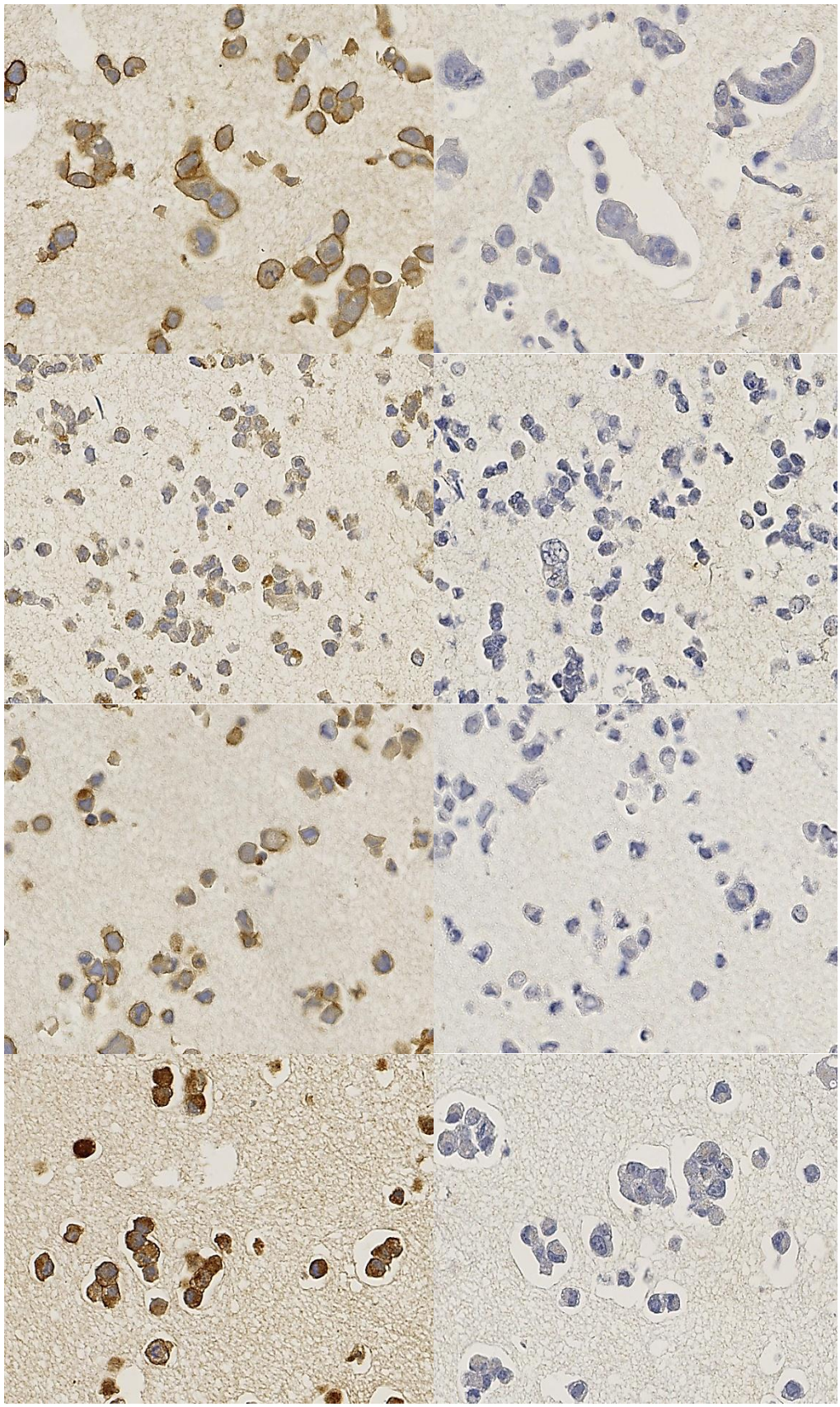

**SNB19**

**Raji**

**U-937**

**HL-60**

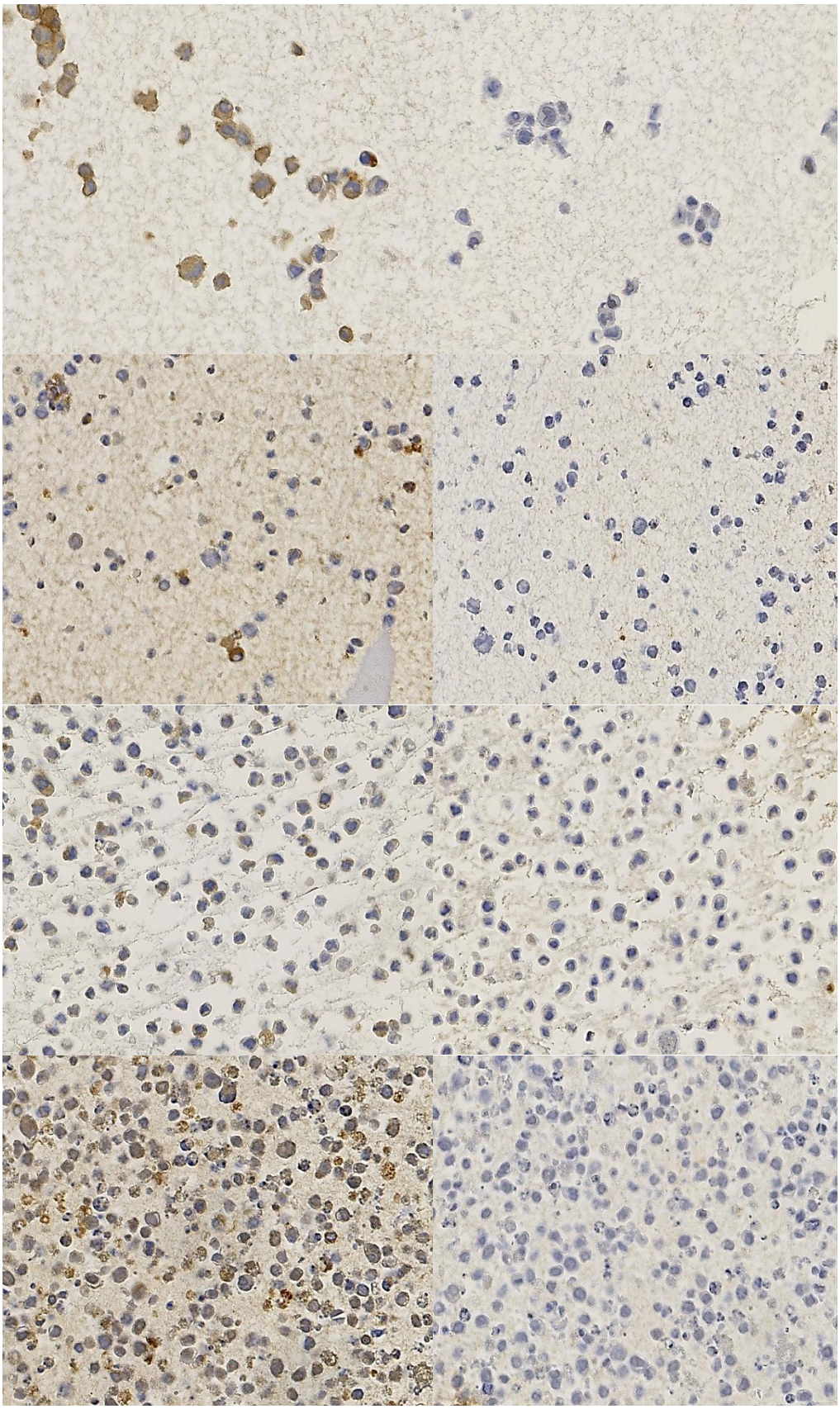

**Granulocytes**

**Lymphocytes**

**Trophoblast cells**

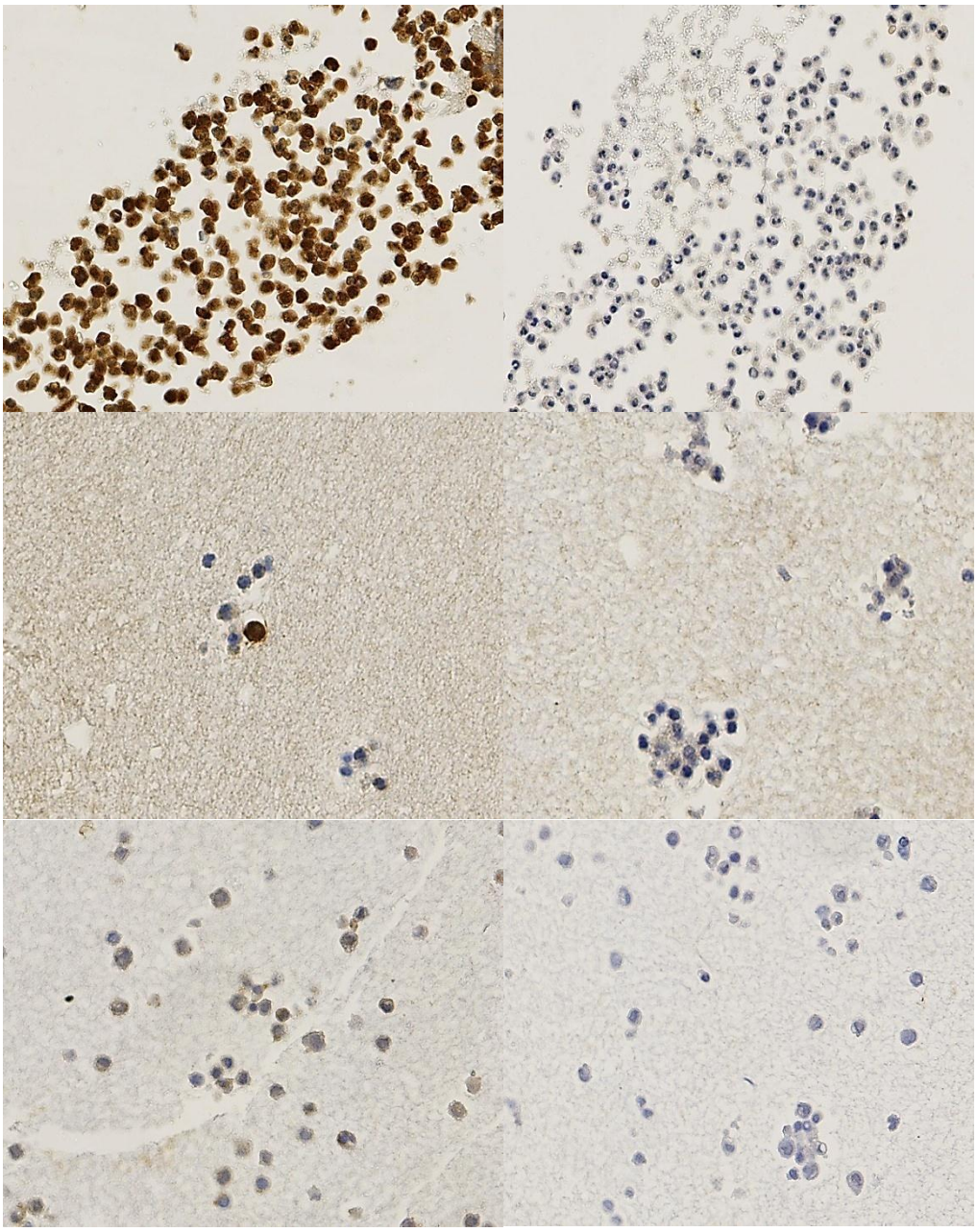

## 11.3 Look-up table for cytofluorometric assays (CLSM)

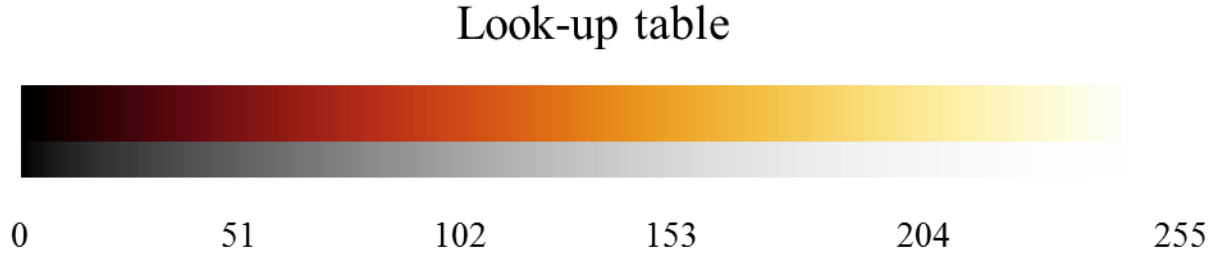

## 11.4 Different fixatives assigned for antibody reactivity testing on tissue specimens.

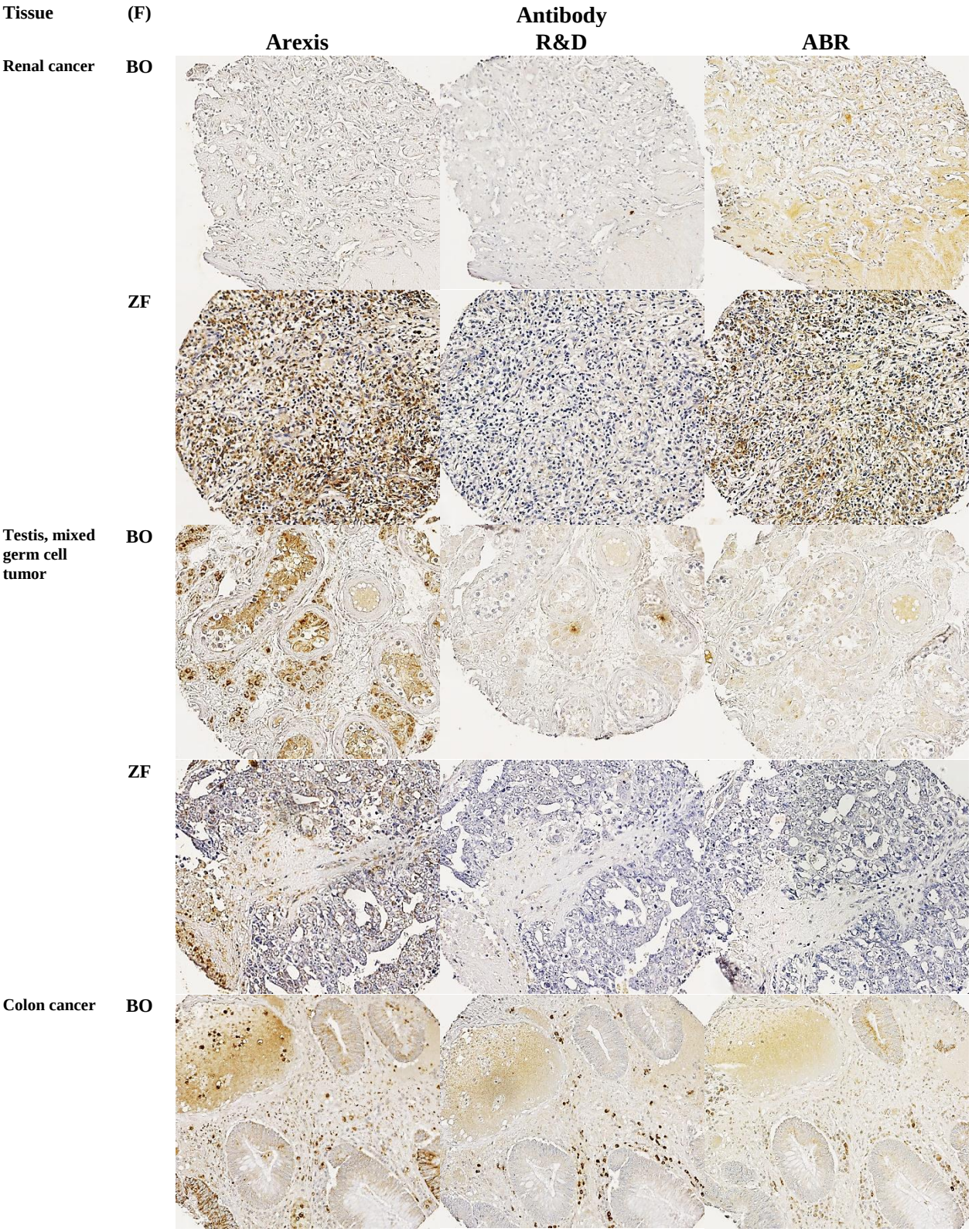

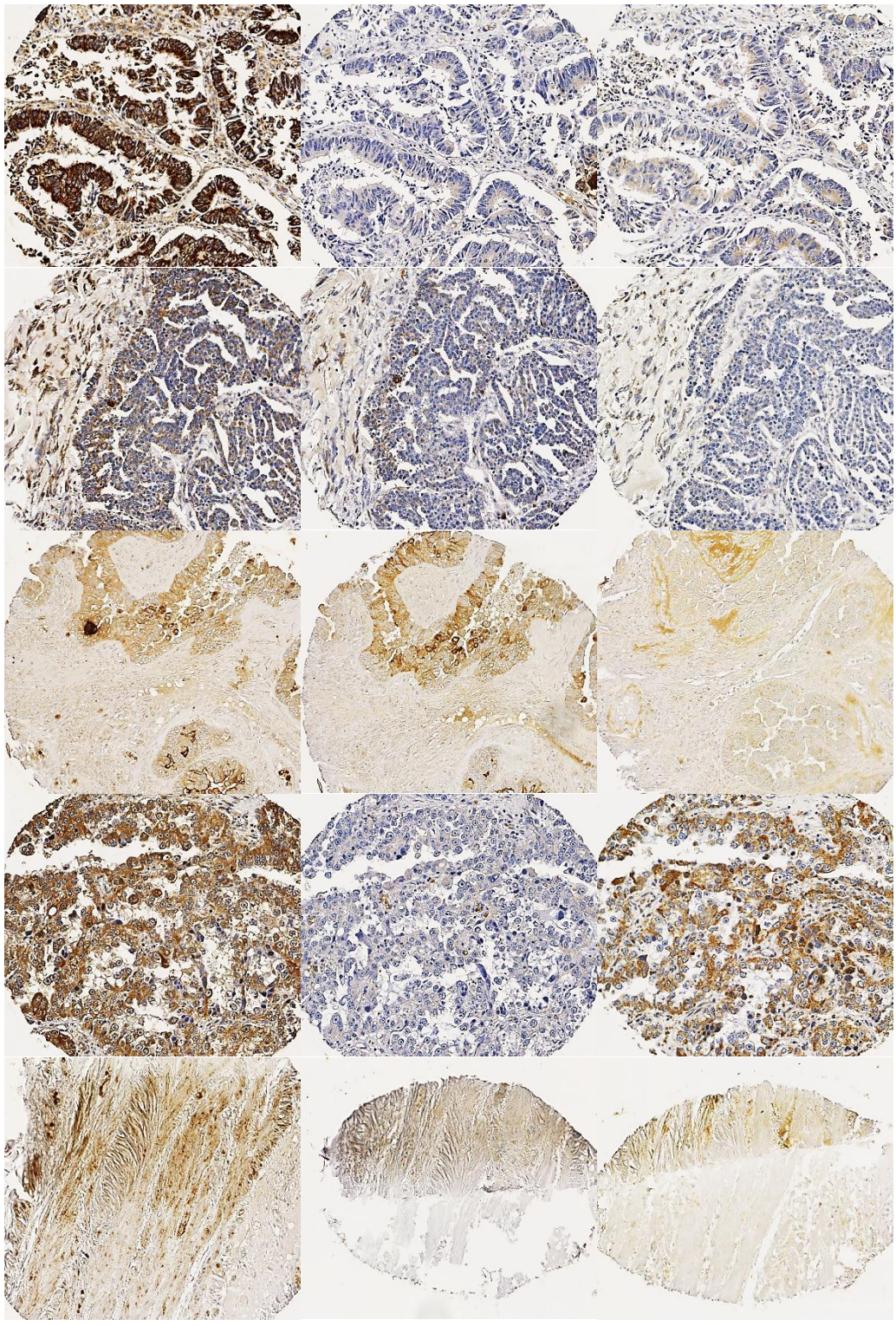
ZF
Ovarian cancer
BF
BO
ZF
Leiomyoma (uterus)
BO

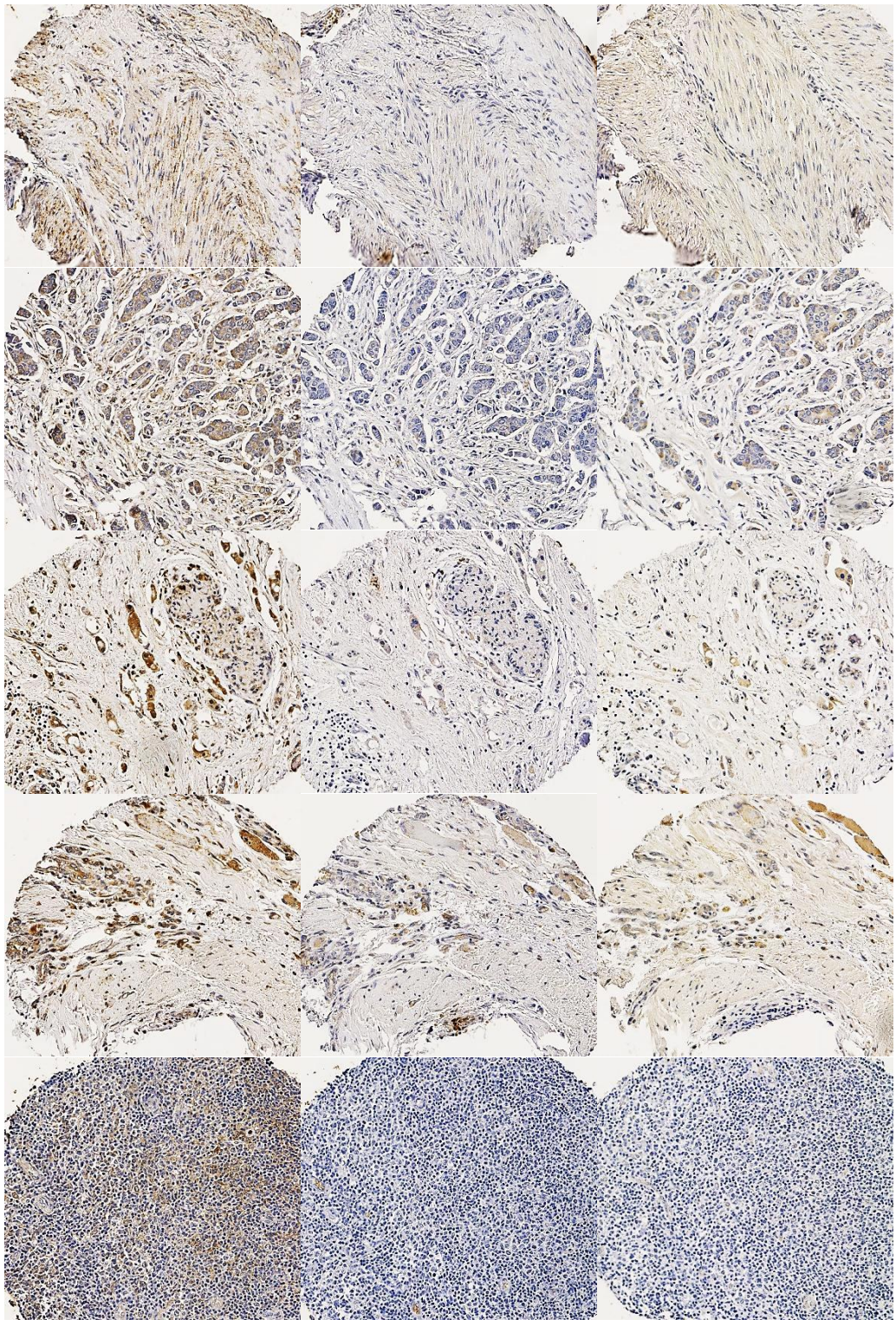
ZF
Breast cancer
BF
ZF
Endometrial tumor
BF
NHL small cleaved cells LN
ZF

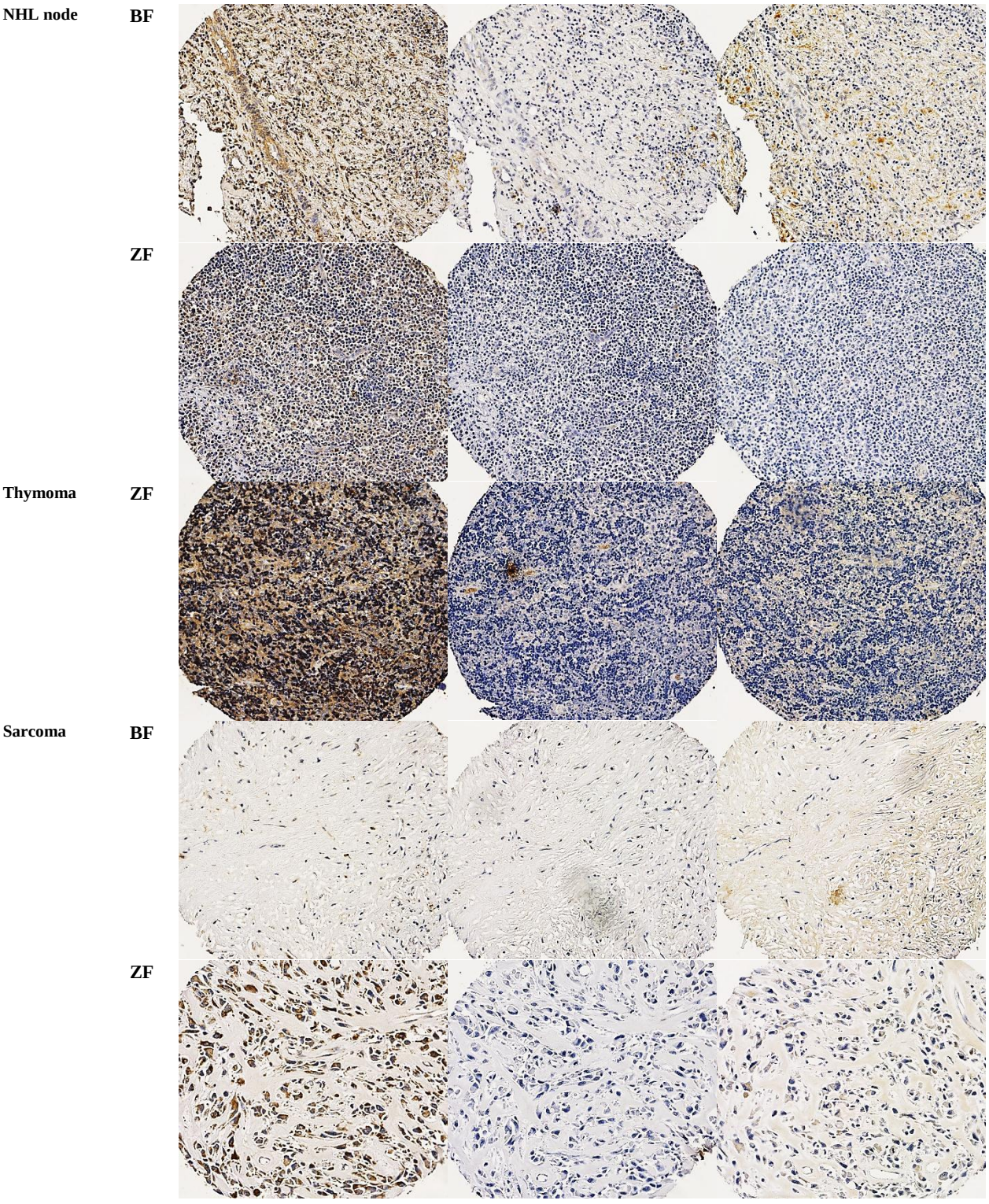
NHL node
BF
ZF
Thymoma
ZF
Sarcoma
BF
ZF

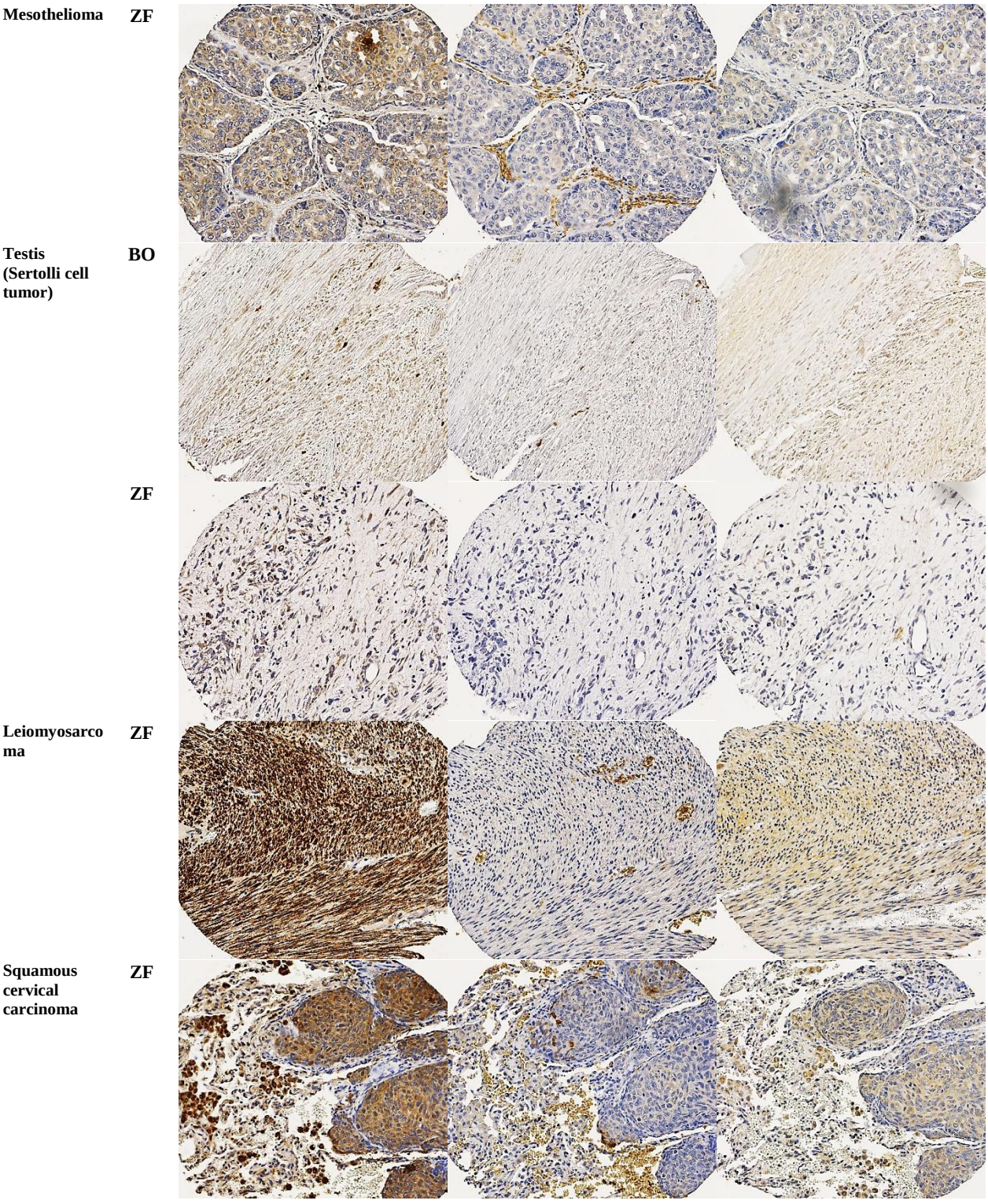
Mesothelioma
ZF
Testis (Sertolli cell tumor)
BO
ZF
Leiomyosarcoma
ZF
Squamous cervical carcinoma
ZF

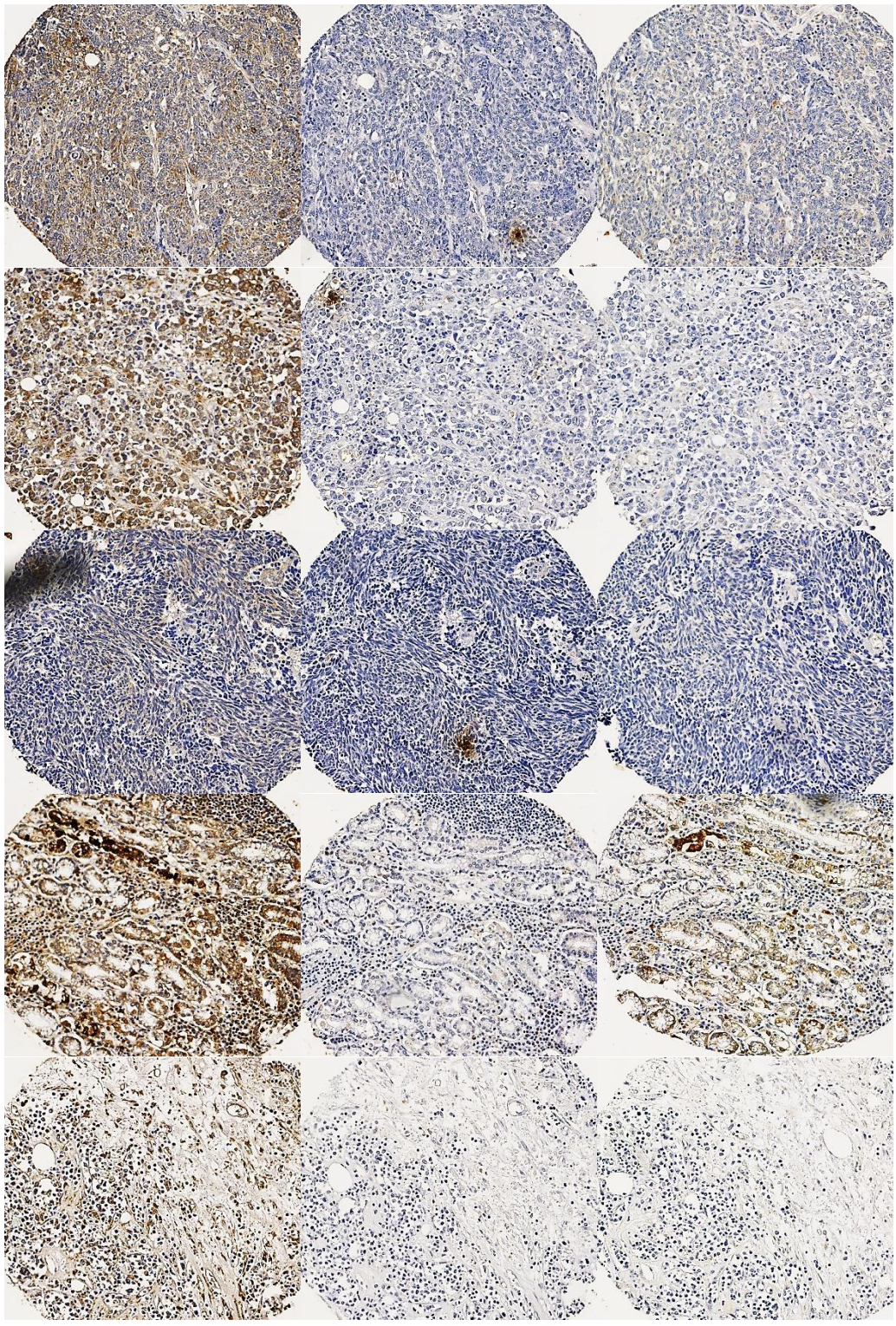
Esophageal cancer
BF
NSCL C
ZF
SCLC
BF
Gastric cancer
BF
NHL
ZF

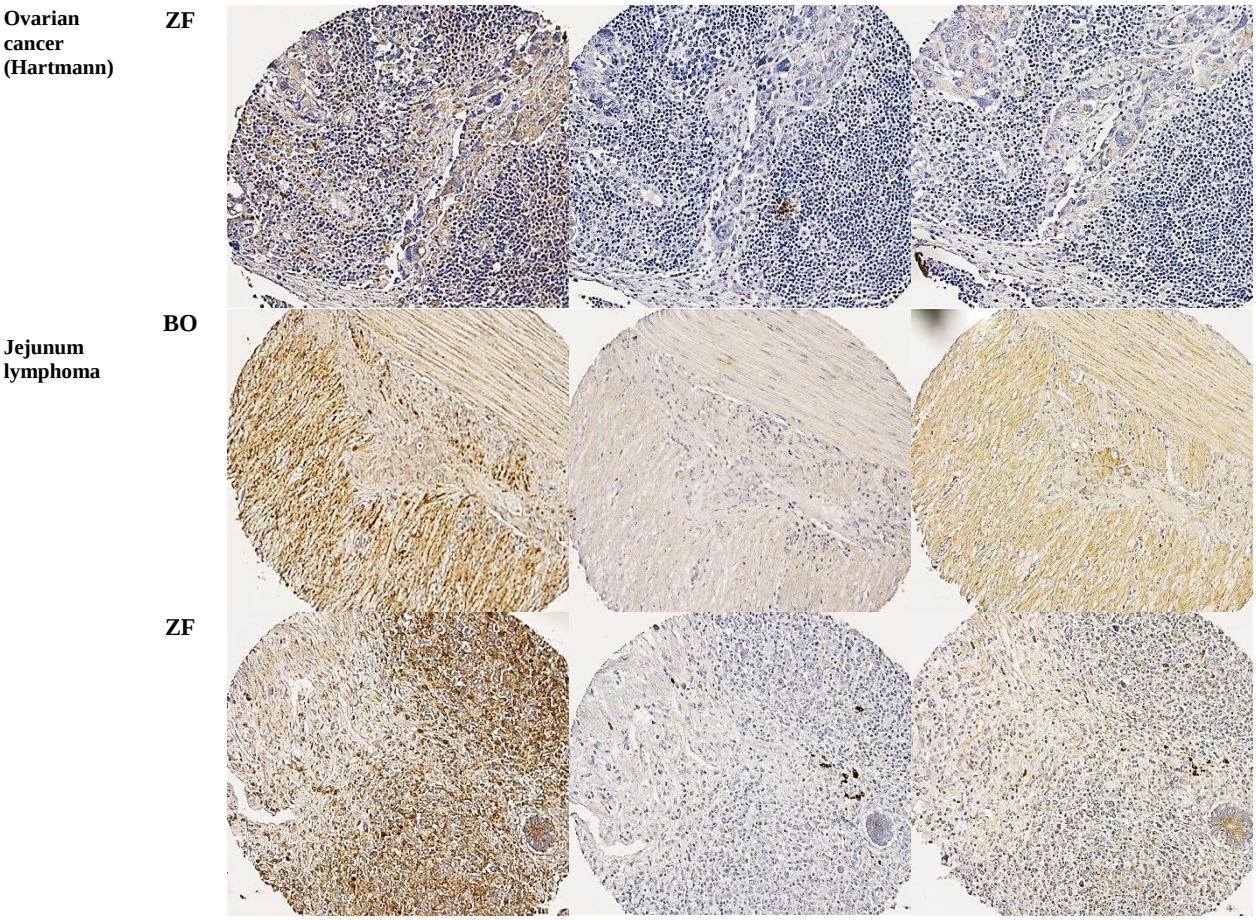


(F) stands for fixative, (BF) for buffered formalin, (ZF) for Z-fix and (BO) for Bouin's solution.

## 11.5 Xcelligence titration curves for the identification of the adequate cell number in cell index assays

| MDA-MB-435 pRc RSV | HaCaT |
|---|---|
| 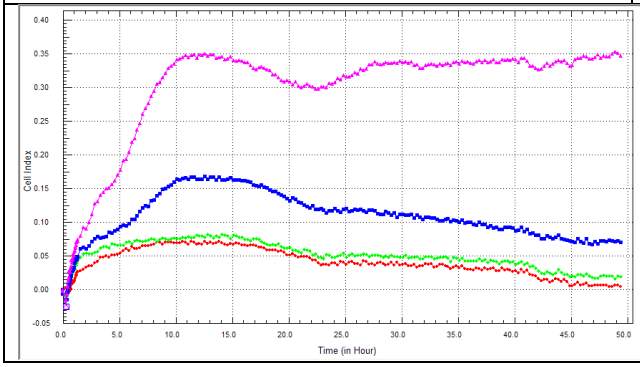 | 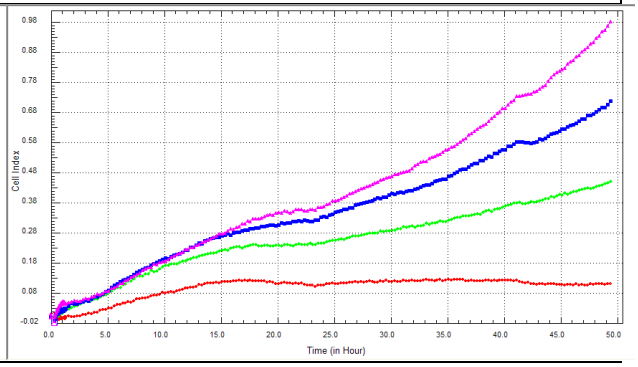 |

| MCF7 | OVMZ-6 pRc RSV |
|---|---|
| 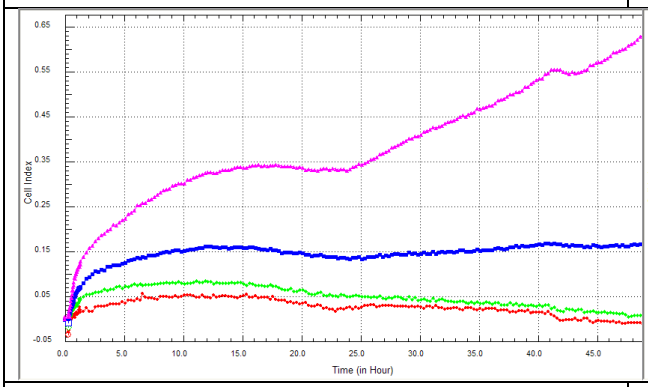 | 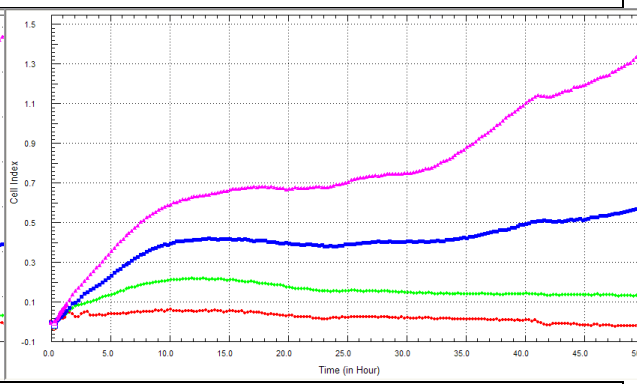 |
| **Number chosen: 10000** | **Legend: cell number**<br>3000 — 9000<br>6000 — 12000 |

## 11.6 Immunohistochemical protocols for KLKs

### 11.6.1 KLK7

| | |
|---|---|
| **1** | Deparaffinization and rehydration in descending row graded alcohols: 2 x 10 min xylene, 2 x 100 % alcohol, 1 x 96 % alcohol, 1 x 70 % alcohol each for 5 min |
| **2** | tris-buffer for 5 min—write down the title of the slides |
| **3** | (pressure cooking, citrate buffer, pH 6.0, 4min after second ring 5 min washing in normal tap water)/(steaming, EDTA pH 9) |
| **4** | Dual Endogenous Enzyme Block (10 min incubation) |
| **5** | tris-buffer 5 min with intervening change |
| **6** | 1st ab: anti-KLK7 1:500 for Arexis/R&D in green diluent -overnight incubation |
| **7** | tris-buffer 5min |
| **8** | (switch antibody anti-goat if I use a goat 1st ab-1:200- 30 min incubation |
| **9** | tris-buffer 5min |
| **10** | Dual link Polymer/HRP 150 µL per slide or some drops-30 min incubation |
| **11** | tris-buffer 5 min |
| **12** | DAB+ Substrate Buffer (K5361) 1mL + DAB+ Chromogen 20 µL (vortex long before use, 8 min) |
| **13** | tris-buffer 5 min |
| **14** | counterstain with hematoxylin for 10 sec if it is dense, otherwise 1 min |
| **15** | wash under flowing normal tap water for 5 min |
| **16** | transfer into $H_2O_{dist}$ for 2 min |
| **17** | ascending row of graded alcohol: 70 % alc, 96 % alc, 96 % alc, 2 x 100 % alc, 2 x xylene each for 25 sec (slides in xylene) |
| **18** | cover-glass lid/ sealing with histomount |

### 11.6.2 KLK4, KLK6 and KLK5

| | |
|---|---|
| **1** | Deparaffinization and rehydration in descending row graded alcohols: 2 x 10 min xylene 2 x 100 % alcohol, 1 x 96 % alcohol, 1 x 70 % alcohol each for 5 min |
| **2** | Tris-buffer for 5 min, with buffer change |
| **3** | Write down the title of the slides |
| **4** | Pressure cooking with citrate buffer, pH 6.0, 4 min after second ring |
| **5** | Washing in normal tap water 5 min |
| **6** | Tris-buffer for 5 min, with buffer change |
| **7** | Dual endogenous enzyme (peroxidases + AP) block (ready-to-use solution, endogenous enzyme block solution, containing 0.5 % hydrogen peroxide and levamisole, detergents, enzyme inhibitors, and preservative, pH 2) 120 µL or two drops per slide for 10 min, RT |
| **8** | Tris-buffer for 5 min, with buffer change! |
| **9** | 1st Antibody (in green diluent)100 µL/slide, overnight incubation, 4 °C |
| **10** | Tris-buffer for 5 min, with buffer change |
| **11** | Switch antibody (in green diluent) (e.g. rabbit anti-goat, if I use goat-Ab as 1st Ab)-Dilution 1:200, incubation 30 min, RT |
| **12** | Tris-buffer for 5 min, with buffer change |
| **13** | Labeled polymer-HRP-antibody( Ready-to-use solution, dextran polymer conjugated with horseradish peroxidase and affinity isolated immunoglobulins anti rabbit and anti-mouse) 120 µL or two drops per slide, incubation 30 min, RT |
| **14** | Tris-buffer for 5 min, with buffer change |
| **15** | Detection with DAB+ (substrate buffer solution: pH 7.5, containing <0.1 % hydrogen peroxide, stabilizers, enhancers, and an antimicrobial agent; chromogen solution: 5 % 3,3'-diaminobenzidine tetrahydrochloride) 1 ml HRP substrate buffer (D) + 20 µL DAB+ chromogen (C) for 10 slides, incubation 7.5 min, RT |
| **16** | Tris-buffer for 5 min, with buffer change |
| **17** | Counterstain with hematoxylin 10 sec if it is dense, otherwise 45 sec |
| **18** | Wash under flowing normal tap water for 5 min |
| **19** | Transfer into $H_2O_{dist}$ for 2 min |
| **20** | Ascending row of graded alcohols 70 % alc., 96 % alc., 2 x 100 % alc., 2 x xylene, each for 25 sec., leave the slides in xylene |
| **21** | Cover-glass sealing with histomount |

## 11.7 SOP uPA/PAI-1

### 11.7.1 Protocol (manual procedure, use of DAKO LSAB/DAB$^+$, 20 – 21 °C)

| | |
|---|---|
| **1** | **Deparaffinization and rehydration of tissue section in descending row of graded ethanol:** 2 x 10 min xylene; then 2 x 100 % isopropanol, 1 x 96 % ethanol, 1 x 70 % ethanol, each step for 5 min followed by 5 min washing in TBS, with an intervening buffer change. |
| **2** | **Blocking of endogenous peroxidase activity**: Incubate sections in 3 % hydrogen peroxide ($H_2O_2$): 45 ml aqua dist. + 5 mL $H_2O_2$ 30 %, for 20 min at room temperature (RT). |
| **3** | **Washing steps**: Short rinse with tap water. Then sections are rinsed using TBS-solution containing 0.05 M Tris and 1,54 M NaCl, pH 7.6) for 5 min with intervening buffer change. |
| **4** | **Blocking step:** Coat tissue section with 10 % goat serum in TBS; apply 130 µL/ slide and incubate for 30 min at RT. Don't wash slides after incubation, just tap off the serum from the slides. |
| **5** | **Apply primary antibody to uPA/PAI-1**: Dilute antibody in green antibody diluent (DAKO, S2022) at RT immediately before use. Apply 130 µL/slide of this dilution; incubate for 2 h at RT. Subsequently, wash for 5 min with TBS, with intervening buffer change. Negative controls do not receive any antibody dilution.<br><br>**Recommended dilutions**<br>**#3689:** 1:500 (stock: 1 mg/mL) → 2 µg/mL. **#3785:** 1:150 (stock: 1 mg/mL) → 6.7 µg/mL<br>**#3786:** 1:35 (stock: 0,42 mg/mL) → 12 µg/mL. #**ADG 25:** 1:35 (stock: 1.7 mg/mL) → 48.6 µg/mL |
| **6** | **Apply Bottle A (yellow) from LSAB-kit** (biotinylated goat anti-mouse immunoglobulin) to tissue section, incubate tissue section for 30 min at RT. Subsequently, wash for 5 min with TBS, with intervening buffer |

| | |
|---|---|
| | change. |
| **7** | **Apply Bottle B (red) from LSAB-kit** (streptavidin-HRP complex); incubate for 30 min at RT. Subsequently, wash for 5 min with TBS, with intervening buffer change. |
| **8** | **Add DAB substrate** from LSAB-kit: Mix content of bottle C and D: 30 µL + 1500 µL for 10 slides; apply 130 µL per slide for 10 min at RT. Subsequently, wash for 5 min with TBS, with intervening buffer change. |
| **9** | **Counterstain** with hematoxylin for appropriate time (e.g. 50 seconds). Blue-dyeing wash for 5 min under flowing tap water. Transfer into aqua dist. for 2 min. |
| **10** | **Dehydrate in ascending row** of graded ethanol: 70 % ethanol, 96 % ethanol, 2 x 100 % ethanol, 2 x xylene, each for 5 min. |
| **11** | **Cover-glass lid sealing** with ASSISTENT Histokitt mounting medium. |

### 11.7.2 Protocol (manual procedure, use of DAKO LSAB/DAB$^+$, 37 °C)

| | |
|---|---|
| **1** | **Deparaffinization and rehydration of tissue section in descending row of graded ethanol:** 2 x 10 min xylene; then 2 x 100 % isopropanol, 1 x 96 % ethanol, 1 x 70 % ethanol, each step for 5 min followed by 5 min washing in TBS, with an intervening buffer change. |
| **2** | **Blocking of endogenous peroxidase activity**: Incubate sections in 3 % hydrogen peroxide ($H_2O_2$): 45 mL aqua dist. + 5 ml $H_2O_2$ 30 %, for 20 min at room temperature (RT). |
| **3** | **Washing steps**: Short rinse with tap water. Then sections are rinsed using TBS-solution containing 0.05 M Tris and 1,54 M NaCl, pH 7.6) for 5 min with intervening buffer change. |
| **4** | **Blocking step:** Coat tissue section with 10 % goat serum in TBS; apply 130 µL/ slide and incubate for 30 min at RT. Don't wash slides after incubation, just tap off the serum from the slides. |
| **5** | **Apply primary antibody to uPA/PAI-1**: Dilute antibody in green antibody diluent (DAKO, S2022) at RT immediately before use. Apply 130 µL/slide of this dilution; incubate for 1 h at 37 °C. Subsequently, wash for 5 min with TBS, with intervening buffer change. Negative controls do not receive any antibody dilution.<br><br>**Recommended dilutions**<br>**#3689:** 1:500 (stock: 1 mg/mL) → 2 µg/mL. **#3785:** 1:150 (stock: 1 mg/mL) → 6.7 µg/mL<br>**#3786:** 1:35 (stock: 0,42 mg/mL) → 12 µg/mL. #**ADG 25:** 1:35 (stock: 1.7 mg/mL) → 48.6 µg/mL |
| **6** | **Apply Bottle A (yellow) from LSAB-kit** (biotinylated goat anti-mouse immunoglobulin) to tissue section, incubate tissue section for 30 min at RT. Subsequently, wash for 5 min with TBS, with intervening buffer change. |
| **7** | **Apply Bottle B (red) from LSAB-kit** (streptavidin-HRP complex); incubate for 30 min at RT. Subsequently, wash for 5 min with TBS, with intervening buffer change. |
| **8** | **Add DAB substrate** from LSAB-kit: Mix content of bottle C and D: 30 µL + 1500 µL for 10 slides, apply 130 µL per slide for 10 min at RT. Subsequently, wash for 5 min with TBS, with intervening buffer change. |
| **9** | **Counterstain** with hematoxylin for appropriate time (e.g. 50 seconds). Blue-dyeing wash for 5 min under flowing tap water. Transfer into aqua dist. for 2 min. |
| **10** | **Dehydrate in ascending row** of graded ethanol: 70 % ethanol, 96 % ethanol, 2 x 100 % ethanol, 2 x xylene, each for 5 min. |
| **11** | **Cover-glass lid sealing** with ASSISTENT Histokitt mounting medium. |

### 11.7.3 Protocol (manual procedure, use of DAKO EnVision/DAB$^+$, 20 - 21 °C)

| | |
|---|---|
| **1** | **Deparaffinization and rehydration of tissue section in descending row of graded ethanol:** 2 x 10 min xylene; then 2 x 100 % isopropanol, 1 x 96 % ethanol, 1 x 70 % ethanol, each step for 5 min followed by 5 min washing in TBS, with an intervening buffer change. |
| **2** | **Blocking of endogenous peroxidase activity** with dual endogenous enzyme (peroxidases + AP) block: 130 µl per tissue section,10 min, RT. |
| **3** | **Washing steps**: Sections are rinsed using TBS-solution containing 0.05 M Tris + 1.54 M NaCl, pH 7.6) for 5 min with intervening buffer change. |
| **4** | **Apply primary antibody to uPA/PAI-1**: Dilute antibody in green antibody diluent (DAKO, S2022) at RT immediately before use. Apply 130 µL/slide of this dilution; incubate for 2 h at RT. Subsequently, wash for 5 min with TBS, with intervening buffer change. Negative controls do not receive any antibody dilution.<br><br>**Recommended dilutions** |

| | |
|---|---|
| | **#3689:** 1:600 (stock: 1 mg/mL) → 1.7 µg/mL. **#3785:** 1:150 (stock: 1 mg/mL) → 6,7 µg/mL<br>**#3786:** 1:45 (stock: 0.42 mg/mL) → 9.3 µg/mL. #**ADG 25:** 1:150 (stock: 1.7 mg/mL) → 11.3 µg/mL |
| **5** | **Apply DAKOCytomation EnVision™+ Dual Link System Peroxidase:** 130 µl per tissue section, 30 min at RT. Subsequently, wash for 5 min with TBS, with intervening buffer change. |
| **6** | **Apply DAB substrate** from DAKO LSAB-kit (K5001): Mix content of bottle C and D: 30 µL + 1500 µL for 10 slides, apply 130 µL per tissue section,10 min at RT. Subsequently, wash for 5 min with TBS, with intervening buffer change. |
| **7** | **Counterstain** with hematoxylin for appropriate time (e.g. 50 seconds) |
| **8** | **Counterstain** with hematoxylin for appropriate time (e.g. 50 seconds). Blue-dyeing wash for 5 min under flowing tap water. Transfer into aqua dist. for 2 min. |
| **9** | **Dehydrate in ascending row** of graded ethanol: 70 % ethanol, 96 % ethanol, 2 x 100 % ethanol, 2 x xylene, each for 5 min. |
| **10** | **Cover-glass lid sealing** with ASSISTENT Histokitt mounting medium. |

### 11.7.4 Protocol (automatic procedure, use of LSAB/ DAB$^+$ for DAKO Autostainer Link48

| | |
|---|---|
| **1** | **Deparaffinization and rehydration of tissue section in descending row of graded ethanol:** 2 x 10 min xylene; then 2 x 100 % isopropanol, 1 x 96 % ethanol, 1 x 70 % ethanol, each step for 5 min followed by 5 min washing in TBS, with an intervening buffer change. Washing in DAKO wash buffer (code S3006). |
| **2** | **Programming of the Autostainer instrument** (Please refer to the template below and to Operators Manual for the respective DAKO Autostainer Instrument):<br>**1. Rinse buffer**<br>**2. Peroxide Block** [3 % $H_2O_2$, 20 min]<br>**3. Rinse Water**<br>**4. Rinse Buffer**<br>**5. NGS** [30 min] (normal goat serum)<br>**6. Blow**<br>**7. Primary Antibody** [120 min]<br>**8. Rinse Buffer**<br>**9. Secondary Reagent** [Bottle A, (DAKO 30 min, Zytomed 20 min)]<br>**10. Rinse Buffer**<br>**11. Tertiary Reagent** [Bottle B, (DAKO 30 min, Zytomed 20 min)]<br>**12. Rinse Buffer**<br>**13. Substrate Batch** [Bottle C+D, 10 min]<br>**14. Rinse Buffer**<br>**15. Auxiliary [Hematoxylin, Dept. Pathologie, TU Munich, e.g. 4 min ]**<br>**16. Rinse Buffer** |
| **3** | **Load the template into the PROGRAM STAINING RUN SCREEN,** specify the number of slides in the run, and load the reagents with incubation times into the template |
| **4** | **Load reagents according to the Slides Layout Map Screen:**<br>Applicable/recommended dilutions for the primary antibody:<br>#3689: 1:500 (2 µg/mL). #3785: 1:200 (5 µg/mL)<br>#3786: 1:60 (7 µg/mL). #ADG25: 1:125 (13.6 µg/mL) |
| **5** | **Load slides according to the Reagents Layout Map Screen** (It is recommended to pre-wet the slides for 5 minutes in DAKO Wash Buffer) |
| **6** | **Check the water and the buffer pumps** |
| **7** | **Start the program** |
| **8** | **After end of program rinse slides in water for 5 min** |
| **9** | **Dehydrate in ascending row** of graded alcohols: 70 % ethanol, 96 % ethanol, 2 x 100 % isopropanol, 2 x xylene, each for 1 min |
| **10** | **Cover-glass lid / sealing** with "Pertex" mounting medium. |

### 11.7.5 Protocol (automatic procedure, use of EnVision/DAB$^+$ for DAKO Autostainer Link 48

| | |
|---|---|
| **1** | **Deparaffinization** and **rehydration** in **descending graded row** of alcohols:<br>2 x 10 min xylene; 2 x 100 % isopropanol, 1 x 96 % ethanol, 1 x 70 % ethanol, each for 5 min |
| | Washing in DAKO Wash Buffer (code S3006) |
| **2** | **Programming of the Autostainer instrument** (Please refer to the template below and to Operators Manual for the respective DAKO Autostainer Instrument):<br>**1. Rinse buffer**<br>**2. Dual Endogenous Enzyme Block [10 min]**<br>**3. Rinse Buffer**<br>**4. Primary Antibody [120 min]**<br>**5. Rinse Buffer**<br>**6. DAKOCytomation EnVision™ + Dual Link System Peroxidase**<br>**7. Rinse Buffer**<br>**8. Substrate Batch [Bottle C+D, 10 min]**<br>**9. Rinse Buffer**<br>**10. Auxiliary [Hematoxylin, Pathologie, TU Munich, e.g. 4 min ]**<br>**11. Rinse Buffer** |
| **3** | **Load the template into the PROGRAM STAINING RUN SCREEN,** specify the number of slides in the run, and load the reagents with incubation times into the template |
| **4** | **Load reagents according to the Slides Layout Map Screen:**<br>Applicable/recommended dilutions for the primary antibody:<br>#3689: 1:700 (1.42 µg/mL). #3785: 1:250 (4 µg/mL)<br>#3786: 1:60 (7 µg/mL). #ADG 25: 1:125 (13.6 µg/mL) |
| **5** | **Load slides according to the Reagents Layout Map Screen (It is recommended to pre-wet the slides for 5 minutes in DAKO Wash Buffer)** |
| **6** | **Check the water and the buffer pumps** |
| **7** | **Start the program** |
| **8** | **After end of program rinse slides in water for 5 min** |
| **9** | **Dehydrate in ascending row of graded alcohol: 70 % ethanol, 96 % ethanol, 2 x 100 % isopropanol, 2 x xylene, each for 1 min** |
| **10** | **Cover-glass lid / sealing** with “Pertex” mounting medium. |

### 11.7.6 Ventana Benchmark XT (working temperature: 37 °C) ultraView®

| | |
|---|---|
| **1** | Apply slide barcode label that corresponds to the primary antibody protocol to be performed. |
| **2** | Load the primary antibody, appropriate detection kit dispensers and required accessory reagents onto the reagent tray and place the reagent tray on the automated slide stainer. Check bulk fluids and waste |
| **3** | Load the slides onto the automated slide stainer. |
| **4** | Start the staining run. |
| **5** | **Baking + Deparaffinization**<br>1. Choose EZ PREP/ Start timed steps/ Mixer off/ Heat the slide at 75 °C and incubate for 4 min/<br>2. Equalize EZ PREP volumes/ Incubate 4 min/Wash slide<br>3. Equalize EZ PREP volumes/ Incubate 4 min/Wash slide<br>4. Equalize EZ PREP volumes/ Apply coverslip<br>5. Heat the slide until 76 °C and incubate for 4 min/ Wash slide<br>6. Equalize deparaffinization volumes/ Apply coverslip<br>7. Slide heat off/ Mixer on<br>[Fast: 8 min Conditioning]/ Wash slide/Apply Cell Conditioner 1 for moderate duration/ Apply Cell Conditioner and coverslip for long<br>[Mild: 30 min Conditioning]/ Apply Cell Conditioner 1 for moderate duration/ Apply coverslip<br>Heat the slide until 100 °C and incubate for 4 min/ Apply coverslip/ Apply Cell Conditioner 1/ Incubate for 4 min/ Apply coverslip<br>8. Add EZPREP CC VOLUME ADJUST/ Incubate for 4 min/ Apply coverslip<br>9. Apply Cell Conditioner 1 for moderate duration/ Incubate for 4 min/ Apply coverslip/ Apply Cell Conditioner 1/ Incubate for 4 min<br>10. Slide heat off/ Incubate for 8 min/ Wash slide/ Adjust slide volumes/ Apply coverslip<br>11. Select reaction buffer/ Heat the slide until 37 °C and incubate for 2 min/ Wash slide/ Adjust slide volumes |
| **6** | Apply 1 drop of the UV Inhibitor, apply coverslip and incubate for 4 min/ Wash slide/Adjust slide volume/ Apply coverslip |
| **7** | **Apply 100 µl of primary antibody in DAKO REAL™ antibody diluent (code S2022)**<br>**#3689 1:300**<br>**#ADG25 1:30**<br>**#3785 1:250**<br>**#3786 1:15**<br>**and incubate for 60 min/ Wash slide/Adjust slide volume** |
| **8** | Apply 1 drop of UV HRP UNIV MULT, apply coverslip and incubate for 8 min/ Wash slide/ Adjust slide volume/ Apply coverslip/ Wash slide/ Adjust slide volume |
| **9** | Apply 1 drop UV DAB and one drop UV DAB $H_2O_2$, apply LCS and incubate for 8 min/ Wash slide |
| **10** | Adjust slide volume |
| **11** | Apply 1 drop of UV COPPER, apply coverslip and incubate for 4 min./ Wash slide/ Adjust slide volume |
| **12** | Apply 1 drop of COUNTERSTAIN 1 (mixture), apply LCS and incubate for 8 min/ Wash slide<br>Adjust slide volume |
| **13** | Apply 1 drop of BLUING REAGENT, apply LCS and incubate for 4 min/ Wash slide |
| **14** | At the completion of the run, remove the slides from the automated slide stainer. |
| **15** | Wash in a mild dishwashing detergent to remove the coverslip solution; dehydrate, clear, and coverslip with permanent mounting media in the usual manner. |
| **16** | The stained slides should be read within two to three days of staining, and are stable for at least two years if properly stored at room temperature (15 to 25 °C). |

### 11.7.7 Ventana Benchmark XT (working temperature: 37 °C) iView®

| | |
|---|---|
| **1** | Apply slide bar code label which corresponds to the antibody protocol to be performed. |
| **2** | Load the primary antibody and appropriate detection kit dispensers and required accessory reagent onto the reagent tray and place them on the automated slide stainer. Check bulk fluids and waste. |
| **3** | Load the slides onto the instrument. |
| **4** | Start the staining run. |
| **5** | **Baking + Deparaffinization**<br>1. Choose EZ PREP/ Start timed steps/ Mixer off/ Heat the slide at 75 °C and incubate for 4 min<br>2. Equalize EZ PREP volumes/ Incubate 4 min/Wash slide<br>3. Equalize EZ PREP volumes/ Incubate 4 min/Wash slide<br>4. Equalize EZ PREP volumes/ Apply coverslip<br>5. Heat the slide until 76 °C and incubate for 4 min/ Wash slide<br>6. Equalize deparaffinization volumes/ Apply coverslip/Heat the slide until 42 °C and incubate for 2 min<br>7. Mixer on/Slide heat off/ Wash slide<br>8. Equalize EZ PREP volumes/ Apply coverslip<br>9. Select reaction buffer/ Heat the slide until 42 °C and incubate for 2 min/ Wash slide/ Adjust slide volumes |
| **6** | Apply 1 drop of i-VIEW Inhibitor, apply coverslip and incubate for 4 min 42 °C/ Wash slide/Adjust slide volume/Apply coverslip/ |
| **7** | **Hand Apply 100 µl of primary antibody in DAKO REAL™ antibody diluent (code S2022)**<br>**#3689 1:300**<br>**#ADG25 1:30**<br>**#3785 1:250**<br>**#3786 1:15**<br>**and incubate for 60 min/ Wash slide/Adjust slide volume** |
| **8** | The slide is rinsed; universal biotinylated secondary antibody is applied. The step takes 8 minutes at 42 °C. |
| **9** | Apply 1 drop of i-VIEW SA-HRP, apply coverslip and incubate for 8 min/ Wash slide/ Adjust slide volume/ Apply coverslip/ Wash slide/ Adjust slide volume |
| **10** | Apply 1 drop i-VIEW DAB and one drop i-VIEW DAB $H_2O_2$, apply coverslip and incubate for 8 min/ Wash slide/Adjust slide volume |
| **11** | Apply 1 drop of i-VIEW COPPER, apply coverslip and incubate for 4 min./ Wash slide/ Adjust slide volume/Apply coverslip<br>Start Timed Steps/Wash slide/ Adjust slide volume |
| **12** | Apply 1 drop of HEMATOXYLIN (Counterstain), apply coverslip and incubate for 8 min/ Wash slide/Adjust slide volume |
| **13** | Apply 1 drop of BLUING REAGENT (Post Counterstain), apply coverslip and incubate for 4 min/ Wash slide |
| **14** | At the completion of the run, remove the slides from the instrument, and wash in a mild dishwashing detergent or alcohol to remove the coverslip solution; dehydrate, clear, and coverslip with permanent mounting media in the usual manner. |

## 11.8 KLK evaluation: list of R&D Systems antibodies employed for detection of KLK5 and KLK7

| Antibody | Immunogen | Host | Clonality | Stock concentration | Best working dilution IHC | IHC tissues used | Dilutions tested on WB | WB results |
|---|---|---|---|---|---|---|---|---|
| **MAB2624** | KLK7 | mouse | monoclonal | 0.5 mg/mL | 1:20 | kidney skin | | |
| **333901** | KLK7 | mouse | monoclonal | | 1:50 | kidney skin | | |

| Antibody | Immunogen | Host | Clonality | Stock concentration | Best working dilution IHC | IHC tissues used | Dilutions tested on WB | WB results |
|---|---|---|---|---|---|---|---|---|
| **333902** | KLK7 | mouse | monoclonal | | 1:50 – 1:100 | kidney<br>skin<br>ovary<br>breast<br>ovca | 1:500 | negative |
| **333908** | KLK7 | mouse | monoclonal | | 1:5000 | kidney<br>skin<br>ovary<br>breast<br>ovca | 1:1000<br>1:5000<br>1:8000 | background<br>background<br>negative |
| **333909** | KLK7 | mouse | monoclonal | | 1:30 | kidney<br>skin | | |
| **333916** | KLK7 | mouse | monoclonal | | 1:30 | kidney<br>skin | | |
| **333918** | KLK7 | mouse | monoclonal | | 1:50 | kidney<br>skin | | |
| **333924** | KLK7 | mouse | monoclonal | | 1:10 | kidney<br>skin | | |
| **333925** | KLK7 | mouse | monoclonal | | 1:100 | kidney<br>skin<br>ovary<br>breast<br>ovca | 1:1000<br>1:500 | negative |
| **333930** | KLK7 | mouse | monoclonal | | 1:10 | kidney<br>skin | | |
| **333930** | KLK7 | mouse | monoclonal | | 1:10 | kidney<br>skin | | |
| **333945** | KLK7 | mouse | monoclonal | | 1:100 | kidney<br>skin | | |
| **AF1108** | KLK5 | goat | polyclonal | 0.2 mg/mL | 1:100 | kidney<br>skin<br>ovary<br>breast<br>ovca<br>benign<br>ov. TMA | 1:500 | no cross-reactivity; tumor extracts |
| **MAB1108** | KLK5 | mouse | monoclonal | 0.5 mg/mL | 1:10 | kidney<br>skin | | |
| **MAB11081** | KLK5 | mouse | monoclonal | 0.5 mg/mL | 1:10 | kidney<br>skin | | |
| **MAB11082** | KLK5 | mouse | monoclonal | 0.5 mg/mL | 1:30 | kidney<br>skin | | |

| Antibody | Immunogen | Host | Clonality | Stock concentration | Best working dilution IHC | IHC tissues used | Dilutions tested on WB | WB results |
|---|---|---|---|---|---|---|---|---|
| **193302** | KLK5 | mouse | monoclonal | | 1:20 | kidney<br>skin | | |
| **193303** | KLK5 | mouse | monoclonal | | 1:100 – 1:300 | kidney<br>skin<br>ovary<br>breast<br>ovca | 1:500<br>1:300<br>1:500 | negative |
| **193304** | KLK5 | mouse | monoclonal | | 1:10 | kidney<br>skin | | |
| **193305** | KLK5 | mouse | monoclonal | | 1:30 | kidney<br>skin | | |
| **193306** | KLK5 | mouse | monoclonal | | 1:10 | kidney<br>skin | | |
| **193308** | KLK5 | mouse | monoclonal | | 1:10 | kidney<br>skin | | |
| **193315** | KLK5 | mouse | monoclonal | | 1:30 | kidney<br>skin | | |

## 12. References


**Abbondanzo, S. L., et al. (1991). "Enhancement of immunoreactivity among lymphoid malignant neoplasms in paraffin-embedded tissues by refixation in zinc sulfate-formalin." Arch Pathol Lab Med 115(1): 31-33.**

**Addis, M. F., et al. (2009). "Generation of high-quality protein extracts from formalin-fixed, paraffin-embedded tissues." Proteomics 9(15): 3815-3823.**

**Adib, T. R., et al. (2004). "Predicting biomarkers for ovarian cancer using gene-expression microarrays." Br J Cancer 90(3): 686-692.**

**Ahlstedt, S., et al. (1974). "Protective capacity of antibodies against E. coli O antigen with special reference to the avidity." Int Arch Allergy Appl Immunol 46(3): 470-480.**

**Anders, C. K., et al. (2010). "Poly(ADP-Ribose) polymerase inhibition: "targeted" therapy for triple-negative breast cancer." Clin Cancer Res 16(19): 4702-4710.**

**Andreasen, P. A., et al. (1986). "Plasminogen activator inhibitor from human fibrosarcoma cells binds urokinase-type plasminogen activator, but not its proenzyme." J Biol Chem 261(17): 7644-7651.**

**Angenete, E., et al. (2009). "uPA and PAI-1 in rectal cancer--relationship to radiotherapy and clinical outcome." The Journal of surgical research 153(1): 46-53.**

**Anisowicz, A., et al. (1996). "A novel protease homolog differentially expressed in breast and ovarian cancer." Mol Med 2(5): 624-636.**

**Astedt, B. and L. Holmberg (1976). "Immunological identity of urokinase and ovarian carcinoma plasminogen activator released in tissue culture." Nature 261(5561): 595-597.**

**Aubele, M., et al. (2007). "PTK (protein tyrosine kinase)-6 and HER2 and 4, but not HER1 and 3 predict long-term survival in breast carcinomas." Br J Cancer 96(5): 801-807.**

**Avgeris, M., et al. (2011). "Kallikrein-related peptidase 4 gene (KLK4) in prostate tumors: Quantitative expression analysis and evaluation of its clinical significance." Prostate.**

**Balbay, M. D., et al. (1999). "Highly metastatic human prostate cancer growing within the prostate of athymic mice overexpresses vascular endothelial growth factor." Clin Cancer Res 5(4): 783-789.**

**Ballestar, E. (2011). "An introduction to epigenetics." Advances in experimental medicine and biology 711: 1-11.**

**Banks (1985). Technical aspects of specimen preparation and special studies. . Surgical Pathology of the Lymph Nodes and Related Organs. Jaffe, W B Saunders Co: 1-21.**

**Batra, J., et al. (2011). "A Kallikrein 15 (KLK15) single nucleotide polymorphism located close to a novel exon shows evidence of association with poor ovarian cancer survival." BMC Cancer 11: 119.**

**Batra, J., et al. (2010). "Kallikrein-related peptidase 10 (KLK10) expression and single nucleotide polymorphisms in ovarian cancer survival." Int J Gynecol Cancer 20(4): 529-536.**

**Baum, H. P., et al. (1994). "Fixation requirements for the immunohistochemical reactivity of PCNA antibody PC10 on cryostat sections." Histochem J 26(12): 929-933.**

**Bayes, A., et al. (2004). "Human kallikrein 6 activity is regulated via an autoproteolytic mechanism of activation/inactivation." Biol Chem 385(6): 517-524.**

**Beaufort, N., et al. (2006). "Interplay of human tissue kallikrein 4 (hK4) with the plasminogen activation system: hK4 regulates the structure and functions of the urokinase-type plasminogen activator receptor (uPAR)." Biol Chem 387(2): 217-222.**

**Beck, T., et al. (1994). "Immunohistochemical detection of hormone receptors in breast carcinomas (ER-ICA, PgR-ICA): prognostic usefulness and comparison with the biochemical radioactive-ligand-binding assay (DCC)." Gynecol Oncol 53(2): 220-227.**

**Becker KF, M. H., Schott C, Hipp S, Rappl A, Piontek G, Höfler, H (2008a). "Extraction of phosphorylated proteins from formalin-fixed cancer cells and tissues." TOPATJ 2: 44-52.**

**Becker KF, S. C., Becker I, Höfler, H (2008b). "Guided protein extraction from formalin-fixed tissues for quantitative multiplex analysis avoids detrimental effects of histological stains." Proteomics Clin. Appl 2: 737-743.**

**Becker, K. F., et al. (2007). "Quantitative protein analysis from formalin-fixed tissues: implications for translational clinical research and nanoscale molecular diagnosis." J Pathol 211(3): 370-378.**

**Bernett, M. J., et al. (2002). "Crystal structure and biochemical characterization of human kallikrein 6 reveals that a trypsin-like kallikrein is expressed in the central nervous system." J Biol Chem 277(27): 24562-24570.**

**Bhattacharjee, A., et al. (2001). "Classification of human lung carcinomas by mRNA expression profiling reveals distinct adenocarcinoma subclasses." Proc Natl Acad Sci U S A 98(24): 13790-13795.**

**Bhoola, K. D., et al. (1992). "Bioregulation of kinins: kallikreins, kininogens, and kininases." Pharmacol Rev 44(1): 1-80.**

**Bignotti, E., et al. (2006). "Differential gene expression profiles between tumor biopsies and short-term primary cultures of ovarian serous carcinomas: identification of novel molecular biomarkers for early diagnosis and therapy." Gynecol Oncol 103(2): 405-416.**

**Binder, B. R., et al. (2007). "uPAR-uPA-PAI-1 interactions and signaling: a vascular biologist's view." Thromb Haemost 97(3): 336-342.**

**Bjerrum, O. J. a. H., N.H.H. (1988). Handbook of Immunoblotting of Proteins. Technical Descriptions, CRC Press.**

**Blaber, S. I., et al. (2007). "The autolytic regulation of human kallikrein-related peptidase 6." Biochemistry 46(17): 5209-5217.**

**Black, M. H. and E. P. Diamandis (2000). "The diagnostic and prognostic utility of prostate-specific antigen for diseases of the breast." Breast Cancer Res Treat 59(1): 1-14.**

**Black, M. H., et al. (2000). "Expression of a prostate-associated protein, human glandular kallikrein (hK2), in breast tumours and in normal breast secretions." Br J Cancer 82(2): 361-367.**

**Blechschmidt, K., et al. (2007). "The E-cadherin repressor snail plays a role in tumor progression of endometrioid adenocarcinomas." Diagnostic molecular pathology : the American journal of surgical pathology, part B 16(4): 222-228.**

**Bollag, D. M., et al. (1996). Protein Methods. New York, Wiley-Liss, Inc.**

**Bondurant, K. L., et al. (2005). "Definition of an immunogenic region within the ovarian tumor antigen stratum corneum chymotryptic enzyme." Clinical cancer research :**

an official journal of the American Association for Cancer Research 11(9): 3446-3454.
Borgono, C. A. and E. P. Diamandis (2004). "The emerging roles of human tissue kallikreins in cancer." Nat Rev Cancer 4(11): 876-890.
Borgono, C. A., et al. (2003a). "Favorable prognostic value of tissue human kallikrein 11 (hK11) in patients with ovarian carcinoma." Int J Cancer 106(4): 605-610.
Borgono, C. A., et al. (2003b). "Human kallikrein 14: a new potential biomarker for ovarian and breast cancer." Cancer Res 63(24): 9032-9041.
Borgono, C. A., et al. (2006). "Human kallikrein 8 protein is a favorable prognostic marker in ovarian cancer." Clin Cancer Res 12(5): 1487-1493.
Borgono, C. A., et al. (2004). "Human tissue kallikreins: physiologic roles and applications in cancer." Molecular cancer research : MCR 2(5): 257-280.
Borgono, C. A., et al. (2007). "Expression and functional characterization of the cancer-related serine protease, human tissue kallikrein 14." J Biol Chem 282(4): 2405-2422.
Boumber, Y. and J. P. Issa (2011). "Epigenetics in cancer: what's the future?" Oncology (Williston Park) 25(3): 220-226, 228.
Brattsand, M. and T. Egelrud (1999). "Purification, molecular cloning, and expression of a human stratum corneum trypsin-like serine protease with possible function in desquamation." J Biol Chem 274(42): 30033-30040.
Brattsand, M., et al. (2005). "A proteolytic cascade of kallikreins in the stratum corneum." J Invest Dermatol 124(1): 198-203.
Brinkhuis, M., et al. (1995). "An evaluation of prognostic factors in advanced ovarian cancer." Eur J Obstet Gynecol Reprod Biol 63(2): 115-124.
Bryans, M., et al. (1992). "Vector methylation inhibits transcription from the SV40 early promoter." FEBS Lett 309(1): 97-102.
Butler, J. E., et al. (1978). "The enzyme-linked immunosorbent assay (ELISA): a measure of antibody concentration or affinity." Immunochemistry 15(2): 131-136.
Byrski, T., et al. (2009). "Response to neoadjuvant therapy with cisplatin in BRCA1-positive breast cancer patients." Breast Cancer Res Treat 115(2): 359-363.
Camp, R. L., et al. (2002). "Automated subcellular localization and quantification of protein expression in tissue microarrays." Nat Med 8(11): 1323-1327.
Cane, S., et al. (2004). "The novel serine protease tumor-associated differentially expressed gene-14 (KLK8/Neuropsin/Ovasin) is highly overexpressed in cervical cancer." Am J Obstet Gynecol 190(1): 60-66.
Cannistra, S. A. (2004). "Cancer of the ovary." N Engl J Med 351(24): 2519-2529.
Carey, L. A., et al. (2007). "The triple negative paradox: primary tumor chemosensitivity of breast cancer subtypes." Clin Cancer Res 13(8): 2329-2334.
Carson (1992 ). Histotechnology: A Self-Instructional Text, ASCP Press: 19.
Catalona, W. J., et al. (1991). "Measurement of prostate-specific antigen in serum as a screening test for prostate cancer." N Engl J Med 324(17): 1156-1161.
Caubet, C., et al. (2004). "Degradation of corneodesmosome proteins by two serine proteases of the kallikrein family, SCTE/KLK5/hK5 and SCCE/KLK7/hK7." J Invest Dermatol 122(5): 1235-1244.
Chacon, R. D. and M. V. Costanzo (2010). "Triple-negative breast cancer." Breast Cancer Res 12 Suppl 2: S3.

**Chang, A., et al. (2002). "Human kallikrein gene 13 (KLK13) expression by quantitative RT-PCR: an independent indicator of favourable prognosis in breast cancer." Br J Cancer 86(9): 1457-1464.**

**Charlesworth, M. C., et al. (1999). "Kininogenase activity of prostate-derived human glandular kallikrein (hK2) purified from seminal fluid." J Androl 20(2): 220-229.**

**Chou, R. H., et al. (2011). "Epigenetic activation of human kallikrein 13 enhances malignancy of lung adenocarcinoma by promoting N-cadherin expression and laminin degradation." Biochem Biophys Res Commun 409(3): 442-447.**

**Christman, J. K. (2002). "5-Azacytidine and 5-aza-2'-deoxycytidine as inhibitors of DNA methylation: mechanistic studies and their implications for cancer therapy." Oncogene 21(35): 5483-5495.**

**Christophi, G. P., et al. (2004). "Distinct promoters regulate tissue-specific and differential expression of kallikrein 6 in CNS demyelinating disease." Journal of neurochemistry 91(6): 1439-1449.**

**Chu, W. S., et al. (2005). "A nondestructive molecule extraction method allowing morphological and molecular analyses using a single tissue section." Lab Invest 85(11): 1416-1428.**

**Chung, C. H., et al. (2004). "Molecular classification of head and neck squamous cell carcinomas using patterns of gene expression." Cancer Cell 5(5): 489-500.**

**Chung, J., Lee S J, Kris Y, Braunschweig T, Traicoff J L, and Hewitt SM (2008). "A well-based reverse-phase protein array applicable to extracts from formalin-fixed paraffin-embedded tissue." Proteomics Clin. Appl 2(10-11): 1539-1547.**

**Clements (1997). The molecular biology of the kallikreins and their roles in inflammation. The Kinin System. F. SG. San Diego, Academic Press. 5: 71-97.**

**Clements, J. and C. Atkins (2001). "Characterization of a non-abscission mutant in Lupinus angustifolius. I. Genetic and structural aspects." Am J Bot 88(1): 31-42.**

**Clements, J. A., et al. (2004). "The tissue kallikrein family of serine proteases: functional roles in human disease and potential as clinical biomarkers." Critical reviews in clinical laboratory sciences 41(3): 265-312.**

**Cloutier, S. M., et al. (2002). "Substrate specificity of human kallikrein 2 (hK2) as determined by phage display technology." Eur J Biochem 269(11): 2747-2754.**

**Cohen, P., et al. (1992). "Prostate-specific antigen (PSA) is an insulin-like growth factor binding protein-3 protease found in seminal plasma." J Clin Endocrinol Metab 75(4): 1046-1053.**

**Conway, C., et al. (2008). "Virtual microscopy as an enabler of automated/quantitative assessment of protein expression in TMAs." Histochemistry and cell biology 130(3): 447-463.**

**Corasanti, J. G., et al. (1980). "Plasminogen activator content of human colon tumors and normal mucosae: separation of enzymes and partial purification." J Natl Cancer Inst 65(2): 345-351.**

**Cornett, W. C., et al. (1985). "Specificity of monoclonal antibodies reactive with Fusobacterium nucleatum: effect of formalin fixation." J Immunol Methods 84(1-2): 321-326.**

**Costantini, V., et al. (1996). "Combined overexpression of urokinase, urokinase receptor, and plasminogen activator inhibitor-1 is associated with breast cancer progression: an immunohistochemical comparison of normal, benign, and malignant breast tissues." Cancer 77(6): 1079-1088.**

**Cregger, M., et al. (2006). "Immunohistochemistry and quantitative analysis of protein expression." Arch Pathol Lab Med 130(7): 1026-1030.**

**Crippa, M. P. (2007). "Urokinase-type plasminogen activator." Int J Biochem Cell Biol 39(4): 690-694.**

**Crookham (1991). Hazardous Chemicals in the Histopathology Laboratory, Anatech.**

**Czekay, R. P., et al. (2003). "Plasminogen activator inhibitor-1 detaches cells from extracellular matrices by inactivating integrins." The Journal of cell biology 160(5): 781-791.**

**Dabbs, D. J. (2010). Diagnostic Immunohistochemistry: Theranostic and Genomic Applications, Saunders.**

**Dano, K., et al. (1985). "Plasminogen activators, tissue degradation, and cancer." Advances in cancer research 44: 139-266.**

**Dapson, R. W. (1993). "Fixation for the 1990's: a review of needs and accomplishments." Biotechnic & histochemistry : official publication of the Biological Stain Commission 68(2): 75-82.**

**Darling, M. R., et al. (2006). "Human kallikrein 6 expression in salivary gland tumors." The journal of histochemistry and cytochemistry : official journal of the Histochemistry Society 54(3): 337-342.**

**Darling, M. R., et al. (2008). "Human kallikrein 8 expression in salivary gland tumors." Head Neck Pathol 2(3): 169-174.**

**Darson, M. F., et al. (1997). "Human glandular kallikrein 2 (hK2) expression in prostatic intraepithelial neoplasia and adenocarcinoma: a novel prostate cancer marker." Urology 49(6): 857-862.**

**Davidson, B. (2004). "Malignant effusions: from diagnosis to biology." Diagn Cytopathol 31(4): 246-254.**

**Davidson, B., et al. (2005). "Kallikrein 4 expression is up-regulated in epithelial ovarian carcinoma cells in effusions." American journal of clinical pathology 123(3): 360-368.**

**Davidson, B., et al. (2007). "Kallikrein 4 is expressed in malignant mesothelioma--further evidence for the histogenetic link between mesothelial and epithelial cells." Diagnostic cytopathology 35(2): 80-84.**

**Davidson, B., et al. (2006). "Gene expression signatures differentiate ovarian/peritoneal serous carcinoma from diffuse malignant peritoneal mesothelioma." Clinical cancer research : an official journal of the American Association for Cancer Research 12(20 Pt 1): 5944-5950.**

**Day, C. H., et al. (2002). "Characterization of KLK4 expression and detection of KLK4-specific antibody in prostate cancer patient sera." Oncogene 21(46): 7114-7120.**

**de Koning, H. J., et al. (2002). "Prostate cancer mortality reduction by screening: power and time frame with complete enrollment in the European Randomised Screening for Prostate Cancer (ERSPC) trial." Int J Cancer 98(2): 268-273.**

**de Witte, J. H., et al. (2001). "Prognostic impact of urokinase-type plasminogen activator receptor (uPAR) in cytosols and pellet extracts derived from primary breast tumours." Br J Cancer 85(1): 85-92.**

**Debela, M., et al. (2008). "Structures and specificity of the human kallikrein-related peptidases KLK 4, 5, 6, and 7." Biol Chem 389(6): 623-632.**

**Debela, M., et al. (2007). "Chymotryptic specificity determinants in the 1.0 A structure of the zinc-inhibited human tissue kallikrein 7." Proc Natl Acad Sci U S A 104(41): 16086-16091.**

**Debela, M., et al. (2006a). "Crystal structures of human tissue kallikrein 4: activity modulation by a specific zinc binding site." Journal of molecular biology 362(5): 1094-1107.**
**Debela, M., et al. (2006b). "Specificity profiling of seven human tissue kallikreins reveals individual subsite preferences." J Biol Chem 281(35): 25678-25688.**
**Deperthes, D., et al. (1996). "Potential involvement of kallikrein hK2 in the hydrolysis of the human seminal vesicle proteins after ejaculation." J Androl 17(6): 659-665.**
**Deraison, C., et al. (2007). "LEKTI fragments specifically inhibit KLK5, KLK7, and KLK14 and control desquamation through a pH-dependent interaction." Mol Biol Cell 18(9): 3607-3619.**
**Derynck, R., et al. (2001). "TGF-beta signaling in tumor suppression and cancer progression." Nat Genet 29(2): 117-129.**
**Descargues, P., et al. (2006). "Corneodesmosomal cadherins are preferential targets of stratum corneum trypsin- and chymotrypsin-like hyperactivity in Netherton syndrome." J Invest Dermatol 126(7): 1622-1632.**
**Desrivieres, S., et al. (1993). "Activation of the 92 kDa type IV collagenase by tissue kallikrein." J Cell Physiol 157(3): 587-593.**
**Dhar, S., et al. (2001). "Analysis of normal epithelial cell specific-1 (NES1)/kallikrein 10 mRNA expression by in situ hybridization, a novel marker for breast cancer." Clin Cancer Res 7(11): 3393-3398.**
**Diamandis, E. P. (1995). "New diagnostic applications and physiological functions of prostate specific antigen." Scand J Clin Lab Invest Suppl 221: 105-112.**
**Diamandis, E. P. (1998a). "Prostate-specific antigen or human kallikrein 3? Recent developments." Tumour Biol 19(2): 65-67; discussion 67-68.**
**Diamandis, E. P. (1998b). "Prostate-specific Antigen: Its Usefulness in Clinical Medicine." Trends Endocrinol Metab 9(8): 310-316.**
**Diamandis, E. P., et al. (2004a). "Human kallikrein 11: an indicator of favorable prognosis in ovarian cancer patients." Clin Biochem 37(9): 823-829.**
**Diamandis, E. P., et al. (2003a). "Immunofluorometric quantification of human kallikrein 5 expression in ovarian cancer cytosols and its association with unfavorable patient prognosis." Tumour biology : the journal of the International Society for Oncodevelopmental Biology and Medicine 24(6): 299-309.**
**Diamandis, E. P., et al. (2002). "Human kallikrein 11: a new biomarker of prostate and ovarian carcinoma." Cancer Res 62(1): 295-300.**
**Diamandis, E. P., et al. (2003b). "Human kallikrein 6 (hK6): a new potential serum biomarker for diagnosis and prognosis of ovarian carcinoma." Journal of clinical oncology : official journal of the American Society of Clinical Oncology 21(6): 1035-1043.**
**Diamandis, E. P., et al. (2004b). "Altered kallikrein 7 and 10 concentrations in cerebrospinal fluid of patients with Alzheimer's disease and frontotemporal dementia." Clin Biochem 37(3): 230-237.**
**Diamandis, E. P. and G. M. Yousef (2002). "Human tissue kallikreins: a family of new cancer biomarkers." Clin Chem 48(8): 1198-1205.**
**Diamandis, E. P., et al. (2000a). "Human kallikrein 6 (zyme/protease M/neurosin): a new serum biomarker of ovarian carcinoma." Clin Biochem 33(7): 579-583.**
**Diamandis, E. P., et al. (2000b). "Immunofluorometric assay of human kallikrein 6 (zyme/protease M/neurosin) and preliminary clinical applications." Clin Biochem 33(5): 369-375.**

**Diamandis, E. P. and H. Yu (1995). "New biological functions of prostate-specific antigen?" J Clin Endocrinol Metab 80(5): 1515-1517.**

**Diamandis, E. P. and H. Yu (1997). "Nonprostatic sources of prostate-specific antigen." Urol Clin North Am 24(2): 275-282.**

**Dinh, P., et al. (2008). "New therapies for ovarian cancer: cytotoxics and molecularly targeted agents." Crit Rev Oncol Hematol 67(2): 103-112.**

**Dolled-Filhart, M., et al. (2010). "Automated analysis of tissue microarrays." Methods in molecular biology 664: 151-162.**

**Dong, Y., et al. (2005). "Compartmentalized expression of kallikrein 4 (KLK4/hK4) isoforms in prostate cancer: nuclear, cytoplasmic and secreted forms." Endocrine-related cancer 12(4): 875-889.**

**Dong, Y., et al. (2003). "Differential splicing of KLK5 and KLK7 in epithelial ovarian cancer produces novel variants with potential as cancer biomarkers." Clin Cancer Res 9(5): 1710-1720.**

**Dong, Y., et al. (2001). "Human kallikrein 4 (KLK4) is highly expressed in serous ovarian carcinomas." Clinical cancer research : an official journal of the American Association for Cancer Research 7(8): 2363-2371.**

**Dong, Y., et al. (2008). "Tissue-specific promoter utilisation of the kallikrein-related peptidase genes, KLK5 and KLK7, and cellular localisation of the encoded proteins suggest roles in exocrine pancreatic function." Biol Chem 389(2): 99-109.**

**Dong, Y., et al. (2010). "Kallikrein-related peptidase 7 promotes multicellular aggregation via the alpha(5)beta(1) integrin pathway and paclitaxel chemoresistance in serous epithelial ovarian carcinoma." Cancer Res 70(7): 2624-2633.**

**Dorn, J., et al. (2006). "Disease processes may be reflected by correlations among tissue kallikrein proteases but not with proteolytic factors uPA and PAI-1 in primary ovarian carcinoma." Biol Chem 387(8): 1121-1128.**

**Dorn, J., et al. (2011). "Circulating biomarker tissue kallikrein-related peptidase KLK5 impacts ovarian cancer patients' survival." Annals of oncology : official journal of the European Society for Medical Oncology / ESMO.**

**Dorn, J., et al. (2007). "Primary tumor levels of human tissue kallikreins affect surgical success and survival in ovarian cancer patients." Clin Cancer Res 13(6): 1742-1748.**

**Dowsett, M. and A. K. Dunbier (2008). "Emerging biomarkers and new understanding of traditional markers in personalized therapy for breast cancer." Clin Cancer Res 14(24): 8019-8026.**

**Duffy, M. J. (2002). "Urokinase-type plasminogen activator: a potent marker of metastatic potential in human cancers." Biochem Soc Trans 30(2): 207-210.**

**Duffy, M. J. and J. Crown (2008). "A personalized approach to cancer treatment: how biomarkers can help." Clin Chem 54(11): 1770-1779.**

**Duffy, M. J., et al. (2009). "Methylated genes as new cancer biomarkers." Eur J Cancer 45(3): 335-346.**

**Eads, C. A., et al. (2000). "MethyLight: a high-throughput assay to measure DNA methylation." Nucleic Acids Res 28(8): E32.**

**Egelrud, T. (1993a). "Purification and preliminary characterization of stratum corneum chymotryptic enzyme: a proteinase that may be involved in desquamation." J Invest Dermatol 101(2): 200-204.**

**Egelrud, T., et al. (2005). "hK5 and hK7, two serine proteinases abundant in human skin, are inhibited by LEKTI domain 6." Br J Dermatol 153(6): 1200-1203.**

**Egelrud, T., et al. (1993b). "Expression of stratum corneum chymotryptic enzyme in reconstructed human epidermis and its suppression by retinoic acid." Acta Derm Venereol 73(3): 181-184.**

**Ehrlich, M. (2002). "DNA methylation in cancer: too much, but also too little." Oncogene 21(35): 5400-5413.**

**Ekholm, E. and T. Egelrud (1999). "Stratum corneum chymotryptic enzyme in psoriasis." Arch Dermatol Res 291(4): 195-200.**

**Ekholm, E., et al. (1998). "Expression of stratum corneum chymotryptic enzyme in human sebaceous follicles." Acta Derm Venereol 78(5): 343-347.**

**Emami, N. and E. P. Diamandis (2008). "Utility of kallikrein-related peptidases (KLKs) as cancer biomarkers." Clin Chem 54(10): 1600-1607.**

**Emanueli, C., et al. (2001). "Local delivery of human tissue kallikrein gene accelerates spontaneous angiogenesis in mouse model of hindlimb ischemia." Circulation 103(1): 125-132.**

**Engvall, E. and P. Perlmann (1972). "Enzyme-linked immunosorbent assay, Elisa. 3. Quantitation of specific antibodies by enzyme-labeled anti-immunoglobulin in antigen-coated tubes." J Immunol 109(1): 129-135.**

**Esteller, M., et al. (2000). "Promoter hypermethylation and BRCA1 inactivation in sporadic breast and ovarian tumors." J Natl Cancer Inst 92(7): 564-569.**

**Felber, L. M., et al. (2006). "Mutant recombinant serpins as highly specific inhibitors of human kallikrein 14." Febs J 273(11): 2505-2514.**

**Feng, B., et al. (2006). "Clinical significance of human kallikrein 10 gene expression in colorectal cancer and gastric cancer." J Gastroenterol Hepatol 21(10): 1596-1603.**

**Fernandez, I. S., et al. (2007). "Crystallization and preliminary crystallographic studies of human kallikrein 7, a serine protease of the multigene kallikrein family." Acta Crystallogr Sect F Struct Biol Cryst Commun 63(Pt 8): 669-672.**

**Ferrier, C. M., et al. (1999). "Comparison of immunohistochemistry with immunoassay (ELISA) for the detection of components of the plasminogen activation system in human tumour tissue." Br J Cancer 79(9-10): 1534-1541.**

**Fevang, B., et al. (2009). "Enhanced levels of urokinase plasminogen activator and its soluble receptor in common variable immunodeficiency." Clin Immunol 131(3): 438-446.**

**Foekens, J. A., et al. (1999). "Expression of prostate-specific antigen (PSA) correlates with poor response to tamoxifen therapy in recurrent breast cancer." Br J Cancer 79(5-6): 888-894.**

**Foekens, J. A., et al. (2000). "The urokinase system of plasminogen activation and prognosis in 2780 breast cancer patients." Cancer Res 60(3): 636-643.**

**Fong, P. C., et al. (2009). "Inhibition of poly(ADP-ribose) polymerase in tumors from BRCA mutation carriers." N Engl J Med 361(2): 123-134.**

**Franco, P., et al. (2006). "Activation of urokinase receptor by a novel interaction between the connecting peptide region of urokinase and alpha v beta 5 integrin." J Cell Sci 119(Pt 16): 3424-3434.**

**Franzke, C. W., et al. (1996). "Antileukoprotease inhibits stratum corneum chymotryptic enzyme. Evidence for a regulative function in desquamation." J Biol Chem 271(36): 21886-21890.**

**Frenette, G., et al. (1997). "Prostatic kallikrein hK2, but not prostate-specific antigen (hK3), activates single-chain urokinase-type plasminogen activator." Int J Cancer 71(5): 897-899.**

**Gabril, M., et al. (2010). "Immunohistochemical analysis of kallikrein-related peptidases in the normal kidney and renal tumors: potential clinical implications." Biol Chem 391(4): 403-409.**

**Gagnon, J. F., et al. (2010). "Immunohistochemistry of Breast Tumor Markers on Archived Bouin-fixed Paraffin-embedded Tissues." Appl Immunohistochem Mol Morphol.**

**Gallagher, S. (1996). Immunoblot Detection Current Protocols in Protein Science. New York, John Wiley and Sons, Inc.**

**Gan, L., et al. (2000). "Sequencing and expression analysis of the serine protease gene cluster located in chromosome 19q13 region." Gene 257(1): 119-130.**

**Gao, J., et al. (2007). "Kallikrein 4 is a potential mediator of cellular interactions between cancer cells and osteoblasts in metastatic prostate cancer." The Prostate 67(4): 348-360.**

**Gao, S., et al. (2005). "CpG methylation of the PAI-1 gene 5'-flanking region is inversely correlated with PAI-1 mRNA levels in human cell lines." Thromb Haemost 94(3): 651-660.**

**Geyer, F. C., et al. (2009). "The role of molecular analysis in breast cancer." Pathology 41(1): 77-88.**

**Gilks, C. B., et al. (2005). "Distinction between serous tumors of low malignant potential and serous carcinomas based on global mRNA expression profiling." Gynecol Oncol 96(3): 684-694.**

**Goyal, J., et al. (1998). "The role for NES1 serine protease as a novel tumor suppressor." Cancer Res 58(21): 4782-4786.**

**Gratio, V., et al. (2010). "Kallikrein-related peptidase 4: a new activator of the aberrantly expressed protease-activated receptor 1 in colon cancer cells." The American journal of pathology 176(3): 1452-1461.**

**Grebenchtchikov, G. A., Creutzburg S, Seiz L, Goettig P, Kotzsch M, Gkazepis A, Schmitt M, Sweep F, and Magdolen V (2007). Polyclonal antibodies (pAbs) against KLK4 and 6: isolation of monospecific pAbs directed against a linear epitope within a flexible surface-exposed loop. IPS. Patras, Greece.**

**Grebenschikov, N., et al. (1997). "A sensitive and robust assay for urokinase and tissue-type plasminogen activators (uPA and tPA) and their inhibitor type I (PAI-1) in breast tumor cytosols." Int J Biol Markers 12(1): 6-14.**

**Grondahl-Hansen, J., et al. (1995). "Prognostic significance of the receptor for urokinase plasminogen activator in breast cancer." Clin Cancer Res 1(10): 1079-1087.**

**Gross, C. M., Sandra Raab, Corinna Propping, Tibor Schuster, Apostolos Gkazepis, Uli Schwarz-Boeger, André B. P. van Kuilenburg, Alfons Meindl, Manfred Schmitt, Marion Kiechle (2011). "Primary triple-negative breast cancers with (epi)genetic alterations in BRCA1 are associated with better patient outcome."**

**Guo, Y., et al. (2002). "Regulation of DNA methylation in human breast cancer. Effect on the urokinase-type plasminogen activator gene production and tumor invasion." J Biol Chem 277(44): 41571-41579.**

**Hachem, J. P., et al. (2005). "Sustained serine proteases activity by prolonged increase in pH leads to degradation of lipid processing enzymes and profound alterations of barrier function and stratum corneum integrity." J Invest Dermatol 125(3): 510-520.**

**Hachem, J. P., et al. (2006). "Serine protease activity and residual LEKTI expression determine phenotype in Netherton syndrome." J Invest Dermatol 126(7): 1609-1621.**

**Hakalahti, L., et al. (1993). "Evaluation of PAP and PSA gene expression in prostatic hyperplasia and prostatic carcinoma using northern-blot analyses, in situ hybridization and immunohistochemical stainings with monoclonal and bispecific antibodies." Int J Cancer 55(4): 590-597.**

**Hamdan, M. H. (2007). Cancer Biomarkers: Analyrical techniques for discovery. New York, John Wiley & Sons.**

**Hansson, L., et al. (2002). "Epidermal overexpression of stratum corneum chymotryptic enzyme in mice: a model for chronic itchy dermatitis." J Invest Dermatol 118(3): 444-449.**

**Hansson, L., et al. (1994). "Cloning, expression, and characterization of stratum corneum chymotryptic enzyme. A skin-specific human serine proteinase." J Biol Chem 269(30): 19420-19426.**

**Harbeck, N., et al. (2002). "Enhanced benefit from adjuvant chemotherapy in breast cancer patients classified high-risk according to urokinase-type plasminogen activator (uPA) and plasminogen activator inhibitor type 1 (n = 3424)." Cancer Res 62(16): 4617-4622.**

**Harris, L., et al. (2007). "American Society of Clinical Oncology 2007 update of recommendations for the use of tumor markers in breast cancer." J Clin Oncol 25(33): 5287-5312.**

**Harvey, T. J., et al. (2003). "Production and characterization of antipeptide kallikrein 4 antibodies. Use of computer modeling to design peptides specific to Kallikrein 4." Methods in molecular medicine 81: 241-254.**

**Hashem, N. N., et al. "Human kallikrein 14 (KLK14) expression in salivary gland tumors." Int J Biol Markers 25(1): 32-37.**

**Hashem, N. N., et al. (2010). "Human kallikrein 14 (KLK14) expression in salivary gland tumors." Int J Biol Markers 25(1): 32-37.**

**Hayat, M. A. (2002). Microscopy, immunohistochemistry and antigen retrieval methods, Kluwer Academic.**

**Hayes, D. F., et al. (1996). "Tumor marker utility grading system: a framework to evaluate clinical utility of tumor markers." J Natl Cancer Inst 88(20): 1456-1466.**

**Heidtmann, H. H., et al. (1999). "Generation of angiostatin-like fragments from plasminogen by prostate-specific antigen." Br J Cancer 81(8): 1269-1273.**

**Henrikson, K. P., et al. (1999). "Role of thrombin receptor in breast cancer invasiveness." Br J Cancer 79(3-4): 401-406.**

**Herman (1988). "Zinc formalin fixative for automated tissue processing." J Histotechnol 11: 85-89.**

**Hermann, A., et al. (1995). "Visualization of tissue kallikrein in human breast carcinoma by two-dimensional western blotting and immunohistochemistry." Biol Chem Hoppe Seyler 376(6): 365-370.**

**Herszenyi, L., et al. (1999). "The role of cysteine and serine proteases in colorectal carcinoma." Cancer 86(7): 1135-1142.**

**Heuzé-Vourc'h, et al. (2009). "High kallikrein-related peptidase 6 in non-small cell lung cancer cells: an indicator of tumour proliferation and poor prognosis." J Cell Mol Med 13(9B): 4014-4022.**

**Hibbs, K., et al. (2004). "Differential gene expression in ovarian carcinoma: identification of potential biomarkers." Am J Pathol 165(2): 397-414.**

**Hipp, S., et al. (2008). "Precise measurement of the E-cadherin repressor Snail in formalin-fixed endometrial carcinoma using protein lysate microarrays." Clin Exp Metastasis 25(6): 679-683.**

**Hoffman, B. R., et al. (2002). "Immunofluorometric quantitation and histochemical localisation of kallikrein 6 protein in ovarian cancer tissue: a new independent unfavourable prognostic biomarker." British journal of cancer 87(7): 763-771.**

**Holzscheiter, L., et al. (2006). "Quantitative reverse transcription-PCR assay for detection of mRNA encoding full-length human tissue kallikrein 7: prognostic relevance of KLK7 mRNA expression in breast cancer." Clin Chem 52(6): 1070-1079.**

**Hooper, J. D., et al. (2001). "Identification and characterization of KLK14, a novel kallikrein serine protease gene located on human chromosome 19q13.4 and expressed in prostate and skeletal muscle." Genomics 73(1): 117-122.**

**Horn, L. C., et al. (2002). "Clinical relevance of urokinase-type plasminogen activator and its inhibitor type 1 (PAI-1) in squamous cell carcinoma of the uterine cervix." Aust N Z J Obstet Gynaecol 42(4): 383-386.**

**Howarth, D. J., et al. (1997). "Immunohistochemical localization of prostate-specific antigen in benign and malignant breast tissues." Br J Cancer 75(11): 1646-1651.**

**Huang, A., et al. (1996). "Immunohistochemical assay for oestrogen receptors in paraffin wax sections of breast carcinoma using a new monoclonal antibody." J Pathol 180(2): 223-227.**

**Hutchinson, S., et al. (2003). "Purification of human kallikrein 6 from biological fluids and identification of its complex with alpha(1)-antichymotrypsin." Clin Chem 49(5): 746-751.**

**Iacobuzio-Donahue, C. A., et al. (2003). "Highly expressed genes in pancreatic ductal adenocarcinomas: a comprehensive characterization and comparison of the transcription profiles obtained from three major technologies." Cancer Res 63(24): 8614-8622.**

**Ikeda, K., et al. (1998). "Extraction and analysis of diagnostically useful proteins from formalin-fixed, paraffin-embedded tissue sections." J Histochem Cytochem 46(3): 397-403.**

**Ishida-Yamamoto, A., et al. (2005). "LEKTI is localized in lamellar granules, separated from KLK5 and KLK7, and is secreted in the extracellular spaces of the superficial stratum granulosum." J Invest Dermatol 124(2): 360-366.**

**Jain, K. (2010). The Handbook of Biomarkers. Basel, Humana Press.**

**Jamaspishvili, T., et al. (2011). "Immunohistochemical localization and analysis of kallikrein-related peptidase 7 and 11 expression in paired cancer and benign foci in prostate cancer patients." Neoplasma 58(4): 298-303.**

**Janicke, F., et al. (1994). "Both the cytosols and detergent extracts of breast cancer tissues are suited to evaluate the prognostic impact of the urokinase-type plasminogen activator and its inhibitor, plasminogen activator inhibitor type 1." Cancer Res 54(10): 2527-2530.**

**Janicke, F., et al. (2001). "Randomized adjuvant chemotherapy trial in high-risk, lymph node-negative breast cancer patients identified by urokinase-type plasminogen activator and plasminogen activator inhibitor type 1." J Natl Cancer Inst 93(12): 913-920.**

**Jänicke, F., Schmitt, M., Hafter, R., Hollrieder, A., Babic, R., Ulm, K., Gössner, W. & Graeff, H.. (1990). "Urokinase-type plasminogen activator (u-PA) antigen is a predictor of early relapse in breast cancer. ." Fibrinolysis (4): 69-78.**

**Jankun, J., et al. (1993). "Expression and localization of elements of the plasminogen activation system in benign breast disease and breast cancers." Journal of cellular biochemistry 53(2): 135-144.**

**Jemal, A., et al. (2008). "Cancer statistics, 2008." CA Cancer J Clin 58(2): 71-96.**

**Jiang, R., et al. (2011). "Kallikrein-5 promotes cleavage of desmoglein-1 and loss of cell-cell cohesion in oral squamous cell carcinoma." J Biol Chem 286(11): 9127-9135.**

**Jin, E., et al. (2003). "Protease-activated receptor (PAR)-1 and PAR-2 participate in the cell growth of alveolar capillary endothelium in primary lung adenocarcinomas." Cancer 97(3): 703-713.**

**Johnson, S. K., et al. (2007). "Kallikrein 7 enhances pancreatic cancer cell invasion by shedding E-cadherin." Cancer 109(9): 1811-1820.**

**Jones, M. J. (1981). "Transition Metal Sacts as Adjuncts to Formalin for Tissue Fixation " Laboratory Investigation 44(32A).**

**Jones, P. A. and S. B. Baylin (2002). "The fundamental role of epigenetic events in cancer." Nat Rev Genet 3(6): 415-428.**

**Kamath, L., et al. (2001). "Signaling from protease-activated receptor-1 inhibits migration and invasion of breast cancer cells." Cancer Res 61(15): 5933-5940.**

**Kaneko, T., et al. (2003). "Urokinase-type plasminogen activator expression correlates with tumor angiogenesis and poor outcome in gastric cancer." Cancer Sci 94(1): 43-49.**

**Kang, S. P., et al. (2008). "Triple negative breast cancer: current understanding of biology and treatment options." Curr Opin Obstet Gynecol 20(1): 40-46.**

**Kapadia, C., et al. (2003). "Human kallikrein 13: production and purification of recombinant protein and monoclonal and polyclonal antibodies, and development of a sensitive and specific immunofluorometric assay." Clin Chem 49(1): 77-86.**

**Kass, S. U., et al. (1993). "Inactive chromatin spreads from a focus of methylation." Mol Cell Biol 13(12): 7372-7379.**

**Kassis, J., et al. (2005). "Tumor microenvironment: what can effusions teach us?" Diagn Cytopathol 33(5): 316-319.**

**Kennedy, R. D., et al. (2004). "The role of BRCA1 in the cellular response to chemotherapy." J Natl Cancer Inst 96(22): 1659-1668.**

**Khandige, S., et al. (2011). "Methylation markers: a potential force driving cancer diagnostics forward." Oncology research 19(3-4): 105-110.**

**Kim, H., et al. (2001). "Human kallikrein gene 5 (KLK5) expression is an indicator of poor prognosis in ovarian cancer." Br J Cancer 84(5): 643-650.**

**Kim, J. T., et al. (2011). "Up-regulation and clinical significance of serine protease kallikrein 6 in colon cancer." Cancer 117(12): 2608-2619.**

**Kim, K., et al. (2009). "Development and validation of a protein-based signature for the detection of ovarian cancer." Clin Lab Med 29(1): 47-55.**

**Kioulafa, M., et al. (2009). "Kallikrein 10 (KLK10) methylation as a novel prognostic biomarker in early breast cancer." Ann Oncol 20(6): 1020-1025.**

**Kishi, T., et al. (2003). "Human kallikrein 8, a novel biomarker for ovarian carcinoma." Cancer Res 63(11): 2771-2774.**

**Kishi, T., et al. (2004). "Development of an immunofluorometric assay and quantification of human kallikrein 7 in tissue extracts and biological fluids." Clin Chem 50(4): 709-716.**

**Klokk, T. I., et al. (2007). "Kallikrein 4 is a proliferative factor that is overexpressed in prostate cancer." Cancer Res 67(11): 5221-5230.**

**Knudson, A. G., Jr. (1971). "Mutation and cancer: statistical study of retinoblastoma." Proc Natl Acad Sci U S A 68(4): 820-823.**

**Kobayashi, H., et al. (1994). "Impact of urokinase-type plasminogen activator and its inhibitor type 1 on prognosis in cervical cancer of the uterus." Cancer Res 54(24): 6539-6548.**

**Kobayashi, H., et al. (1991). "Cathepsin B efficiently activates the soluble and the tumor cell receptor-bound form of the proenzyme urokinase-type plasminogen activator (Pro-uPA)." J Biol Chem 266(8): 5147-5152.**

**Komatsu, N., et al. (2007a). "Human tissue kallikrein expression in the stratum corneum and serum of atopic dermatitis patients." Exp Dermatol 16(6): 513-519.**

**Komatsu, N., et al. (2007b). "Aberrant human tissue kallikrein levels in the stratum corneum and serum of patients with psoriasis: dependence on phenotype, severity and therapy." Br J Dermatol 156(5): 875-883.**

**Komatsu, N., et al. (2006). "Elevated human tissue kallikrein levels in the stratum corneum and serum of peeling skin syndrome-type B patients suggests an over-desquamation of corneocytes." J Invest Dermatol 126(10): 2338-2342.**

**Komatsu, N., et al. (2002). "Elevated stratum corneum hydrolytic activity in Netherton syndrome suggests an inhibitory regulation of desquamation by SPINK5-derived peptides." J Invest Dermatol 118(3): 436-443.**

**Komatsu, N., et al. (2003). "Expression and localization of tissue kallikrein mRNAs in human epidermis and appendages." J Invest Dermatol 121(3): 542-549.**

**Kononen, J., et al. (1998). "Tissue microarrays for high-throughput molecular profiling of tumor specimens." Nat Med 4(7): 844-847.**

**Konstantoudakis, G., et al. (2010). "Kallikrein-related peptidase 13 (KLK13) gene expressional status contributes significantly in the prognosis of primary gastric carcinomas." Clin Biochem 43(15): 1205-1211.**

**Koomen, J. M., et al. (2008). "Proteomic contributions to personalized cancer care." Mol Cell Proteomics 7(10): 1780-1794.**

**Kountourakis, P., et al. (2009). "Expression and prognostic significance of kallikrein-related peptidase 8 protein levels in advanced ovarian cancer by using automated quantitative analysis." Thromb Haemost 101(3): 541-546.**

**Krebs, M., et al. (1999). "Protein C inhibitor is expressed in keratinocytes of human skin." J Invest Dermatol 113(1): 32-37.**

**Kroll, J., et al. (2008). "Isolation of high quality protein samples from punches of formalin fixed and paraffin embedded tissue blocks." Histol Histopathol 23(4): 391-395.**

**Kuhn, W., et al. (1994). "Urokinase (uPA) and PAI-1 predict survival in advanced ovarian cancer patients (FIGO III) after radical surgery and platinum-based chemotherapy." Gynecol Oncol 55(3 Pt 1): 401-409.**

**Kuhn, W., et al. (1999). "Prognostic significance of urokinase (uPA) and its inhibitor PAI-1 for survival in advanced ovarian carcinoma stage FIGO IIIc." Br J Cancer 79(11-12): 1746-1751.**

**Kulasingam, V., et al. (2010). "Integrating high-throughput technologies in the quest for effective biomarkers for ovarian cancer." Nat Rev Cancer 10(5): 371-378.**
**Kurlender, L., et al. (2004). "Differential expression of a human kallikrein 5 (KLK5) splice variant in ovarian and prostate cancer." Tumour biology : the journal of the International Society for Oncodevelopmental Biology and Medicine 25(3): 149-156.**
**Kyriakopoulou, L. G., et al. (2003). "Prognostic value of quantitatively assessed KLK7 expression in ovarian cancer." Clin Biochem 36(2): 135-143.**
**L'Hoste (1995). "Using zinc formalin as a routine fixative in the histology laboratory." Lab Med 26: 210-214.**
**L&K-Biosciences. (2009). "The L&K Process Guide."**
**Leong, F. J. and J. O. McGee (2001). "Automated complete slide digitization: a medium for simultaneous viewing by multiple pathologists." J Pathol 195(4): 508-514.**
**Li, M., et al. (2011). "Over-expression of Ephb4 is associated with carcinogenesis of gastric cancer." Dig Dis Sci 56(3): 698-706.**
**Li, X., et al. (2009). "Parallel underexpression of kallikrein 5 and kallikrein 7 mRNA in breast malignancies." Cancer Sci 100(4): 601-607.**
**Liedtke, C., et al. (2008). "Response to neoadjuvant therapy and long-term survival in patients with triple-negative breast cancer." J Clin Oncol 26(8): 1275-1281.**
**Lijnen, H. R. (2002). "Matrix metalloproteinases and cellular fibrinolytic activity." Biochemistry. Biokhimiia 67(1): 92-98.**
**Lijnen, H. R. (2005). "Pleiotropic functions of plasminogen activator inhibitor-1." J Thromb Haemost 3(1): 35-45.**
**Lilja, H. (1985). "A kallikrein-like serine protease in prostatic fluid cleaves the predominant seminal vesicle protein." J Clin Invest 76(5): 1899-1903.**
**Little, S. P., et al. (1997). "Zyme, a novel and potentially amyloidogenic enzyme cDNA isolated from Alzheimer's disease brain." J Biol Chem 272(40): 25135-25142.**
**Liu, X. L., et al. (1996). "Identification of a novel serine protease-like gene, the expression of which is down-regulated during breast cancer progression." Cancer Res 56(14): 3371-3379.**
**Livak, K. J. and T. D. Schmittgen (2001). "Analysis of relative gene expression data using real-time quantitative PCR and the 2(-Delta Delta C(T)) Method." Methods 25(4): 402-408.**
**Lovgren, J., et al. (1999). "Measurement of prostate-specific antigen and human glandular kallikrein 2 in different body fluids." J Androl 20(3): 348-355.**
**Lu, C. Y., et al. (2009). "Aberrant DNA methylation profile and frequent methylation of KLK10 and OXGR1 genes in hepatocellular carcinoma." Genes, chromosomes & cancer 48(12): 1057-1068.**
**Lu, K. H., et al. (2004). "Selection of potential markers for epithelial ovarian cancer with gene expression arrays and recursive descent partition analysis." Clin Cancer Res 10(10): 3291-3300.**
**Lundstrom, A. and T. Egelrud (1991). "Stratum corneum chymotryptic enzyme: a proteinase which may be generally present in the stratum corneum and with a possible involvement in desquamation." Acta Derm Venereol 71(6): 471-474.**
**Luo, L., et al. (1998). "Structural characterization and mapping of the normal epithelial cell-specific 1 gene." Biochem Biophys Res Commun 247(3): 580-586.**
**Luo, L. Y., et al. (2001a). "Human kallikrein 10: a novel tumor marker for ovarian carcinoma?" Clin Chim Acta 306(1-2): 111-118.**

**Luo, L. Y., et al. (2002). "Higher expression of human kallikrein 10 in breast cancer tissue predicts tamoxifen resistance." Br J Cancer 86(11): 1790-1796.**
**Luo, L. Y. and W. Jiang (2006). "Inhibition profiles of human tissue kallikreins by serine protease inhibitors." Biol Chem 387(6): 813-816.**
**Luo, L. Y., et al. (2003a). "The serum concentration of human kallikrein 10 represents a novel biomarker for ovarian cancer diagnosis and prognosis." Cancer Res 63(4): 807-811.**
**Luo, L. Y., et al. (2001b). "Prognostic value of human kallikrein 10 expression in epithelial ovarian carcinoma." Clin Cancer Res 7(8): 2372-2379.**
**Luo, L. Y., et al. (2001c). "Expression of the normal epithelial cell-specific 1 (NES1; KLK10) candidate tumour suppressor gene in normal and malignant testicular tissue." Br J Cancer 85(2): 220-224.**
**Luo, L. Y., et al. (2003b). "Human tissue kallikreins and testicular cancer." APMIS : acta pathologica, microbiologica, et immunologica Scandinavica 111(1): 225-232; discussion 232-223.**
**Luther, T., et al. (1996). "Tissue factor expression during human and mouse development." Am J Pathol 149(1): 101-113.**
**Magklara, A., et al. (2003). "Characterization of the enzymatic activity of human kallikrein 6: Autoactivation, substrate specificity, and regulation by inhibitors." Biochem Biophys Res Commun 307(4): 948-955.**
**Magklara, A., et al. (2001). "The human KLK8 (neuropsin/ovasin) gene: identification of two novel splice variants and its prognostic value in ovarian cancer." Clin Cancer Res 7(4): 806-811.**
**Magklara, A., et al. (2000). "Decreased concentrations of prostate-specific antigen and human glandular kallikrein 2 in malignant versus nonmalignant prostatic tissue." Urology 56(3): 527-532.**
**Malinowsky, K., et al. (2010). "Targeted therapies in cancer - challenges and chances offered by newly developed techniques for protein analysis in clinical tissues." J Cancer 2: 26-35.**
**Mange, A., et al. (2008). "Specific increase of human kallikrein 4 mRNA and protein levels in breast cancer stromal cells." Biochem Biophys Res Commun 375(1): 107-112.**
**Markus, G., et al. (1980). "Content and characterization of plasminogen activators in human lung tumors and normal lung tissue." Cancer Res 40(3): 841-848.**
**Masand, R. P., et al. (2011). "Adenosquamous carcinoma of the head and neck: relationship to human papillomavirus and review of the literature." Head Neck Pathol 5(2): 108-116.**
**Matsuoka, H., et al. (2006). "Plasminogen-mediated activation and release of hepatocyte growth factor from extracellular matrix." Am J Respir Cell Mol Biol 35(6): 705-713.**
**Mavridis, K., et al. (2010). "Expression analysis and study of the KLK15 mRNA splice variants in prostate cancer and benign prostatic hyperplasia." Cancer Sci 101(3): 693-699.**
**McKiernan, E., et al. (2008). "Protein kinase Cdelta expression in breast cancer as measured by real-time PCR, western blotting and ELISA." Br J Cancer 99(10): 1644-1650.**
**Meani, F., et al. (2009). "Clinical application of proteomics in ovarian cancer prevention and treatment." Mol Diagn Ther 13(5): 297-311.**

**Menashi, S., et al. (1994). "Regulation of 92-kDa gelatinase B activity in the extracellular matrix by tissue kallikrein." Ann N Y Acad Sci 732: 466-468.**

**Mengele, K., et al. (2010). "Characteristics of the level-of-evidence-1 disease forecast cancer biomarkers uPA and its inhibitor PAI-1." Expert Rev Mol Diagn 10(7): 947-962.**

**Mikolajczyk, S. D., et al. (1999). "Prostatic human kallikrein 2 inactivates and complexes with plasminogen activator inhibitor-1." International journal of cancer. Journal international du cancer 81(3): 438-442.**

**Mikolajczyk, S. D., et al. (1997). "Ala217 is important for the catalytic function and autoactivation of prostate-specific human kallikrein 2." Eur J Biochem 246(2): 440-446.**

**Miller, R. T. (2001a). Control Slides: How many and what kind do you need? TECHNICAL IMMUNOHISTOCHEMISTRY: Achieving Reliability and Reproducibility of Immunostains. QUALITIY CONTROL OF DIAGNOSTIC IHC.**

**Miller, R. T. (2001b). TECHNICAL IMMUNOHISTOCHEMISTRY: Achieving Reliability and Reproducibility of Immunostains, Society for Applied Immunohistochemistry.**

**Milliat, F., et al. (2008). "Essential role of plasminogen activator inhibitor type-1 in radiation enteropathy." Am J Pathol 172(3): 691-701.**

**Mo, L., et al. (2010). "Human kallikrein 7 induces epithelial-mesenchymal transition-like changes in prostate carcinoma cells: a role in prostate cancer invasion and progression." Anticancer research 30(9): 3413-3420.**

**Moebus, V., et al. (1992). "Morphological, immunohistochemical and biochemical characterization of 6 newly established human ovarian carcinoma cell lines." Int J Cancer 52(1): 76-84.**

**Moeder, C. B., et al. (2009). "Quantitative, fluorescence-based in-situ assessment of protein expression." Methods in molecular biology 520: 163-175.**

**Moldenhauer, G., et al. (1987). "Epithelium-specific surface glycoprotein of Mr 34,000 is a widely distributed human carcinoma marker." Br J Cancer 56(6): 714-721.**

**Moodley, R., et al. (2005). "Visualisation of transforming growth factor-beta 1, tissue kallikrein, and kinin and transforming growth factor-beta receptors on human clear-cell renal carcinoma cells." Biol Chem 386(4): 375-382.**

**Mugnaini, E. and A. L. Dahl (1983). "Zinc-aldehyde fixation for light-microscopic immunocytochemistry of nervous tissues." The journal of histochemistry and cytochemistry : official journal of the Histochemistry Society 31(12): 1435-1438.**

**Na, Y. J., et al. (2009). "Ovarian cancer: markers of response." Int J Gynecol Cancer 19 Suppl 2: S21-29.**

**Nagahara, H., et al. (2005). "Clinicopathologic and biological significance of kallikrein 6 overexpression in human gastric cancer." Clinical cancer research : an official journal of the American Association for Cancer Research 11(19 Pt 1): 6800-6806.**

**Nakamura, T., et al. (2001). "Alternative splicing isoforms of hippostasin (PRSS20/KLK11) in prostate cancer cell lines." The Prostate 49(1): 72-78.**

**Nakamura, T., et al. (2003a). "The usefulness of serum human kallikrein 11 for discriminating between prostate cancer and benign prostatic hyperplasia." Cancer Res 63(19): 6543-6546.**

**Nakamura, T., et al. (2003b). "Quantitative analysis of hippostasin/KLK11 gene expression in cancerous and noncancerous prostatic tissues." Urology 61(5): 1042-1046.**

**Napieralski, R., et al. (2007). "Methylation of tumor-related genes in neoadjuvant-treated gastric cancer: relation to therapy response and clinicopathologic and molecular features." Clin Cancer Res 13(17): 5095-5102.**

**Nekarda, H., et al. (1994). "Prognostic impact of urokinase-type plasminogen activator and its inhibitor PAI-1 in completely resected gastric cancer." Cancer Res 54(11): 2900-2907.**

**Nelson, P. S., et al. (1999). "Molecular cloning and characterization of prostase, an androgen-regulated serine protease with prostate-restricted expression." Proc Natl Acad Sci U S A 96(6): 3114-3119.**

**Ni, X., et al. (2004). "Characterisation of human kallikrein 6/protease M expression in ovarian cancer." British journal of cancer 91(4): 725-731.**

**Nielsen, L. S., et al. (1986). "Monoclonal antibodies to human 54,000 molecular weight plasminogen activator inhibitor from fibrosarcoma cells--inhibitor neutralization and one-step affinity purification." Thromb Haemost 55(2): 206-212.**

**NIH (2010).**

**Nirmalan, N. J., et al. (2009). "Development and validation of a novel protein extraction methodology for quantitation of protein expression in formalin-fixed paraffin-embedded tissues using western blotting." J Pathol 217(4): 497-506.**

**Noack, F., et al. (1999). "CD87-positive tumor cells in bone marrow aspirates identified by confocal laser scanning fluorescence microscopy." Int J Oncol 15(4): 617-623.**

**Noack, F., et al. (2000). "A new approach to phenotyping disseminated tumor cells: methodological advances and clinical implications." Int J Biol Markers 15(1): 100-104.**

**Nocito, A., et al. (2001). "Tissue microarrays (TMAs) for high-throughput molecular pathology research." Int J Cancer 94(1): 1-5.**

**O'Shaughnessy, J., et al. (2011). "Iniparib plus chemotherapy in metastatic triple-negative breast cancer." N Engl J Med 364(3): 205-214.**

**Obiezu, C. V. and E. P. Diamandis (2000). "An alternatively spliced variant of KLK4 expressed in prostatic tissue." Clin Biochem 33(7): 599-600.**

**Obiezu, C. V. and E. P. Diamandis (2005). "Human tissue kallikrein gene family: applications in cancer." Cancer letters 224(1): 1-22.**

**Obiezu, C. V., et al. (2001). "Higher human kallikrein gene 4 (KLK4) expression indicates poor prognosis of ovarian cancer patients." Clinical cancer research : an official journal of the American Association for Cancer Research 7(8): 2380-2386.**

**Obiezu, C. V., et al. (2005). "Human kallikrein 4: quantitative study in tissues and evidence for its secretion into biological fluids." Clin Chem 51(8): 1432-1442.**

**Obiezu, C. V., et al. (2002). "Detection of human kallikrein 4 in healthy and cancerous prostatic tissues by immunofluorometry and immunohistochemistry." Clin Chem 48(8): 1232-1240.**

**Oertel, J. and D. Huhn (2000). "Immunocytochemical methods in haematology and oncology." Journal of cancer research and clinical oncology 126(8): 425-440.**

**Oesterling, J. E. (1991). "Prostate specific antigen: a critical assessment of the most useful tumor marker for adenocarcinoma of the prostate." J Urol 145(5): 907-923.**

**Ogawa, K., et al. (2005). "Clinical significance of human kallikrein gene 6 messenger RNA expression in colorectal cancer." Clinical cancer research : an official journal of the American Association for Cancer Research 11(8): 2889-2893.**

**Ohta, T., et al. (2003). "Protease-activated receptor-2 expression and the role of trypsin in cell proliferation in human pancreatic cancers." Int J Oncol 23(1): 61-66.**

**Oikonomopoulou, K., et al. (2010). "Kallikrein-related peptidases: proteolysis and signaling in cancer, the new frontier." Biol Chem 391(4): 299-310.**

**Oka, T., et al. (1991). "Immunohistochemical evidence of urokinase-type plasminogen activator in primary and metastatic tumors of pulmonary adenocarcinoma." Cancer Res 51(13): 3522-3525.**

**Pakneshan, P., et al. (2005). "Hypomethylation of urokinase (uPA) promoter in breast and prostate cancer: prognostic and therapeutic implications." Curr Cancer Drug Targets 5(7): 471-488.**

**Paliouras, M. and E. P. Diamandis (2006). "The kallikrein world: an update on the human tissue kallikreins." Biol Chem 387(6): 643-652.**

**Pampalakis, G., et al. (2006). "The epigenetic basis for the aberrant expression of kallikreins in human cancers." Biol Chem 387(6): 795-799.**

**Pampalakis, G., et al. (2004). "Cloning and characterization of novel isoforms of the human kallikrein 6 gene." Biochem Biophys Res Commun 320(1): 54-61.**

**Pampalakis, G., et al. (2009). "A tumor-protective role for human kallikrein-related peptidase 6 in breast cancer mediated by inhibition of epithelial-to-mesenchymal transition." Cancer Res 69(9): 3779-3787.**

**Pampalakis, G. and G. Sotiropoulou (2006). "Multiple mechanisms underlie the aberrant expression of the human kallikrein 6 gene in breast cancer." Biol Chem 387(6): 773-782.**

**Papachristopoulou, G., et al. (2011). "Quantitative expression analysis and study of the novel human kallikrein-related peptidase 14 gene (KLK14) in malignant and benign breast tissues." Thromb Haemost 105(1): 131-137.**

**Papachristopoulou, G., et al. (2009). "Expression analysis and study of KLK4 in benign and malignant breast tumours." Thromb Haemost 101(2): 381-387.**

**Papsidero, L. D., et al. (1980). "A prostate antigen in sera of prostatic cancer patients." Cancer Res 40(7): 2428-2432.**

**Parkin, D. M., et al. (2005). "Global cancer statistics, 2002." CA Cancer J Clin 55(2): 74-108.**

**Pavlopoulou, A., et al. (2010). "Evolutionary history of tissue kallikreins." PLoS One 5(11): e13781.**

**Pedersen, H., et al. (1994a). "Prognostic impact of urokinase, urokinase receptor, and type 1 plasminogen activator inhibitor in squamous and large cell lung cancer tissue." Cancer Res 54(17): 4671-4675.**

**Pedersen, H., et al. (1994b). "Urokinase and plasminogen activator inhibitor type 1 in pulmonary adenocarcinoma." Cancer Res 54(1): 120-123.**

**Perou, C. M., et al. (2000). "Molecular portraits of human breast tumours." Nature 406(6797): 747-752.**

**Petraki, C. D., et al. (2003a). "Immunohistochemical localization of human kallikreins 6, 10 and 13 in benign and malignant prostatic tissues." Prostate cancer and prostatic diseases 6(3): 223-227.**

**Petraki, C. D., et al. (2006a). "Prognostic implications of the immunohistochemical expression of human kallikreins 5, 6, 10 and 11 in renal cell carcinoma." Tumour**

**biology : the journal of the International Society for Oncodevelopmental Biology and Medicine 27(1): 1-7.**

**Petraki, C. D., et al. (2003b). "Human kallikrein 13 expression in normal tissues: an immunohistochemical study." J Histochem Cytochem 51(4): 493-501.**

**Petraki, C. D., et al. (2001). "The spectrum of human kallikrein 6 (zyme/protease M/neurosin) expression in human tissues as assessed by immunohistochemistry." The journal of histochemistry and cytochemistry : official journal of the Histochemistry Society 49(11): 1431-1441.**

**Petraki, C. D., et al. (2006b). "Cellular distribution of human tissue kallikreins: immunohistochemical localization." Biol Chem 387(6): 653-663.**

**Pettus, J. R., et al. (2009). "Multiple kallikrein (KLK 5, 7, 8, and 10) expression in squamous cell carcinoma of the oral cavity." Histol Histopathol 24(2): 197-207.**

**Planque, C., et al. (2006). "Expression of the human kallikrein genes 10 (KLK10) and 11 (KLK11) in cancerous and non-cancerous lung tissues." Biol Chem 387(6): 783-788.**

**Planque, C., et al. (2008a). "Quantitative RT-PCR analysis and immunohistochemical localization of the kallikrein-related peptidases 13 and 14 in lung." Biol Chem 389(6): 781-786.**

**Planque, C., et al. (2010). "Alternative splicing variant of kallikrein-related peptidase 8 as an independent predictor of unfavorable prognosis in lung cancer." Clin Chem 56(6): 987-997.**

**Planque, C., et al. (2005). "KLK5 and KLK7, two members of the human tissue kallikrein family, are differentially expressed in lung cancer." Biochem Biophys Res Commun 329(4): 1260-1266.**

**Planque, C., et al. (2008b). "A multiparametric serum kallikrein panel for diagnosis of non-small cell lung carcinoma." Clin Cancer Res 14(5): 1355-1362.**

**Prezas, P., et al. (2006a). "Overexpression of the human tissue kallikrein genes KLK4, 5, 6, and 7 increases the malignant phenotype of ovarian cancer cells." Biol Chem 387(6): 807-811.**

**Prezas, P., et al. (2006b). "The role of human tissue kallikreins 7 and 8 in intracranial malignancies." Biol Chem 387(12): 1607-1612.**

**Psyrri, A., et al. (2008). "Human tissue kallikrein 7, a novel biomarker for advanced ovarian carcinoma using a novel in situ quantitative method of protein expression." Ann Oncol 19(7): 1271-1277.**

**Rabbani, S. A. and R. H. Xing (1998). "Role of urokinase (uPA) and its receptor (uPAR) in invasion and metastasis of hormone-dependent malignancies." Int J Oncol 12(4): 911-920.**

**Rabien, A., et al. (2008). "High expression of KLK14 in prostatic adenocarcinoma is associated with elevated risk of prostate-specific antigen relapse." Tumour Biol 29(1): 1-8.**

**Rabien, A., et al. (2011). "KLK15 is a prognostic marker for progression-free survival in patients with radical prostatectomy." Int J Cancer 127(10): 2386-2394.**

**Rajah, R., et al. (1997). "Insulin-like growth factor (IGF)-binding protein-3 induces apoptosis and mediates the effects of transforming growth factor-beta1 on programmed cell death through a p53- and IGF-independent mechanism." J Biol Chem 272(18): 12181-12188.**

**Ramani, V. C. and R. S. Haun (2008a). "Expression of kallikrein 7 diminishes pancreatic cancer cell adhesion to vitronectin and enhances urokinase-type plasminogen activator receptor shedding." Pancreas 37(4): 399-404.**

**Ramani, V. C. and R. S. Haun (2008b). "The extracellular matrix protein fibronectin is a substrate for kallikrein 7." Biochem Biophys Res Commun 369(4): 1169-1173.**

**Ramani, V. C., et al. (2008). "Desmoglein 2 is a substrate of kallikrein 7 in pancreatic cancer." BMC Cancer 8: 373.**

**Rehault, S., et al. (2001). "Insulin-like growth factor binding proteins (IGFBPs) as potential physiological substrates for human kallikreins hK2 and hK3." Eur J Biochem 268(10): 2960-2968.**

**Rehbock, J., et al. (1995). "Identification of immunoreactive tissue kallikrein in human ductal breast carcinomas." J Cancer Res Clin Oncol 121(1): 64-68.**

**Reilly, D., et al. (1992). "Type-1 plasminogen activator inhibitor in human breast carcinomas." Int J Cancer 50(2): 208-214.**

**Reis-Filho, J. S. and A. N. Tutt (2008). "Triple negative tumours: a critical review." Histopathology 52(1): 108-118.**

**Rhiem, K., et al. (2010). "Sporadic breast carcinomas with somatic BRCA1 gene deletions share genotype/phenotype features with familial breast carcinomas." Anticancer Res 30(9): 3445-3449.**

**Rijken, D. C. (1995). "Plasminogen activators and plasminogen activator inhibitors: biochemical aspects." Bailliere's clinical haematology 8(2): 291-312.**

**Rittenhouse, H. G., et al. (1998). "Human Kallikrein 2 (hK2) and prostate-specific antigen (PSA): two closely related, but distinct, kallikreins in the prostate." Crit Rev Clin Lab Sci 35(4): 275-368.**

**Roman-Gomez, J., et al. (2004). "The normal epithelial cell-specific 1 (NES1) gene, a candidate tumor suppressor gene on chromosome 19q13.3-4, is downregulated by hypermethylation in acute lymphoblastic leukemia." Leukemia : official journal of the Leukemia Society of America, Leukemia Research Fund, U.K 18(2): 362-365.**

**Rosen, D. G., et al. (2005). "Potential markers that complement expression of CA125 in epithelial ovarian cancer." Gynecol Oncol 99(2): 267-277.**

**Ruckert, F., et al. (2008). "Co-expression of KLK6 and KLK10 as prognostic factors for survival in pancreatic ductal adenocarcinoma." Br J Cancer 99(9): 1484-1492.**

**Safra, T. (2009). "Hereditary ovarian cancer: biology, response to chemotherapy and prognosis." Womens Health (Lond Engl) 5(5): 543-553.**

**Sander, B., et al. (1991). "Assessment of cytokines by immunofluorescence and the paraformaldehyde-saponin procedure." Immunological reviews 119: 65-93.**

**Sano, A., et al. (2007). "Kallikrein 11 expressed in human breast cancer cells releases insulin-like growth factor through degradation of IGFBP-3." Int J Oncol 30(6): 1493-1498.**

**Santin, A. D., et al. (2004a). "The serine protease stratum corneum chymotryptic enzyme (kallikrein 7) is highly overexpressed in squamous cervical cancer cells." Gynecol Oncol 94(2): 283-288.**

**Santin, A. D., et al. (2005a). "Human kallikrein 6: a new potential serum biomarker for uterine serous papillary cancer." Clinical cancer research : an official journal of the American Association for Cancer Research 11(9): 3320-3325.**

**Santin, A. D., et al. (2004b). "Gene expression profiles in primary ovarian serous papillary tumors and normal ovarian epithelium: identification of candidate**

**molecular markers for ovarian cancer diagnosis and therapy." Int J Cancer 112(1): 14-25.**

**Santin, A. D., et al. (2005b). "Gene expression fingerprint of uterine serous papillary carcinoma: identification of novel molecular markers for uterine serous cancer diagnosis and therapy." British journal of cancer 92(8): 1561-1573.**

**Saville, D. J. (1990). "Multiple Comparison Procedures: The Practical Solution." The American Statistician 44(2): 174-180.**

**Schachter, M. (1979). "Kallikreins (kininogenases)--a group of serine proteases with bioregulatory actions." Pharmacol Rev 31(1): 1-17.**

**Schechter, N. M., et al. (2005). "Inhibition of human kallikreins 5 and 7 by the serine protease inhibitor lympho-epithelial Kazal-type inhibitor (LEKTI)." Biol Chem 386(11): 1173-1184.**

**Schmalfeldt, B., et al. (1995). "Primary tumor and metastasis in ovarian cancer differ in their content of urokinase-type plasminogen activator, its receptor, and inhibitors types 1 and 2." Cancer Res 55(18): 3958-3963.**

**Schmitt, M., et al. (1997). "Clinical impact of the plasminogen activation system in tumor invasion and metastasis: prognostic relevance and target for therapy." Thromb Haemost 78(1): 285-296.**

**Schmitt, M., et al. (1992). "Tumor-associated urokinase-type plasminogen activator: biological and clinical significance." Biological chemistry Hoppe-Seyler 373(7): 611-622.**

**Schmitt, M., et al. (2008). "Assessment of Urokinase-Type Plasminogen Activator and Its Inhibitor PAI-1 in Breast Cancer Tissue: Historical Aspects and Future Prospects." Breast care 3(s2): 3-10.**

**Schmitt, M., et al. (2010). "Clinical utility of level-of-evidence-1 disease forecast cancer biomarkers uPA and its inhibitor PAI-1." Expert Rev Mol Diagn 10(8): 1051-1067.**

**Schouten, J. P., et al. (2002). "Relative quantification of 40 nucleic acid sequences by multiplex ligation-dependent probe amplification." Nucleic Acids Res 30(12): e57.**

**Scorilas, A., et al. (2004). "Human kallikrein 13 protein in ovarian cancer cytosols: a new favorable prognostic marker." J Clin Oncol 22(4): 678-685.**

**Seiz, L., et al. (2010). "Polyclonal antibodies against kallikrein-related peptidase 4 (KLK4): immunohistochemical assessment of KLK4 expression in healthy tissues and prostate cancer." Biol Chem 391(4): 391-401.**

**Shan, S. J., et al. (2007). "Transcriptional upregulation of human tissue kallikrein 6 in ovarian cancer: clinical and mechanistic aspects." British journal of cancer 96(2): 362-372.**

**Shan, S. J., et al. (2006). "Unfavorable prognostic value of human kallikrein 7 quantified by ELISA in ovarian cancer cytosols." Clin Chem 52(10): 1879-1886.**

**Shaw, J. L. and E. P. Diamandis (2007). "Distribution of 15 human kallikreins in tissues and biological fluids." Clin Chem 53(8): 1423-1432.**

**Sher, Y. P., et al. (2006). "Human kallikrein 8 protease confers a favorable clinical outcome in non-small cell lung cancer by suppressing tumor cell invasiveness." Cancer Res 66(24): 11763-11770.**

**Shi, S. R., et al. (2006). "Protein extraction from formalin-fixed, paraffin-embedded tissue sections: quality evaluation by mass spectrometry." J Histochem Cytochem 54(6): 739-743.**

**Shigemasa, K., et al. (2004a). "Human kallikrein gene 11 (KLK11) mRNA overexpression is associated with poor prognosis in patients with epithelial ovarian cancer." Clin Cancer Res 10(8): 2766-2770.**

**Shigemasa, K., et al. (2001). "Expression of the protease inhibitor antileukoprotease and the serine protease stratum corneum chymotryptic enzyme (SCCE) is coordinated in ovarian tumors." Int J Gynecol Cancer 11(6): 454-461.**

**Shigemasa, K., et al. (2004b). "Human kallikrein 8 (hK8/TADG-14) expression is associated with an early clinical stage and favorable prognosis in ovarian cancer." Oncol Rep 11(6): 1153-1159.**

**Shinoda, Y., et al. (2007). "Association of KLK5 overexpression with invasiveness of urinary bladder carcinoma cells." Cancer Sci 98(7): 1078-1086.**

**Shvartsman, H. S., et al. (2003). "Overexpression of kallikrein 10 in epithelial ovarian carcinomas." Gynecol Oncol 90(1): 44-50.**

**Sidiropoulos, M., et al. (2005). "Downregulation of human kallikrein 10 (KLK10/NES1) by CpG island hypermethylation in breast, ovarian and prostate cancers." Tumour biology : the journal of the International Society for Oncodevelopmental Biology and Medicine 26(6): 324-336.**

**Sier, C. F., et al. (1991). "Immunolocalization of urokinase-type plasminogen activator in adenomas and carcinomas of the colorectum." Histopathology 19(3): 231-237.**

**Simon, R., et al. (2003). "Tissue microarrays in cancer diagnosis." Expert Rev Mol Diagn 3(4): 421-430.**

**Singh, A. K., et al. (2010). "Epigenetic silencing of BRCA1 gene associated with demographic and pathologic factors in sporadic breast cancer: a study of an Indian population." Eur J Cancer Prev.**

**Singh, J., et al. (2008). "Expression of kallikrein-related peptidases (KRP/hK5, 7, 6, 8) in subtypes of human lung carcinoma." Int Immunopharmacol 8(2): 300-306.**

**Skacel, M., et al. (2002). "Tissue microarrays: a powerful tool for high-throughput analysis of clinical specimens: a review of the method with validation data." Appl Immunohistochem Mol Morphol 10(1): 1-6.**

**Skelly, M. M., et al. (1997). "Urokinase-type plasminogen activator in colorectal cancer: relationship with clinicopathological features and patient outcome." Clin Cancer Res 3(10): 1837-1840.**

**Skytt, A., et al. (1995). "Primary substrate specificity of recombinant human stratum corneum chymotryptic enzyme." Biochem Biophys Res Commun 211(2): 586-589.**

**SlidePath (2008). Tissue Image Analysis user guide.**

**Smith, E., et al. (1974). "Hapten-reactive T and B mouse lymphocytes. Affinity of antibodies and binding strength of cellular receptors as factors of dose and time after immunization." Scand J Immunol 3(1): 61-70.**

**Sondell, B., et al. (1997). "In situ evidence that the population of Langerhans cells in normal human epidermis may be heterogeneous." Br J Dermatol 136(5): 687-693.**

**Sondell, B., et al. (1995). "Evidence that stratum corneum chymotryptic enzyme is transported to the stratum corneum extracellular space via lamellar bodies." J Invest Dermatol 104(5): 819-823.**

**Sondell, B., et al. (1994). "Immunolocalization of stratum corneum chymotryptic enzyme in human skin and oral epithelium with monoclonal antibodies: evidence of a proteinase specifically expressed in keratinizing squamous epithelia." J Histochem Cytochem 42(4): 459-465.**

**Sorlie, T., et al. (2001). "Gene expression patterns of breast carcinomas distinguish tumor subclasses with clinical implications." Proc Natl Acad Sci U S A 98(19): 10869-10874.**

**Sotiropoulou, G., et al. (2003). "Emerging interest in the kallikrein gene family for understanding and diagnosing cancer." Oncol Res 13(6-10): 381-391.**

**Spentzos, D., et al. (2004). "Gene expression signature with independent prognostic significance in epithelial ovarian cancer." J Clin Oncol 22(23): 4700-4710.**

**Stavropoulou, P., et al. (2005). "Expression analysis and prognostic significance of human kallikrein 11 in prostate cancer." Clin Chim Acta 357(2): 190-195.**

**Stefansson, O. A., et al. (2011). "CpG island hypermethylation of BRCA1 and loss of pRb as co-occurring events in basal/triple-negative breast cancer." Epigenetics 6(5): 638-649.**

**Stephan, C., et al. (2003). "Quantitative analysis of kallikrein 15 gene expression in prostate tissue." J Urol 169(1): 361-364.**

**Stephenson, S. A., et al. (1999). "Localization of a new prostate-specific antigen-related serine protease gene, KLK4, is evidence for an expanded human kallikrein gene family cluster on chromosome 19q13.3-13.4." J Biol Chem 274(33): 23210-23214.**

**Sutkowski, D. M., et al. (1999). "Growth regulation of prostatic stromal cells by prostate-specific antigen." J Natl Cancer Inst 91(19): 1663-1669.**

**Svanberg, L. and B. Astedt (1979). "Release of plasminogen activator from normal and neoplastic endometrium." Experientia 35(6): 818-819.**

**Svenson, S. B. and K. Larsen (1977). "An enzyme-linked immunosorbent assay (ELISA) for the determination of diphtheria toxin antibodies." J Immunol Methods 17(3-4): 249-256.**

**Sweep, F. C., et al. (2003). "Considerations on development, validation, application, and quality control of immuno(metric) biomarker assays in clinical cancer research: an EORTC-NCI working group report." Int J Oncol 23(6): 1715-1726.**

**Takahashi, T., et al. (2005). "Plasminogen activator inhibitor type 1 promotes fibrosarcoma cell migration by modifying cellular attachment to vitronectin via alpha(v)beta(5) integrin." Semin Thromb Hemost 31(3): 356-363.**

**Takayama, T. K., et al. (2001). "Characterization of hK4 (prostase), a prostate-specific serine protease: activation of the precursor of prostate specific antigen (pro-PSA) and single-chain urokinase-type plasminogen activator and degradation of prostatic acid phosphatase." Biochemistry 40(50): 15341-15348.**

**Talieri, M., et al. (2011). "Expression analysis and clinical evaluation of kallikrein-related peptidase 10 (KLK10) in colorectal cancer." Tumour Biol 32(4): 737-744.**

**Talieri, M., et al. (2004). "Expression analysis of the human kallikrein 7 (KLK7) in breast tumors: a new potential biomarker for prognosis of breast carcinoma." Thromb Haemost 91(1): 180-186.**

**Talieri, M., et al. (2009a). "The use of kallikrein-related peptidases as adjuvant prognostic markers in colorectal cancer." Br J Cancer 100(10): 1659-1665.**

**Talieri, M., et al. (2009b). "Clinical significance of kallikrein-related peptidase 7 (KLK7) in colorectal cancer." Thromb Haemost 101(4): 741-747.**

**Tanimoto, H., et al. (2001). "Increased expression of protease M in ovarian tumors." Tumour biology : the journal of the International Society for Oncodevelopmental Biology and Medicine 22(1): 11-18.**

**Tanimoto, H., et al. (1999). "The stratum corneum chymotryptic enzyme that mediates shedding and desquamation of skin cells is highly overexpressed in ovarian tumor cells." Cancer 86(10): 2074-2082.**

**Tarui, T., et al. (2006). "Direct interaction of the kringle domain of urokinase-type plasminogen activator (uPA) and integrin alpha v beta 3 induces signal transduction and enhances plasminogen activation." Thromb Haemost 95(3): 524-534.**

**Taylor, C. R. (2009). Immunohistochemical Standardization and Ready-to-Use Antibodies. Dako Immunohistochemical Staining Methods**

**Termini, L., et al. (2010). "Analysis of human kallikrein 7 expression as a potential biomarker in cervical neoplasia." Int J Cancer 127(2): 485-490.**

**Tian, X., et al. (2004). "Expression of human kallikrein 7 (hK7/SCCE) and its inhibitor antileukoprotease (ALP/SLPI) in uterine endocervical glands and in cervical adenocarcinomas." Oncol Rep 12(5): 1001-1006.**

**Tissot, J. D., et al. (1982). "Isolation from human plasma of a plasminogen activator identical to urinary high molecular weight urokinase." The Journal of clinical investigation 70(6): 1320-1323.**

**Tome, Y., et al. (1990). "Preservation of cluster 1 small cell lung cancer antigen in zinc-formalin fixative and its application to immunohistological diagnosis." Histopathology 16(5): 469-474.**

**Torr-Brown, S. R. and B. E. Sobel (1993). "Attenuation of thrombolysis by release of plasminogen activator inhibitor type-1 from platelets." Thrombosis research 72(5): 413-421.**

**Toyama, T., et al. (2008). "Frequently increased epidermal growth factor receptor (EGFR) copy numbers and decreased BRCA1 mRNA expression in Japanese triple-negative breast cancers." BMC Cancer 8: 309.**

**Tschesche, H., et al. (1989). "Tissue kallikrein effectively activates latent matrix degrading metalloenzymes." Adv Exp Med Biol 247A: 545-548.**

**Tuma, R. S. (2009). "PARP inhibitors: will the new class of drugs match the hype?" J Natl Cancer Inst 101(18): 1230-1232.**

**Turner, J. M., et al. (2004). "BRCA1, histone H2AX phosphorylation, and male meiotic sex chromosome inactivation." Curr Biol 14(23): 2135-2142.**

**Turner, N. C., et al. (2007). "BRCA1 dysfunction in sporadic basal-like breast cancer." Oncogene 26(14): 2126-2132.**

**Ulisse, S., et al. (2009). "The urokinase plasminogen activator system: a target for anti-cancer therapy." Curr Cancer Drug Targets 9(1): 32-71.**

**Underwood, L. J., et al. (1999). "Cloning of tumor-associated differentially expressed gene-14, a novel serine protease overexpressed by ovarian carcinoma." Cancer Res 59(17): 4435-4439.**

**Ursitti, J. A., et al. (1995). Electroblotting from Polyacrylamide Gels. . Current Protocols in Protein Science. New York, John Wiley and Sons, Inc.**

**van der Stoep, N., et al. (2009). "Diagnostic guidelines for high-resolution melting curve (HRM) analysis: an interlaboratory validation of BRCA1 mutation scanning using the 96-well LightScanner." Human mutation 30(6): 899-909.**

**van Mourik, J. A., et al. (1984). "Purification of an inhibitor of plasminogen activator (antiactivator) synthesized by endothelial cells." J Biol Chem 259(23): 14914-14921.**

**Vasilopoulos, Y., et al. (2004). "Genetic association between an AACC insertion in the 3'UTR of the stratum corneum chymotryptic enzyme gene and atopic dermatitis." J Invest Dermatol 123(1): 62-66.**

**Veveris-Lowe, T. L., et al. (2005). "Kallikrein 4 (hK4) and prostate-specific antigen (PSA) are associated with the loss of E-cadherin and an epithelial-mesenchymal transition (EMT)-like effect in prostate cancer cells." Endocrine-related cancer 12(3): 631-643.**

**Vial, D. and P. J. McKeown-Longo (2008). "PAI1 stimulates assembly of the fibronectin matrix in osteosarcoma cells through crosstalk between the alphavbeta5 and alpha5beta1 integrins." Journal of cell science 121(Pt 10): 1661-1670.**

**Voduc, D. and T. O. Nielsen (2008). "Basal and triple-negative breast cancers: impact on clinical decision-making and novel therapeutic options." Clin Breast Cancer 8 Suppl 4: S171-178.**

**Walch, A., et al. (2008). "MALDI imaging mass spectrometry for direct tissue analysis: a new frontier for molecular histology." Histochem Cell Biol 130(3): 421-434.**

**Wang, M. C., et al. (1981). "Prostate antigen: a new potential marker for prostatic cancer." Prostate 2(1): 89-96.**

**Wang, M. C., et al. (1979). "Purification of a human prostate specific antigen." Invest Urol 17(2): 159-163.**

**Wang, S. N., et al. (1994). "Antigen expression associated with lymph node metastasis in gastric adenocarcinomas." Pathol Int 44(12): 844-849.**

**Watanabe, Y. and M. Maekawa (2010). "Methylation of DNA in cancer." Advances in clinical chemistry 52: 145-167.**

**Watkinson, A., et al. (2001). "Water modulation of stratum corneum chymotryptic enzyme activity and desquamation." Arch Dermatol Res 293(9): 470-476.**

**Watt, K. W., et al. (1986). "Human prostate-specific antigen: structural and functional similarity with serine proteases." Proc Natl Acad Sci U S A 83(10): 3166-3170.**

**Wei, M., et al. (2005). "BRCA1 promoter methylation in sporadic breast cancer is associated with reduced BRCA1 copy number and chromosome 17 aneusomy." Cancer Res 65(23): 10692-10699.**

**Weisenberger, D. J., et al. (2005). "Analysis of repetitive element DNA methylation by MethyLight." Nucleic Acids Res 33(21): 6823-6836.**

**Welsh, J. B., et al. (2003). "Large-scale delineation of secreted protein biomarkers overexpressed in cancer tissue and serum." Proc Natl Acad Sci U S A 100(6): 3410-3415.**

**Wen, Y. G., et al. (2011). "Identification and validation of Kallikrein-ralated peptidase 11 as a novel prognostic marker of gastric cancer based on immunohistochemistry." J Surg Oncol.**

**White, N. M., et al. (2009). "KLK6 and KLK13 predict tumor recurrence in epithelial ovarian carcinoma." Br J Cancer 101(7): 1107-1113.**

**WHO (2008) "Cancer."**

**Winnepenninckx, V., et al. (2006). "Gene expression profiling of primary cutaneous melanoma and clinical outcome." J Natl Cancer Inst 98(7): 472-482.**

**Wolf, W. C., et al. (2001). "A synthetic tissue kallikrein inhibitor suppresses cancer cell invasiveness." Am J Pathol 159(5): 1797-1805.**

**Wu, M., et al. (1977). "Purification and characterization of a plasminogen activator secreted by cultured human pancreatic carcinoma cells." Biochemistry 16(9): 1908-1913.**

**Wun, T. C., et al. (1982). "Isolation and characterization of urokinase from human plasma." J Biol Chem 257(6): 3276-3283.**

**Xi, Z., et al. (2004a). "Kallikrein 4 is associated with paclitaxel resistance in ovarian cancer." Gynecol Oncol 94(1): 80-85.**

**Xi, Z., et al. (2004b). "Kallikrein 4 is a predominantly nuclear protein and is overexpressed in prostate cancer." Cancer Res 64(7): 2365-2370.**

**Xing, R. H. and S. A. Rabbani (1996). "Overexpression of urokinase receptor in breast cancer cells results in increased tumor invasion, growth and metastasis." Int J Cancer 67(3): 423-429.**

**Xing, R. H. and S. A. Rabbani (1999). "Transcriptional regulation of urokinase (uPA) gene expression in breast cancer cells: role of DNA methylation." Int J Cancer 81(3): 443-450.**

**Xuan, Q., et al. (2008). "Expression of the serine protease kallikrein 7 and its inhibitor antileukoprotease is decreased in prostate cancer." Arch Pathol Lab Med 132(11): 1796-1801.**

**Yamashiro, K., et al. (1997). "Molecular cloning of a novel trypsin-like serine protease (neurosin) preferentially expressed in brain." Biochim Biophys Acta 1350(1): 11-14.**

**Yoshida, E., et al. (1995). "Prostate-specific antigen activates single-chain urokinase-type plasminogen activator." International journal of cancer. Journal international du cancer 63(6): 863-865.**

**Yoshida, S., et al. (2009). "Expression profiles of genes involved in poor prognosis of epithelial ovarian carcinoma: a review." Int J Gynecol Cancer 19(6): 992-997.**

**Yoshida, S., et al. (1998a). "Sequence analysis and expression of human neuropsin cDNA and gene." Gene 213(1-2): 9-16.**

**Yoshida, S., et al. (1998b). "cDNA cloning and expression of a novel serine protease, TLSP." Biochim Biophys Acta 1399(2-3): 225-228.**

**Yousef, G. M., et al. (2004a). "In-silico analysis of kallikrein gene expression in pancreatic and colon cancers." Anticancer research 24(1): 43-51.**

**Yousef, G. M., et al. (2002a). "Quantitative analysis of human kallikrein gene 14 expression in breast tumours indicates association with poor prognosis." Br J Cancer 87(11): 1287-1293.**

**Yousef, G. M., et al. (2004b). "In silico analysis of the human kallikrein gene 6." Tumour biology : the journal of the International Society for Oncodevelopmental Biology and Medicine 25(5-6): 282-289.**

**Yousef, G. M., et al. (2000a). "Identification and characterization of KLK-L4, a new kallikrein-like gene that appears to be down-regulated in breast cancer tissues." J Biol Chem 275(16): 11891-11898.**

**Yousef, G. M. and E. P. Diamandis (1999). "The new kallikrein-like gene, KLK-L2. Molecular characterization, mapping, tissue expression, and hormonal regulation." J Biol Chem 274(53): 37511-37516.**

**Yousef, G. M. and E. P. Diamandis (2000). "The expanded human kallikrein gene family: locus characterization and molecular cloning of a new member, KLK-L3 (KLK9)." Genomics 65(2): 184-194.**

**Yousef, G. M. and E. P. Diamandis (2001). "The new human tissue kallikrein gene family: structure, function, and association to disease." Endocr Rev 22(2): 184-204.**
**Yousef, G. M. and E. P. Diamandis (2002). "Human tissue kallikreins: a new enzymatic cascade pathway?" Biol Chem 383(7-8): 1045-1057.**
**Yousef, G. M., et al. (2003a). "Steroid hormone regulation and prognostic value of the human kallikrein gene 14 in ovarian cancer." Am J Clin Pathol 119(3): 346-355.**
**Yousef, G. M., et al. (2003b). "The human kallikrein protein 5 (hK5) is enzymatically active, glycosylated and forms complexes with two protease inhibitors in ovarian cancer fluids." Biochim Biophys Acta 1628(2): 88-96.**
**Yousef, G. M., et al. (2001a). "Quantitative expression of the human kallikrein gene 9 (KLK9) in ovarian cancer: a new independent and favorable prognostic marker." Cancer Res 61(21): 7811-7818.**
**Yousef, G. M., et al. (1999a). "Molecular characterization of zyme/protease M/neurosin (PRSS9), a hormonally regulated kallikrein-like serine protease." Genomics 62(2): 251-259.**
**Yousef, G. M., et al. (2001b). "Cloning of a new member of the human kallikrein gene family, KLK14, which is down-regulated in different malignancies." Cancer Res 61(8): 3425-3431.**
**Yousef, G. M., et al. (2000b). "KLK12 is a novel serine protease and a new member of the human kallikrein gene family-differential expression in breast cancer." Genomics 69(3): 331-341.**
**Yousef, G. M., et al. (2002b). "Differential expression of Kallikrein gene 5 in cancerous and normal testicular tissues." Urology 60(4): 714-718.**
**Yousef, G. M., et al. (1999b). "Prostase/KLK-L1 is a new member of the human kallikrein gene family, is expressed in prostate and breast tissues, and is hormonally regulated." Cancer Res 59(17): 4252-4256.**
**Yousef, G. M., et al. (2003c). "Human kallikrein 5: a potential novel serum biomarker for breast and ovarian cancer." Cancer Res 63(14): 3958-3965.**
**Yousef, G. M., et al. (2003d). "Parallel overexpression of seven kallikrein genes in ovarian cancer." Cancer Res 63(9): 2223-2227.**
**Yousef, G. M., et al. (2002c). "Down-regulation of the human kallikrein gene 5 (KLK5) in prostate cancer tissues." The Prostate 51(2): 126-132.**
**Yousef, G. M., et al. (2000c). "Genomic organization, mapping, tissue expression, and hormonal regulation of trypsin-like serine protease (TLSP PRSS20), a new member of the human kallikrein gene family." Genomics 63(1): 88-96.**
**Yousef, G. M., et al. (2001c). "Molecular cloning of the human kallikrein 15 gene (KLK15). Up-regulation in prostate cancer." J Biol Chem 276(1): 53-61.**
**Yousef, G. M., et al. (2003e). "Prognostic value of the human kallikrein gene 15 expression in ovarian cancer." Journal of clinical oncology : official journal of the American Society of Clinical Oncology 21(16): 3119-3126.**
**Yousef, G. M., et al. (2002d). "Human kallikrein gene 5 (KLK5) expression by quantitative PCR: an independent indicator of poor prognosis in breast cancer." Clin Chem 48(8): 1241-1250.**
**Yousef, G. M., et al. (2002e). "The androgen-regulated gene human kallikrein 15 (KLK15) is an independent and favourable prognostic marker for breast cancer." Br J Cancer 87(11): 1294-1300.**
**Yousef, G. M., et al. (2000d). "The KLK7 (PRSS6) gene, encoding for the stratum corneum chymotryptic enzyme is a new member of the human kallikrein gene**

**family - genomic characterization, mapping, tissue expression and hormonal regulation." Gene 254(1-2): 119-128.**
**Yousef, G. M., et al. (2003f). "The prognostic value of the human kallikrein gene 9 (KLK9) in breast cancer." Breast Cancer Res Treat 78(2): 149-158.**
**Yousef, G. M., et al. (2003g). "Differential expression of the human kallikrein gene 14 (KLK14) in normal and cancerous prostatic tissues." Prostate 56(4): 287-292.**
**Yousef, G. M., et al. (2004c). "The kallikrein gene 5 splice variant 2 is a new biomarker for breast and ovarian cancer." Tumour biology : the journal of the International Society for Oncodevelopmental Biology and Medicine 25(5-6): 221-227.**
**Yousef, G. M., et al. (2005). "Identification of new splice variants and differential expression of the human kallikrein 10 gene, a candidate cancer biomarker." Tumour Biol 26(5): 227-235.**
**Yousef, G. M., et al. (2004d). "Kallikrein gene downregulation in breast cancer." Br J Cancer 90(1): 167-172.**
**Yousef, G. M., et al. (2004e). "Kallikrein gene downregulation in breast cancer." British journal of cancer 90(1): 167-172.**
**Yu, H. and E. P. Diamandis (1995). "Measurement of serum prostate specific antigen levels in women and in prostatectomized men with an ultrasensitive immunoassay technique." J Urol 153(3 Pt 2): 1004-1008.**
**Yu, H., et al. (1996). "Prostate specific antigen in breast cancer, benign breast disease and normal breast tissue." Breast Cancer Res Treat 40(2): 171-178.**
**Yu, H., et al. (1995). "Prostate-specific antigen is a new favorable prognostic indicator for women with breast cancer." Cancer Res 55(10): 2104-2110.**
**Yu, H., et al. (1998). "Prognostic value of prostate-specific antigen for women with breast cancer: a large United States cohort study." Clin Cancer Res 4(6): 1489-1497.**
**Zhang, S. Q., et al. (2009). "Kallikrein 4 overexpression in endometrial carcinoma and upregulation by estrogen via mitogen-activated protein kinase signal pathway." Int J Gynecol Cancer 19(8): 1377-1383.**
**Zhang, Y., et al. (2010). "Frequent transcriptional inactivation of Kallikrein 10 gene by CpG island hypermethylation in non-small cell lung cancer." Cancer Sci 101(4): 934-940.**
**Zhang, Y., et al. (2011). "Methylation of multiple genes as a candidate biomarker in non-small cell lung cancer." Cancer letters 303(1): 21-28.**
**Zhao, H., et al. (2010). "Correlation of the expression of human kallikrein-related peptidases 4 and 7 with the prognosis in oral squamous cell carcinoma." Head Neck 33(4): 566-572.**
**Zhao, H., et al. (2011). "Correlation of the expression of human kallikrein-related peptidases 4 and 7 with the prognosis in oral squamous cell carcinoma." Head & neck 33(4): 566-572.**
**Zhao, Y., et al. (2008). "Urokinase directly activates matrix metalloproteinases-9: a potential role in glioblastoma invasion." Biochem Biophys Res Commun 369(4): 1215-1220.**
**Zorio, E., et al. (2008). "Fibrinolysis: the key to new pathogenetic mechanisms." Curr Med Chem 15(9): 923-929.**